UNIVERSITE MONTPELLIER II
SCIENCES ET TECHNIQUES DU LANGUEDOC

THESE

Pour obtenir le grade de

DOCTEUR DE L'UNIVERSITE MONTPELLIER II

Discipline : Structure et Evolution de la Terre et des Planètes

Ecole Doctorale : SIBAGHE (Système Intégrés en Biologie, Agronomie, Géosciences, Hydrosciences, Environnement)

Présentée et soutenue Publiquement

Par

Shahryar SOLAYMANI AZAD

Le 28 Avril 2009

EVALUATION DE L'ALEA SISMIQUE POUR LES VILLES DE TEHERAN, TABRIZ ET ZANDJAN DANS LE NW DE L'IRAN APPROCHE MORPHOTECTONIQUE ET PALEOSISMOLOGIQUE

SEISMIC HAZARD ASSESSEMENT FOR TEHRAN, TABRIZ AND ZANDJAN CITIES (NW IRAN) BASED ON MORPHOTECTONICS AND PALEOSEISMOLOGY

Composition du Jury

Olivier BELLIER	Professeur, Université d'Aix-Marseille III	Rapporteur
Damien DHONT	Maître de Conférence, Université de Pau	Rapporteur
Roger BAYER	Professeur, Université Montpellier II	Examinateur
Hervé PHILIP	Professeur, Université Montpellier II	Directeur de thèse
Jean-François RITZ	Chargé de Recherche, CNRS, Univ. Montpellier II	Co-directeur de thèse
Stéphane DOMINGUEZ	Chargé de Recherche, CNRS, Univ. Montpellier II	Invité
Khaled HESSAMI	Professeur assistant, IIEES, Iran	Examinateur
Mohammad-Reza ABBASSI	Professeur assistant, IIEES, Iran	Invité

UNIVERSITE MONTPELLIER II
SCIENCES ET TECHNIQUES DU LANGUEDOC

THESE

Pour obtenir le grade de

DOCTEUR DE L'UNIVERSITE MONTPELLIER II

Discipline : Structure et Evolution de la Terre et des Planètes

Ecole Doctorale : SIBAGHE (Système Intégrés en Biologie, Agronomie, Géosciences, Hydrosciences, Environnement)

Présentée et soutenue Publiquement

Par

Shahryar SOLAYMANI AZAD

Le 28 Avril 2009

EVALUATION DE L'ALEA SISMIQUE POUR LES VILLES DE TEHERAN, TABRIZ ET ZANDJAN DANS LE NW DE L'IRAN APPROCHE MORPHOTECTONIQUE ET PALEOSISMOLOGIQUE

SEISMIC HAZARD ASSESSEMENT FOR TEHRAN, TABRIZ AND ZANDJAN CITIES (NW IRAN) BASED ON MORPHOTECTONICS AND PALEOSEISMOLOGY

Composition du Jury

Olivier BELLIER	Professeur, Université d'Aix-Marseille III	Rapporteur
Damien DHONT	Maître de Conférence, Université de Pau	Rapporteur
Roger BAYER	Professeur, Université Montpellier II	Examinateur
Hervé PHILIP	Professeur, Université Montpellier II	Directeur de thèse
Jean-François RITZ	Chargé de Recherche, CNRS, Univ. Montpellier II	Co-directeur de thèse
Stéphane DOMINGUEZ	Chargé de Recherche, CNRS, Univ. Montpellier II	Invité
Khaled HESSAMI	Professeur assistant, IIEES, Iran	Examinateur
Mohammad-Reza ABBASSI	Professeur assistant, IIEES, Iran	Invité

Remerciements

Je sais bien que pour lancer un grand travail de recherche scientifique qui contient deux projets internationaux et trois projets nationaux, ce n'est pas seulement mon effort qui peut m'aider. Ce mémoire de thèse est le résultat d'une grande collaboration qui m'a accompagnée pendant 347 jours de travail sur le terrain dans trois domaines du nord-ouest de l'Iran, région la plus peuplée de ce pays. Pour faire ça, j'ai profité des conseils scientifiques et aussi d'aide de beaucoup d'amis, de collègues et de maitres soit en Iran, mon pays d'origine, soit en France, mon pays d'adoption.

Au terme de mon travail de recherche dans le cadre d'une collaboration scientifique franco-iranienne entre le laboratoire Géosciences de l'université Montpellier II et IIEES, un regard rétrospectif sur cette période passée m'apprend à quel point je suis redevable pour à toutes les gentillesses et tous les soutiens si nombreux autour de moi et qui méritent l'expression d'une reconnaissance pleine de respect et de modestie de ma part. Ma mémoire pourrait difficilement en faire une liste exhaustive, aussi je vous prie de pardonner mes oublis.

Dans un premier temps, je tiens à exprimer toute ma reconnaissance à l'IIEES, à mes amis et collègues en Iran qui m'ont laissé un souvenir agréable de plus d'une décade de recherche en leur compagnie. J'adresse également mes plus sincères remerciements à tous mes amis et collègues au laboratoire Géosciences Montpellier et à l'équipe TAG pour un accueil amical et marqué par la gentillesse et les sourires d'encouragement permanents. Ainsi, je présente mes meilleurs remerciements au service culturel de l'ambassade de France en Iran, à messieurs Duhamel et Blanchy et aussi à madame Mirbaha.

Je voudrais exprimer ma plus profonde reconnaissance à Hervé PHILIP, Jeff RITZ et Stéphane DOMINGUEZ mes bons amis, frères (mes familles françaises) et professeurs pour avoir assuré la direction de ce travail, ainsi que pour leur gentillesse envers ma famille et moi-même. Les nombreux conseils qu'ils m'ont promulgués m'ont permis d'avancer et d'apprendre. Je leur serais reconnaissant pour toujours. Et comment ne pas remercier ici leurs épouses, Samira, Guila et Cécile dont la présence a été une source permanente de confiance et de soutien pour moi et pour ma famille. Nous n'oublierons jamais leur gentillesse.

Je ne peux parler de ce travail de thèse sans adresser mes remerciements aux responsables de la faculté de sismologie (Mehdi Zaré) et de l'équipe sismotectonique d'IIEES (Khaled Hessami) que je préfère compter parmi mes amis parce que, ils m'ont toujours permis d'effectuer mon travail de recherche dans un environnement amical. Ainsi, je présente mes meilleurs remerciements à messieurs Mohammad Reza Abbassi (mon codirecteur iranien de la parti Mosha-Nord Téhéran de ma thèse), Khalil Feghhi, Esmail Shabanian, Hadi Tabassi et à mesdames Farbod et Mobayen de l'équipe sismotectonique et messieurs Mohssen Zolfaghari, Mossayeb Hadavi, Morteza Osati, M Rezai, Farzad Kushki, Iraj Zahedi, Mehdi Massudi, M Hosseini, Abass Tassbihi, M Aghai, Maissam Kushki, Hamid Nadjmizadeh, Hassan Handjani, Mohammad Chizari, Ebrahim Akbari qui m'ont gentiment accompagné en amis et camarades sans souci au bout de ce long chemin.

J'aimerais également présenter ici tous mes remerciements à mes amis dont la compagnie pendant cette courte période de séjour à Montpellier m'a facilité la vie loin de mon pays : Hamid Nazari, Hossein Lotfalizadeh, Modjtaba Hosseini Nassab, Mohsen Rahmani-Tabar, Yahya Djamour, Payam Kaboli, Ali Amini, Hamed Fazlikhani, Reza Khaledian ainsi qu'Hassan Rajabi et leurs familles.

Je remercie très vivement Brigitte Smith et son épous Marc Daignieres, que j'ai eu l'honneur de fréquenter avec ma famille, pour leur amitié très sincère.

Ce travail de recherche doit sans doute sa plus ample valeur à de nombreux amis et chercheurs qui ne m'ont pas privé de leurs idées et conseils. Ainsi, je remercie Denis Hatzfeld, Roger Bayer, Olivier Bellier, Damien Dhont, Serge Lallemand, Shannon Mahan, Sanda Balescu, M Lamothe, Maurice Brunel, Jean Chery, Samira Rabai et surtout Anne Delplanque et Mojgan Yazdani et certainement mes chers amis ; Fabien Graveleau, Hamid Nazari, Riccardo Vassalo, Vahan Davtyan, Florian Meresse, Reza Salamati, Magali Riza, Tomas Tounessie, Yaghoub Hatam, Bruno Sclabrino, Mohsen Sadeghzadeh, Pierre Sabatier, Thomas Jacob et Olivier Raynal. J'aimerais également présenter ici tous mes remerciements à mes amis au Laboratoire GM : Nathalie Mouly, Marie-France Roch, Bernadette Marie, José Atienza, Dominique Arnau, Erik Doerflinger, Yves Lagabrielle et Fabrice Grosbeau.

Et je remercie du fond de mon cœur mon père et ma mère qui ont patiemment abreuvé de leur jeunesse les fleurs de notre famille, ainsi que ma sœur Sanaz et mon frère Hessam qui ont accepté avec sourire et gentillesse notre absence. Je remercie également ma belle famille pour leur soutient indéfectible.

Enfin, je suis reconnaissant envers mon épouse Mahshid qui a consacré sans hésitation sa vie et ses passions pour défendre mes idées et projets pour que je puisse avancer. Je remercie du fond de cœur mes fils Kourosh et Afshin qui a dû supporter mon absence durant mes longues missions répétées. Même si j'en ai beaucoup souffert moi-même, j'espère qu'ils ne m'en tiendront pas rigueur. J'espère également qu'ils garderont un bon souvenir de cette expérience.

C'est ainsi que je dédie ce mémoire de thèse, qui représente un effort sincère pour l'avancée, même infime, des sciences de la terre et pour l'image de mon pays Iran, à ces trois êtres chers.

Avant-propos

L'Iran est un pays qui est situé entre les latitudes 25°- 40° N et longitudes 44°- 64° E au Moyen-Orient sur une superficie de 1 648 195 km^2. Le pays dispose en outre de deux façades maritimes, sur la Mer Caspienne au nord, et sur le Golfe Persique et le Golfe d'Oman, au sud. L'Iran est l'un des pays les plus montagneux du monde. Une grande partie du territoire iranien est occupée par un haut plateau central d'une altitude moyenne de 1300 m, bordée par des chaînes de hautes montagnes. A cause du climat semi-aride du plateau iranien et donc le problème de ressource en eau, la répartition de la population (65,9 millions estimée en 2008) est très inégale. La grande majorité de la population se concentre en effet au pied des chaînes de montagnes surtout au nord et à l'ouest du pays. La majorité de ces chaînes de montagnes sont limitées par des failles actives. Les séismes liés à ces failles actives sont bien documentés dans les catalogues de la sismicité.

Basés sur les catalogues de la sismicité historique, plus de 450 grands séismes sont rapportés en Iran depuis 600 ans avant J. C.. De fait, le risque sismique fait partie intégrante du quotidien des iraniens, et ce depuis toujours. Dans le but d'étudier ce risque sismique, un projet collaboration franco-iranien entre le laboratoire Géosciences Montpellier de l'université Montpellier 2 (UM2) et l'International Institute of Earthquake Engineering and Seismology (IIEES) a été mis en place. L'objectif de ce projet est l'évaluation de l'aléa sismique dans le NW de l'Iran. C'est dans ce cadre que j'ai réalisé cette thèse de doctorat

L'Iran se situe dans la partie centrale de la ceinture sismique « Alpes-Himalayenne » qui s'étend sur 10000 kilomètres de l'Europe occidentale à l'Asie orientale. Sur le plateau iranien, cette ceinture sismique se sépare en deux chaînes de montagnes, le Zagros vers le sud et l'Alborz vers le nord. La zone de jonction de ces chaînes de montagnes est située au nord-ouest de l'Iran. La déformation actuelle et la sismicité historique qui sont liées à cette zone, combinée à la forte densité de population et aux nombreux centres économiques font de cette région l'une des plus menacée du point de vue du risque sismique.

Le travail présenté dans cette thèse est une contribution à l'estimation de l'alea sismique (localisation et caractérisation des sources sismiques) pour les villes de Téhéran, Tabriz et Zandjan. Les approches mises en œuvre sont l'analyse morphotectonique et la paléosismologie. Le mémoire de thèse contient 5 chapitres: le premier chapitre présente le contexte géodynamique général de l'Iran en détaillant la région nord-ouest. Les chapitres 2, 3 et 4 présentent les résultats des études morphotectonique et paléosismologique sur les failles de Mosha et de Nord Téhéran (chapitre 2), le segment SE de la faille Nord Tabriz (chapitre 3) et le système de failles de Zandjan (chapitre 4). Le chapitre 5 synthétise les principaux résultats de cette étude et conclue sur la géodynamique du nord-ouest de l'Iran.

Dans le but de valoriser et de communiquer au mieux les résultats de ce travail, nous avons choisi de présenter les résultats de cette étude sous la forme d'articles en anglais qui seront soumis à des journaux internationaux à comités de lecture. Chaque article reprend la problématique propre à chaque région étudiée (Téhéran, Tabriz et Zandjan) en détaillant le contexte tectonique de la région concernée.

TABLE DES MATIERES

CHAPITRE 1

INTRODUCTION GENERALE

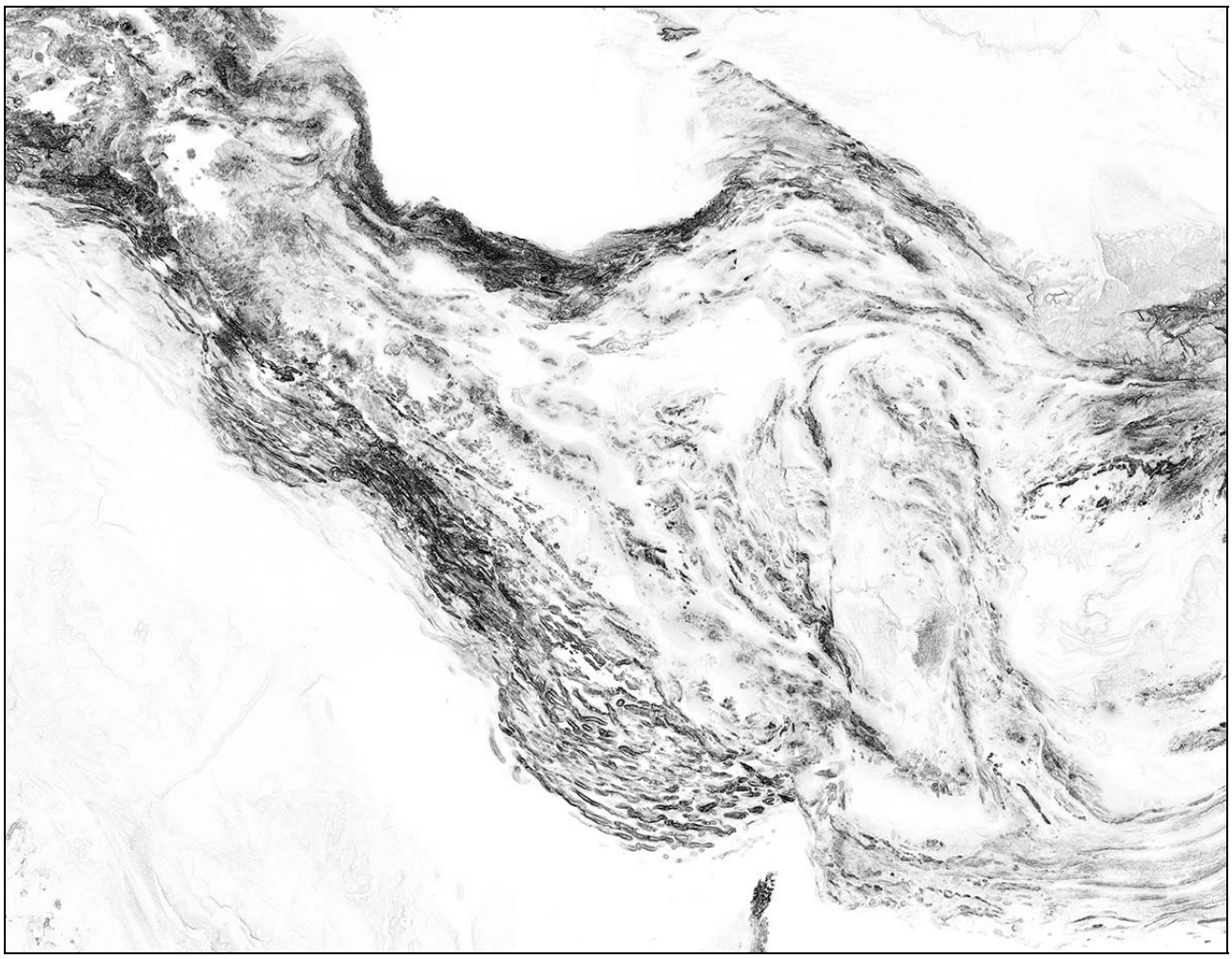

Carte du gradient topographique de l'Iran. L'Iran contient deux chaînes de montagnes majeures, le Zagros (dans la partie SW) et l'Alborz (dans la partie N). Ces chaînes de montagne encadrent un grand plateau (plateau d'Iran Central).

A- Contexte géographique et géodynamique de l'Iran

1- Géographie et Climat

L'Iran est un pays montagneux du Moyen-Orient situé entre la plaque Arabie au sud et la plate-forme de Turan, considérée comme faisant partie de l'Eurasie stable, au nord. Il s'étend sur 1648 195 km² et possède une population de près de 70 millions d'habitants (source : Wikipedia). Au nord, il possède des frontières communes avec l'Arménie (35 km), l'Azerbaïdjan (611 km) et le Turkménistan (992 km), et a 740 km de côtes sur la mer Caspienne. Les frontières occidentales sont partagées avec la Turquie au nord-ouest et l'Irak au sud-ouest, finissant au Chatt-el-Arab (en persan : Arvand Rud). Le paysage iranien est dominé par plusieurs chaînes de montagnes qui séparent divers bassins et plateaux les uns des autres. La partie occidentale, la plus peuplée, est la plus montagneuse, avec des chaînes comme le Zagros et l'Alborz (Elbourz) ; c'est dans cette dernière que se trouve le sommet le plus haut de l'Iran, le volcan Damavand qui culmine à 5671 m. L'Iran est l'un des pays les plus montagneux du monde. Une grande partie du territoire iranien est occupée par un haut plateau central d'une altitude moyenne de 1300m, bordée par des chaînes de hautes montagnes. Le plateau iranien est la zone située entre les chaînes de montagnes localisées à l'est et à l'ouest du pays. La moitié orientale consiste essentiellement en une série de bassins désertiques inhabités (comme le désert Kavir) parsemés de rares lacs salés.

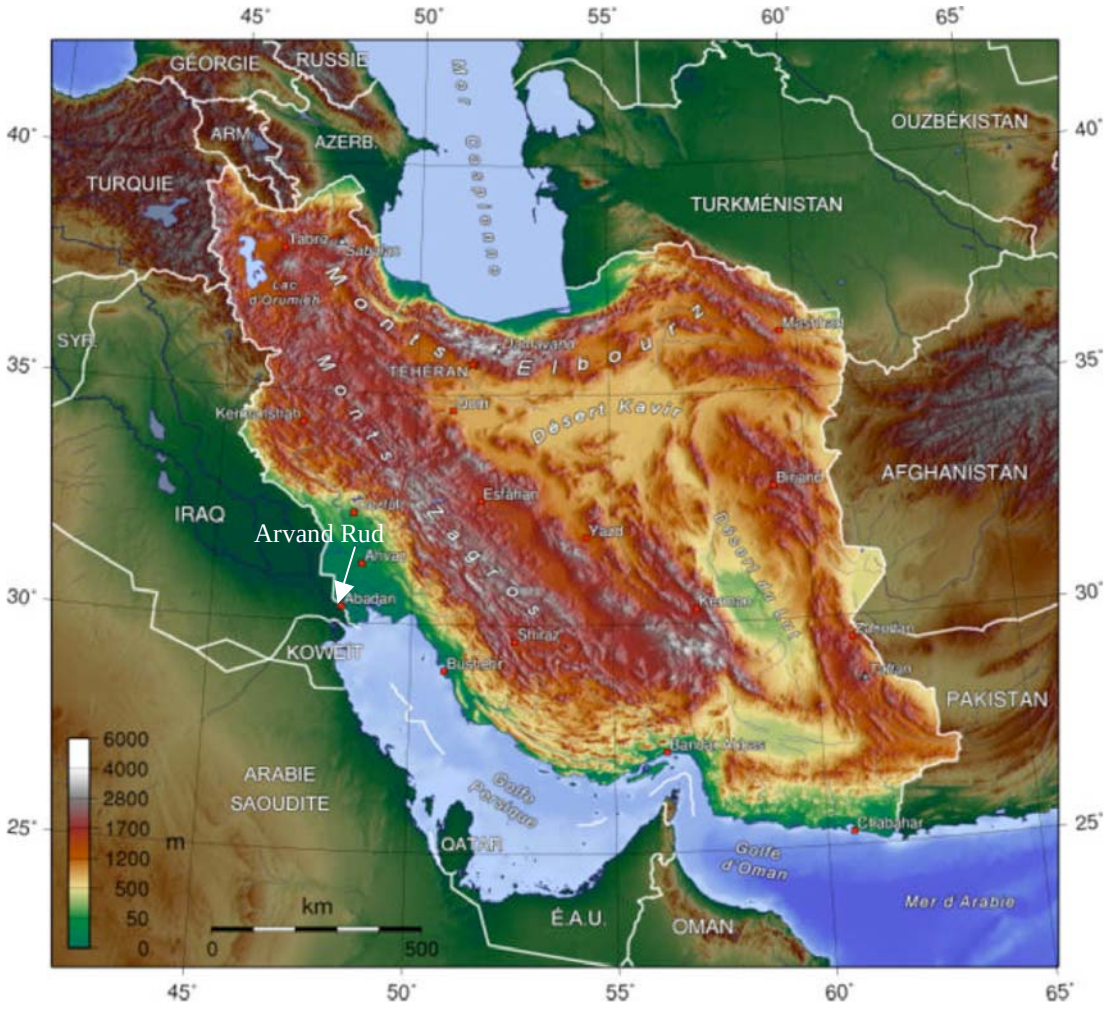

Figure 1- Carte géographique générale de l'Iran et sa situation géographique par rapport aux pays voisins.

Le climat de l'Iran est principalement aride ou semi-aride. La plaine côtière de la mer Caspienne fait exception avec un climat subtropical : les températures y tombent rarement en dessous de 0°C en hiver et le climat reste humide toute l'année. Les températures estivales montent rarement au

dessus de 29 °C, et les précipitations annuelles sont de 680 mm à l'est et de 1700 mm à l'ouest. Dans l'ouest du pays, les régions habitées dans les vallées des monts Zagros connaissent des températures moins clémentes, des températures moyennes en dessous de 0°C et de fortes chutes de neige. Les bassins orientaux et centraux sont très arides, avec moins de 200 mm de précipitations annuelles et des températures estivales dépassant les 38°C. Les plaines côtières du golfe Persique ont des hivers tempérés, et des étés très chauds et très humides. Les précipitations y varient entre 135 et 355 mm (source Wikipedia).

A: B:

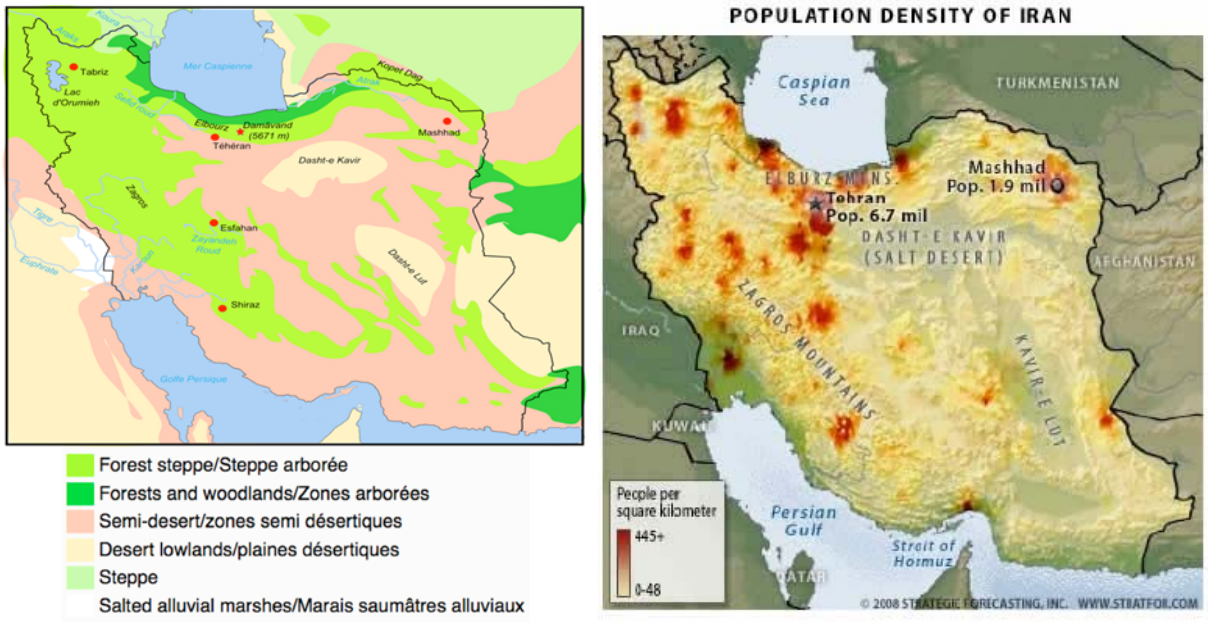

Figure 2- Cartes de la végétation (A) et de la densité de la population en IRAN (B) (Strategic forecasting, INC, 2008).

2- Géologie et contexte géodynamique

D'un point de vue tectonique, l'Iran est une zone de collision intracontinentale active appartenant à de la ceinture orogénique Alpes-Himalayenne qui s'étend sur près de 10000 km depuis l'Ouest de l'Europe jusque dans le Sud-Est de l'Asie. Les deux autres parties de cette ceinture sont liées à la collision Afrique-Europe (10 mm/an, Cisternas et Philip, 1997) à l'ouest et à la collision Inde-Asie (35 mm/an) à l'est.

L'Iran peut être divisé en plusieurs unités géologiques principales ; une unité sud, correspondant à la plaque arabique et comprenant la chaîne du Zagros, une unité centrale, correspondant à un assemblage de micro blocs qui se sont accrétés à la marge sud de l'Eurasie. Cette unité comprend en particulier la zone métamorphique de Sanandaj-Sirjan au nord du Zagros, les blocs de l'Iran Central et du Lut à l'est et la chaîne de l'Alborz et une unité nord, correspondant à la marge sud du continent Eurasiatique, comprenant la chaîne du Kopet Dagh et la plate-forme de Turan au Turkménistan.

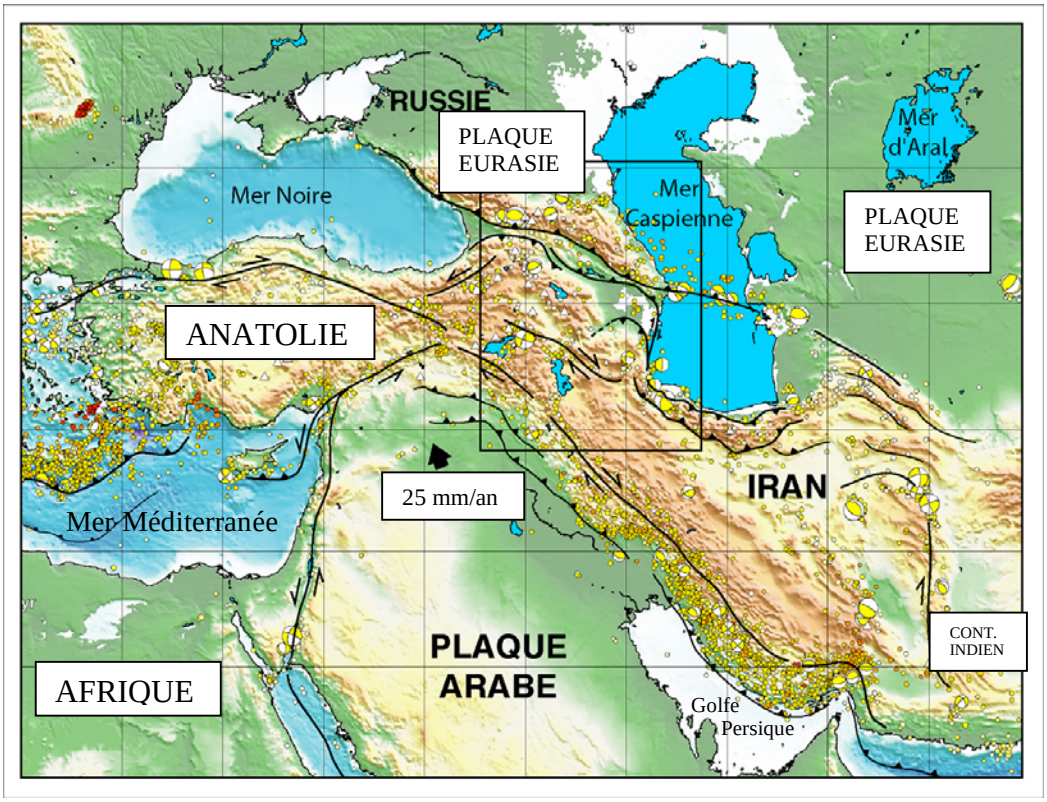

Figure 3- Contexte géodynamique général de l'Iran dans le territoire Moyen-Orient, la localisation du domaine NW Iran et la distribution de la déformation sismique (les cercles jaunes) dans ce territoire.

La structure géologique de l'Iran et son évolution au cours du temps ne se comprennent bien que si l'on examine le pays dans son cadre général. Les chaînes montagneuses qui occupent la majeure partie du territoire appartiennent à un ensemble s'étendant de la Turquie à l'Afghanistan et au Pakistan. Cet ensemble est pris en tenaille entre les grandes masses continentales suivantes (« plaques » au sens large du terme) : au nord, l'Eurasie (Caucase et plaine du Touran) ; au sud-ouest, l'Arabie ; au sud-est, le continent indien (Figure 3). Au sud, un hiatus entre les blocs de l'Arabie et de l'Inde est représenté par la mer d'Oman et l'Océan Indien. Toute l'évolution géologique de l'Iran est commandée par les mouvements relatifs de ces plaques : convergence Arabie-Eurasie (22-25 mm/an, Nilforoushan et al. 2003 ; Vernant et al., 2004), qui est à l'origine des chaînes des parties sud-ouest (Zagros) et nord (Alborz) ; convergence Inde-Eurasie, dont le poinçonnement au niveau du Pamir induit, par l'intermédiaire des montagnes d'Afghanistan et du Pakistan, les chaînes orientales de direction nord-sud (Sistan), les rotation de blocs (bloc du Lut) et, indirectement, l'arc du Makran-Baloutchistan, face à la mer d'Oman.

Le territoire iranien épouse assez bien les formes des principales unités géologiques. La partie nord est représentée par la chaîne de l'Alborz et son appendice oriental, le Kopet Dagh. En dépit de ses sinuosités, cette chaîne est globalement de direction est-ouest (son point culminant en est le Damavand à 5671 m). Sur son versant Nord s'étend la dépression Caspienne et la plaine de Touran, au sud, la grande dépression intramontagneuse désertique du Dasht-e Kavir. Toutes les parties ouest et sud-ouest sont occupés par un ensemble montagneux de direction NW-SE, de plus de 1500 km de longueur, allant de la Turquie orientale jusqu'au niveau du détroit d'Hormoz. Cette chaîne appelée globalement Zagros, s'élèvent jusqu'à 4550 m au Zard-Kuh. Comme toutes les chaînes orogéniques, elle est bordée par une dépression frontale, localisée ici au sud-ouest: la plaine de Mésopotamie et le golfe Persique. Elle est limitée au nord-est par un grand alignement volcanique qui va du Sahand, au NW, jusqu'au Bazman, au SE (l'arc magmatique Urumieh-Dokhtar).

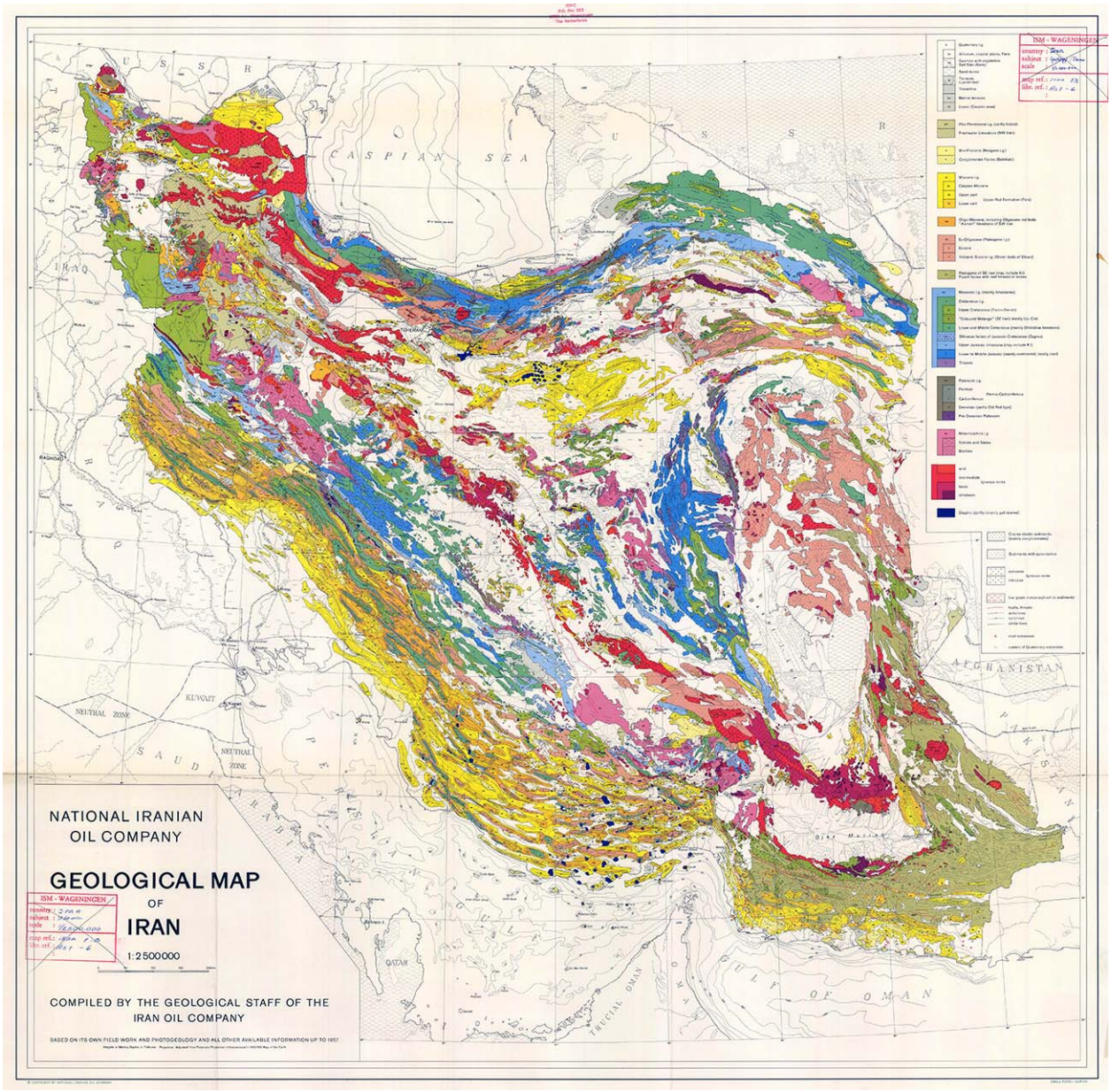

Figure 4- Carte Géologique de l'Iran (National Iranian Oil Company, NIOC, 1957). Globalement, la distribution des formations géologiques ont contrôlé par les basins et… . formés par les activités des structures majeures comme des failles et des plis.

Accolé à l'Alborz au niveau de l'Azerbaïdjan, l'ensemble montagneux du Zagros s'en écarte en direction du sud-est, laissant place à la dépression du Dasht-e Kavir et aux blocs de l'Iran Central et du Lut. Alavi (1994) a distingué plusieurs domaines tectono-métamorphiques dans la zone de collision Arabie-Eurasie (Figure 5). En allant du NW vers le SE, on rencontre :

1- L'arc magmatique d'Urumieh-Dokhtar, caractérisé par des roches intrusives et extrusives calc-alkalines d'âge Eocène à Quaternaire. Son origine est liée à la subduction de la plaque Arabie sous l'Eurasie (e.g. Berberian, 1981; Forster et al., 1982).

2- La ceinture métamorphique de Sanandaj-Sirjan

3- Le prisme d'accrétion du Zagros

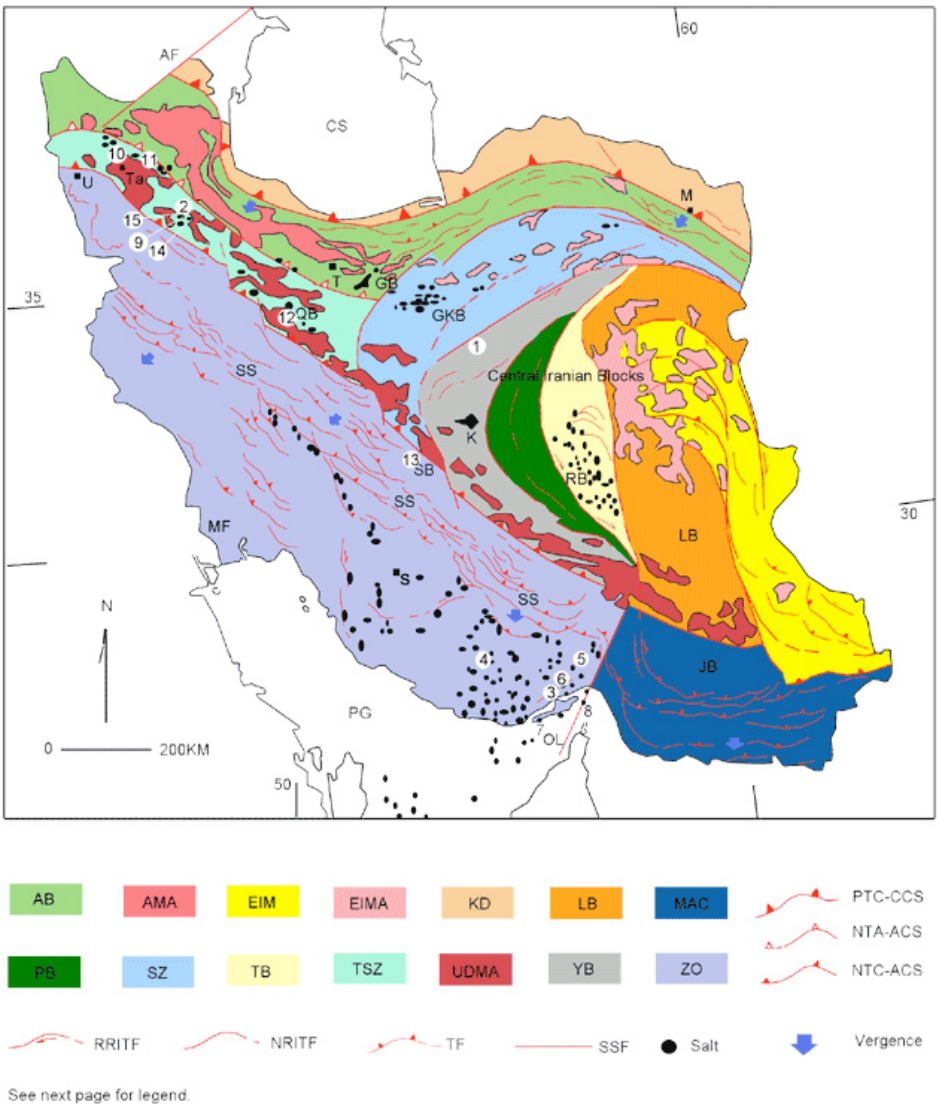

Figure 5- Carte tectonique générale de l'Iran (Alavi, 1991). AB: chaîne de l'Alborz. AF: faille d'Aras. AMA: Ensemble magmatique de l'Alborz. CS: Mer Caspienne. EIB: chaînes de l'Iran oriental. EIMA: Ensemble magmatique de l'Iran oriental. GB: basin de Garmsar. JB: basin de Jazmurian. K: Kalut. KD: Kopet Dagh. LB: bloc du Lut. M: Mashhad. MAC: Complexe d'accrétion du Makran. MF: basin d'avant-pays Mésopotamien. NTA-ACS: Neo-Tethyan arc-arc collision suture. NTC-ACS: Neo-Tethyan continent-arc collision suture. NRITF: Non-rotational related intracontinental transfer fault. OL: Oman Line. PBB: bloc du Posht-Badam. PG: Persian Gulf foreland basin. PTC-CCS: Paleo-Tethyan continent-continent collision suture. QB: Bassin de Qum. RB: Bassin de Ravar. RRITF: rotational related intracontinental transfer fault. S: Shiraz. SB: Bassin de Sirjan. SS: Zone Sanandaj-Sirjan. SSF: faille décrochante. SZ: Zone de Sabzevar. T: Téhéran. Ta: Tabriz. TB: Bloc de Tabas. TF: faille inverse. TSZ: zone de Tabriz-Saveh. U: Urumieh. UDMA: Ensemble magmatique Urumieh-Dokhtar. YB: Bloc de Yazd. ZO: Zagros orogen. 1-Kour. 2-Iljaq. 3-Pol. 4-Karmohstaj. 5-Syahoo. 6-Anguran. 7-Qeshm. 8-Larak. 9-Mianaj. 10-Chupanloo. 11-Nahand. 12-Qum. 13-Varzaneh. 14-Ghareh-Gol. 15-Ghareh-Aghaj.

La partie sud-est du pays, plus complexe, est formée de chaînes qui moulent le bloc du Lut : l'arc du Makran, de direction est-ouest bordant le golfe d'Oman; les chaînes du Baloutchistan et du Sistan, de direction nord-sud longeant les frontières de l'Afghanistan et du Pakistan.

Au cœur de ce dispositif de géométrie triangulaire s'étalent des massifs montagneux (de directions N-S, dans la région de Kerman, et NW-SE dans la région de Birdjand enfermant la dépression désertique du Lut. Ces ensembles (Iran Central et Lut) peuvent être considérés comme des « blocs médians » par rapport aux chaînes qui les encadrent.

Comme la proposée Stöcklin (1968; 1977), auteur de plusieurs synthèses sur la géologie de l'Iran, l'analyse géologique doit s'appuyer essentiellement sur les caractéristiques majeures des unités rencontrées (quelle que soit l'importance de leur extension géographique), à savoir :

-la nature et l'âge du soubassement crustal (d'origine continentale ou océanique) ;
-les conditions paléogéographiques de dépôt des sédiments de couverture ;
-la géodynamique (présence et nature d'un volcanisme), l'âge et le style des déformations.

Comme toutes les chaînes du Moyen-Orient, celles de l'Iran sont exemplaires du fait de la présence, en leur sein, de zone à ophiolites, ensembles de roches particulièrement intéressantes car elles représentent d'anciennes croûtes océaniques (océans, mer marginales ou rifts). Bien entendu, ces domaines océaniques ont été refermés par les rapprochements des continents adjacents (par exemple, Arabie-Eurasie), et ils apparaissent comme des cicatrices, encore appelées sutures. Malgré leur étroitesse relative, ces sutures sont du plus grand intérêt pour retracer l'histoire géologique de ces régions.

La péninsule arabique, qui s'avance jusqu'au golfe Persique, est constituée par un socle complexe de terrains cristallins précambriens. La couverture sédimentaire débute à l'Infracambrien avec des niveaux d'évaporites (sel) et se poursuit sans perturbation tectonique jusqu'à la période actuelle ; les sédiments, restés sub-horizontaux, y sont épicontinentaux, entrecoupés de lacunes (les mêmes caractéristiques ou presque se retrouvent dans le Zagros externe).

De fait, l'Iran est un exemple majeur de collision continentale juvénile active dans laquelle les structures héritées, ainsi que les probables hétérogénéités de la lithosphère, exercent un contrôle majeur sur la localisation et le style des déformations.

3- Cinématique des déformations actuelles

La cinématique de la convergence entre l'Arabie et l'Eurasie est bien contrainte par l'analyse des anomalies magnétiques en mer et le champ de déplacement GPS (Figures 6 et 7). A la longitude du Détroit d'Hormuz, la vitesse de convergence des plaques Eurasie au nord et Arabie au sud est d'environ 3 cm/an. Dues au mouvement de rotation anti-horaire de l'Arabie, l'orientation et la vitesse de convergence Arabie-Eurasie varient d'ouest en est.

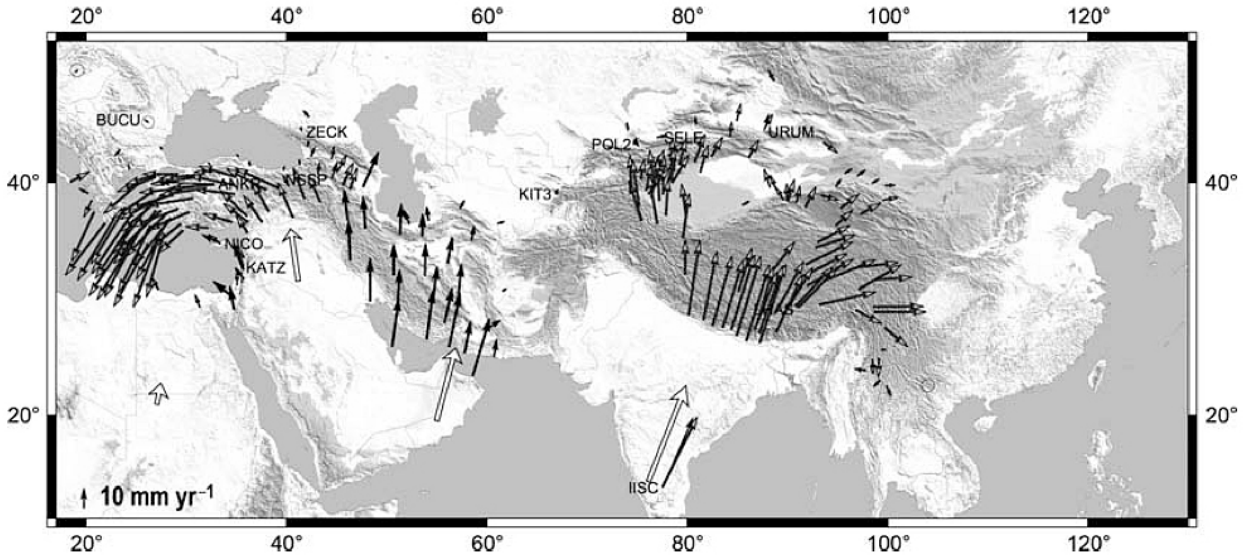

Figure 6- Vitesses GPS horizontales (Référence Eurasie fixe) le long de la ceinture orogénique Alpine-Himalayenne (dans Vernant et al. 2004 et d'après Mc Clusky et al., 2000 et Wang et al., 2001). Les vecteurs en blanc correspondent aux vitesses calculées à partir du modèle NUVEL-1A.

La chaîne de collision du Zagros s'étend sur plus de 200 km selon une direction NO-SE depuis la Faille Est Anatolienne dans l'est de la Turquie, jusqu'à la zone de faille de Minab-Zendan, au nord du détroit d'Hormuz. A l'est de ce détroit, le continent Arabie laisse place à un domaine océanique (le Golfe d'Oman) qui subducte vers le nord sous le prisme d'accrétion émergé du Makran. Ce dernier, d'orientation E-O, s'étend sur 100 km, depuis la faille de Minab-Zendan jusqu'au système de failles d'Ornach-Nal et Chaman.

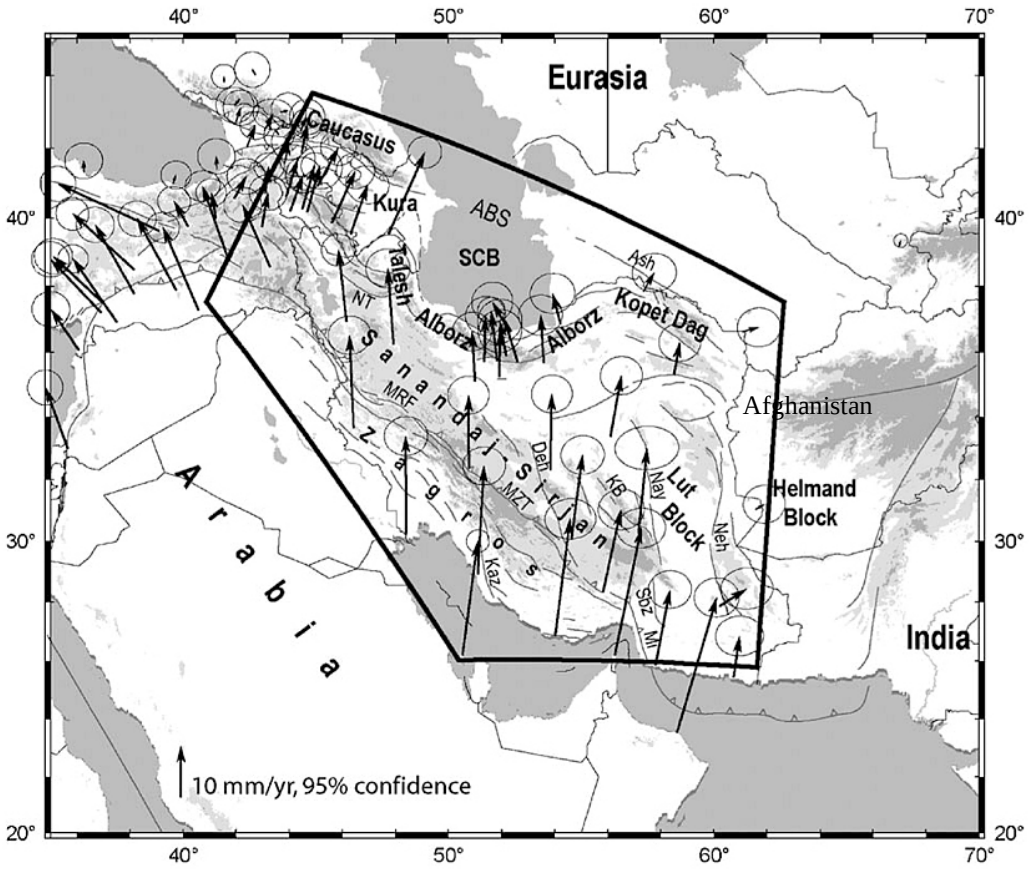

Figure 7- Champ de vitesse GPS horizontal en Iran en fixant comme référentiel l'Eurasie (Vernant et al. 2006). Compilation réalisée à partir des travaux de McClusky et al, (2000), Vernant et al., (2004a; 2004b).

Le raccourcissement intracontinental se concentre dans le Zagros au sud et dans les chaînes du Caucase, de l'Alborz et du Kopet Dag au nord. Les zones majeures de décrochement séparent les différents blocs tels que l'Iran Central, le Lut ou la partie méridionale (à lithosphère océanique) de la Mer Caspienne (Berberian, 1983).

4- Sismicité historique et instrumentale

La sismicité iranienne se concentre principalement sur les zones de contact que constituent le Makran au sud, le Zagros au sud-ouest, le Talesh, l'Alborz central et le Kopet Dagh au Nord. On note également une sismicité le long des grandes failles NNW-SSE à mouvement dextre en Iran central. La distribution des séismes met clairement en évidence l'existence de ces blocs, dont les limites sont souvent jalonnées d'ophiolites, témoins des processus d'accrétion anciens. Enfin, les données paléomagnétiques suggèrent que la convergence entre l'Arabie et l'Eurasie a également été accompagnée par des rotations importantes de certains des blocs lithosphériques de l'Iran Central. (Figure 8).

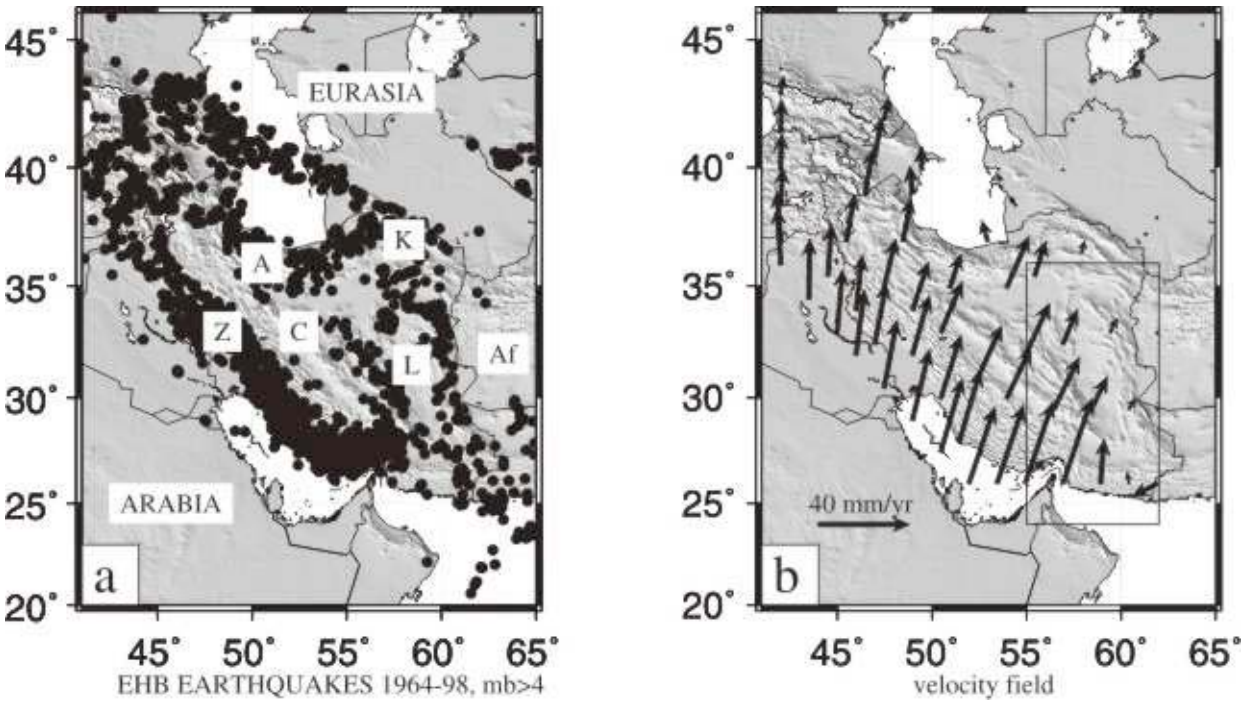

Figure 8- Sismicité générale de l'Iran (Catalogue Engdahl, 1998 – Période couverte 1964-1998) et champ de vitesse déduit des variations des taux de contraintes issus des séismes (Jackson et al. 1995). Globalement, la sismicité dans le domaine de l'Iran est concentrée sur les zones actives de: Z; Zagros, A; Alborz, C; les frontières de l'Iran Centrale, K; Kopeh-Dagh, L; Lut et de Af; Afghanistan.

D'après les catalogues de sismicité historique, plus de 450 séismes destructeurs ont été répertoriés en Iran depuis 600 avant Jésus-Christ (Ambraseys et Melville, 1982; Berberian et Yeats 1999; 2001). Au cours du dernier siècle, de forts séismes (M> 6.5) sont produits, avec une fréquence moyenne de 5-6 ans (e.g. Silakhor Ms=7.4, 1909, Salmas Ms=7.4, 1930, Torud Ms=6.5, 1953, Lar Ms=6.7, 1960, Buin Zahra Ms=7.2, 1962, Dasht-e-Bayaz Ms=7.4, 1968, QIR Ms=6.9, 1972, Khorgu Ms=7.0, 1977, Tabas Ms=7.7, 1978, Qayen Ms=7.1, 1979, Rudbar-Manjil Ms=7.3, 1990, Sefidabeh Ms=6.1, 1994, Ardebil Ms=6.1, 1997, Birjand Ms=7.3, 1997, Fandog Ms=6.6, 1998).

La distribution de la sismicité instrumentale est cohérente en général avec la carte des séismes historiques et montre que les régions du Zagros, Alborz, Kopet Dagh, et les bordures du Lut sont les plus actives (Figure 9). Néanmoins, il est intéressant à noter la forte sismicité historique dans le NW en comparaison avec le sud et le sud-ouest, et une distribution contraire en ce qui concerne la sismicité instrumentale. De fait, depuis 1900 AD, les grandes villes iraniennes, comme Téhéran ou Tabriz qui ont été détruites par de grands séismes historiques, ne montrent qu'une faible sismicité instrumentale. Cet état de fait place ces grandes villes dans une situation « critique » car elles ont grandies très rapidement (population, superficie, économie) au cours du dernier siècle sans connaitre de séismes, et du coup sans que l'aléa sismique - pourtant estimé par les instances compétentes iraniennes (Figure 10) - soit pris en compte au niveau sociétal.

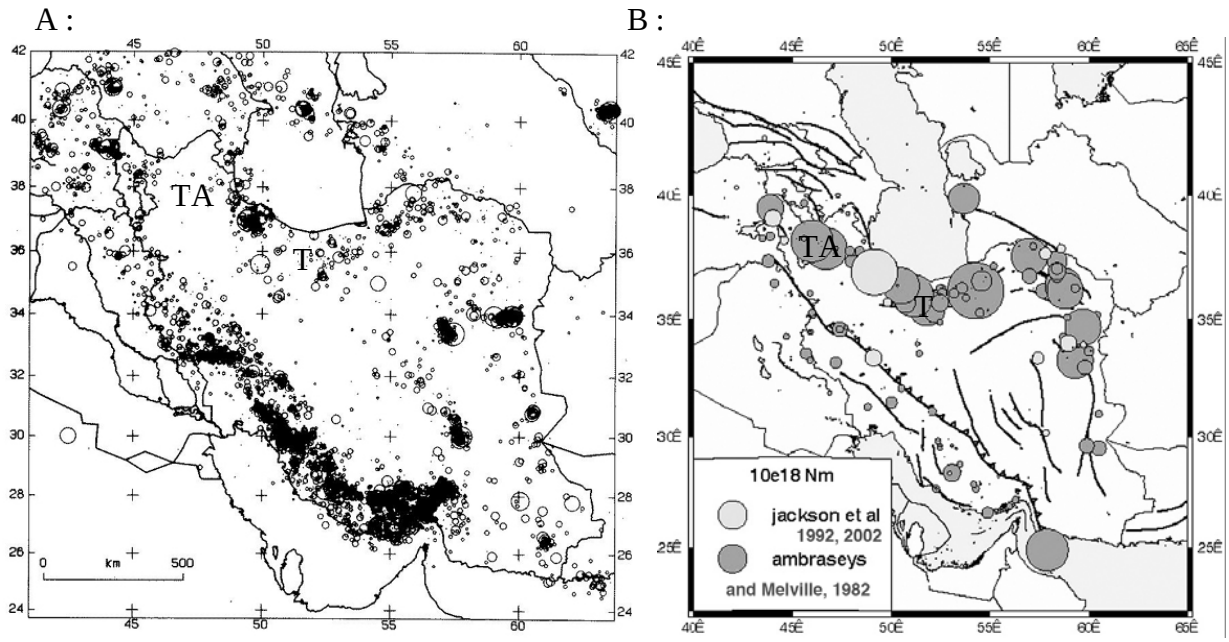

Figure 9- Cartes de la sismicité récente (IIEES ; 1965-2007) (A) et historique (Hatzfeld, 2005) (B) de l'Iran. T; la ville de Téhéran, TA; la ville de Tabriz.

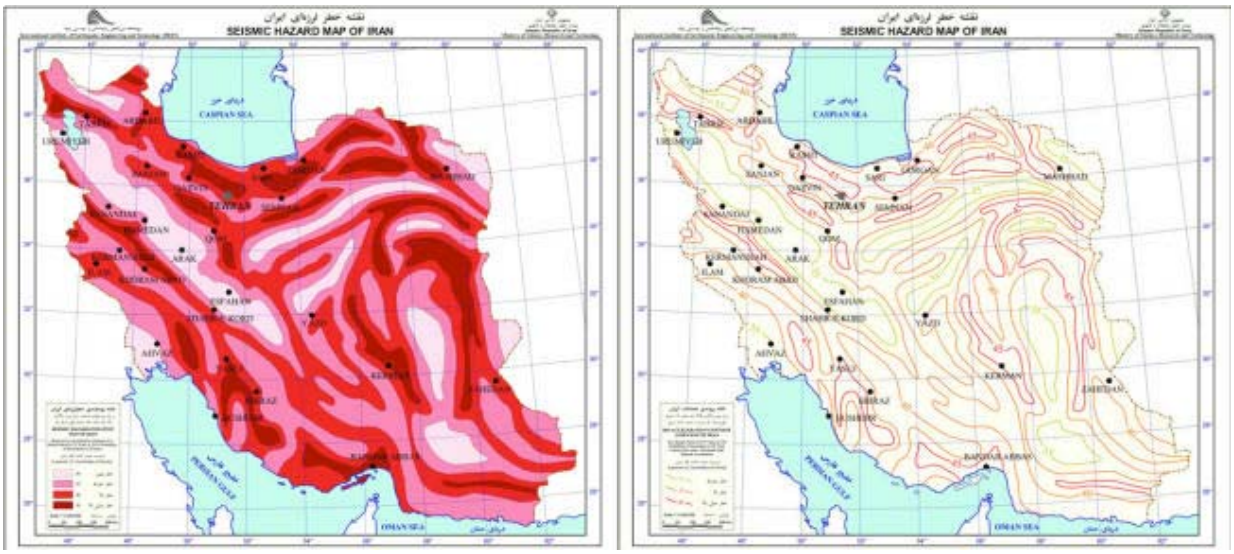

Figure 10- Cartes de l'aléa et du risque sismique en Iran (IIEES, Tavakoli et al., 2000). Une majorité de villes iraniennes sont situées dans des zones actives (en rouges).

5- Tectonique et failles actives

D'une façon générale, l'analyse de la sismicité instrumentale en Iran montre que la profondeur des séismes est comprise entre 0 et 30 km, avec des magnitudes M >6.5. Du point de vue des mécanismes, la plupart des foyers sismiques correspondent à des ruptures en failles inverses ou décrochantes (Figure 11).

Ces deux types de mécanismes caractérisent par exemple la déformation actuelle dans le Zagros, avec des failles orientées NW-SE correspondant à du chevauchement et du décrochement dextre. A noter qu'en ce qui concerne les chevauchements, ils sont aveugles dans le Zagros, alors qu'ils atteignent la surface dans la plupart des cas dans le reste du pays. Ces deux types de mécanismes caractérisent également la déformation actuelle dans la partie orientale, dans la partie centrale et dans le nord et nord-est de l'Iran.

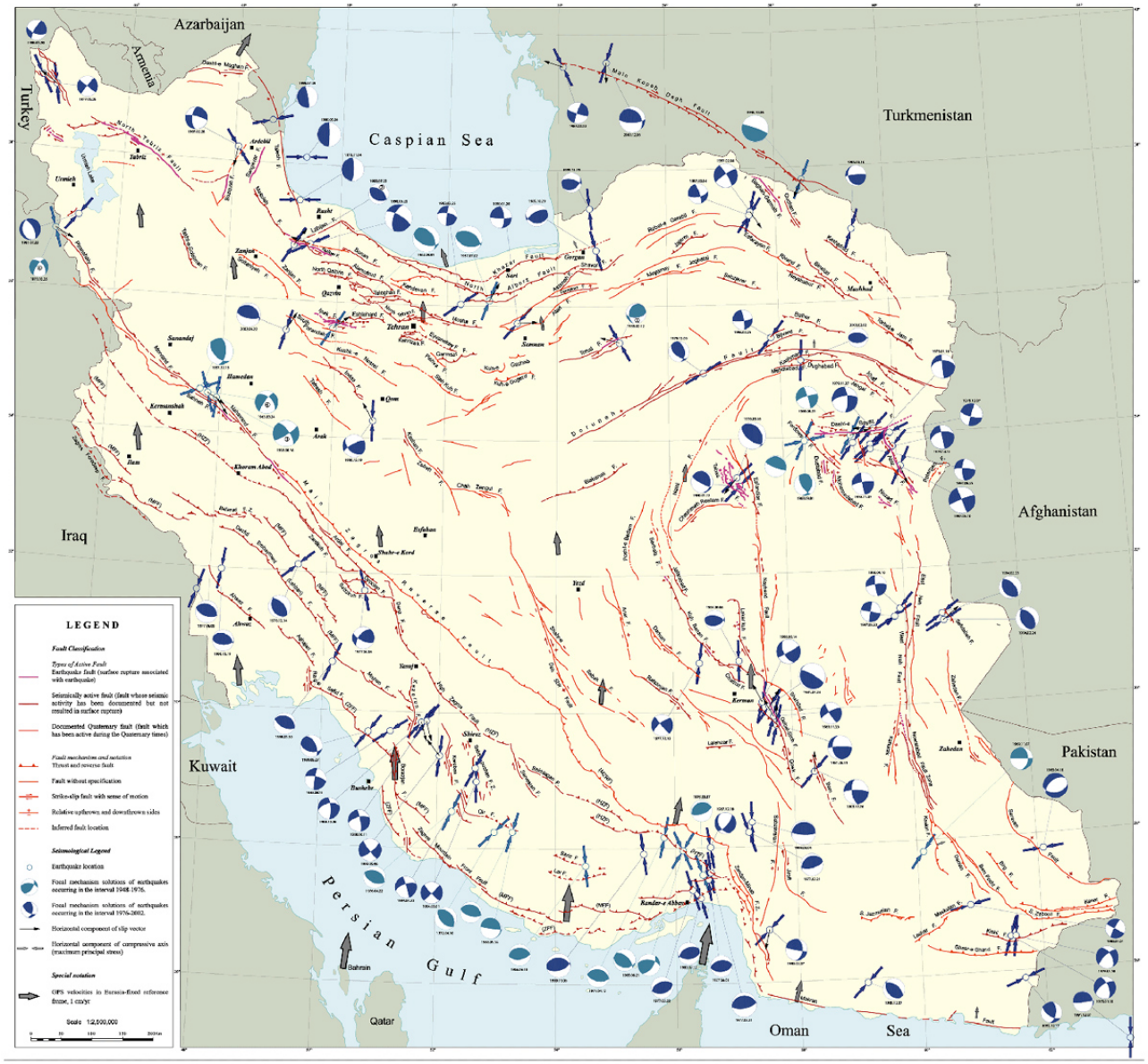

Figure 11- Carte sismo-tectonique de l'Iran (Hessami et al., 2003). Mécanismes aux foyers (Harvard CMT pour la période de1976 à 2002 et d'après Chandra, 1984, Shirokova, 1976, Jackson et McKenzie, 1984 pour la période de 1948 à 1976). Globalement, on peut trouver deux types de mécanismes principaux accommodant la convergence Arabie-Eurasie : I) du raccourcissement intracontinental qui se manifeste sous la forme de chaînes de montagnes, et II) des grands décrochements lithosphériques.

B- Contexte géographique et géodynamique du NW de l'Iran

1- Topographie

Le NW de l'Iran est compris entre les longitudes 45°E et 53°E et les latitudes 35°N et 40°N. Cette région située entre l'Iran et le Caucase correspond au domaine de jonction entre les chaînes du Zagros, du Caucase et de l'Alborz. Ces chaînes de montagnes sont limitées par des failles majeures actives. La partie la plus au NW de ce domaine est une partie du plateau turc-iranien d'une altitude moyenne de 2000m. Les montagnes les plus hautes correspondent à des volcans Néogène à Quaternaire (Damavand 5671 m, Sabalan 4820 m et Sahand 3695 m) et constituent trois points topographiques remarquables (Figure 12). A l'inverse, les lacs de cette région, comme le Lac d'Urumieh, correspondent à des dépressions tectoniques associées au fonctionnement des grandes zones de failles, comme le système de faille de Tabriz. Notons, que l'analyse paléogéographique des dépôts dans ces dépressions montre que celles-ci étaient beaucoup plus larges au Mio-Pliocène.

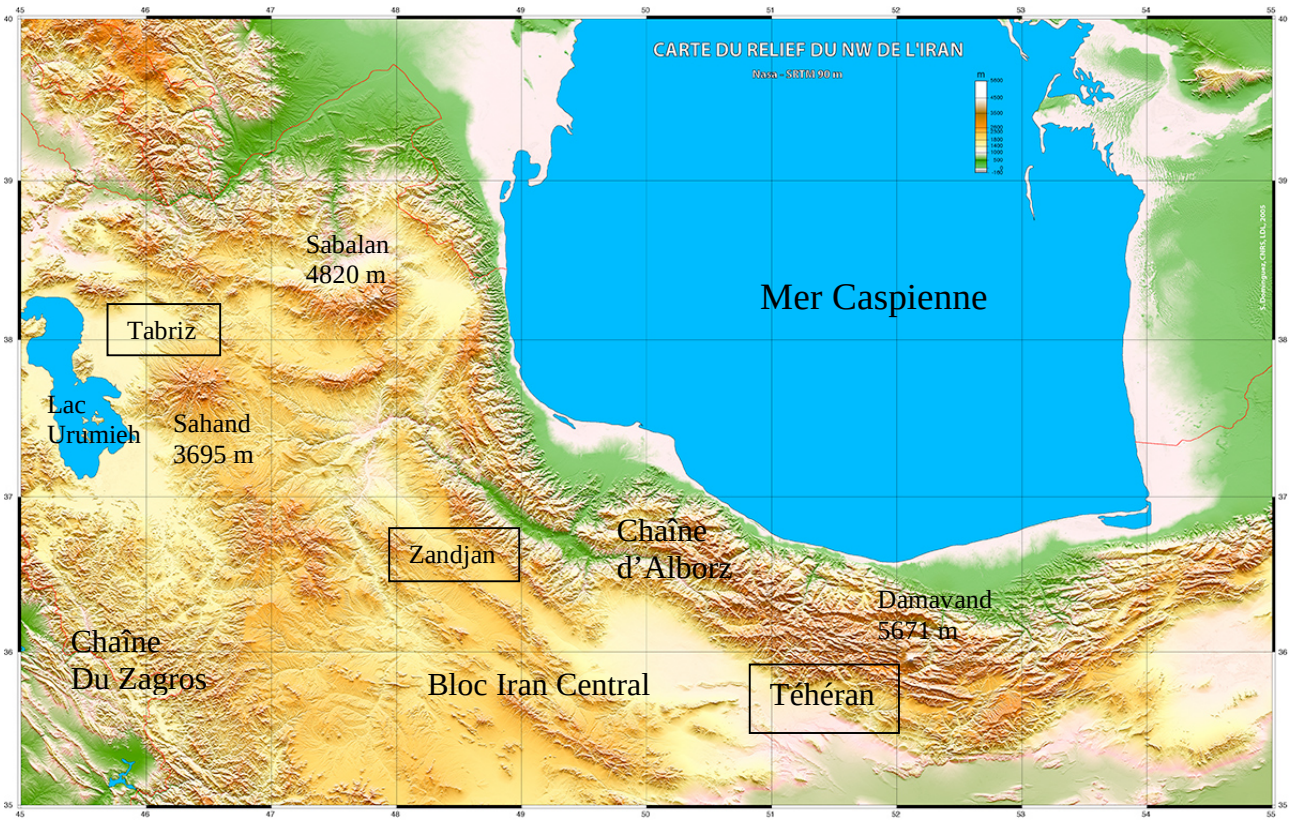

Figure 12- Carte topographique du NW de l'Iran (MNT SRTM V3, NASA). Le nord-ouest de l'Iran est une région montagneuse, bordée par le bloc Iran Central (vers le sud). Les chaînes montrent les domaines déformables autour de blocs plus rigides que sont l'Iran central et le basin sud Caspien. Les failles parallèles aux chaînes contrôlent la morphologie de celles-ci.

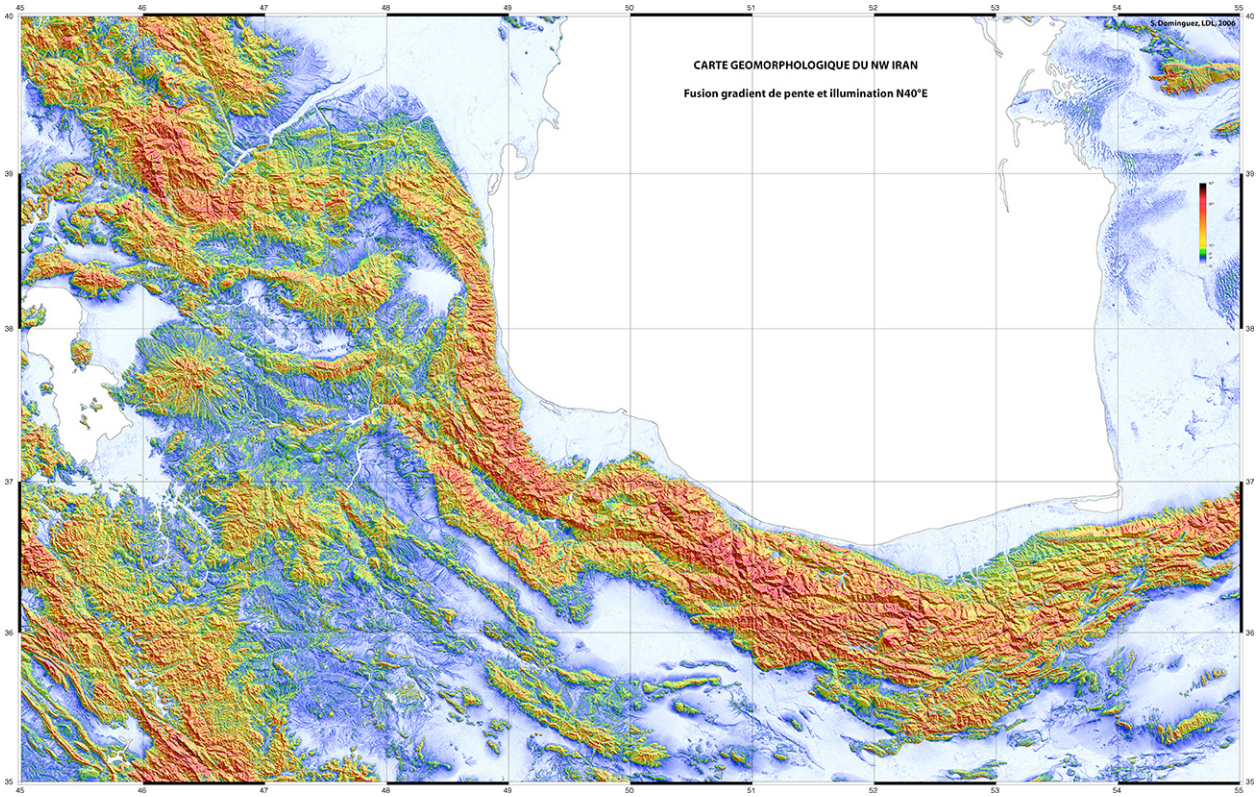

Figure 13- Carte morphométrique combinant les gradients topographiques en couleur et le MNT ombré. Les surfaces planes apparaissent en bleu et blanc tandis que régions plus escarpées apparaissent en jaune et rouge. Cette carte permet de mettre en évidence les principales caractéristiques morphologiques (dépressions, directions structurales, zones de forte incision, zones de plateau peu déformées) du NW de l'Iran. Les forts gradients de pente soulignent le tracé des failles majeures.

2- Géologie

La situation géologique actuelle du NW de l'Iran est le résultat d'une histoire complexe. Pendant le Précambrien, plusieurs massifs et plateaux magmatiques se forment dans ce territoire (Eftekharnezhad, 1975). Les couches du Paléozoique inférieur comporte une lacune sédimentaire remarquable attestant de mouvements calédoniens (Nabavi, 1976). D'après Eftekharnezhad (1975), le résultat principal de ces mouvements au Dévonien inférieur est la paléo-faille de Tabriz, qui depuis cet époque, a structuré ce domaine en deux parties. Cette zone de faille a controlé la sédimentation des formations géologiques jusqu'à la fin du Carbonifère (Eftekharnezhad, 1975). Au Trias supérieur, après un contexte paléogéographique de plateforme, ce domaine subit un plissement (le premier mouvement de la phase orogénique alpine). Au Cénozoique, le NW de l'Iran est affecté par une seconde phase de plissement associé à un magmatisme d'âge Eocène. D'après Eftekharnezhad (1975), l'activité des failles et des volcans au Plio-Quaternaire correspond à l'épisode tectonique le plus important dans ce domaine.

Globalement, la chaîne de l'Alborz est située à l'est de notre région étudiée. Les montagnes de l'Alborz s'étendent sur plus de 900 kilomètres depuis le Petit Caucase à l'ouest jusqu'à l'Indu-Kush à l'est. Dans sa partie orientale, l'Alborz se parallélise avec le Kopet Dagh situé juste au nord. A l'heure actuelle, beaucoup de géologues lorsqu'ils parlent des chaînes de l'Alborz et du Kopet Dagh considèrent que la première correspond à la chaîne qui borde le sud de la Mer Caspienne (et qui correspond traditionnellement à l'Alborz central) et que la seconde correspond à la chaîne qui s'étend depuis Apchéron à l'est de la mer Caspienne jusqu'en Afghanistan (Figure 7). L'Alborz central contient différentes unités géologiques allant du Précambrien au Quaternaire. Ces unités

sont assemblées dans des systèmes complexes de chevauchements et de plis qui se sont formé au cours de plusieurs orogenèses dont la plus importante en termes de déformations cassantes s'est produite à la fin du Cénozoïque (Alavi 1996). Les failles du côté septentrional de la chaîne sont chevauchantes vers le nord, celles de la partie sud vers le sud (Stöcklin 1974a). Sur l'ensemble de la chaîne, l'azimut des plis et des failles change, passant d'une direction WNW à l'ouest à une direction ENE à l'est. Des failles décrochantes (toutes sénestres actuellement) se produisent sur toute la longueur de l'Alborz parallèlement aux chevauchements et aux plis. Dans les terminaisons orientale et occidentale de l'Alborz, la direction des structures change progressivement pour passer à une direction Nord-Sud à la jonction avec le Talesh à l'ouest et E-W à la jonction avec le Kopet Dagh a l'est (Berberian 1997; Allen et al, 2003a).

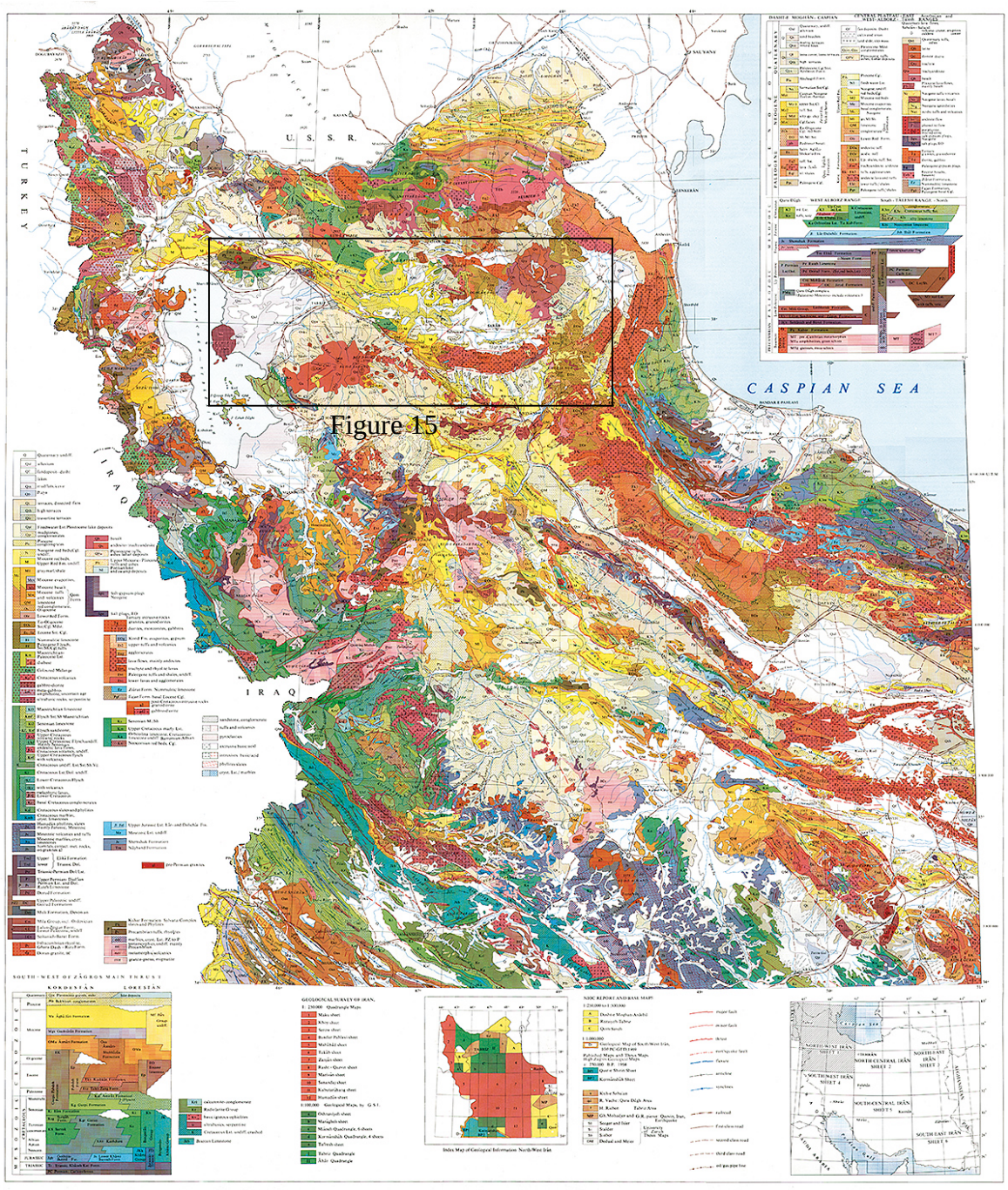

Figure 14- Carte géologique du NW de l'IRAN

Une des caractéristiques importantes du NW de l'Iran est la présence d'un volcanisme plio-quaternaire très bien exprimé. Il existe en effet plusieurs volcans récents dans le domaine

transcaucasien (par exemple l'Ararat, situé à cheval entre la Turquie et l'Arménie) et dans le NW de l'Iran (le Sahand, le Sabalan, le Damavan).

Situé à 40 km au SE de Tabriz, le Sahand est un strato-volcan qui culmine à 3695 m d'altitude et s'étend sur une surface de 4500 km^2. Les plus anciennes traces de son activité remontent à 12 Ma (Miocène moyen) et les plus récentes à seulement 140000 ans (Moinvaziri et Aminsobhani, 1986). Il est constitué de roches volcaniques de types rhyolite, dacite et andésite ainsi que de tufs et de cendres.

Le Sabalan se trouve à 40 km au SW de la ville d'Ardebil. Il a une superficie de 1200 km^2 et atteint une altitude de 4820 m. Il s'agit d'un volcan de type stratovolcan, composé de roches de types trachy-andésite, de dacites, d'andésites et de basalte. Sa période d'activité est principalement Pliocène mais il existe des évidences d'une activité plus récente (Würm).

Le Damavand est situé à 65 km au NE de Téhéran (Figure 12). C'est un édifice volcanique de type stratovolcan couvrant 400 km^2 et culminant à 5671 m. Son activité a débuté par des effusions de type basalte et trachy-basalte puis a évolué vers des roches plus intermédiaires de type trachyte. L'éruption connue la plus ancienne est d'âge Würm (Alenbach, 1966). Les laves barrant le Lac de Lar ont été datées à 38500 ans.

Ce volcanisme est classiquement interprété comme étant lié à la collision continentale N-S entre les plaques Arabie et Eurasie, provoquant l'expulsion du bloc Anatolie vers l'ouest et d'une partie de l'Iran vers l'Est (e.g. Cisternas et Philip, 1997). Cette déformation d'échelle lithosphérique se traduit par un épaississement crustal global, une augmentation générale du gradient géothermique et plus localement à des amincissement crustaux liés aux mouvements relatifs des blocs tectoniques impliqués dans la déformation (e.g. Berberian, 1997).

On peut également noter que d'après Karakhanian et al. (2002-2004), plusieurs grands séismes historiques ont été accompagnés par des activités volcaniques comme ce fut le cas pour le séisme d'Ararat en 1840 A.D.

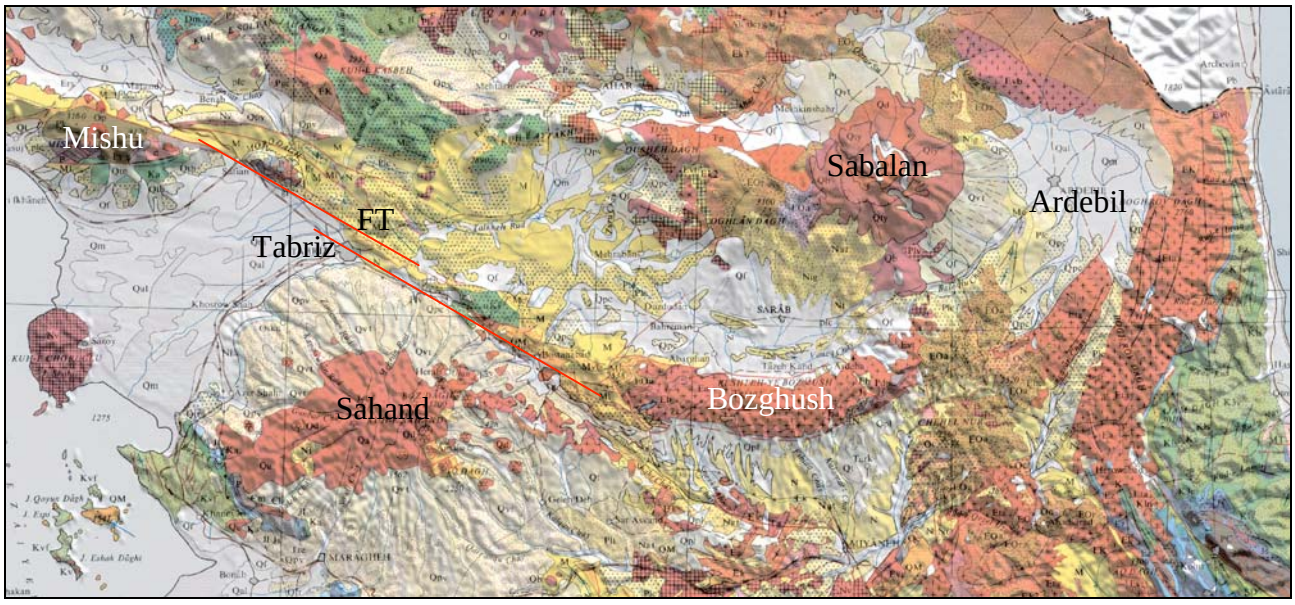

Figure 15- Détail de la carte géologique plaquée sur un MNT dans la région de la Faille de Tabriz (FT). Ici, les mouvements décrochants dextres de la faille Nord Tabriz sont amortis à l'ouest et à l'est par les zones compressives de Mishu et de Bozghush, respectivement.

3- Sismicité

Le nord-ouest de l'Iran a connu parmi les plus forts séismes destructeurs enregistrés au cours du dernier siècle de l'Iran, avec notamment le tremblement de terre de Rudbar-Manjil en 1990, dans le domaine de l'Alborz occidental (Figure 16), région pour laquelle on ne connaissait pas de séisme historique. Au contraire, la région de Tabriz apparait calme du point de vue de la sismicité instrumentale, alors qu'elle a été dévastée par deux cycles de séismes au XVIIIe siècle (Figure 17). Ceci montre clairement que les bases de données instrumentales et historiques ne suffisent pas à caractériser l'activité sismique d'une région, surtout en domaine intracontinental. Et de fait, très souvent, l'échelle des temps caractéristiques des grands tremblements de terre continentaux n'est pas accessible au souvenir des hommes.

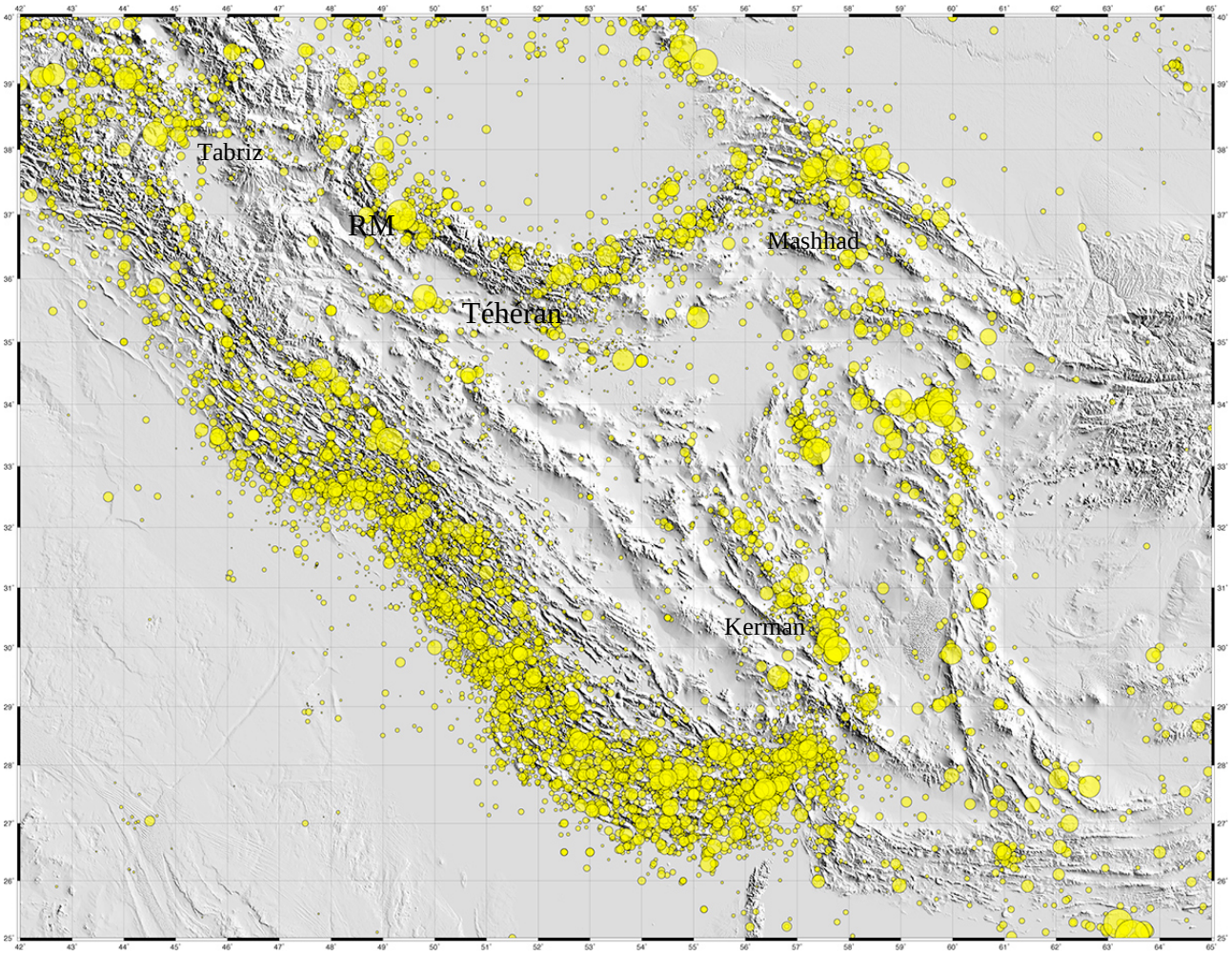

Figure 16- Carte de la sismicité instrumentale réalisée à partir du catalogue de l'IIEES (période couverte de 1900 jusqu'à 2008). Notons que d'après cette base de données, les régions de Téhéran et de Tabriz sont calmes. RM ; la localisation du séisme de Rudbar-Manjil en 1990.

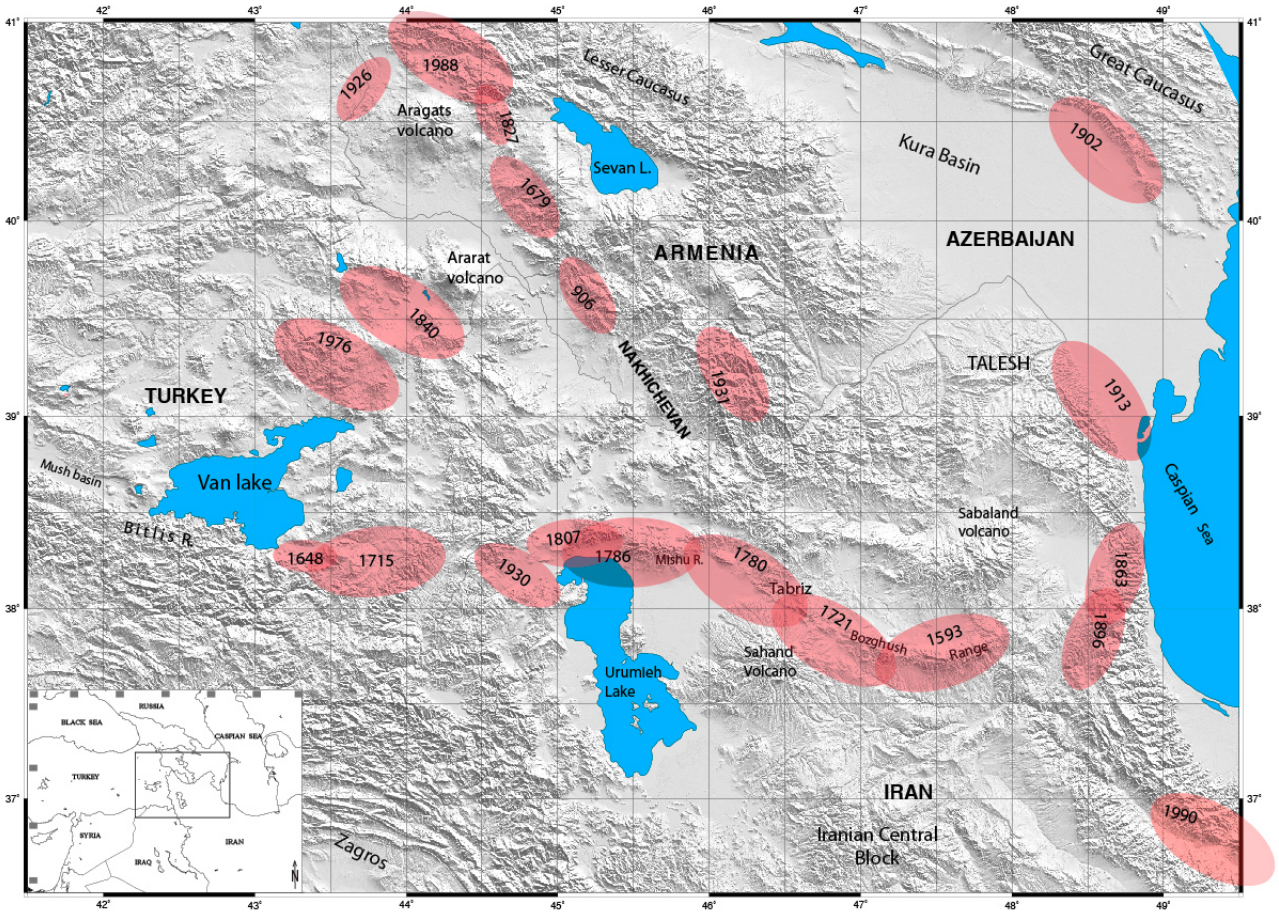

Figure 17- Carte de la sismicité historique simplifiée du NW de l'Iran et des pays limitrophes.

4- Tectonique et failles actives

Sur les bases d'une synthèse obtenue à partir de cartes sismotectoniques de la région nord-ouest de l'Iran comme celles de Berbérian, 1997 ou Hessami et al. , 2003 on remarquera que les failles actives majeures comme celle de Tabriz (dans le domaine occidental) et de Rudbar-Manjil (dans le domaine oriental) ont des directions identiques NO-SE mais des cinématiques décrochantes opposée (Figure 18), c'est à dire dextre pour la faille de Tabriz et senestre pour celle de Rudbar-Manjil. Ce dispositif souligne l'importance sur le plan tectonique et géodynamique de la région de transition entre deux domaines : la terminaison occidentale de la chaîne de l'Alborz et le domaine Tabriz-Talesh. . D'après Vernant et al. (2004) et Djamour (2004), la déformation dans la chaîne de l'Alborz est partitionnée en 5 mm/an du raccourcissement nord-sud et en 4 mm/an cisaillement sénestre. La majeure partie du cisaillement sénestre est localisée dans la partie sud de l'Alborz. Dans le domaine Tabriz-Azerbaïdjan iranien, d'après Vernant et al. (2004) et Masson et al. (2006), il y a 5 à 8 mm/an de cisaillement dextre qui est concentré sur la faille de Tabriz.

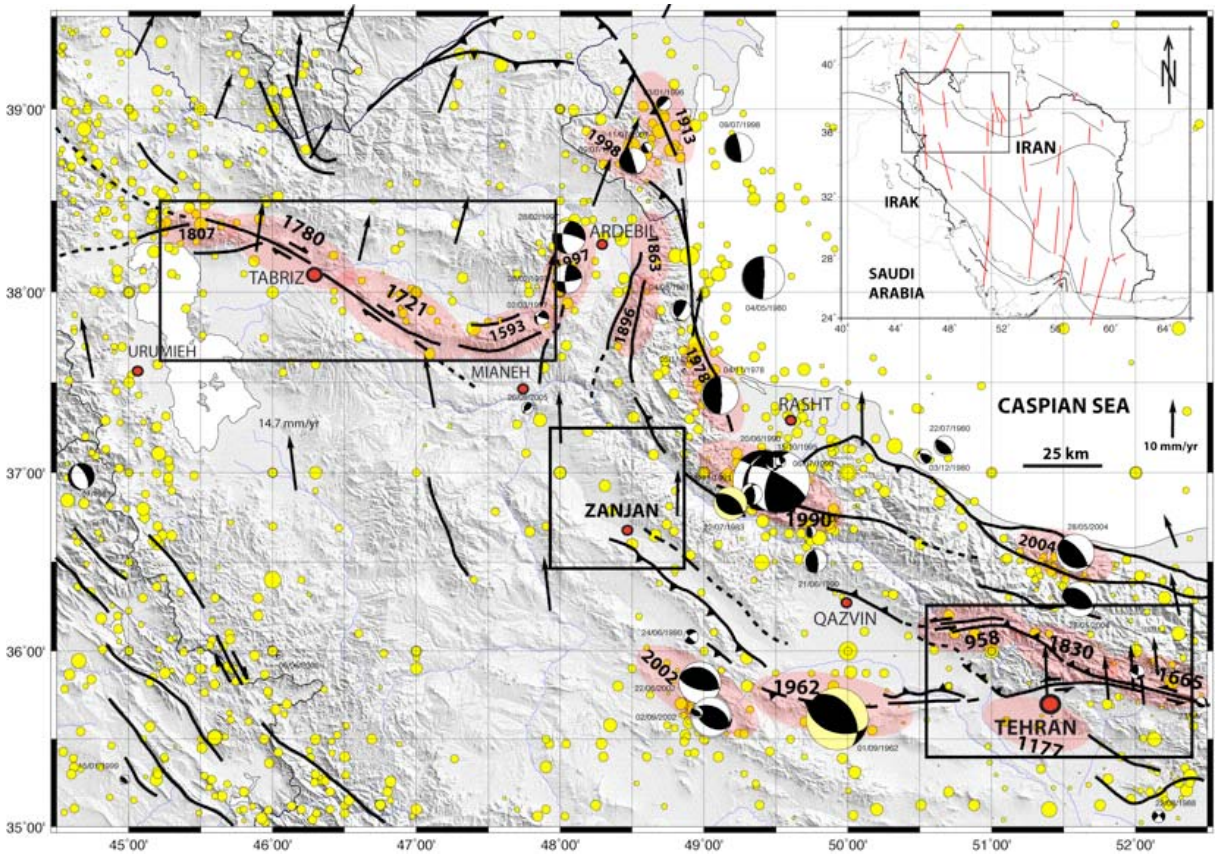

Figure 18- Carte sismo-tectonique simplifiée du NW de l'Iran avec les vecteurs GPS, mécanismes au foyer, sismicité historique et instrumentale.

Dans cette région de l'Iran se trouve des villes importantes comme Tabriz (dans le domaine occidental) et Téhéran (dans le domaine oriental) qui sont situées au voisinage de failles sismogéniques. Entre ces deux domaines, on trouve également des villes importantes comme Zandjan qui sont situées dans la zone de jonction entre les deux domaines mentionnés, mais qui n'ont pas expérimenté de grands séismes historiques et instrumentaux.

<u>Dans ce travail de thèse, nous nous sommes fixés comme objectifs:</u>

1-d'améliorer l'évaluation de l'aléa sismique pour les villes de Téhéran, Tabriz et Zandjan;
2-de comprendre la cinématique récente et actuelle des grandes failles dans les domaines oriental, occidental et central du NO de l'Iran;
3-d'améliorer notre connaissance de la géodynamique du nord-ouest de l'Iran.

5- Approche mise en oeuvre

Jusqu'à présent, en Iran, l'évaluation de l'aléa sismique était basée souvent sur les données de la sismicité instrumentale et historique. Cette période est généralement insuffisante pour préciser les périodes de retour des séismes majeurs qui dépassent souvent la période couverte par les données historiques (2600 ans) dans les régions intracontinentales (comme le nord-ouest de l'Iran). Pour essayer d'obtenir des données géologiques sur des périodes de temps plus anciennes que celle couverte par la sismicité, nous avons mis en œuvre des méthodes basées sur des études morphotectoniques et paléosismologiques.

Nous avons suivi les étapes suivantes:

1- Analyses d'images satellites et de photos aériennes.
2- Réalisation et analyse de modèles numériques de Terrain (MNT) à l'échelle générale et locale.
3- Cartographie des failles actives et analyse géomorphologique des matériaux quaternaires sur le terrain.

Après ces étapes, nous avons sélectionné plusieurs sites favorables pour effectuer des études paléosismologiques et réaliser des tranchées traversant les zones de faille précédemment cartographiée.

Pour les études paléosismologiques, il est nécessaire d'abord de dessiner le log de chaque tranchée, c'est à dire de faire un relevé détaillé de la géométrie des couches sédimentaires, et d'identifier les différentes strates qui ont été affectées successivement par la faille. La datation de chaque niveau important (comme les Event Horizons ou Post-event Horizons), peut permettre de trouver l'âge de chaque événement sismique et de définir les caractéristiques sismogéniques de la faille tels que, sa vitesse de glissement et l'intervalle de récurrence des grands séismes. Enfin, avec l'évaluation des déplacements co-sismiques (déplacement par évènement) on peut estimer les magnitudes des différents événements sismiques identifiés dans les tranchées.

CHAPITRE 2

LES FAILLES ACTIVES DANS LA REGION NORD DE TEHERAN

Dans ce chapitre, nous abordons l'étude d'une région clé en qui concerne le risque sismique en Iran, puisqu'il s'agit de la capitale iranienne, Téhéran, qui compte aujourd'hui, avec les villes adjacentes (Karadj, Lavasanat etc...), plus de 15 millions d'habitants. Cette région très fortement peuplées et où se concentre une grande partie de l'activité économique iranienne est une des zones les plus vulnérable du point de vue de l'aléa sismique. En effet, de nombreuses failles actives bordent cette immense zone urbaine située sur le piedmont méridional de la chaine active de l'Alborz central. Parmi celles-ci, les failles de Mosha et de Nord Téhéran sont les principales. L'étude de la cinématique actuelle des différents segments qui composent ces deux zones de failles permet de mieux définir l'aléa sismique qu'elles représentent, et de contraindre le modèle géodynamique régional.

To be submitted to Tectonophysics

Left-lateral active deformation along the Mosha-North Tehran fault system (Iran): morphotectonics and paleoseismological investigations

Shahryar SOLAYMANI AZAD[1, 2], Jean-François RITZ[1], Mohammad Reza ABBASSI[2]

1: Université Montpellier 2, Laboratoire Géosciences Montpellier, UMR CNRS 5243, France.
2: International Institute of Earthquake Engineering and Seismology (IIEES), North Dibaji, West Arghavan,# 26,Tehran, Iran.

Abstract: The Mosha and North Tehran faults correspond to the nearest seismic sources for the northern part of the Tehran megacity. The present structural relationships and the kinematics of these two faults, especially at their junction in Lavasanat region, is still a matter of debate. In this paper, we present the results of a morphotectonics analysis (aerial photos and field investigations) within the central part of the Mosha and eastern part of the North Tehran faults between the Mosha valley and Tehran city clarifying the two points. Our investigations show that, generally, the traces of activity do not follow the older traces corresponding to previous long-term dip-slip thrusting movements. The recent faulting movements is mainly occurring on new traces trending E-W to ENE-WSW, affecting quaternary features (streams, ridges, risers, young glacial markers) cutting straight through the topography. Often defining en echelon patterns (right and left stepping), these new traces correspond to steep faults with either north- or south-dipping directions, along which clear evidences for left-lateral strike-slip faulting are found. At their junction zone, the two sinistral faults display a left stepping *en-echelon* pattern defining a flower structure system clearly visible near Ira village. Further west, the left-lateral strike-slip motion is transferred along the ENE-WSW trending Niavaran fault and other faults. The cumulative offsets associated with this left-lateral deformation is small compared with the topography associated with the previous Late Tertiary thrusting motion, showing that it corresponds to a recent change of kinematics.

Keywords: Iran, Central Alborz, Mosha fault, North Tehran fault, active fault, morphotectonics

1 Introduction

The Mosha and North Tehran faults correspond to two major structures in the southern border of the Central Alborz, the active mountain range surrounding the southern margin of the South Caspian basin (e.g. Berberian, 1983; Jackson et al., 2002; Allen et al., 2003a). These faults are located at the immediate vicinity of the highly-populated region of Tehran, where more than 15 million peoples are living (Figure 1). The Mosha and North Tehran faults represent an important seismic hazard for the Iranian capital considering the historical seismicity recorded in the area (e.g. Ambraseys and Melville, 1982; Berberian and Yeats, 1999) and the active tectonics features observed along them (e.g. Berberian et al.1985; Trifonov et al. 1996; Ritz et al., 2003; Solaymani et al. 2003; Nazari, 2006; Ritz et al., 2006).

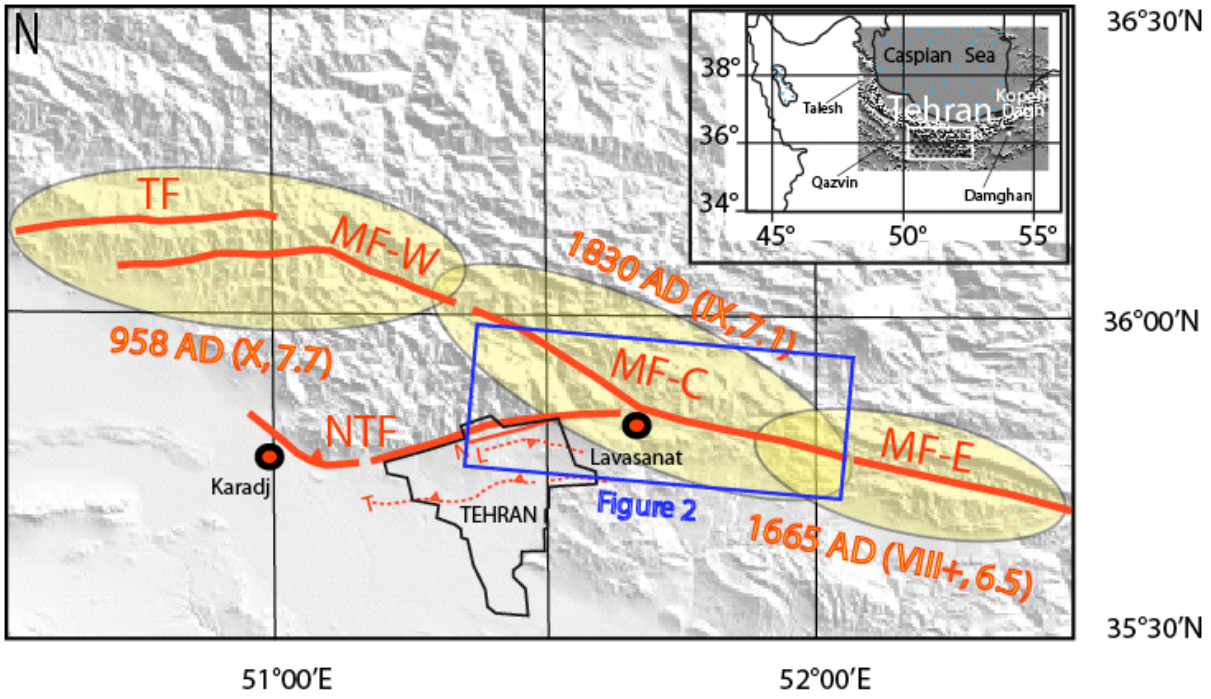

Figure1: Sketch map of the Mosha and the North Tehran faults in the southern border of the Central Alborz mountain range, and the three damaging historical earthquakes classically attributed to this area. MF: Mosha fault, NTF: North Tehran fault, TF: Taleghan fault, MF-W: Western Mosha fault, MF-E: Eastern Mosha fault, MF-C: Central Mosha fault. N: Niavaran fault; L: Lavizan fault; T: Tarasht fault. The blue frame indicates our study area within the macroseismal zone of the 1830 AD event. The macroseismic areas are from Berberian and Yeats (1999) and their evaluated intensities and magnitudes are from Ambraseys and Melville (1982). L and T fault traces after Abbassi and Farbod (2009).

The present kinematics of these two faults, especially at their junction is still a matter of debate. Geologically, at a large scale, the Mosha and North Tehran faults are mapped as north-dipping thrust faults, along which Jurassic and older formations (for the Mosha fault)

and Eocene formations (for the North Tehran fault) are thrusting over Eocene rocks and Plio-Quaternary deposits, respectively (e.g. Geological survey of Iran, 1993). As concerns their present kinematics, the two faults are classically described as mainly thrusting faults (e.g. Tchalenko, 1975; Berberian, 1976; Berberian and Yeats, 1999; Berberian and Yeats, 2001), that join together within the Lavasanat region (e.g. Tchalenko, 1975; Berberian et al., 1985; Bachmanov et al., 2004).

However, recent active tectonics studies describe clear active left-lateral strike-slip deformation along the WNW-ESE trending eastern Mosha fault (e.g. Ritz et al., 2003; Solaymani et al., 2003; Allen et al., 2003b; Ashtari et al., 2005; Ritz et al., 2006). Recent left-lateral strike-slip deformation as a component of a main transpressional deformation is also described along the North Tehran fault, within its eastern NE-SW trending section (e.g. Hessami et al., 2003; Bachmanov et al., 2004; Landgraf et al., 2009).

The present geometry, spatial extent and kinematics of the two active faults within their junction zone (Lavasanat region, see Figure 1) remain in question. In this paper, by means of a morphotectonics study using aerial photo interpretations and field investigations, we analyze the present structural relationships and kinematics between the central part of the Mosha fault and the eastern part of the North Tehran fault.

2 Tectonic Setting

The Alborz mountain range corresponds to an active mountain belt surrounding the south Caspian oceanic domain (e.g. Berberian, 1983; Jackson et al., 2002; Allen et al., 2003a), and can be described as the northern part of the Alpine-Himalayan orogen in Western Asia (e.g. Stöcklin et al., 1974). This sinuous range extends over 900 km and can be subdivided in three major parts. The longer one, the Central Alborz, extends for about 600 km along the southern side of the Caspian Sea from Qazvin (49°00’E, 36°15’N) to Damghan (54°30’E, 36°15’N) (see regional map enclosed in Figure 1). We define the Western Alborz as the portion of the mountain range setting from Qazvin to the Talesh, and the Eastern Alborz as the part situated between Damghan and the Kopeh Dagh mountain range. The Central Alborz formed a ~100 km wide belt, characterized by range-parallel folds and faults showing opposite vergences (e.g. Stöcklin et al., 1968 and 1974; Berberian, 1983; Jackson et al., 2002; Allen et al., 2003b). Between longitudes 50°E to 54°E, a wide “V” shape structure characterizes its general form, with folds and faults trending NW-SE in the western part and

NE-SW in the eastern part (see regional map enclosed in Figure 1). The geological and tectonics history of Alborz is complex with several orogen episodes (e.g. Alavi, 1996) separated by extensional phases (e.g. Berberian, 1983; Zanchi et al., 2006). Estimates of total shortening across Central Alborz vary from 35-38 km (Nazari, 2006) to 53 km (Guest et al., 2006). Most of this shortening occurred recently (since Neogene). Allen et al. (2003) and Nazari (2006) estimated both 25-30 km of shortening during the Neogene.

Neotectonics and seismological studies show that the present deformation in Alborz is partitioned along range-parallel thrusts and left-lateral strike-slip faults (e.g. Jackson et al., 2002; Allen et al., 2003a; Ritz et al., 2006; Nazari, 2006; Hollingsworth, 2007). Evidences of left-lateral deformation are documented by focal mechanisms of earthquakes along the Rudbar-Manjil fault zone (e.g. Jackson et al., 2002; Tatar and Hatzfeld, 2009) or along the Mosha fault (e.g. Hedayati et al., 1976; Ashtari et al, 2005), and by fault kinematics deduced from morphotectonics studies along several range parallel faults such as the Mosha fault (e.g. Trifonov et al. 1996; Ritz et al., 2003; Solaymani et al., 2003; Allen et al., 2003; Hessami et al., 2003; Bachmanov et al., 2004) or the Taleghan fault (Nazari, 2006; Nazari et al., 2009).

According to Jackson et al. (2002), this active strain partitioning is a result of oblique compression due to the combination of the Arabia-Eurasia northwards convergence and the north-westward motion of the South Caspian basin with respect to stable Eurasia. A recent GPS study quantified the partitioning at the scale of the whole range: the N-S shortening across the range occurs at 5 ± 2 mm/yr, while the left-lateral shear across it occurs at a rate of 4 ± 2 mm/yr (Vernant et al., 2004; Djamour, 2004). A recent update of the geodetic data gives shortening rates varying from 0 to 5.5 mm/y (most of it being in the north-western part) and a left-lateral shearing across the range from 1.5 to 6.0 mm/y (most of it setting in the south-eastern part) within the Central Alborz (Djamour et al., 2008).

To explain this present tectonic setting, authors invoke a regional kinematical change during the Neogene: first, the Alborz started to shorten under a North-South compression leading to the formation of ~E-W trending parallel folds and thrusts structures. A recent study documented that the southward propagation of thrusting and folding within southern Alborz occurred beyond ~6.2 Ma, which is the age of the Hezardarreh formation corresponding to the conglomerates found at the base of the foreland basin in the Tehran region (Ballato et al., 2008). During this stage, the South Caspian basin would have been fixed with respect to Eurasia (e.g. Jackson et al., 2002). Then, during a second stage, the South Caspian basin started moving towards the north-west with respect to Eurasia. The timing of the onset of the

north-west motion is still in debate and varies between 10 Ma (Hollingsworth et al., 2008), ~5 Ma (Axen et al., 2001; Allen et al., 2003a) to 1.5 Ma (Ritz et al., 2006). Recently, Ritz (Geology, accepted) suggested that the recent motion of the South-Caspian basin occurred in two stages: during a first stage at the end of the Miocene, the basin started subducting north beneath the Apsheron Sill, and then a westward component of motion has been added during the Pleistocene.

The historical and pre-historical seismic records within the Alborz mountain range suggest the occurrence of strong earthquakes with often long-term recurrence intervals (e.g. Ambraseys and Melville, 1982; Negahban, 1977; Berberian, 1994; Talai, 1998; Berberian and Yeats, 1999, 2001). In the Tehran region, which was named initially Shahr-e Rey, several destructive historical earthquakes have been recorded since 958 AD. Earthquakes in 958 AD (Ms=7.7, Io=X), 1177 AD (Ms=7.2, Io=VIII+), 1665 AD (Ms=6.5, Io=VIII+) and 1830 AD (Ms=7.1, Io= VIII+) have been described in few studies such as Ambraseys and Melville (1982) and Berberian and Yeats (1999, 2001). The seismic events of 958 AD , 1665 AD and 1830 AD have been correlated to the Mosha, North Tehran and Taleghan faults at the north vicinity of Tehran region (e.g. Berberian and Yeats, 1999) (see Figure 1). These destructive historical earthquakes show the important seismic hazard that the Iranian metropolis is facing nowadays. Two hundred years ago, in 1807 AD, the ancient Tehran was about 2 km^2 and 50,000 peoples. Today, Tehran and its suburbs areas represent a sprawling urban area of more than 1,000 km^2, growing faster each day, where more than 15 million peoples are living.

Structural relationships and kinematics of the Mosha and North Tehran faults – The Mosha and North Tehran faults (see Figures 1 and 2), are located at the southern border of the Central Alborz and were first described by Dellenbach (1964) and Reiben (1955), respectively. Most of the pioneer works described the Mosha fault as a major reverse or thrust fault (e.g. Dellenbach, 1964; Allenbach, 1966; Steiger, 1966; Sieber, 1970; Tchalenko et al. 1974; Nabavi, 1976; Berberian, 1976; Berberian et al., 1985). Standing out in the highest part of the Central Alborz mountain range, the Mosha fault corresponds to the thrusting of the "High Alborz" (a complex folded zone of Paleozoic-Mesozoic and Tertiary formations) over the Border Folds to the south (Tchalenko et al., 1974). As for the Mosha fault, the North Tehran fault was first described as an active reverse fault controlling the thrusting of the Central Alborz reliefs above the Neogene foreland basin (e.g. Reiben, 1955; Dresch, 1961; Knill and Jones, 1968; Breddin, 1970; Tchalenko et al., 1974; Berberian et al., 1985).

Further studies allowed precising the recent kinematics of these two faults. Along the Mosha fault, mainly within its eastern part, several morphotectonics studies showed evidences of left-lateral strike-slip faulting (Trifonov et al., 1996; Berberian and Yeats, 1999; Ritz et al., 2003; Solaymani et al., 2003; Bachmanov et al., 2004; Allen et al., 2003b; Ritz et al., 2006). These results are consistent with microseismic data showing active left-lateral movements along the eastern Mosha fault (e.g. Hedayati et al., 1976; Ashtari et al., 2005). Along the eastern Mosha fault, this left-lateral motion is associated with a normal component (Ritz et al., 2006) as also observed along the Taleghan fault (Nazari et al., in press). This component is explained by the obliquity of the fault with respect to the general trend of the range (Ritz, in press).

Along the North Tehran fault, recent left-lateral component of motion was also suggested from the interpretation of the geometry of the faults within its NE-SW trending part, where three en-echelon branches are observed (Tchalenko et al., 1974). Further studies (Trifonov et al., 1996; Hessami et al., 2003; Bachmanov et al., 2004, Landgraf et al., 2009) presented some other evidences of left-lateral deformation associated with the main thrusting movement along the North Tehran fault. Along its western NW-SE section, the North Tehran fault shows clear evidences of active thrusting (Nazari, 2006; Nazari et al., in revision).

In their recent work, using fault kinematics analysis, Landgraf et al. (2009) interpret the succession of three faulting regimes within the North Tehran and Mosha faults system: a former dextral transpressional stage under a NW-shortening was followed by a Pliocene to recent NE-shortening during which the North Tehran and Mosha faults formed a sinistral transpressional duplex. Finally, an extensional youngest stage would invert the kinematics of structures. The chronology between the first and second stages is interpreted to be associated with the clockwise rotation of Shmax from NW-SE to NE-SW as was previously proposed by Abbassi et al. (2003).

According to Abbassi and Farbod (2009) there is no evidence for active faulting along the North Tehran fault as defined classically at the mountain front zone of Tehran. The active deformation seems, instead, to have switched southwards within the Niavaran, Lavizand and Tarasht faults (see Figure 1). The Niavaran fault was first recognized by Delenbach (1964) and by Tchalenko (1975). It is situated ~1 km southwards the NTF and is roughly parallel to it. Berberian (1985) and Berberian and Yeats (1999) mapped the fault as a 12 km long, steep north dipping thrust fault. In his 1985 report, Berberian presented some evidences of left-lateral horizontal component along the eastern part of the fault. Within its western part,

Abbassi and Farbod (2009) described active left-lateral strike-slip features, plus associated minor faults situated northwards of the Niavaran fault. According to Abbassi and Farbod (2009), the thrusting deformation is now occurring south of the Niavaran fault, along the roughly E-W trending Lavizan and Tarasht faults.

3 Morphotectonics analysis along the Central Mosha fault and the North Tehran fault

We studied the central part of the Mosha fault and its junction zone with the eastern section of the North Tehran fault within nine different sites (Figure 2). The central part of the Mosha fault can be defined as the portion of the fault extending from Mosha village to Shahrestanak village (Solaymani et al., 2003) (Figure 2). Along its central part, the fault shows a smooth deviation in strike at Lavasanat area. West of this area, the strike of the Mosha fault is 130°E whereas east of this area, the fault is striking 110°E. In this paper, we name these two parts West-Central and East-Central Mosha faults, respectively. The junction of the North Tehran with the Central Mosha fault sets at the bend between the west-central Mosha fault and east-central Mosha fault. Our study was first based on the interpretation of aerial photographs. We used the oldest set of photographs (i.e. 1955) to work on landscapes preserved from the effects of the recent increase of human activities in the region. Our preliminary morphotectonics mapping was then completed by field studies.

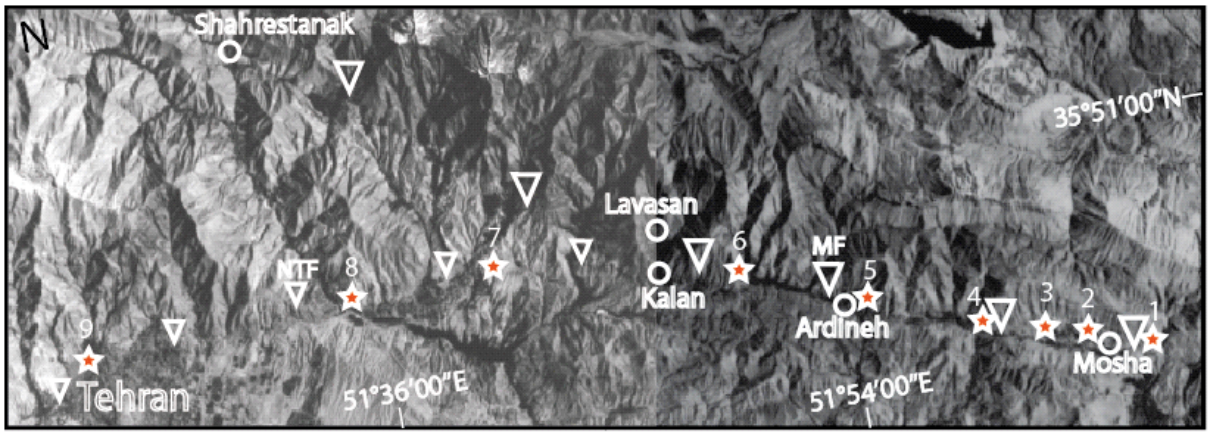

Figure 2: Cosmos satellite image of the region situated in the NE of Tehran city. Triangles point out the traces of the central part of the Mosha fault (MF) and the eastern part of the North Tehran fault (NTF). Red stars indicate the 9 sites studied in details.

3.1 The Central Mosha fault within the Mosha valley

The Mosha valley is situated at the eastern part of the East-Central Mosha fault and corresponds to a glacial valley with fluvio-glacial and colluviums deposits that can be

attributed to the Würm and Riss periods (after observations at the western end of the valley by Pedrami, 1983). These Quaternary sediments are affected by a linear fault scarp defining a steep dipping fault between Mosha village and the Abali ski resort (Figure 3). The scarp defines a straight alignment with a difference in height of 20-40 m between the northern and the southern parts (Figure 4). This main Quaternary rupture re-activates an older structure separating Paleozoic and older formations to the north from Eocene (Karaj formation) and younger formations to the south. Based on fault slip data (075, 80S, -28) within the eastern part of the valley, several small N070°-N080° trending sinistral fault branches connect the main N100° trending linear scarp (Figure 3). The fact that the height of the main fault scarp is a little (~10 m) higher to the east than to the west can be related to these secondary features. This eastern section of the fault scarp is also characterized by the occurrence of surficial travertines indicating water circulation within the fault zone.

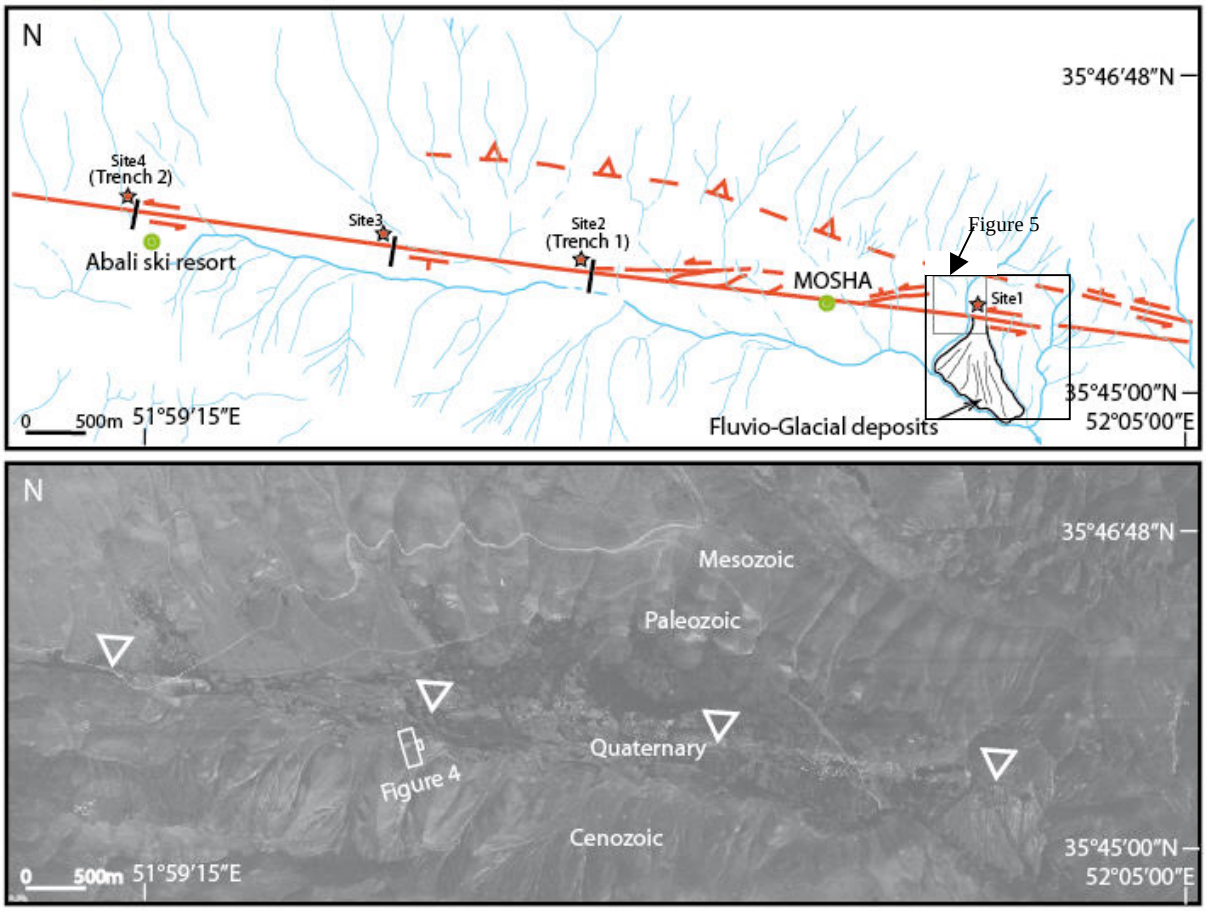

Figure 3: Aerial picture and its interpretation of the East-Central Mosha fault within the Mosha Valley between Mosha and the Abali ski resort.

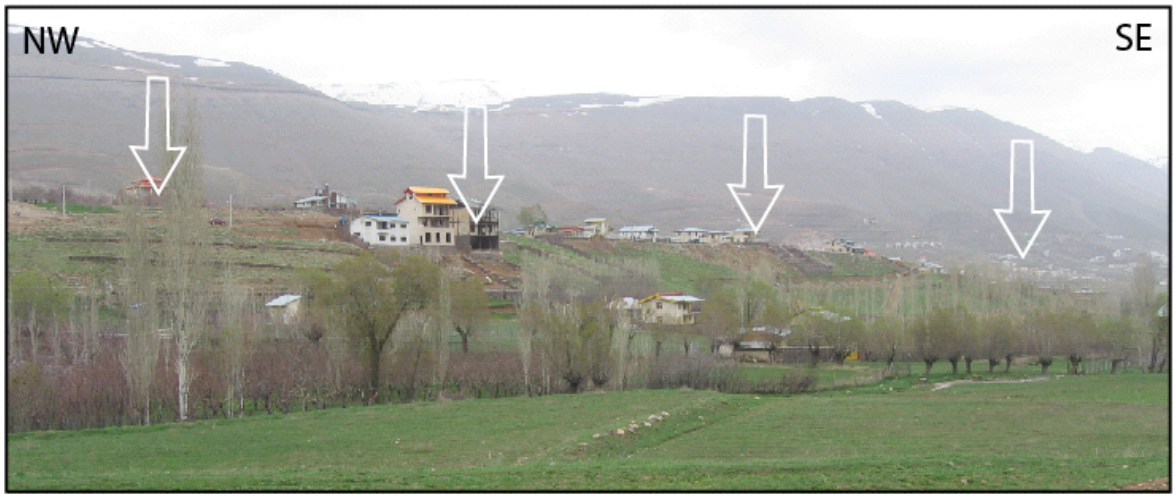

Figure 4: View towards the NE of The Mosha fault scarp within the Mosha valley. The scarp defines a straight alignment with 20-40 m difference in height.

The intensive agricultural activities during the last decades and the recent building constructions have modified and erased most of the recent morphological features, precluding the possibility of evidencing easily kinematics indicators at large scale. However, clear features of left-lateral strike-slip faulting can be observed east of the Mosha valley within the overlapping zone between the central and eastern portions of the fault (site 1, Figure 3). There, a cone made of glacial out-washes shows a cumulative left-lateral displacement comprised between 140 and 390 m (265 ± 125 m) (Figure 5).

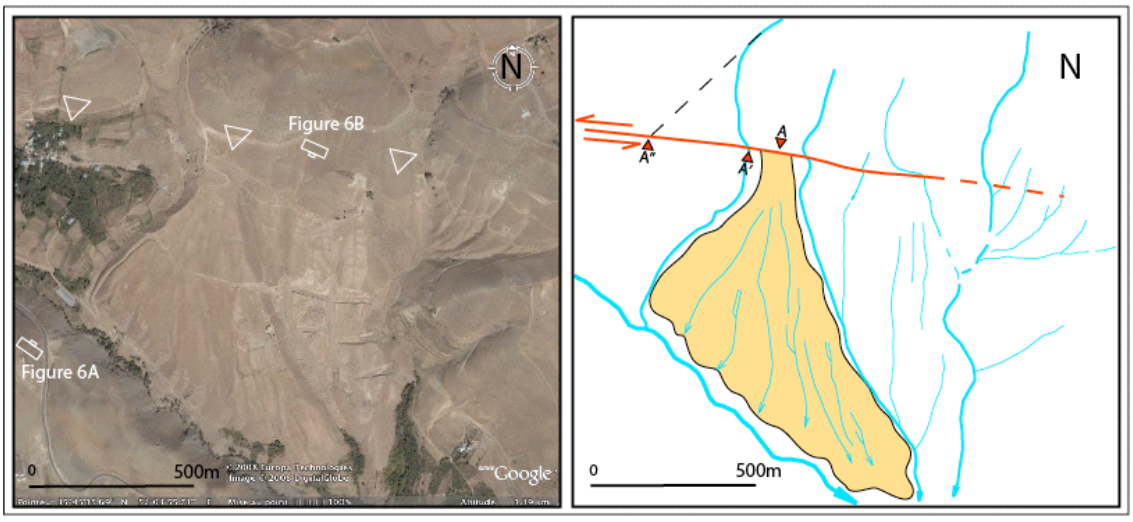

Figure 5: Google earth image and its interpretation of the East-Central part of the Mosha fault at eastern end of the Mosha Valley (site 1 in Figure 3) showing the left-lateral displacement of an out-wash cone. A corresponds to the apex of the cone. A-A' and A-A" define the minimum and maximum offsets, respectively. The black dashed line shows the southward extension of the up streambed of the offset drainage.

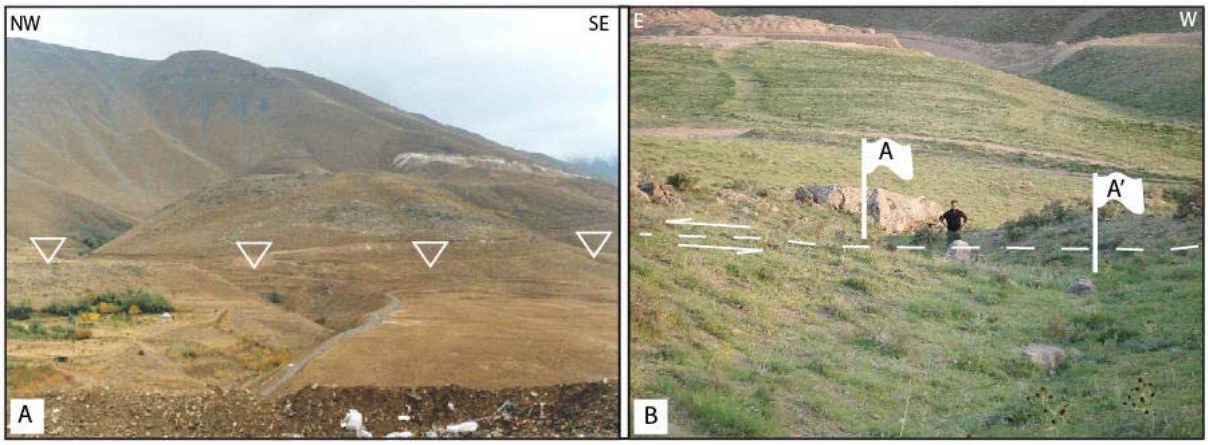

Figure 6: A: North-eastwards view of the Mosha fault scarp at the eastern part of the Mosha Valley. B: South-westwards view of a 5 m left-lateral offset drainage (A-A") along the Mosha fault.

Figure 6A shows a north-eastwards view of the outwash. The difference in height between the erosional surface within the bedrock to the north and the surface of the outwash deposits to the south is ~40 m. Assuming that this difference in height corresponds to a vertical offset postdating the deposition of the debris cone yields a mean ratio of ~7 between the horizontal and the vertical components. A detailed analyze within this site allows observing offset streams incisions with left-lateral displacements of 5 m, 30 m and 75 m (Fig. 6B).

Three kilometers westwards, within a small hill located on the upper part of the fault scarp, we cleaned an east-facing artificial riser - made for agricultural purpose (site 2 in Figure 3). For logistical and administrative reasons, we could not open a long trench reaching the toe of the fault scarp. The study of this 32 m long west wall shows a 25 m wide faulted zone capped by a flat abrasive unit mainly composed of sands and silts from which developed a soil unit (Figure 7). Two main faulted zones can be observed: to the north, one observes a steep south-dipping rupture (FI). This rupture is sealed by the organic-rich sandy-silty unit in which we found ceramic fragments. Slickensides along the rupture plane characterize a sinistral movement with a small normal component (075, 80S, -28 for strike, dip and rake, respectively). Northwards of FI rupture, we observe parallel secondary planes (070, 74S, -28). To the south, we observe two sets of ruptures. A first set of ruptures (FII), dipping steeply to the south, cuts the Holocene soil unit containing ceramic fragments and show fault slip data (103, 81S, -09) indicating left-lateral strike-slip fault with a small normal component. A

second set (FIII) is dipping steeply to the north. In terms of strike, the steep fault planes (FII) correspond to the main scarp direction observed in the morphology, while the fault planes observed within FI seem to correspond to the riddle planes oblique to the main line FII. This pattern is consistent with our plan-view interpretation of the fault traces (see Figure 3).

Westwards, 1.5 km from site 2, at the base of the fault scarp where new buildings were under construction, we found a section across Plio-Quaternary deposits (site 3 in figure 3). Within this NNE-SSW section, we observed two steep faults dipping 52° south and cutting through detrital material dipping ~60-65° south (Figure 8). Striation measurements within the two faults (096, 52S, -44) attest of a left-lateral-normal motion.

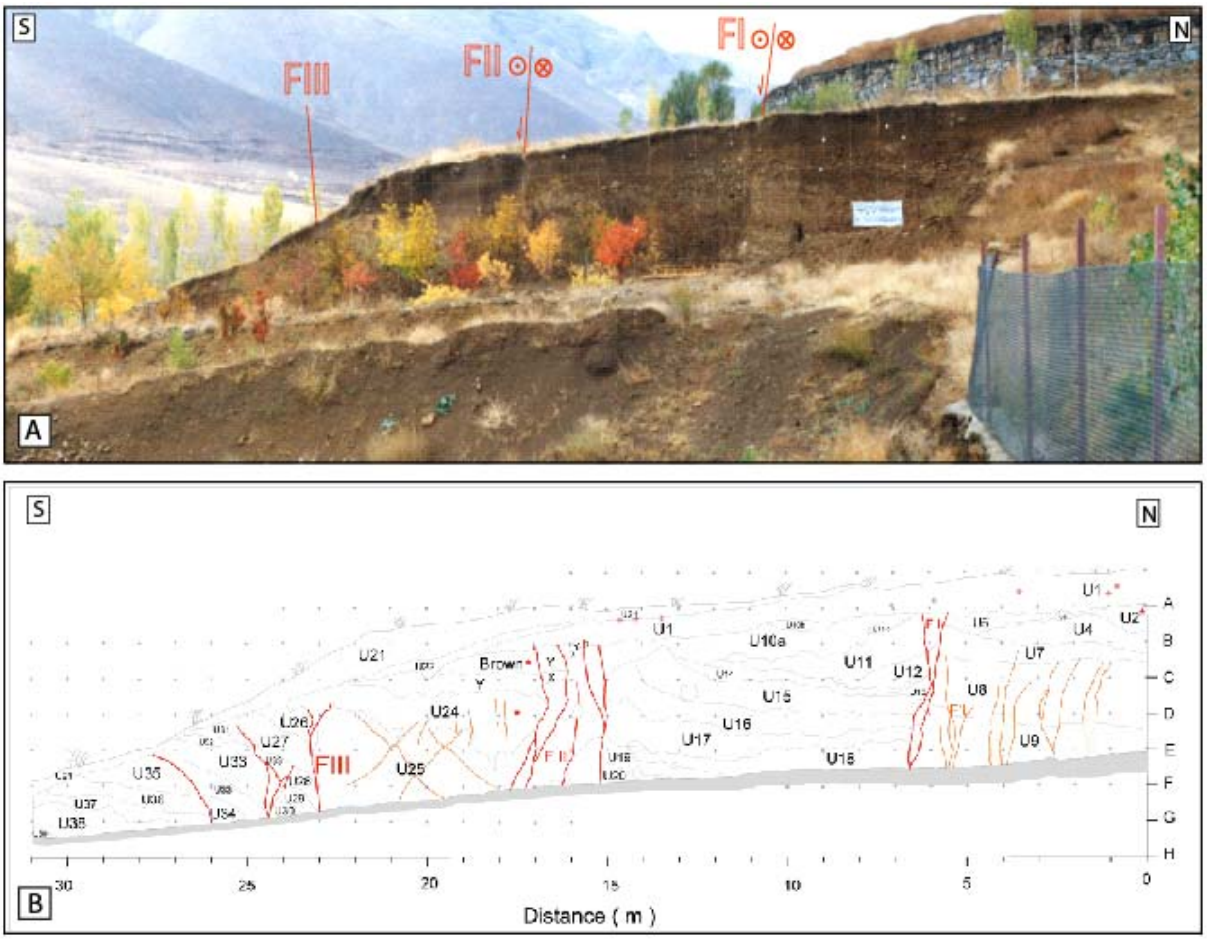

Figure 7: Picture (A) and interpretation (B) of the east-facing artificial riser studied at site 2. Red lines correspond to ruptures along which are observed displacements. Orange lines define fractures without obvious displacements.

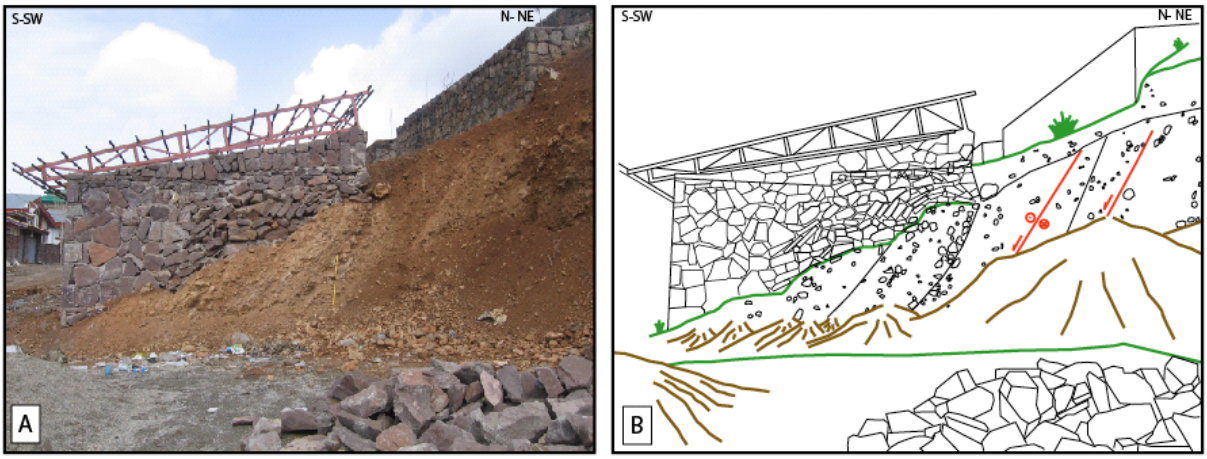

Figure 8: Picture (A) and interpretation (B) of a section at the base of the Mosha fault scarp (site 3 in Figure 3) showing steeply-dipping Plio-Quaternary deposits affected by fault planes.

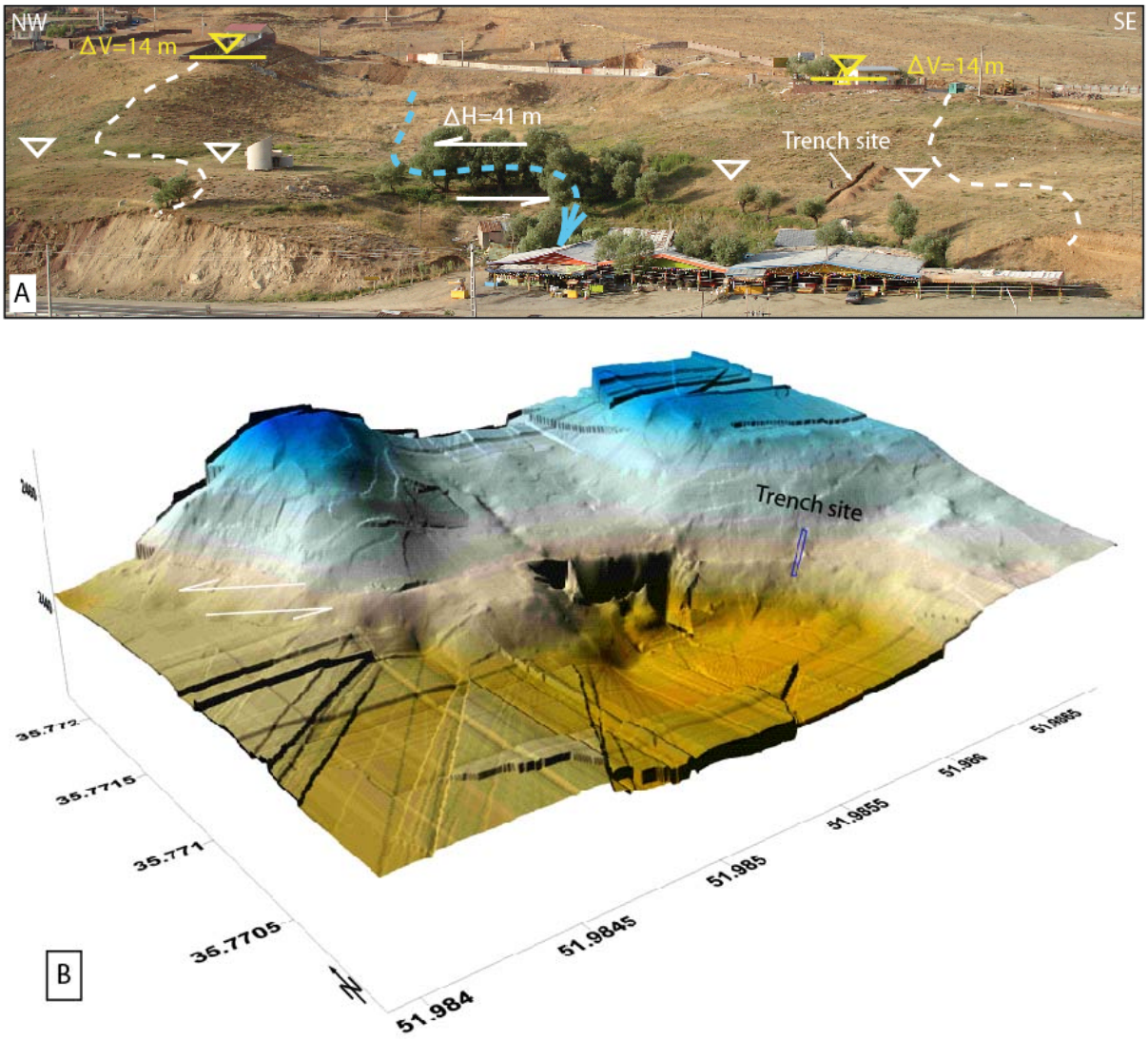

Figure 9:Photo (A) and DEM (B) of the two ridges left-laterally displaced west of Abali ski resort (Mosha fault)

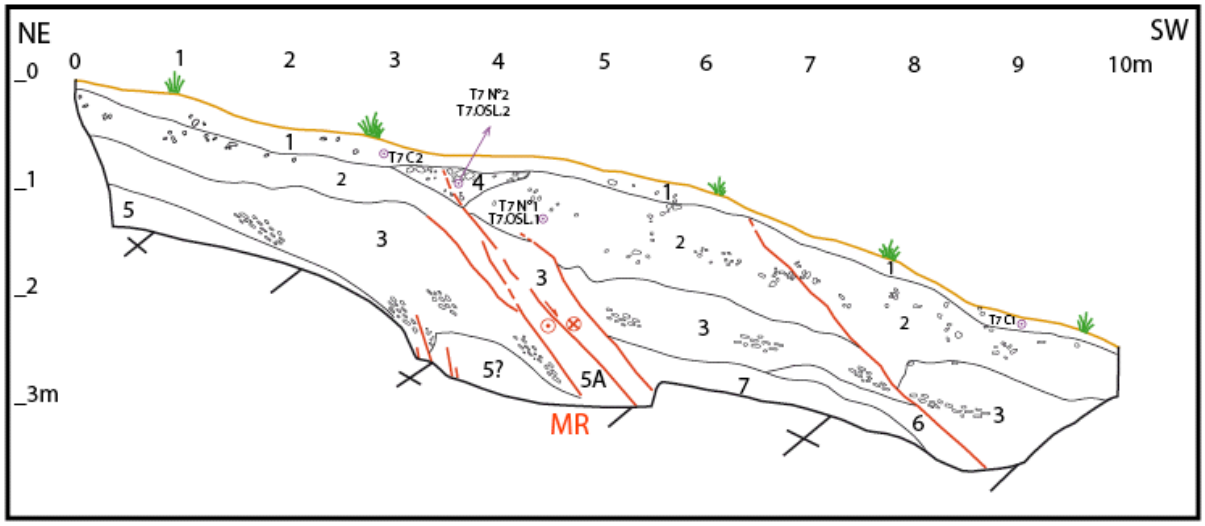

Figure 10: Log of the trench opened across the Mosha fault scarp westwards of Abali ski resort. Red lines correspond to ruptures with displacements. MR: Main Rupture. Here, based on optical stimulation luminescence dating of the unit 4 (simple n° T7N°2 T7OSL.2) as the last event-horizon unit, we identified the maximum age of the last seismic event (see text for more information).

Westwards of site 3, immediately to the west of the Abali ski resort, the stereo analysis of the 1/20.000 and 1/10.000 scale aerial photographs allowed finding another evidences for two left-laterally offset ridges along the Mosha fault (site 4 in Figure 3). This feature is not obvious to observe today because of human activity (road, agriculture, and buildings) that modified the original morphology (Figure 9A). Figure 9B shows the DEM obtained by surveying the site with GPS kinematics. From the DEM, we determined a horizontal offset of a 41 ± 4 m and a vertical offset of 14 ±1 m, yielding a ratio H/V of ~3. We measured a strike of N100°E and a dip of 70°S for the main rupture in a trench excavated across the fault scarp (Figure 10, see location in Figure 9). Combining H, V and the dip allowed us to calculate a rake of -20°. The dating of the colluvial unit 4, the most recent unit affected by the fault, allows us to estimate the elapsed time since the last rupture along the fault. OSL dating of the unit yielded an age of ~1120 years. This event could correspond to one of the two historical seismic events that occurred in 1665 AD and 1830 AD, with a preferred interpretation for the 1830 AD earthquake taken the macroseismal areas (e.g. Berberian and Yeats, 1999; see Figure 1).

3.2 The Central Mosha fault between Abali ski resort and Ardineh

Between Abali ski resort and Ardineh village, the active parts of the Mosha fault zone define two 110°E trending left-lateral left-stepped en-echelon fault branches (Figure 11).

These branches cut through or reactivate ancient thrusts faults between paleozoic and younger formations. East of Mobarak-Abad village, the fault trace is covered by an active landslide that could have been triggered during the October 2, 1930 (M=5.2) earthquake, event during which several landslides occurred in the nearby Ardineh-Ira valley (see Ambraseys and Melville, 1982; in this reference the Ardineh valley is named the Ira-rud valley).

West of Hazar-Dasht, several small left-lateral offset features are observed, and the shape of the Mobarak-Abad River suggests a left-lateral cumulative displacement comprised between 0.8 (A-A') and 3.8 km (A-A") (Figure 11).

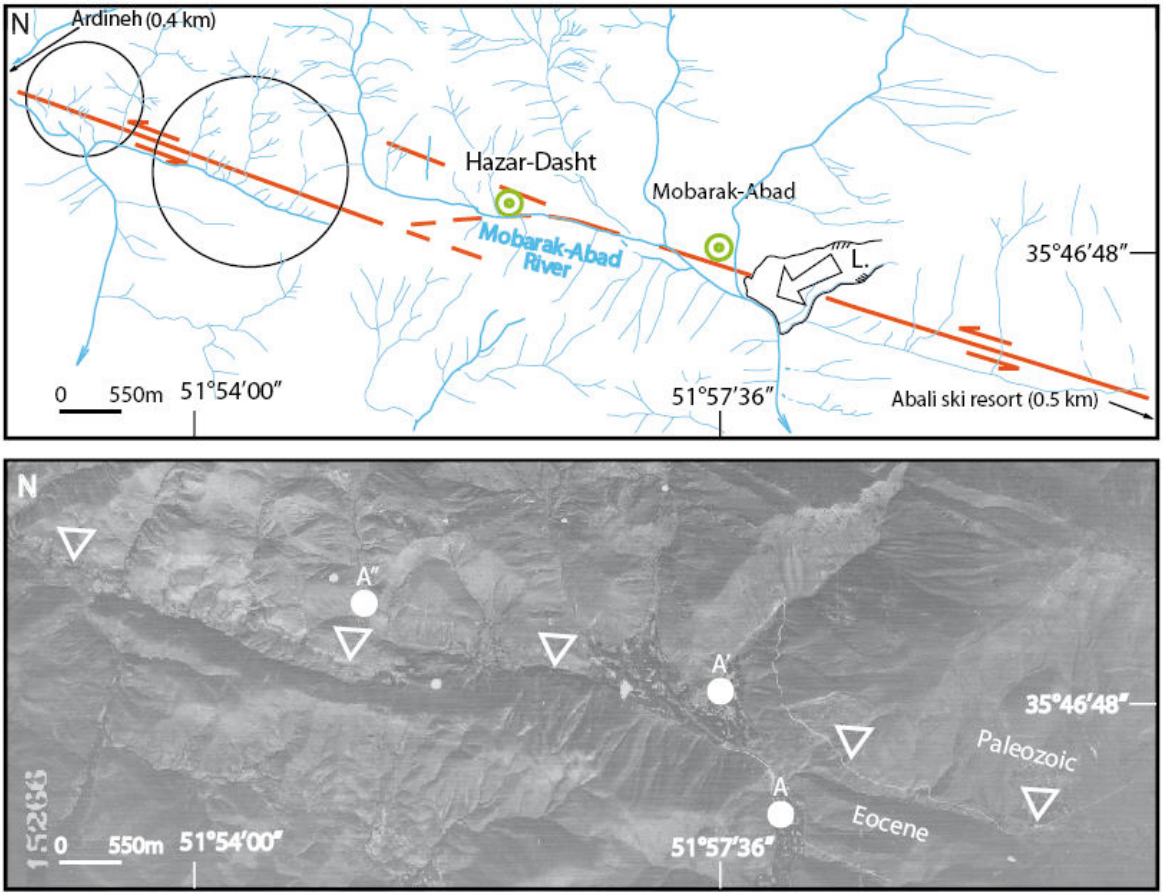

Figure 11: Aerial photograph and its interpretation of the Mosha fault within the Mobarak-Abad region, between Abali ski resort and Ardineh. Circles point out offset drainage feature. A-A' and A-A" define the minimum and maximum offsets, respectively. L: Mobark-Abad landslide.

3.3 The Central Mosha fault between Ardineh and Ira.

Between Ardineh and Ira, sets a linear valley where the Ira-Rud River runs. The linearity of the valley is controlled by the N110°E trending strike of the Mosha fault which generally separates the Jurassic from Eocene formations to the north, and the Jurassic from

the Paleogene formations to the south (Figure 12). Large scale offset features within the drainage indicate a cumulative left-lateral displacements of ~3 km (A-A'). The total cumulative left-lateral slip cannot correspond to the ~6 km between points A and A", because the catchment basin upstream A" is too small. North of this main left-lateral strike-slip linear segment, we observe a parallel branch along which the deformation is also left-lateral (see below) and would evolves gradually to oblique left-lateral-reverse considering the gradual change of strike from N110°E to N130°E.

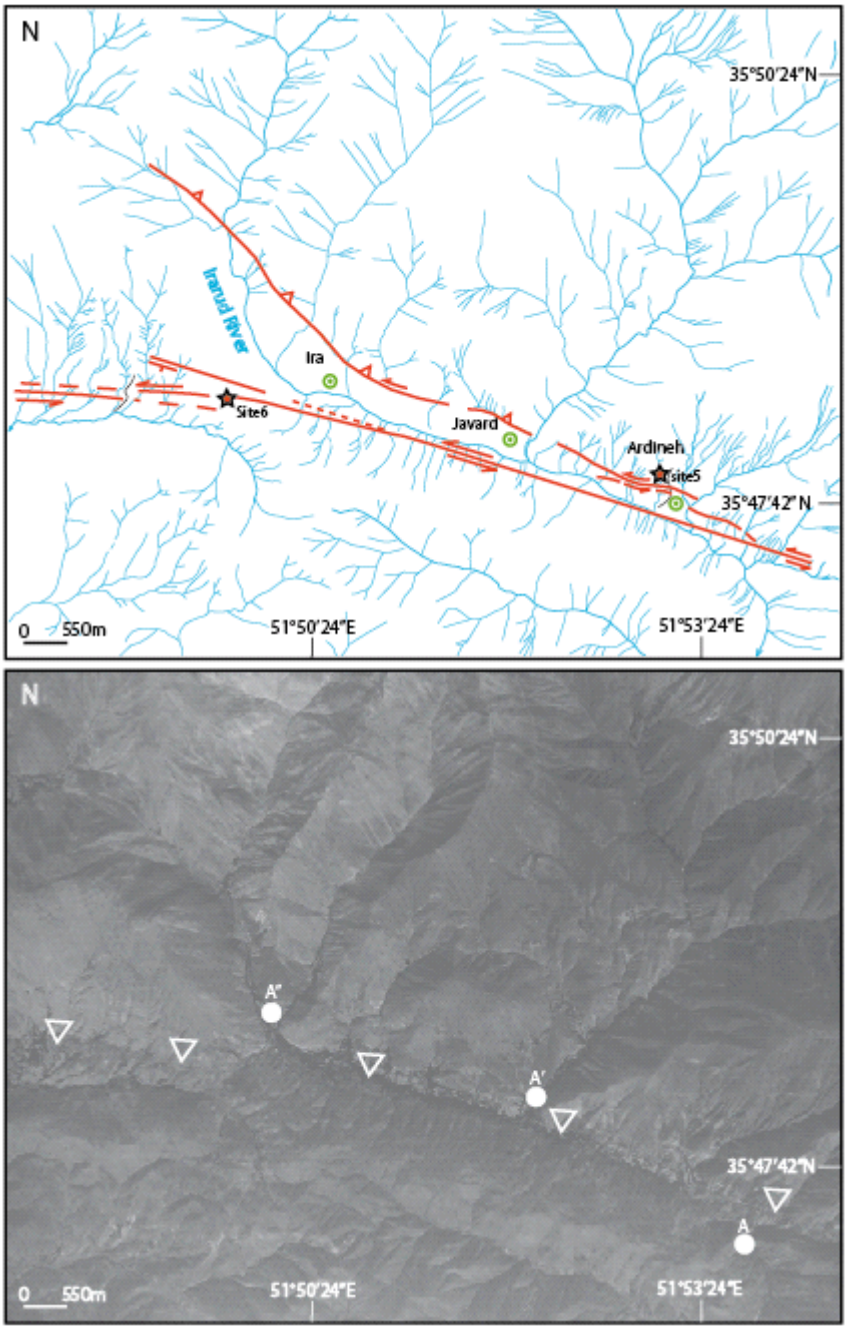

Figure 12: Aerial photograph and its interpretation of the Mosha fault zone within the Ardineh-Ira valley, between Ardineh and Ira villages.

Field observations in the eastern part of the Ardineh-Ira valley allowed us to better constrain the kinematics of recent faulting in this area. Site 5 is located where we interpreted the occurrence of two parallel active branches from large-scale observations (see Figure 12). This site is located on the northern branch, just to the north of Ardineh village. There, we observed a topographic ridge shuttered left-laterally by two parallel rupture lines (Figure 13) cumulating together a horizontal displacement of ~55 m (A-A'). We estimated also a vertical component of ~18 m, which yields a ratio H/V of ~3.

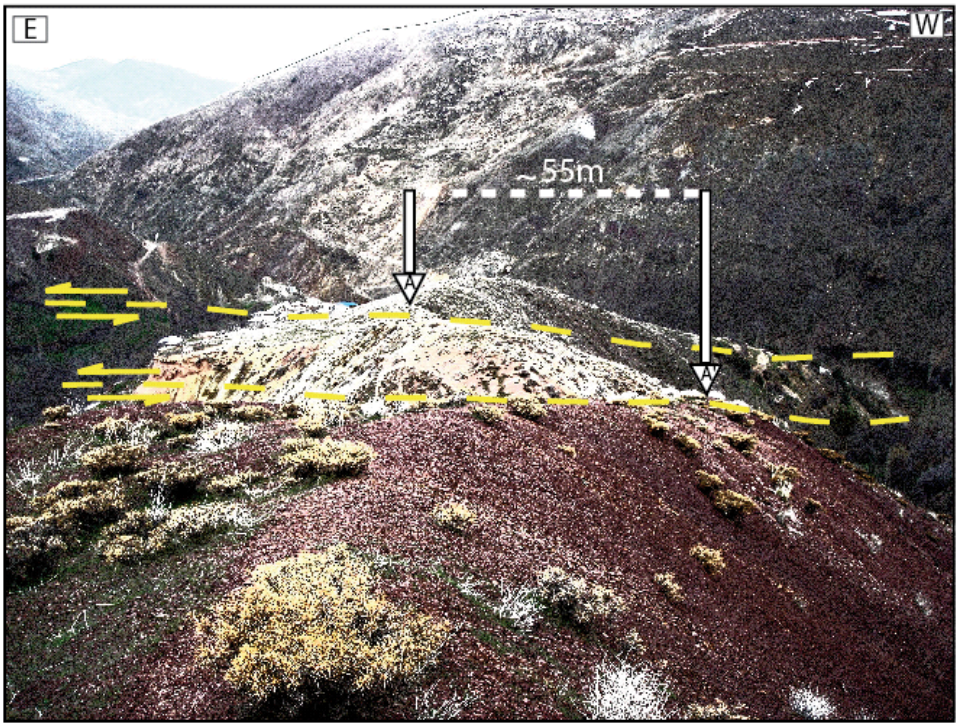

Figure 13: South view of the double-shutter-ridge north of Ardineh village (A-A' ~55 m).

3.4 The junction zone between the Central Mosha fault and the eastern North Tehran fault

From 51°50'24"E, the left-lateral strike-slip deformations observed along the Central Mosha fault stepped to the left within left-stepping branches bending progressively to the west (see Figure 12). We consider that this left-stepping pattern corresponds to the junction zone between the active Mosha fault and the active North Tehran fault. One kilometer west of Ira, we observed a symmetric hump in the morphology cut by a trench (site 6, see Figure 12). This artificial section shows a fault zone displaying several ruptures between bedrock

(Cenozoic and older formations) and Quaternary reddish soil units (Figure 14). Fault slip data (105, 83, 33) within the vertical ruptures indicate sinistral slips associated with a reverse component. Considering this kinematics data together with the general rupture pattern, we interpret the overall feature as positive flower structure associated with a main left-lateral strike-slip deformation.

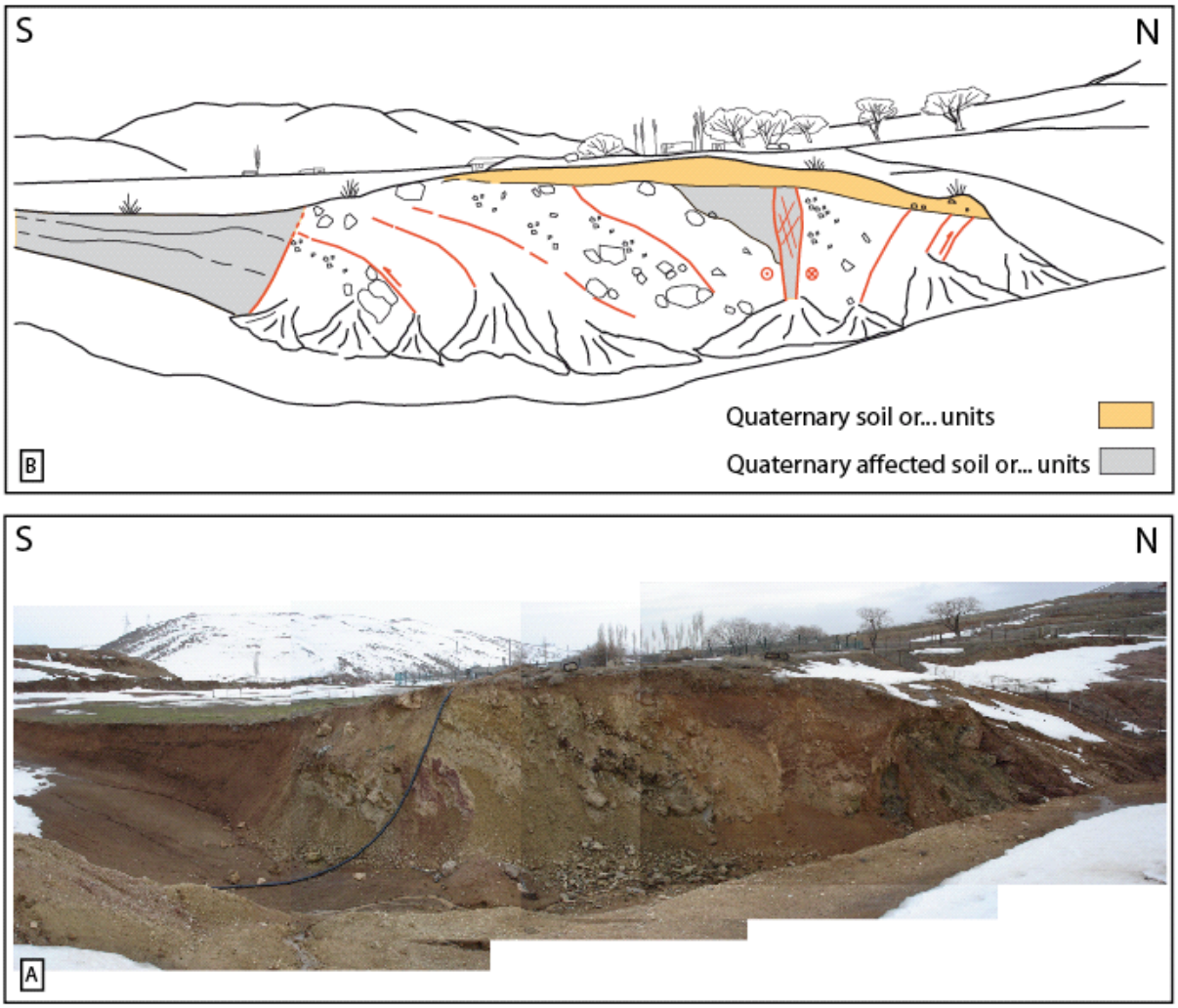

Figure 14: Field picture (A) and interpretation (B) of a flower structure observed west of Ira village.

Further west, towards Chahar-Bagh sets the eastern Lavasanat area. Our aerial photographs interpretation allows characterizing an overlapping zone of ~3 km length between the Central Mosha fault and the eastern termination of the North Tehran fault (Figure 15). Westwards Kalan village, we observed several left-lateral offset features within drainages and ridges along a ~N105°E trending linear trace corresponding to the North Tehran fault (Figure 16). Cumulative horizontal slip varies from 80, 330 to ~600 m.

To the north of the North Tehran fault, it is difficult to conclude about activity along the West-Central Mosha fault and its kinematics. Few morphotectonics features suggest that

the active left-lateral deformation continues westwards along a rupture bending from ~N105°E to N130°E. Considering this bending, the kinematics of this section of the Central Mosha fault (West-Central Mosha fault) would evolve gradually from mainly left-lateral to oblique reverse-left-lateral. Further north-westwards, we observed clearer evidences of oblique reverse-left-lateral deformations within the morphology and also Quaternary deposits. Slickensides along the rupture plane north of Afdjeh village characterize a thrust movement with a sinistral component (305, 70, 65 for strike, dip and rake, respectively).

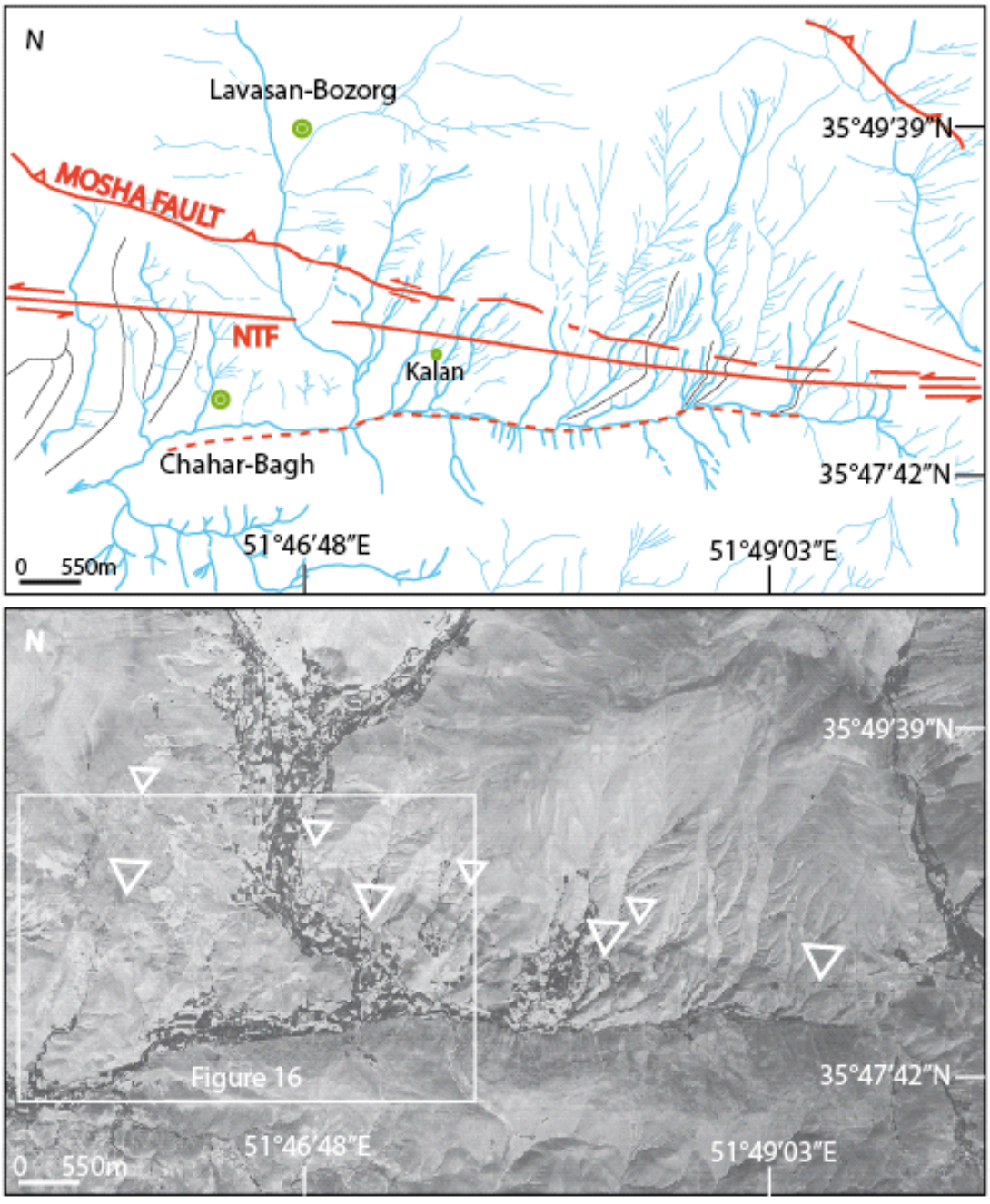

Figure 15: Aerial photo and its interpretation of the overlapping zone between the Central Mosha and North Tehran faults (NTF) within the eastern Lavasanat area (Lavasanat is the regional name of the area).

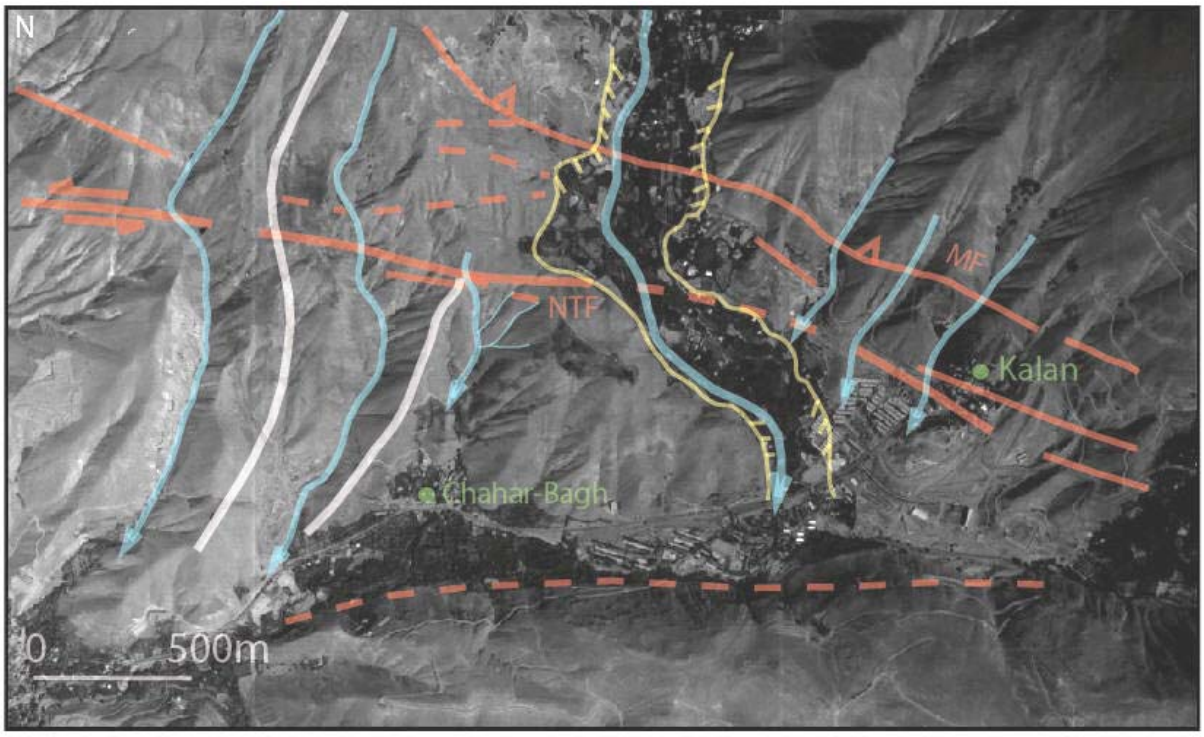

Figure 16: Enlargement of the junction zone between the Mosha (MF) and the North Tehran (NTF) faults at the immediate vicinity of Kalan village.

3.5 The eastern North Tehran fault within Lavasanat area between Chahar-Bagh and Galandoak

Within the central Lavasanat area, between Chahar-Bagh and Sabu-Bozorg the alignment of several offset streams and ridges define the active trace of the eastern North Tehran fault (Figure 17). This active trace corresponds generally to the tectonic contact between Eocene and Plio-Quaternary formations. The trace of the fault can be followed from Chahar-Bagh to Niknam-Deh and further west. Its linearity indicates that the fault plane has a steep dip. West of Niknam-Deh village, the large-scale deflection of a river indicates a cumulative left-lateral displacement of ~900 m (Figure 18), while the present river bed shows a deflection of ~200 m.

West of 51°42’18”E, the trace of the fault bends slightly from N095°E to N085°E, and several parallel ~1-2 km long fault strands can be traced southwards of the main trace. One of these parallel strands is located at the north-eastern vicinity of Sabu-Bozorg village (site 7 in Figures 3 and 17), and corresponds to the offset of two drainages and their interfluve. We estimated the horizontal and the vertical cumulative displacements to be ~40 (A-A’) m and ~10 m, respectively (Figure 19).

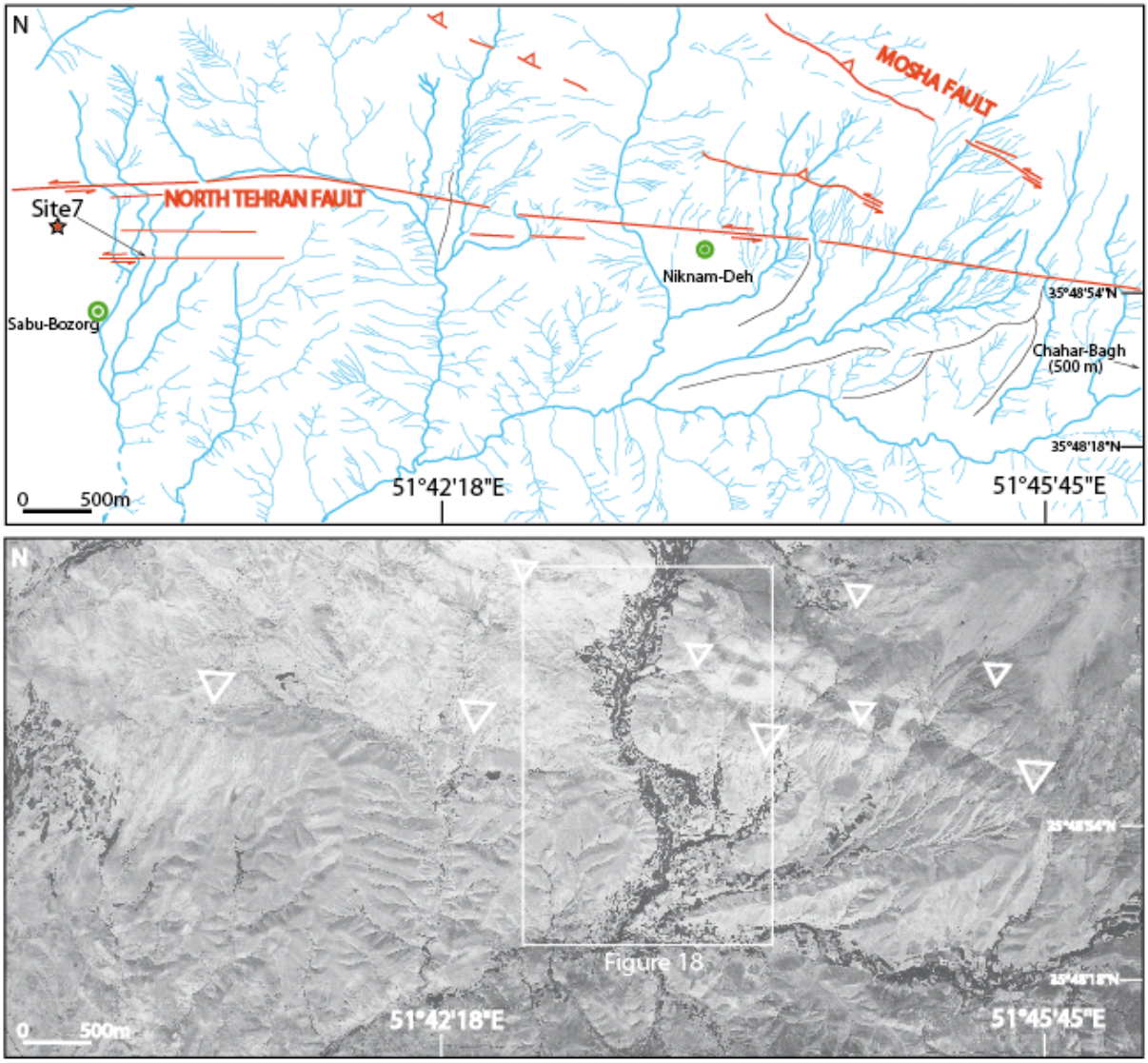

Figure 17: Aerial photo and its interpretation of active features observed along the North Tehran fault between Chahar-Bagh and Sabu-Bozorg in the Lavasanat area.

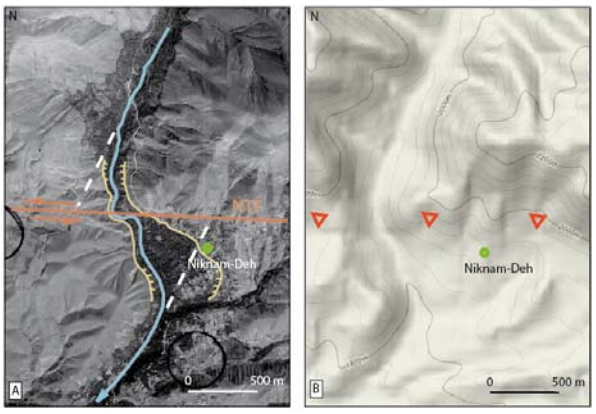

Figure 18: Enlargement of the North Tehran fault trace westwards from Niknam-Deh village (Lavasanat area). (A) Aerial photograph with main morphotectonics features: The white dashed lines define the maximum left-lateral offset (900 m) estimated from the deflection of the river. (B) Contour lines from Google maps with red triangles pointing out the North Tehran fault trace.

Figure 19: Southwards view of a left-laterally offset drainage and interfluve at the north-eastern vicinity of Sabu-Bozorg village within the central Lavasanat area (site 7, Figure 17).

Within the western Lavasanat area, the trace of the North Tehran fault is difficult to follow in the morphology due to the modifications of the landscape by human activities. Figure 20 shows an interpretation of the morphology within the Galandoak village (Galandoak is now a city). In the eastern part of the 1955 aerial photograph, the Afdjeh river shows a deflection feature matching the westwards extension of the North Tehran fault mapped in Sabu-Bozorg (see Figure 20 and enclosed contour map).

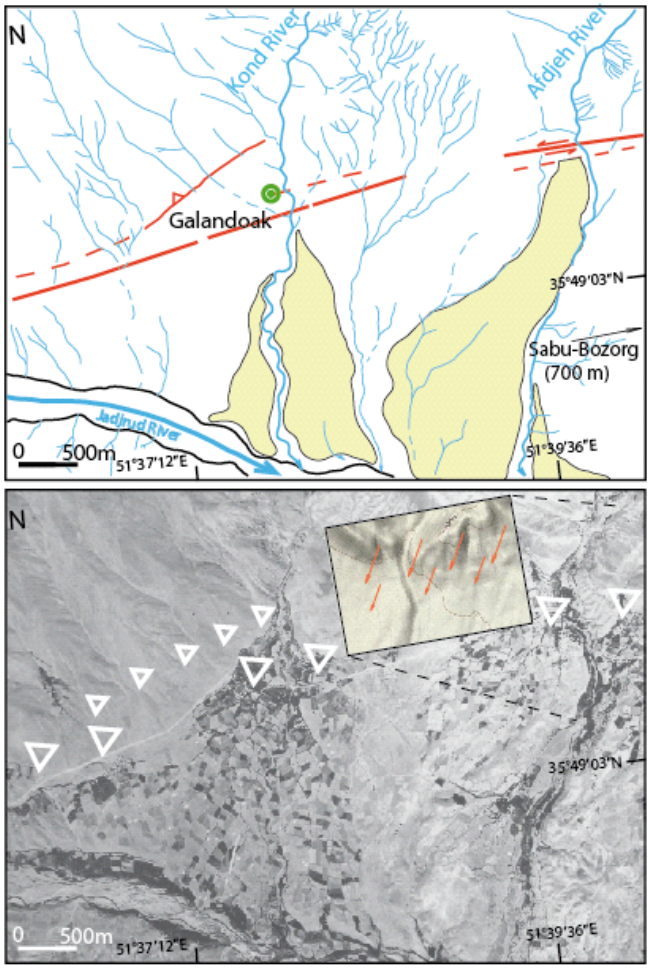

Figure 20: Aerial photograph and its interpretation of the North Tehran fault zone within the western part of the Lavasanat area. The contour map enclosed in aerial photo is from Google map and shows the trace of the North Tehran fault cutting through the Afdjeh River. The yellowish surfaces show the alluvial fan deposits associated with the Afdjeh and Kond rivers.

3.6 The North Tehran fault within the northeast of Tehran city

West of the Jadjrud River, between Lashgarak and Suhanak, several evidences for left-lateral strike-slip faulting can be observed in the morphology (Figure 21). Within the Jadjrud River, the trace of the fault is rather simple with two branches trending N075° and defining a right-stepping system. Further west, towards Suhanak, the active traces are more complex and define a fault zone displaying several straight branches.

Kinematics indicators are observed within the Jadjrud River. Along the eastern branch, active faulting is localized within a narrow fault zone, showing left-laterally offset drainages (Figure 22). Figure 23 represents a cross section at the western tip of the fault branch (site 8 in Figure 21) showing a set of steep north-dipping contacts affecting Eocene Karaj formation and Plio-Quaternary alluvium. Taken the left-lateral movement observed in the morphology

and the structures pattern observed in cross-section, we interpret the overall features as a positive flower structure associated with the active left-lateral strike-slip deformation along the fault.

The western branch shows a northern dip when it crosses the Jadjrud River but a southern dip further west (Figure 24). Evidences of left-lateral strike-slip movements are seen within the left bank of Jadjrud River showing a horizontal displacement of about 100 m (Figure 21), and further west where small drainage shows also horizontal deflections (Figure 24).

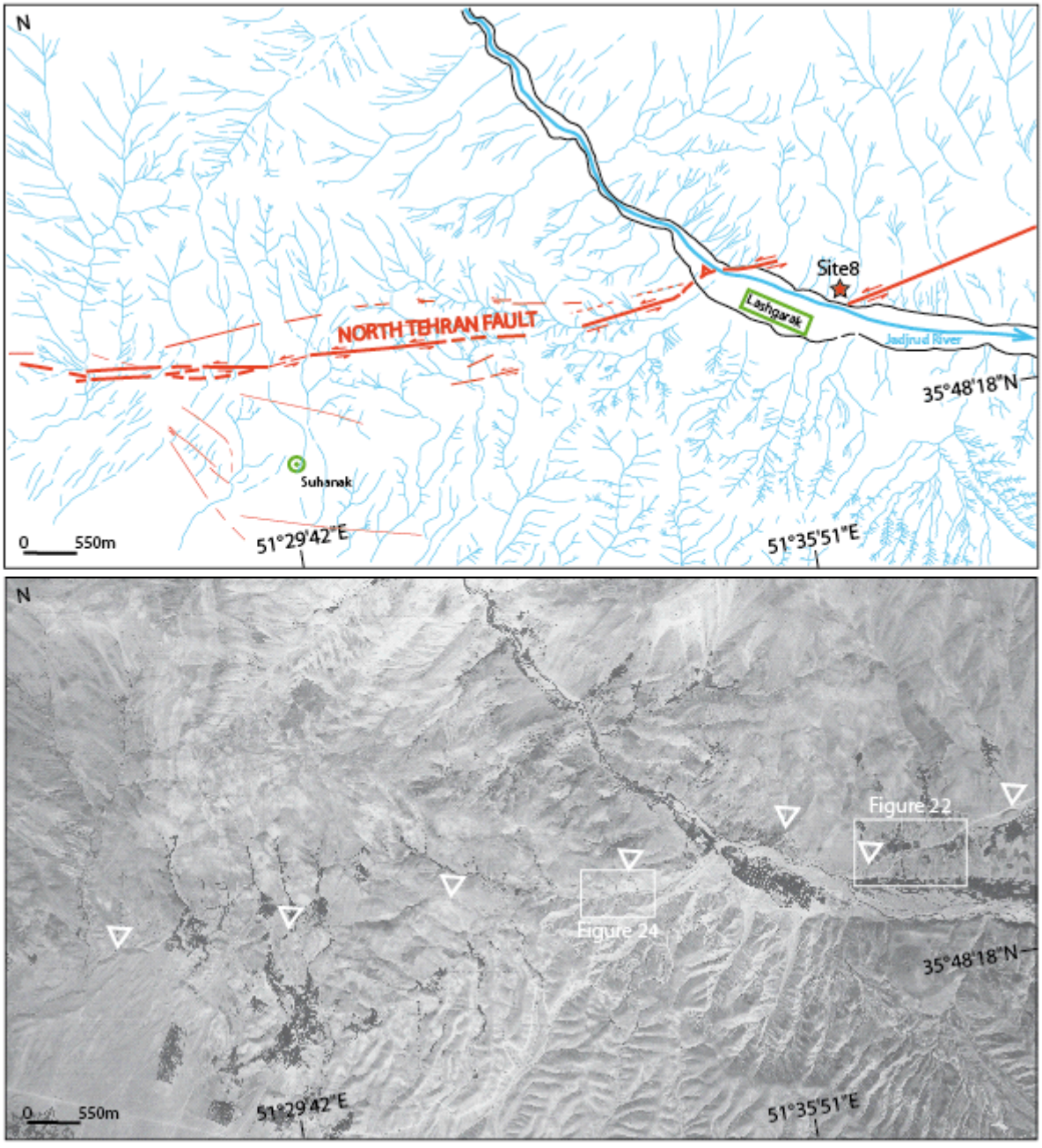

Figure 21: Aerial photograph and its interpretation of the North Tehran fault within the Lashgarak-Suhanak region.

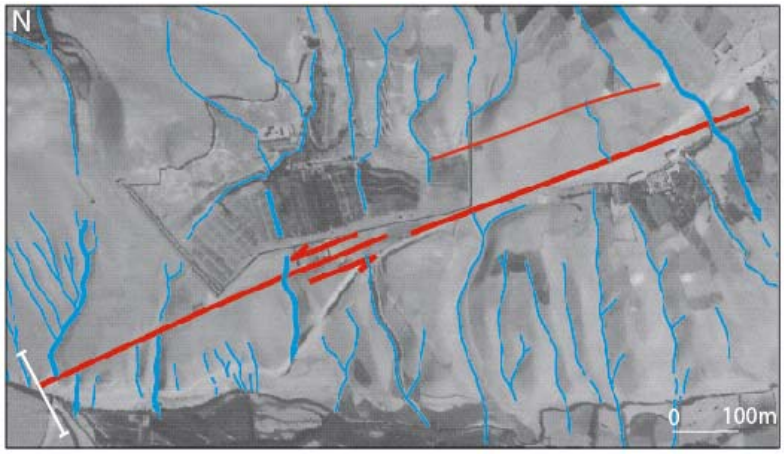

Figure 22: Large scale aerial photo with interpretation of morphotectonics features along the North Tehran fault, east of Lashgarak. The white solid line indicates the cross section presented in Figure 23A.

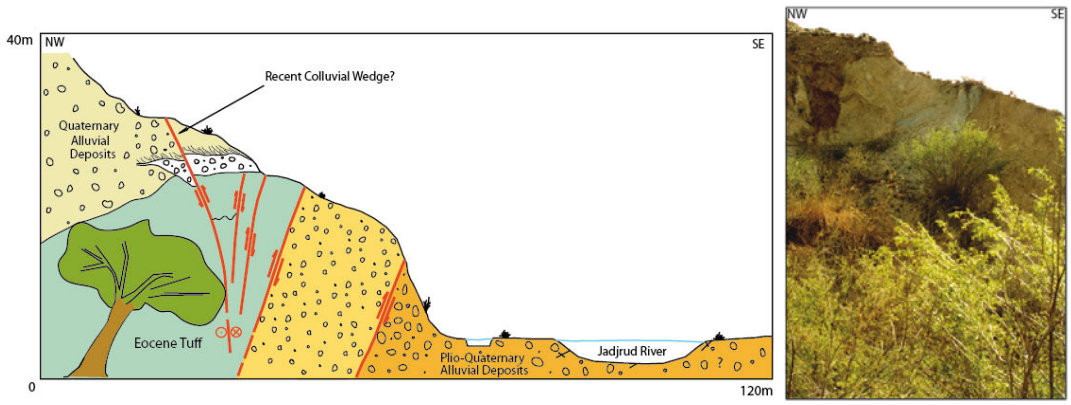

Figure 23: A: Schematic cross section of the North Tehran fault scarp within Jadjrud River (site 8; see Figure 21 for location). B: Picture of the fault zone.

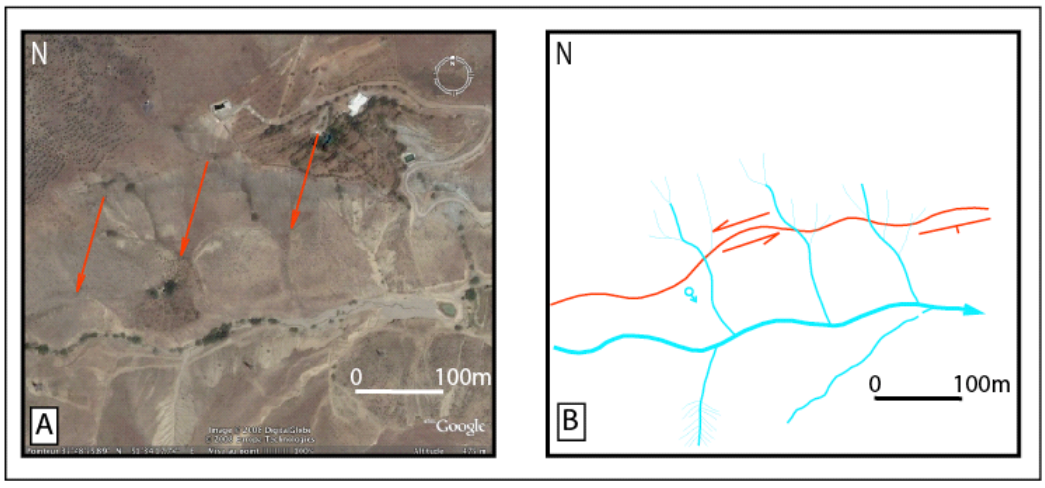

Figure 24: Google earth satellite image of the North Tehran fault west of Lashgarak Valley. The trace of the fault is located along the north slope of this morphologically linear valley (see Figure 21 for location).

3.7 The North Tehran fault within the northeast of Tehran between Suhanak and Darabad.

Between Suhanak and Darabad, within the northeastern Tehran region, at the western end of the Lashgarak linear valley, the active tectonics features corresponding to the North Tehran fault, are distributed on several strands defining a general ~E-W trend (Figure 25). Left-lateral offset features are observed in the morphology ~1 km northwards of Suhanak village, where several streams and ridges are left-laterally shifted with a displacement of about ~150-200 m (Figure 26). No obvious vertical component seems to be associated with this left-lateral strike-slip deformation.

At Darabad village, the active left-lateral movements observed along the North Tehran fault are transferred along the Niavaran fault, looking as a right-stepping en echelon of the North Tehran fault. Evidences for recent deformations keep straight across Tehran city along the Niavaran fault, which morphotectonics features indicating left-lateral strike-slip displacements more than 500 m (Figure 27).

No clear evidences of recent activity is noticed along the North Tehran fault strictly speaking, classically mapped as a thrust fault following the sinuosity of the southern mountain front. Figure 28 shows the north-dipping North Tehran fault, 1 km west of Jamaran, cutting through the andesitic tuffs layers of the Karaj formation, Eocene in age. Fault slip data (277, ~70N, 23) within the steeped rupture indicate sinistral slips associated with a reverse component. Nearby this site, a rock avalanche seems to be affected by the fault scarp (Figure 25) but this feature observed on aerial photograph could not be confirmed in the field.

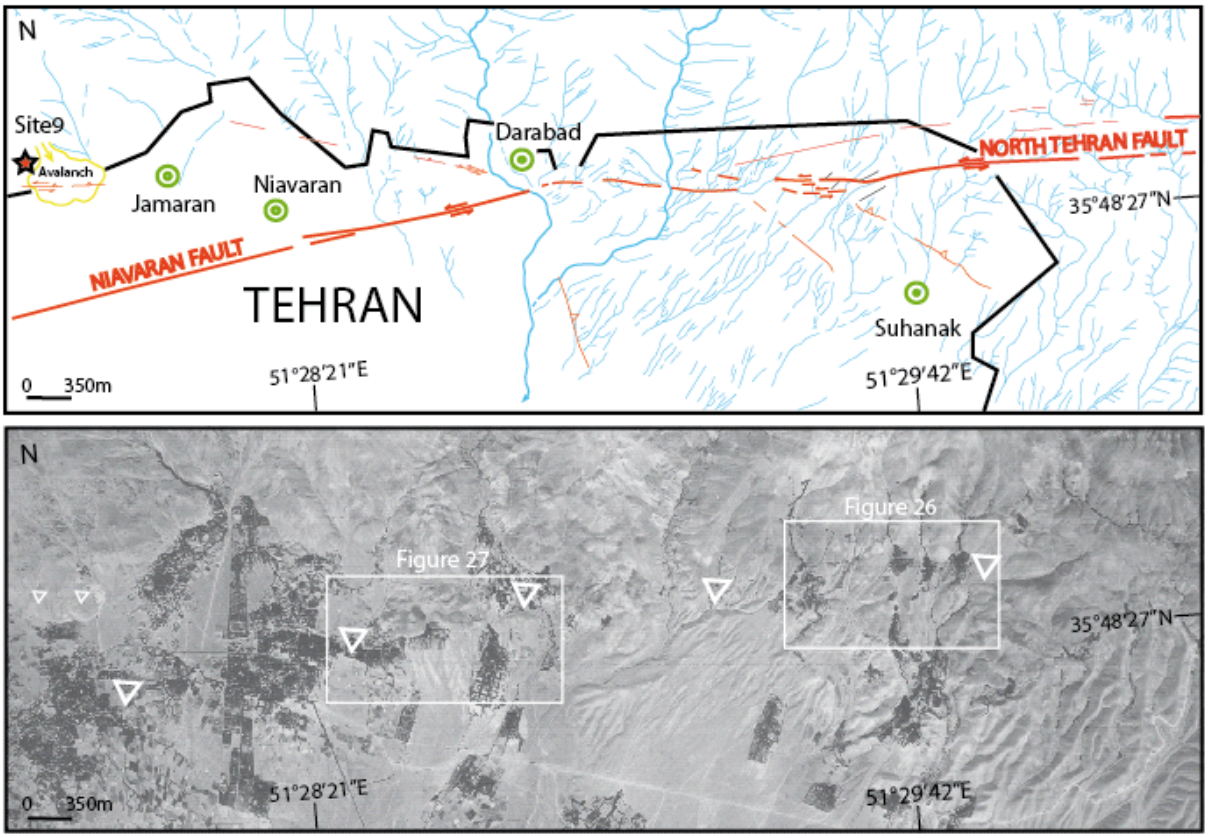

Figure 25: Aerial photo and its interpretation of the North Tehran and Niavaran faults northeast of Tehran. At Darabad village, the active left-lateral movement observed along the North Tehran fault is transferred along the Niavaran fault, which appears as a right-stepping en echelon of the North Tehran fault.

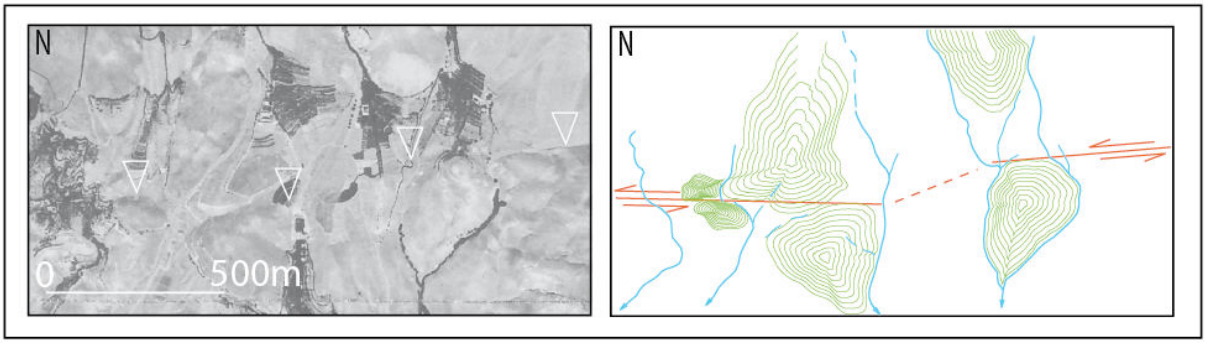

Figure 26: Enlargement of the North Tehran fault trace shows en echelon geometry north of Suhanak village. Here, the drainage beds and ridges offset clearly left-laterally.

Figure 27: Aerial photograph of the Niavaran fault. Note the left-lateral offset (> 500m) of the terrace riser.

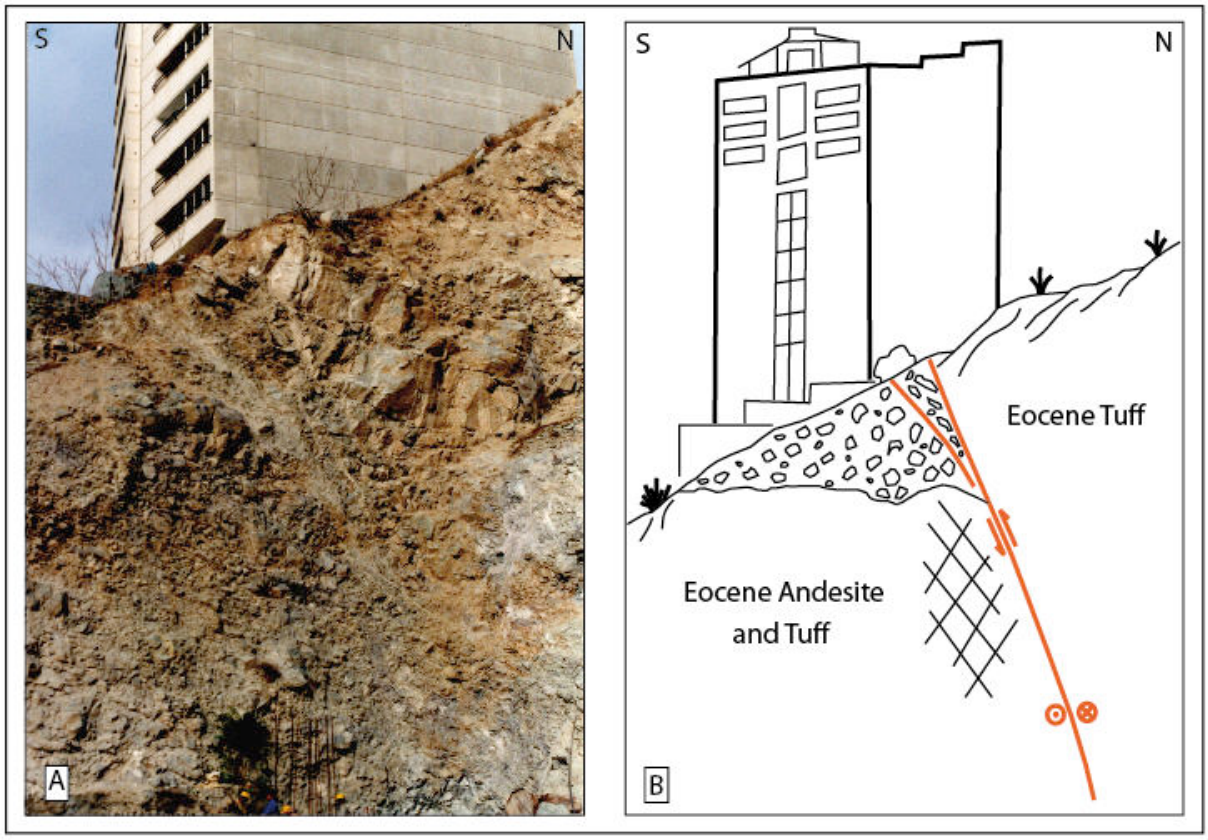

Figure 28: Picture of a quarry and its interpretation showing the North Tehran fault 1 km west of Jamaran (site 9 in Figures 2 and 25). Note the steep north-dipping shear zone in the Eocene tuffs (Karaj formation), with brecciation of the layers near the surface.

4. Discussion and Conclusions

In this paper, we clarified both the present structural relationships and kinematics of the Mosha and North Tehran faults at their junction. Mosha and North Tehran active traces affect quaternary features such as Late Pleistocene glacial markers, streams, ridges, or terrace risers. Cutting straight across the topography, these traces define steep faults with either north- or south-dipping directions, along which clear evidences for left-lateral strike-slip faulting are found.

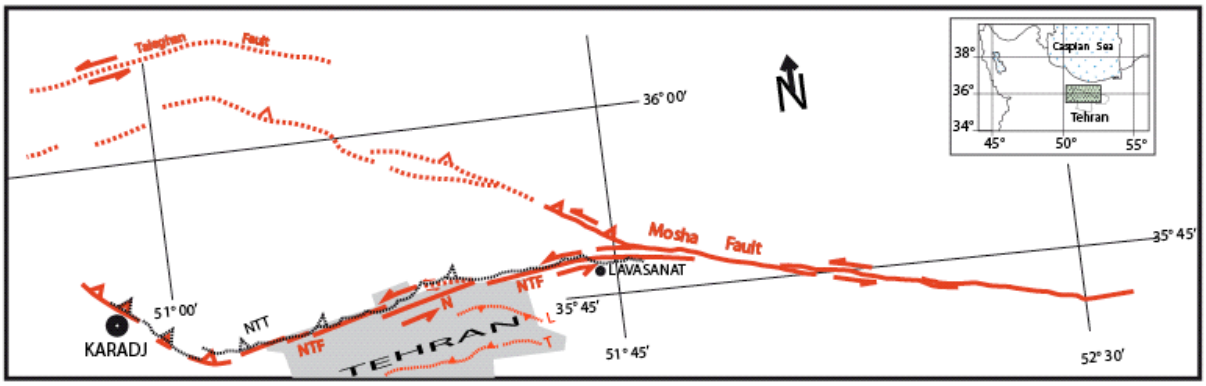

Figure 29: Sketch map of active faulting within northern Tehran region. The traces of activity within our study area (red solid red lines) generally do not follow the older traces corresponding to previous long-term dip-slip thrusting movements (black doted line with NTT for North Tehran Thrust). The recent faulting movements are occurring on new traces trending from WNW-ESE to the east to WSW-ENE to the west, affecting quaternary features. NTF: North Tehran Fault, N: Niavaran fault, L: Lavizan fault and T: Tarasht fault (L and T locations after Abbassi and Farbod, 2009).

Evidences of predominant active left-lateral strike-slip faulting are found from the eastern Mosha valley to the Tehran city, all along the junction zone between the Mosha and the North Tehran faults. Eastwards of the junction zone, within the Mosha valley (site 1) and around Ardineh village (site 5), we estimate a ratio between horizontal and vertical displacements of (H/V) $\geq$ 3. This result differs from previous studies that estimated ratios of ~2 and ~1 at these same sites, respectively (Trifonov et al, 1996; Bachmanov et al., 2004). The difference of interpretation is even larger when one considers that the vertical displacement corresponds generally to a normal component and not a reverse component as interpreted by the above-mentioned authors. This local slight transtensional deformation is generally associated to left-stepping en echelon pattern. It is explained by the obliquity of the

WNW-ESE trending Central Mosha fault zone with respect to the general NE-SW trend of the range (Ritz et al., 2006; Ritz, Geology, accepted).

The left-lateral strike-slip motion is then transferred westwards along a fault zone bending progressively from WNW-ESE to WSW-ENE, along the eastern North Tehran fault zone. There, newly-formed fault branches show right-stepping en echelon pattern suggesting local transpressional deformation. One of this main right-stepping en echelon features is occurring between the eastern part of North Tehran fault and the Niavaran fault, a left-lateral strike-slip WSW-ENE trending fault, crossing straight across the northern part of the Tehran megacity. This right stepping en echelon left-lateral strike-slip fault pattern would extent further west until Karadj region, where are observed active NW-SE trending thrust faults (Nazari et al. JGR, in revision).

Our investigations show that along the eastern part of the central Mosha fault, the traces of recent activity follow generally older structures. On the other hand, recent faulting features do not often follow the previous long-term dip-slip thrusting movements along the North Tehran fault at the foothills of the reliefs but instead occur on new traces trending WSW-ENE (Figure 29). This result differs from Landgraf et al (2009) study interpreting sinistral component along the geological trace of the North Tehran fault.

The cumulative offsets associated with this left-lateral deformation is small compared with the topography associated with the previous Late Tertiary thrusting motion, suggesting a recent change of fault kinematics. This is consistent with the interpretations of several works that described similar changes of kinematics from mainly reverse to mainly left-lateral at local scale (e.g. Shabanian and Abbassi, 1999; Solaymani et al., 2003; Abbassi and Farbod, 2009). This change correlates well also with the regional model proposed by Ritz et al. (2006) and Ritz (Geology, accepted) for the South-Caspian region and Alborz. In our study, we estimate ~3 km of cumulative left-lateral displacement along the Central Mosha fault between Abali and Ira (see figures 11, 12). This is the same cumulative offset than Ritz et al. (2006) estimated along the eastern Central Mosha fault, from which they inferred an age of 1-1.5 Ma for the kinematical change (dividing the 3 km of cumulative offset by a 2.2 mm/yr horizontal slip rate). The same timing is proposed by Nazari et al. (2009a) along the Taleghan fault, by dividing the 450 m of observed cumulative vertical deformation by a 0.5 mm/yr vertical slip rate. Note that the cumulative left-lateral offsets that we observed along the NTF is lower (0.6 to ~1 km) than along the Mosha fault (~3 km) suggesting either that the kinematic change has propagated from east to west, or that the left-lateral slip rate decreases from east to west. We do not have yet enough data to conclude.

Our observations are also consistent with geodetic data (Djamour et al. 2008, Djamour et al., in revision) showing that the southern Central Alborz is mainly characterized by left-lateral interseismic deformation rather than vertical deformation.

At last, our study highlights at different way the question of the source for the past 1830 AD, Ms 7.1 historical earthquake. Interpreted classically as being associated with the Western Central Mosha fault (Berberian and Yeats, 1999). Our observation suggests that its mechanism was left-lateral and its source probably closer to Tehran than proposed earlier, within the junction zone between the Mosha fault and the North Tehran fault.

Acknowledgments

This work was supported by the International Institute of Earthquake Engineering and Seismology (IIEES) and the laboratory of Geosciences Montpellier of the University Montpellier 2. We are grateful to M. Osati and I. Zahedi for their logistics help in the field, and to F. and M. Kushki for digging the trench in Abali. We thank H. Tabassi, E. Shabanian and K. Fegghi for fruitful discussions, and S. Mahan for OSL dating of unit 4 in the Abali trench.

References

Abbassi, M. R., Shabanian-B, E., Farbod, Y., Feghhi, Kh. And Tabassi, H., 2003. The state of contemporary stress in the southern flank of Central Alborz. International Institute of Earthquake Engineering and Seismology: Tehran, Iran, 122 p., Publication No: 81-2003-7 (in Persian).

Abbassi, M. R., Farbod, Y., 2009. Faulting and folding in quaternary deposits of Tehran's piedmont (Iran). Journal of Asian Earth Science 34, 522–531.

Alavi, M., 1996. Tectonostratigraphic synthesis and structural style of the Alborz mountain system in northern Iran. Journal of Geodynamics 21, 1 – 33.

Allen, M.B., S.J. Vincent, I. Alsop, A. Ismail-zadeh, R Flecker, 2003a. Late Cenozoic deformation in the South Caspian region: effects of a rigid basement block within a collision zone, Tectonophysics 366, 223– 239.

Allen, M.B., Ghassemi, M.R., Shahrabi, M., and Qorashi, M., 2003b. Accommodation of late Cenozoic oblique shortening in the Alborz range, northern Iran: Journal of Structural Geology, 25, p. 659–672.

Allenbach, P., 1966. Geologie und petrographie des Damavand und seiner Umgebung (Zentral Elburz), Iran, Geol. Mitt. Geol. Inst. ETH Univ. Zurich, n. s., 63, 144p.

Ambraseys, N.N. & Melville, C.P., 1982. *A History of Persian Earthquakes*. Cambridge University Press, New York.

Ashtari, M., Hatzfeld, D., and Kamalian, M., 2005. Microseismicity in the region of Tehran: Tectonophysics, 395, p. 193–208.

Axen, G. J., P. J. Lam, M. Grove, D. F. Stockli, andJ. Hassanzadeh, 2001. Exhumation of the westcentral Alborz mountains, Iran, Caspian subsidence,and collision-related tectonics, Geology, 29, 559 – 562, doi:10.1130/0091-7613(2001)029<0559:EOTWCA>2.0.CO;2.

Bachmanov, D.M., Trifonov, V.G., Hessami, Kh.T., Kozhurin, A.I., Ivanova, T.P., Rogozhi, E.A., Hademi, M.C., and Jamali, F.H., 2004. Active faults in the Zagros and central Iran: Tectonophysics, v. 380, p. 221–241.

Ballato, P., N. R. Nowaczyk, A. Landgraf, M R. Strecker, A. Friedrich, and S. H. Tabatabaei, 2008. Tectonic control on sedimentary facies pattern and sediment accumulation rates in the Miocene foreland basin of the southern Alborz mountains, northern Iran. Tectonics, 27, TC6001, doi:10.1029/2008TC002278. (3.413).

Berberian, M., 1976. Contribution on the Seismotectonics of Iran: Part I. Geological Survey of Iran, Tehran. 517 pp.

Berberian, M., 1983. The southern Caspian: a compressional depression floored by a trapped, modified oceanic crust. Canadian Journal of Earth Sciences 20, 163–183.

Berberian, M., Qorashi, B., Arzhang-ravesh, A., Mohajer-Ashjai, 1985. Recent tectonics, seismotectonics and earthquake fault hazard investigations in the greater Tehran region: contribution to the seismotectonics of Iran: Part V, Geological Survey of Iran, report 56, 316 pp, 1985.

Berberian, M., Yeats, R.S., 1999. Patterns of historical earthquake rupture in the Iranian plateau. Bulletin of the Seismological Society of America 89, 120–139.

Berberian, M., Yeats, R.S., 2001. Contribution of archaeological data to studies of earthquake history in the Iranian plateau. Journal of Structural Geology 23, 563– 584.

Berberian,M .(1994).Natural Hazards and the First Earthquake catalogue of Iran, vol. 1, Historical Hazards in Iran Prior to 1900,A UNESCO/IIEES Publication during UN/IDND International Institute of Earthquake Engineering and Seismology Tehran, 603 + 66 pp.

Dellenbach, J., 1964. Contribution à l'étude géologique de la region située a l'est de Téhéran (Iran). Faculté des Science de l'Universite Strasbourg (France), 117pp.

Djamour, Y., Bayer, R., Vernant, P., Hatam, Y., Ritz, J. F., Hinderer, J., Luck, B., Nankali, H., Le Moigne, N., Sedighi, M., Boy, J. P. 2008, The present-day deformation in Alborz (Iran) depicted by GPS and absolute gravity observations: Paris, France, SGF

Djamour, Y., 2004. Contribution de la Géodésie (GPS et nivellement) à l'étude de la déformation tectonique et de l'aléa seismique sur la région de Téhéran (montagne de l'Alborz, Iran), Faculté des Sciences et des techniques du Languedoc l'Université Montpellier II (France), 180pp.

Dresch, J., 1961, Le piedmont de Téhéran, Les observations de géographie physique en Iran septentrional : Centre Docum. Cart. Geogr., Mem. et Docum., 8, 85-101.

Geological Survey of Iran, 1993. 1:100,000 Geology map of Tehran. Geological Survey of Iran, Tehran.

Guest, B., D. F. Stockli, M. Grove, G. J. Axen, P. S. Lam, and J. Hassanzadeh, 2006b. Thermal histories from the central Alborz mountains, northern Iran: Implications for the spatial and temporal distribution of deformation in northern Iran, Geol. Soc. Am. Bull., 118, 1507 – 1521, doi:10.1130/B25819.1.

Guest, B., G. J. Axen, P. S. Lam, and J. Hassanzadeh , 2006a. Late Cenozoic shortening in the west central Alborz mountains, northern Iran, by combined conjugate strike-slip and thin-skinned deformation, Geosphere, 2, 35 – 52, doi:10.1130/GES00019.1.

Hedayati, A., Brander, J.L., Berberian, M., 1976. Microearthquake survey of Tehran region, Iran. Bull. Seismol. Soc. Am. 66, 1713–1725.

Hessami, K., Jamali, F., Tabassi, H., 2003. the map of major active faults of Iran., International Institute of Earthquake Engineering and Seismology.

Holingsworth, J., Jackson, J., Walker, R., Nazari, H., 2008. Extrusion tectonics and subduction in the eastern South Caspian, J. Geology, V. 36, N. 10, 763-766.

Hollingsworth, J., 2007. Active Tectonics of NE Iran , PhD thesis University of Cambridge, 220 pp.

Ritz J-F, H. Nazari, H.A., R. Salamati, A. Shafeii, S. Solaymani, 2006. Active transtension inside Central Alborz: a new insight into the Northern Iran–Southern Caspian geodynamics, Geology 34, 477–480.

Jackson, J., Priestley, K., Allen, M., Berberian, M., 2002. Activetectonics of the South Caspian Basin. Geophysical Journal International 148, 214– 245.

Knill and Jones , K.S., 1968, Ground water conditions in Greater Tehran. Quart. J. Eng. Geol., 1, 181-194.

Landgraf A., P. Ballato, M. R. Strecker, A. Friedrich, S. H. Tabatabaei and M. Shahpasandzadeh, 2009, Fault-kinematic and geomorphic observations along the North Tehran Thrust and Mosha Fasham Fault, Alborz mountains Iran: implications for fault-system evolution and interaction in a changing tectonic regime, *Geophys. J. Int.* 177**,** 676–690

Nabavi, M. H., 1976, Preface to geology of Iran, Geological survey of Iran, 109 p.

Nazari H., Ritz J-F., A. Shafei, A. Ghassemi, R. Salamati, J-L. Michelot and M. Massault, 2009a. Morphological and paleoseismological analyses of the Taleghan fault, Alborz, Iran, GJI, accepted

Nazari H., Ritz J-F., Balescu S., Lamothe M., R. Salamati, A. Ghassemi, A. Shafei, M. Ghoraishi, A. Saidi, J-L. Michelot and M. Massaut, 2009b, Paleoseismological analysis of the North Tehran Fault, Iran: Analysing Prehistoric ruprures for the past 30.000 years, JGR, in revision

Nazari, H., 2006. Analyse de la tectonique récente et active dans l'Alborz Central et la région de Téhéran : Approche morphotectonique et paléoseismologique, Faculté des Sciences et des techniques du Languedoc l' Université Montpellier II (France), 246pp.

Negahban, E.O., 1977. Report of Preliminary excavations at Tapeh Sagzabadin the Qazvin plain. Marlik, Journal of the Institute and Department of Archaeology, 2, Faculty of Letters and Humanities, Tehran University, pp. 26 and 45 (in Persian and English).

Pedrami, M., 1983, Plio-Pleis resch, J., 1961. Le piedmont de Téhéran, In observations de géographie physique en Iran septentrional : Centre Docum.Cart. Geogr.,Mem. et Docum., 8, 85-101.

Rieben, E.H., 1955. The geology of Tehran plain. American Journal of Science 253, 617–639.

Ritz J.-F., Extrusion tectonics and subduction in the eastern South Caspian region since 10 Ma: Comment, Geology, in press.

Ritz, J.-F., Balescu, S., Soleymani, S., Abbassi, M., Nazari, H., Feghhi, K., Shabanian, E., Tabassi, H., Farbod, Y., Lamothe, M., Michelot, J.-L., Massault, M., Che´ry, J., Vernant, P., 2003. Determining the long-term slip rate along the Mosha fault, Central Alborz, Iran. Implications in Terms of Seismic Activity, S.E.E. 4 Meeting, Tehran, 12–14 May.

Sieber, N., 1970. Zur geologie des gebietes sudlich des Taleghan-tales, Zentral Elburz (Iran), Europaische Hochsch, Schrschriften, 19(2), 126p.

Solaymani, Sh., Feghhi, Kh., Shabanian, E., Abbassi, M.R., Ritz, J.F., 2003. Preliminary paleoseismological studies on the Mosha Fault at Mosha Valley. International Institute of Earthquake Engineering and Seismology, 89 p. (in Persian).

Steiger, R., 1966. Die geologie der west-Firuzkuh area (Zentral Elburz/Iran), Mitteilung Geologisches Institut, ETH-Zurich, 145p.

Stöcklin, J. 1974. Northern Iran: Alborz Mountains. *In* Mesozoic-Cenozoic belts. *Edited by* A. M. Spencer. Geological Society of London, Special Publications, 4, pp. 213-234.

Stöcklin, J., 1968. Structural history and tectonics of Iran. A review: Bull. Amer. Assoc. Petrol.Geol. 52 (7), pp. 1229-1258.

Tala'i, H., 1998. Preliminary report of the 10th excavation season (1998) at Tappeh Sagzabad, Qazvin Plain. Archaeological Institute, Tehran University, unpublished internal report, 31 p.

Tatar, M., Hatzfeld, D., 2009. Microseismic evidence of slip partitioning for the Rudbar-Tarom earthquake (*M*s 7.7) of 1990 June 20 in NW Iran, Geophisical Journal International **176,** 529–541

Tchalenko, J.S., 1975. Seismotectonics framework of the North Tehran fault. Tectonophysics 29, 411– 420.

Tchalenko, J.S., Berberian, M., Iranmanesh, H., Bailly, M., Arsovsky, M., 1974. Tectonic framework of the Tehran region, Geological Survey of Iran, Report n° 29.

Trifonov, V.G., Hessami, K.T., Jamali, F., 1996. West-Trending Oblique Sinitral–Reverse Fault system in Northern Iran. IIEES Special Publication 75. Tehran, Iran.

Vernant, P., Nilforoushan, F., Che´ry, J., Bayer, R., Djamour, Y., Masson, F., Nankali, H., Ritz, J.F., Sedighi, M., and Tavakoli, F., 2004, Deciphering oblique shortening of central Alborz in Iran using geodetic data: Earth and Planetary Science Letters 223, p. 177–185.

Zanchi , A., F. Berra, M. Mattei, M.R. Ghassemi and J. Sabouri, 2006. Inversion tectonics in central Alborz, Iran, J. Struct. Geol., 20, 1-15.

CHAPITRE 3

LA FAILLE NORD TABRIZ

Ce chapitre est consacré à l'une des failles active les plus connues de l'Iran. Malgré cela beaucoup de problèmes la concernant restent à résoudre, en particulier ce qui regarde l'aléa. Ce problème est important compte tenu de la proximité de la faille à l'une des villes les plus peuplées d'Iran. Comme pour Téhéran, la faille de Tabriz passe dans les quartiers nord de la ville. D'autre part, la ville a été détruite à deux reprises au XVIII ème siècle.
Sur le plan tectonique, le tracé de la faille est à préciser, notamment à ces extrémités qui peuvent constituer les zones où sont absorbés les déplacements horizontaux de la partie centrale.

Paleoseismological and morphological evidences of slip variations along the North Tabriz Fault (NW Iran)

SOLAYMANI AZAD S. (1,2), PHILIP H. (1), DOMINGUEZ S. (1), HESSAMI K. (2), SHAHPASAND ZADEH M. (2), FORUTAN M-R (3), TABASSI H. (2), LAMOTHE M. (4)

1: Université Montpellier 2, Laboratoire Géosciences Montpellier, UMR CNRS 5243, France.
2: International Institute of Earthquake Engineering and Seismology (IIEES), Dibaji, 19531, Tehran-Iran.
3: Geological Survey of Iran, P.O.Box: 13185 1494, Tehran-Iran.
4: Quebec University, P.O.Box: 8888, H3C 3P8, Canada

Abstract: The NW of Iran is characterized by a high level of historical seismicity related to the ongoing collision between Arabia and Eurasia plates. In this region, the right-lateral strike-slip North Tabriz Fault represents the major seismic source. It is responsible of at least three strong and damaging earthquakes since 858 AD. The last major and destructive seismic events occurred in 1721 AD and 1780 AD, rupturing, respectively, the southeastern and northwestern main fault segments. The North Tabriz Fault represents the central portion of a larger regional fault system (the Tabriz Fault System). The North Mishu, South Mishu, Tassuj, Sufian, and Shabestar faults constitute its NW termination while its SE termination corresponds to the North Bozghush, South Bozghush, Sarab and Duzduzan faults. To better constrain the seismic hazard for the Tabriz city (which present population exceeds 1200000) and surrounding areas we carried out paleoseismological trenching together with quantitative geomorphologic investigations. We focused our studies on the SE part of the North Tabriz Fault, over an area located between Bostanabad and Tabriz cities. Field works interpretations allowed us to recognize evidence for repeated faulting events since Late Quaternary. The first results show that, since 33.5 ky, the SE segment of the North Tabriz Fault experienced at least three major (M=7.2-7.4) seismic events including the last one in 1721 AD. Additional interpretations show that, the amount of strong seismic events along NW segment of the fault appears to be significantly greater than along the SE segment. This observation could indicate that, co-seismic fault slip rate along the North Tabriz Fault decreases from NW to SE.

Keywords: NW Iran, North Tabriz Fault, Morphotectonics, Paleoseismology, Earthquake, Seismic hazard

I) Introduction

Iran belongs to the Alpine-Himalaya orogenic belt, which extends over more than 10000 km from West Europe to Southeast Asia. The NW of Iran is situated in the central part of the Arabian-Eurasian collision zone where crustal deformation since upper Miocene is mainly dominated by N-S shortening associated to E-W extension. This stress field induces intense faulting, strong earthquakes occurrence and controls recent volcano distribution (Figure 1). GPS measurements reveal that present day northward motion of Arabia relative to Eurasia is about 22 +/- 2 mm/yr (20-25 mm/yr) (Nilfolroushan et al., 2003;Vernant et al. 2004). This velocity is less than the 31 mm/yr (at longitude of 52°E) predicted by the NUVEL-1A model, based on seafloor spreading magnetic anomalies over the last 3 Myr (DeMets et al. 1990). The NUVEL-1A overestimation could be related to a gradual slowing of the Arabian plate induced by collision and increasing of gravitational body forces within Caucasus and Zagros mountain belt (Sella et al., 2002). Moreover, GPS estimated rate by Vernant et al. (2006) confirm the one estimated by McQuarrie et al. (2003) over the last ten Myr.

In the west of Iran (between 45°E and 54°E), the Arabia-Eurasia convergence is mainly accommodated by crustal deformation concentrated on both parts of the Central Iranian Plateau that can be considered as a passive rigid block (e.g. Stöcklin et al. 1968 and 1974). Relatively little internal deformation associated to a very low seismic activity within the Central Iranian Plateau support this assumption. Based on GPS measurements (Vernant et al. 2006), strain rates reach about 4 +/-2 mm/yr in the Zagros and about 14 +/- 2 mm/yr between the Central Iranian Block and the Russian Platform. Here, most of the convergence is accommodated in the Caucasus and the Kura foreland basin that undergo N-S compression while in the North-West of Iran, large right lateral strain (about 8 mm/yr) is measured. In this region, GPS measurements reveal that right-lateral strike-slip movement is mainly concentrated along the North Tabriz fault (Masson et al., 2006) and its western prolongation along the Guilato-Siahcheshmeh-Khoy fault system (GSK F) (Figure 1).
Historical seismologic records in NW of Iran (e.g. Ambraseys and Melville, 1982; Berberian, 1994; Berberian, 1997; Karakhanian et al., 2004) show that the Tabriz region is the most important in terms of seismic activity. In this area, the main active fault corresponds to the North Tabriz Fault (NTF), which is located in the immediate vicinity of the Tabriz city. This fault ruptured during several destructive and tragic earthquakes in the past millennium. During the past two centuries, however, it has been seismically inactive and at the same time, the Tabriz city greatly developed in terms of population and urban extension. Based on these observations, it appears clearly that the North Tabriz Fault is one of the most important seismic sources of NW Iran and Transcaucasian regions. Consequently, this fault increases to a high level the seismic risk for the Tabriz City and surrounding regions where, present day population is up to two million people.

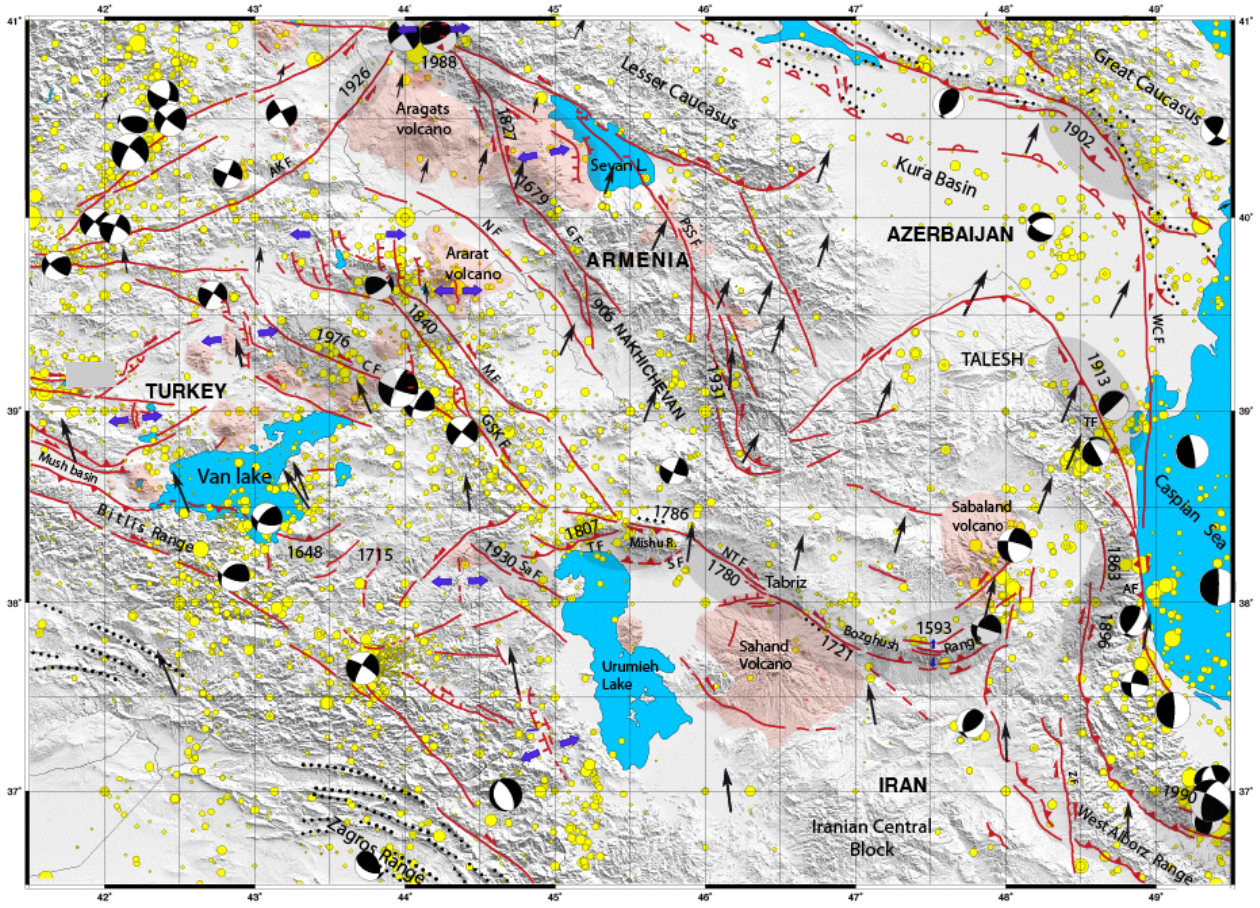

Figure 1: Active tectonic map showing the general pattern of recent deformation in the north-central portion of the Arabia-Eurasia collision zone and the situation of the North Tabriz Fault (NTF) within NW Iran-Transcaucasian region. Here, right and left-lateral strike-slip faulting occur along NW and NE fault trends, respectively. Fold and thrust belts and normal faulting, associated to active volcanoes, revealed active N-S compression and E-W extension (see text for details). The instrumental seismicity (yellow cycles) is from IRIS. The focal-mechanisms are from Jackson et al. (2002) and from IRIS. GPS arrows from Reilinger et al. (2006). The historical seismicity is from Berberian (1997) and Ambraseys and Melville (1982). The pointed lines show the active fold axis. The main faults: GSKF: *Guilato-Siahshechmeh-Khoy faults;, NAF: North Anatolian fault;, CF: Chalderan fault;, AKF: Akurian fault;, MF: Maku fault;, TF: Tassuj fault;, SaF; Salmas fault;, GF: Garni fault;, PSSF: Pambak-Sevan-Sunik fault;, WCF: West Caspian fault;, AF: Astara fault;, TF: Talesh fault;, ZF: Zandjan faul (Solaymani Azad et al., in preparation).*

According to some authors (e.g. Berberian 1997; Karakhanian et al. 2004), the North Tabriz Fault constitutes the eastern prolongation of the Guilato-Siahcheshmeh-Khoy-Tabriz Fault system (GSKT) that plays a significant role in transmitting the right-lateral movements of the North Anatolian Fault toward the east (e.g. Westaway 1990; Jackson 1992), however these two faults are not connected. The first studies dealing with the North Tabriz Fault (NTF) (e.g. Nabavi 1976; Eftekharnezhad 1975; Berberian and Arshadi 1976) showed that this fault is a major tectonic structure in NW of Iran that played a fundamental role in controlling geological formations and facies distribution. Nabavi (1976) noticed that Devonian and Carboniferous formations are missing within the southern block of the fault suggesting that it follows the northern limit of the Iranian Caledonian domain. He concludes that the fault reactivate an old structure inherited at least from Lower Paleozoic time. Despite these works, some first order characteristics of the Tabriz fault system remain under debate like its segmentation, detailed kinematics and long-term seismologic behavior.

In this paper, based on field investigations, including geomorphologic, seismotectonic and paleoseismologic studies, we present new data that complement the first paleoseismological study performed by Hessami et al. (2003) on the NW segment of the fault. We discussed more specifically, how cumulated and co-seismic deformations are distributed along the NTF; and how deformation is accommodated in both fault terminations. The final objective of our study is to bring new constrains on the seismologic behavior of the fault (Maximum magnitude, slip per event and recurrence time) to better assess the seismic hazard for the Tabriz city and surrounding areas.

II) North Tabriz Fault

The NTF strikes N135°E over a length of about 120 km. The fault is not continuous and presents several segments as previously mentioned by some authors (e.g. Berberian 1997; Karakhanian et al. 2004) that identified two main NW and SE fault segments. Due to repeating earthquake surface ruptures, the NTF has a clear surface expression along most of its trace and exhibits, then, several geomorphic evidences of recent activity. The main fault plane appears to be close to vertical dip at a first order.
Morphologically, several evidences of en-echelon right-stepping fault segments, that sign the strike-slip activity of the fault, can be identified at regional and local scales (e.g. Berberian, 1997; Karakhanian et al., 2004). Numerous shutter ridges, dextrally offsetting alluvial fans and drainage patterns can be also observed (Figure 2)

Figure 2: Shutter ridge feature, which formed by right-lateral strike-slip movements along the NTF west of Bostanabad (looking NE). The amount of right-lateral strike-slip cumulated displacement of this drainage is about 150 m.

Right-lateral strike-slip movements along the North Tabriz fault were first documented by Nabavi (1976) based on the study of geological offsets, then by Berberian and Arshadi (1976) using aerial photo interpretations, and by Karakhanian et al. (2002, 2004) and finally by Hessami et al. (2003) from morphotectonics observations. According to interseismic geodetic measurements (GPS monitoring) in the NW of Iran (Masson et al. 2006; Vernant et al. 2006), the short-term slip rate of the North Tabriz Fault could reach 5-8 mm/yr, This estimation is of the same order and consistent with the geological long-term slip rates proposed by Karakhanian et al. (2004) and Hessami et al. (2003), 2 mm/yr and 3.1-6.4 mm/yr respectively.

In terms of morphology and geometry, the North Tabriz Fault can be divided in two major NW and SE fault segments with right stepping pattern. This feature is consistent with the study of seismic ruptures distribution based on historical (e.g. Ambraseys and Melville, 1982; Berberian and Yeats, 1999) and pre-historical seismic records (e.g. Hessami et al., 2003) along this fault. Karakhanian et al. (2004) showed that the main overlap zone between these two fault segments corresponds to a large pull-apart basin situated in the Tabriz city area (Figure 5). Within the pull-apart basin, the fault scarp topography is mainly controlled by the variations of the vertical slip component along normal fault branches trending probably NNW-SSE.

Historical records indicate that the North Tabriz Fault ruptured during several large and destructive earthquakes in the past millenium. Indeed, since 858 AD, the Tabriz city experienced at least twelve destructive seismic events in 858, 1042, 1273, 1304, 1550, 1641, 1650, 1657, 1664, 1717, 1721 and 1780 AD (e.g. Ambraseys and Melville, 1982). The strong earthquakes of 1042 AD (M=7.3), 1721 AD (M=7.3) and 1780 AD (M= 7.4), were associated to the North Tabriz Fault and produced clear surface ruptures (Ambraseys and Melville, 1982; Berberian, 1997; Berberian and Yeats, 1999; Hessami et al., 2003). Since that time, the NTF has remained seismically inactive, accumulating a period of quiescence of more than two centuries. However, recent seismological studies along the fault show numerous evidences of shallow micro-seismic activity limited at depths of 7 to 21 kilometers (e.g. Siahkali Moradi, 2008). Even if the return period of strong earthquakes whole along the fault is not yet constrained, it presents a high level of seismic risk for the Tabriz City and surrounding regions.

At a more regional scale, the Mishu and Bozghush Ranges mark, respectively, the NW and SE ends of the North Tabriz Fault (see Figure 1). These ranges, trending roughly E-W, have almost similar dimensions of 85 km x 25 km and average altitudes of about 3000 m. Mishu and Bozghush ranges are bordered by several oblique and reverse faults trending roughly E-W that connect to the NTF.
The occurrence of five successive and destructive seismic events of Sarab (1593 AD), SE Tabriz (1721 AD), NW Tabriz (1780 AD), Marand (1786 AD) and Tassuj (1807 AD) along these faults show potentially a seismic migration from the SE toward the NW over a period of 214 years (Figure 3). This feature not only could correspond to earthquake clustering, as presented by some authors (e.g. Kagan and Jackson, 1991; Berberian, 1997; Karakhanian et al., 2004), but also can reveal fault segment interactions in the framework of the Tabriz Fault System (TFS).

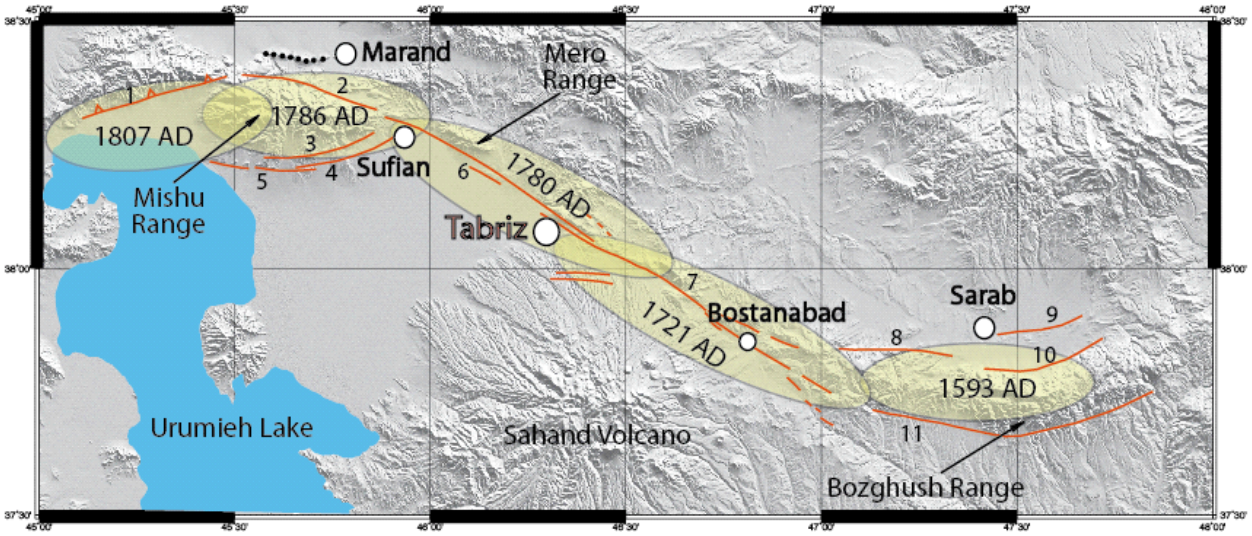

Figure 3: The occurrence of five successive and destructive seismic events of Sarab (1593 AD), SE Tabriz (1721 AD), NW Tabriz (1780 AD), Marand (1786 AD) and Tassuj (1807 AD) could correspond to a seismic migration sequence from the SE toward the NW over a period of 214 years. This situation can be related to fault segment interactions in the framework of the Tabriz Fault System (TFS). Note the east-west trending active folding (pointed line) west of the Marand City. 1: Tassuj fault; 2: North Mishu fault; 3: South Mishu fault; 4: Sufian fault; 5: Shabestar fault; 6: NW segment of the North Tabriz Fault; 7: SE segment of the North Tabriz fault; 8: Duzduzan fault; 9: South Sarab fault; 10: North Bozghush fault; 11 South Bozghush fault. The historical seismicity is from Berberian (1997), Berberian and Yeats (1999) and Ambraseys and Melville (1982).

1- The Western part of the Tabriz Fault system (TFS)

Morphologically, this portion of the TFS is limited to the west by the Mishu Range and includes the South Mishu, Sufian and Shabestar faults toward the south and the North Mishu and Tassuj faults toward the north (see Figure 3). Geologically, the Mishu Range is constituted by Proterozoic and lower Paleozoic igneous rocks (granite, rhyolite and gabbro), separated on both side from Neogene formations by the Tassuj, North Mishu and South Mishu faults.

More to the south, the Sufian and Shabestar faults, that trend parallel the South Mishu fault, separate Neogene formations to Quaternary alluvial fan deposits. All of these faults correspond to pure and oblique thrusts with right-lateral component trending roughly E-W, which merge together west of Sufian city (see Figure 3). North-south trending active compression is attested west of Marand city by a large E-W Quaternary fold, which presents a clearly antecedent stream pattern (Figure 4). Southwest of the fold, morphologic evidences of dextral strike-slip faulting associated to the North Mishu fault is also observed, indicating that slip partitioning is occurring in this region. This feature confirms that the tectonic regime is mostly transpressive in this region.

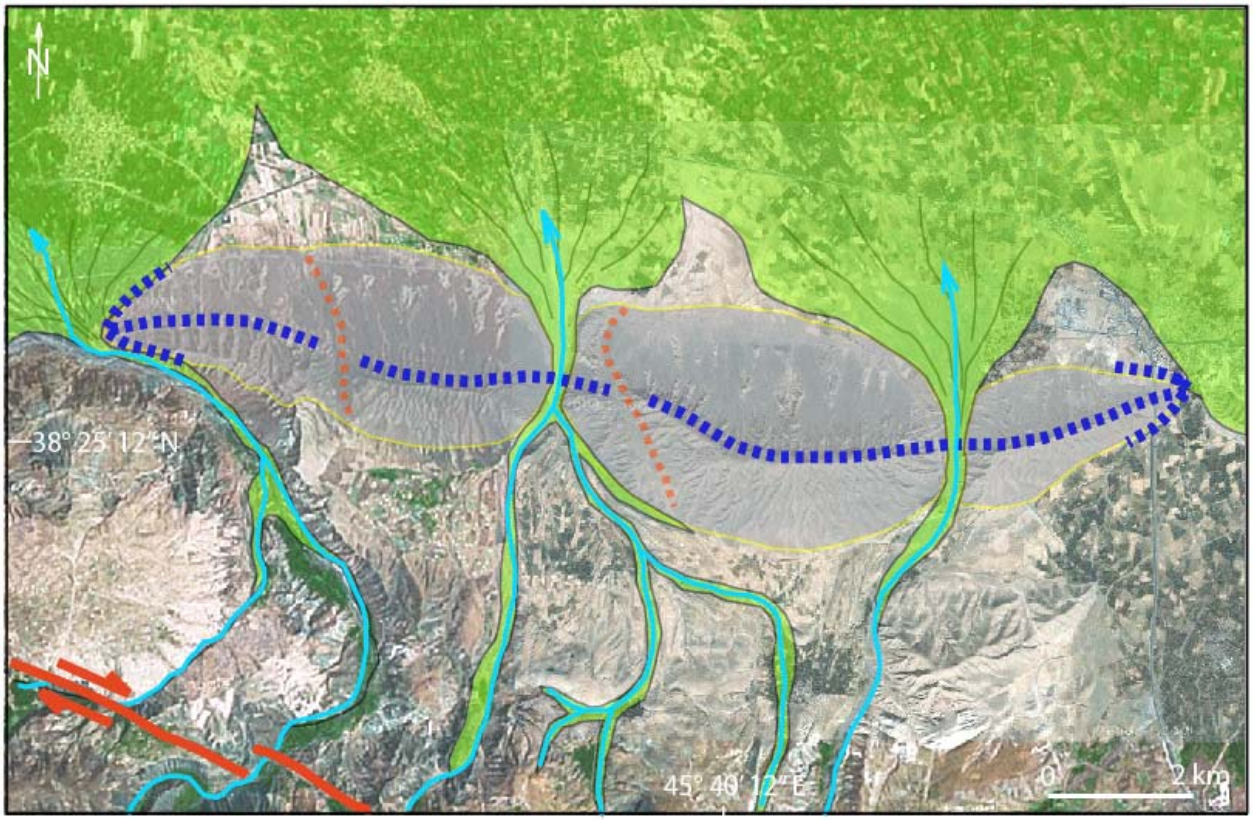

Figure 4: Google Earth satellite image from west of Marand city. A large E-W trending Quaternary fold induced by active N-S shortening shows a clearly antecedent stream pattern (see Figure 3 for location). Red dashed lines correspond wind gap features. Southwest of the fold, a clear dextral strike-slip fault is also observed, indicating that slip partitioning is occurring in this region. This feature confirms that the tectonic regime is transpressive.

The Mishu Range can be considered as a compressive relay, which absorbs part of the displacement along the NW right-lateral strike-slip segment of the NTF. Based on this observation, the seismic events of 1786 AD and 1807 AD that occurred along Mishu Range can be interpreted, most probably, as thrust or oblique-slip events.

2- The West-Central part of the Tabriz Fault System

The west-central part of the TFS corresponds to the NW segment of the North Tabriz Fault, as defined classically. The eastern termination of this segment corresponds to the northern boundary of the pull-apart basin of the Tabriz city. Morphologically, this segment of the NTF follows the southern flank of the Mero Range, from Sufian city to the west to Tabriz city to the east (see Figures 3 and 5). The recent co-seismic surface faultings along this portion of the Tabriz Fault System favor an easy observation of the fault trace over more than 50 kilometers.

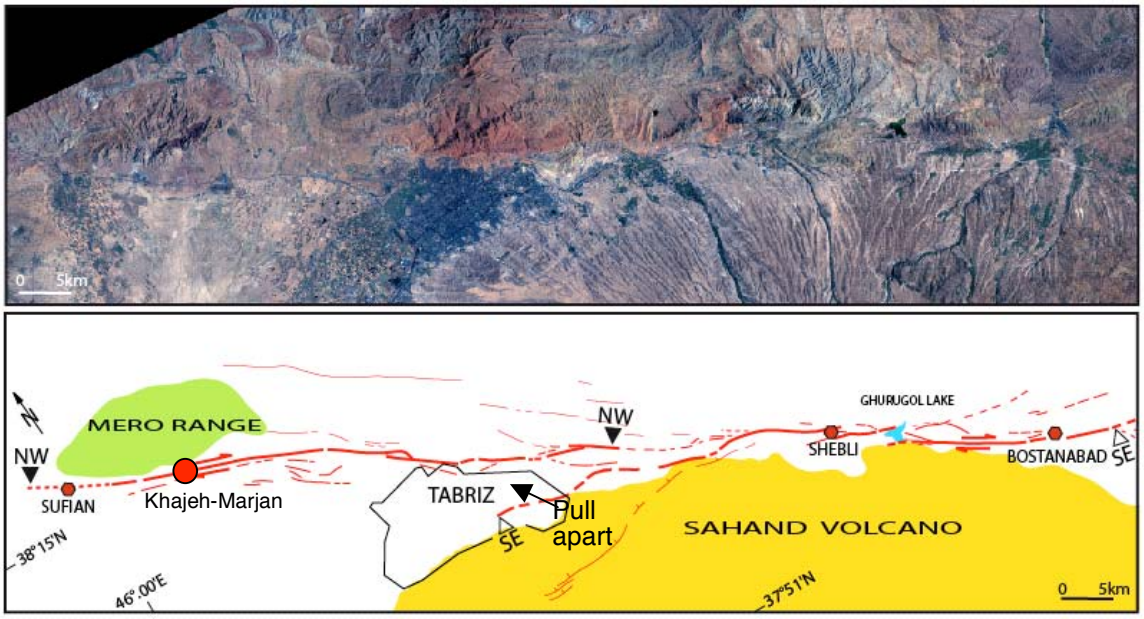

Figure 5: Landsat 7 satellite image of the Tabriz region and its tectonic interpretation (see Figure 3 for location). The limits of the 50 km long NW and 60 km long SE segments of the NTF are represented by black and white triangles, respectively. These fault segments bound the southern flank of the Mero and the northeast flank of the Sahand volcano. The Tabriz city is situated in the overlap zone of about 15 km long between these two segments of the TFS in a large pull-apart basin position. Generally, the SE segment of the NTF, that constitutes the East-Central part of the TFS, exhibits several right stepped fault branches and has a wider fault zone compared to the NW fault segment of the fault that constitutes the West-Central part of the fault system.

A maximum cumulated right-lateral offset of 256 meters was documented by Hessami et al. (2003) for this segment of the NTF. Our observations, however, show that the amount of cumulated dextral displacement along this segment of the fault close to Khajeh-Marjan village could reach about 500 meters (Figure 6A). More to the east, an 800 m horizontal morphologic offset is also observable which represents the greatest measured cumulated displacement whole along the TFS (Figure 6B).
The minimum and maximum values of horizontal slip rate along the NTF deduced from geological and geodetic estimations are 2 mm/yr (Karakhanian et al., 2004) and 8 mm/y (Masson et al., 2006), respectively. Based on the assumption that the mean value of slip rate is 5 mm/yr (coherent with geological observation of Hessami et al., 2003 and geodetic estimation of Vernant et al., 2006) the age of the 500-800 meters of right-lateral observed offsets will be situated between 100000 and 160000 years. If we assume the fault slip rate is constant over several ten millions of years, the geological offset proposed by Nabavi (1976) between Mishu and Mero Ranges is about 20-25 km (according our estimation), then the age of right-lateral strike-slip faulting along the NTF reach 4 to 5 My (see Figures 1 and 3 for situation). If the 20-25 km of displacement corresponds to the total horizontal geological offset, then, the NTF started to play as a right-lateral strike-slip fault during Pliocene. This age is consistent with the starting time of the North Anatolian Fault propagation proposed by Barka, 1992, which is also the starting time of the process of expulsion of the Anatolian block and NW of Iran towards west and east, respectively (diachronously after the closing of the Neothetys)(e.g. Cisternas and Philip, 1997).

Based on historical seismic records (e.g. Ambraseys and Melville 1982; Berberian and Yeats 1999) the NW segment of the TFS ruptured lastly in 1780 AD. The length of the co-

seismic surface faulting of this strong earthquake that extends roughly from Tabriz to Sufian is about 50 km.

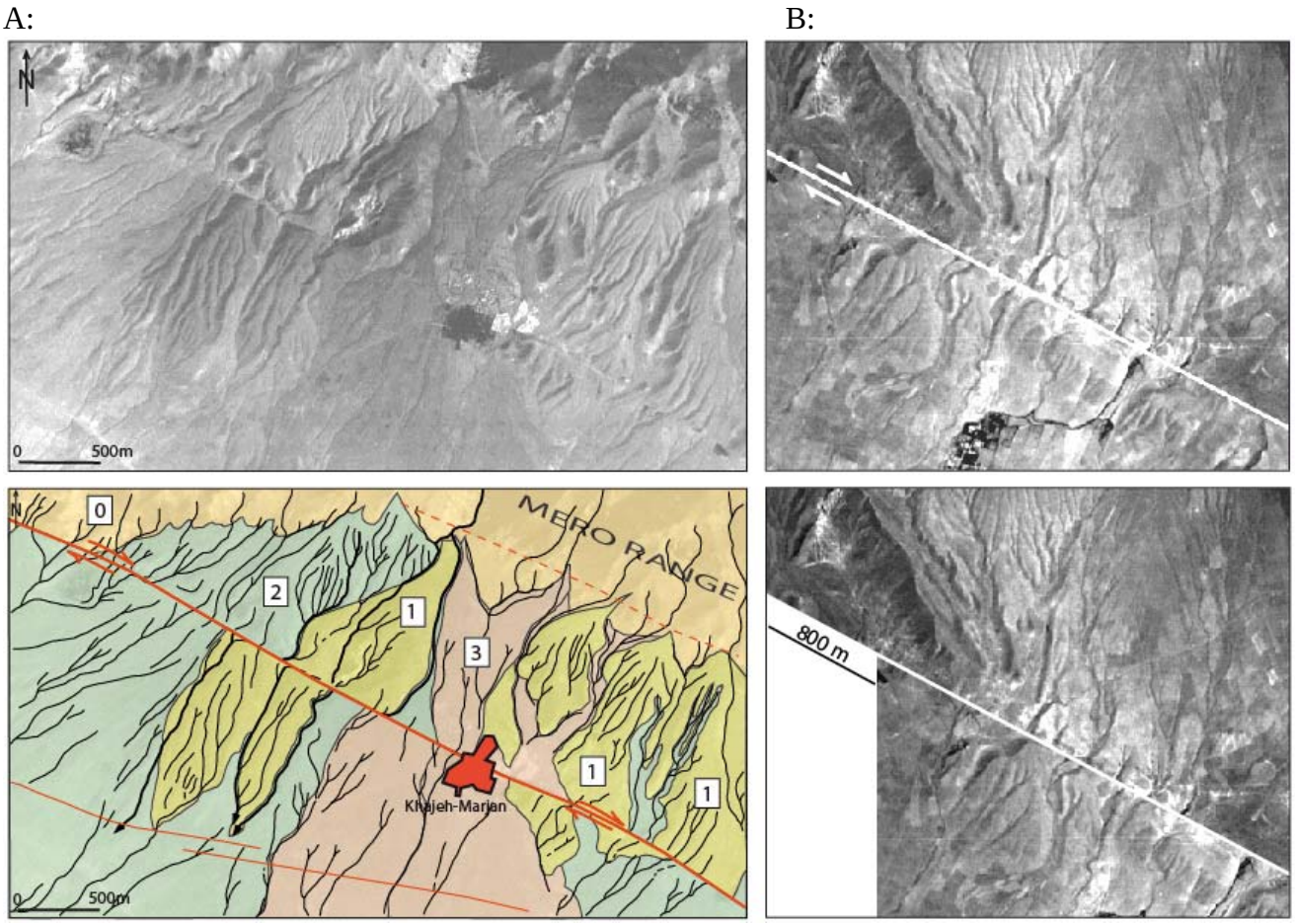

Figure 6: (A) Near the Khajeh-Marjan village, the NW segment of the NTF fault crosscuts several generations of alluvial fans (the chronological classification is based on down cutting erosion). Zero shows the bedrock. The observed maximum cumulated right-lateral offsets of the alluvial fans are about 500 m. More to the east (B), an 800 m horizontal morphologic offset is also observable which represents the greatest measured cumulated displacement whole along the TFS.

3- The East-Central part of the Tabriz Fault System

This segment, identified classically as the SE segment of the NTF, trends N135E°-145°E and measures 60 kilometers long. The fault trace bounds the northeast flank of the Sahand Volcano (see Figures 3 and 5) and extends from the Tabriz city to the southeast of Bostanabad. This south-east prolongation of the NTF was firstly proposed by Ambraseys and Melville (1982) when considering the location of the surface rupture associated to the 1721 AD seismic event.

At least, three right stepped branches can be observed along the SE segment of the NTF. These branches of the main strike-slip fault segment are stepped to the right two times, first west of the Ghurugol Lake and then, west of the Shebli village (see Figure 5). Moreover, several secondary branches are distributed on both sides of the main fault over a zone of several kilometers wide (rather than The West-Central part of the Tabriz Fault System) (see Figures 5).

The western termination of the SE segment corresponds to the southern boundary of the Tabriz city pull-apart basin. The eastern termination is located SE of Bostanabad where the fault divides into two branches, the main one strikes gradually toward the east to follow the southern flank of the Bozghush Range and the second one continues 65 km toward the south-east in direction of Siahchaman. The field observations that we performed SE of Bostanabad show geological evidences of a NW-SE trending fault zone, which could be associated to a moderate seismic event in 1965 AD (M=5.1, I0=VII). These observations are coherent with interpretations of Ambraseys and Melville (1982).

Our field observations along this segment of the fault system west of the Ghurugol Lake show some evidences of active dextral faulting with a little normal vertical component (Figure 7). This secondary normal slip component observed along the main right-lateral strike-slip faulting can be caused locally by the right-stepping geometry observed within its fault branches (Figure 8).

Figure 7: SE segment of the NTF: View to the east of the main fault plane west of Ghurugol Lake (between Shebli and the lake in Figure 5). Here, the fault cuts a Quaternary colluvium (on the left side) and shifted it against the Mio-Pliocene bedrock (to the right side). At this site we measured dextral-normal striations: 145°E, 65° N, 22° SE.

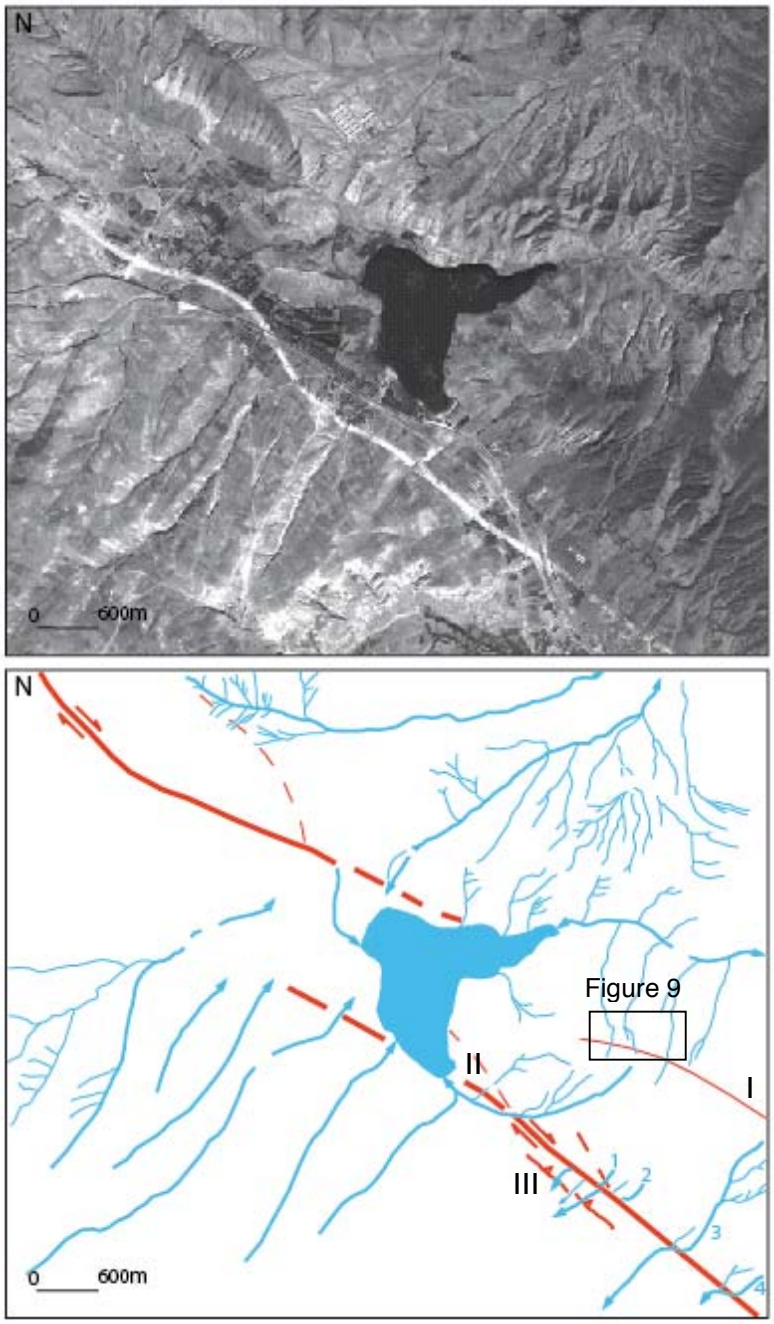

Figure 8: Aerial photograph and morpho-tectonic interpretation of the two right-stepped en-echelon branches of the SE segment of the NTF that limited the Ghurugol Lake (west of Bostanabad). Based on these observations, the Ghurugol Lake can be interpreted as small a pull-apart basin formed in response to the right-lateral strike-slip movements along the fault branches. On the other hand, the drainage pattern on both sides of the lake shows a paleostream direction toward the northeast. North of the lake, it has changed recently toward the southwest probably because fault activity induced uplift on the northern compartment of the fault. At the eastern side of the lake, several right-lateral strike-slip offset features show evidences of repeated co-seismic surface faulting (stream beds 1, 2, 3 and 4) during past earthquakes. The mean value of maximum cumulated dextral displacement of four stream beds along this part of the TFS is about 300 meters.

East of Ghurugol Lake (12 km west of Bostanabad), the fault zone widens to about 1500 m and three parallel fault branches are observable (I, II and III in Figure 8). The first one (as the northern one) is located morphologically on the northern limb of a small range parallel fault and cuts the ground surface (Figure 9).

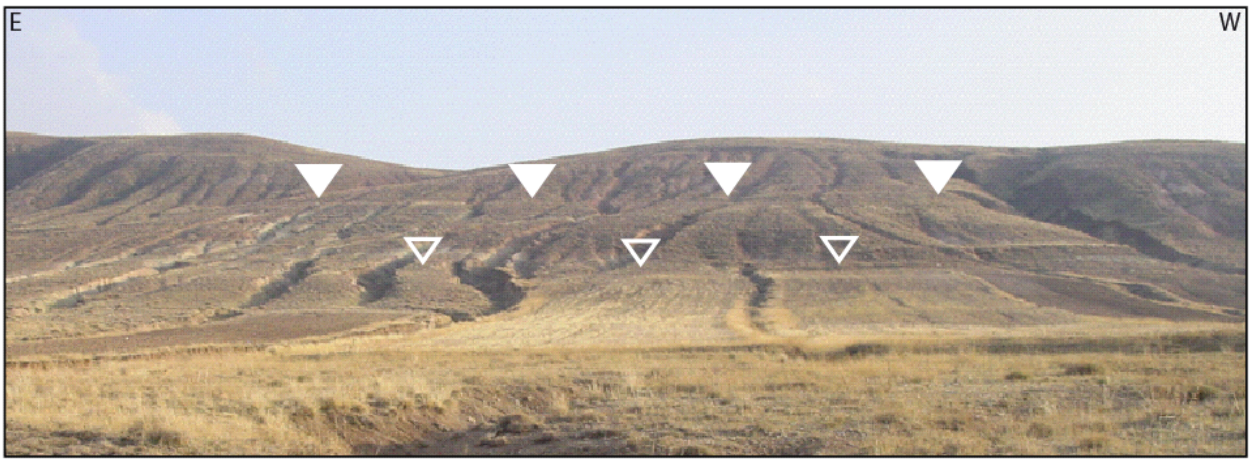

Figure 9: The northern fault branch of the NTF zone east of Ghurugol Lake (looking south). Morphologically, this range parallel fault zone cut the surface and then shows evidence of active faulting.

1450 m towards the south, another branch corresponds to the main fault trace, which is clearly a right-lateral strike-slip fault (Figure 2, and II in Figure 8,). Along this fault branch, the amount of cumulated offset features such as drainages and ridges varied from 9 to 300 m (see Figures 8, 11 and 12). Based on satellite image and aerial photo interpretations, this fault branch extends between the southeast of Bostanabad city (to the SE) and the Gurugol Lake to the NW (see Figure 5).

Finally, the third one is situated at a distance about 140 m south of the second fault branch. The morphology of the fault scarp shows a reverse to thrust fault dipping NE. The trend of the fault trace (N 140-145° E) is a little oblique rather than the second mentioned fault branch (N 135° E)(III in Figure 8).
According to historical seismicity catalogues (e.g. Ambraseys and Melville 1982; Berberian 1994), this portion of the Tabriz Fault System lastly ruptured in 1721 AD. The co-seismic surface faulting of this event has been documented along more than 60 km from Tabriz to Bostanabad.
Here, along the main fault branch we focused our studies on two sites (Figures 12 and 13).

4- The Eastern part of the Tabriz Fault System

Morphologically, this portion of the fault system is associated to the fault network affecting the Bozghush Range. It is constituted by the South Bozghush fault to the south and the North Bozghush, South Sarab and Duzduzan faults to the north (see Figure 3).
Geologically, the Bozghush Range corresponds to a large antiform structure mainly composed of Eocene volcanic (trachyandesite and lava flows) rocks. We interpret an E-W longitudinal depression on top of Bozghush range as a graben that results from extrados extension. Faults are present on both side of the range (Figure 10). The South and North Bozghush faults separate the volcanic formations from Neogene and Quaternary sediments. More to the north, the South Sarab and Duzduzan faults (parallel the North Bozghush fault) are located in Quaternary alluvial fan deposits. All of these faults are generally E-W trending dip-slip (thrust) and oblique-slip (reverse-dextral) faults.

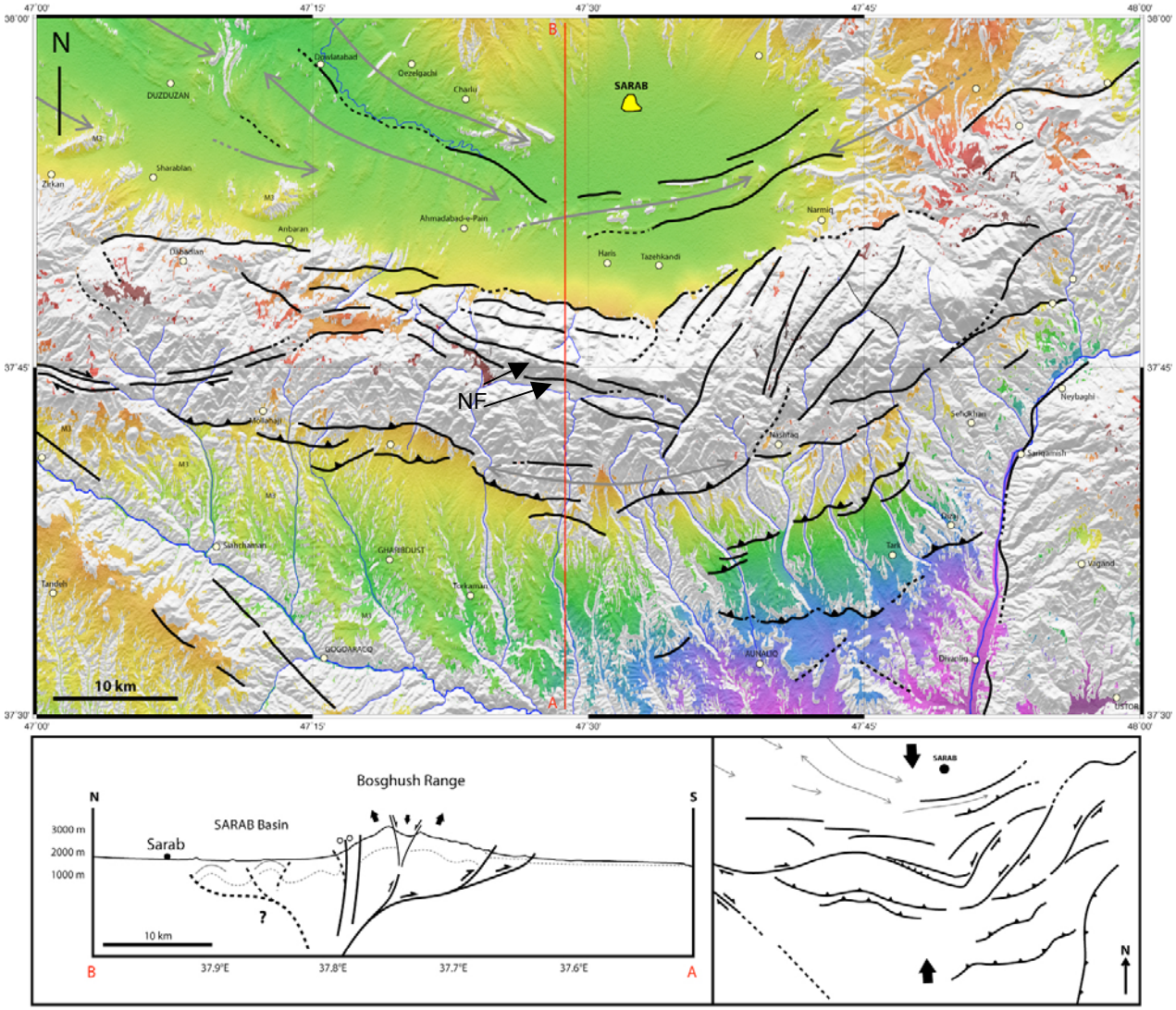

Figure 10: Morpho-structural map and north-south cross-section of the eastern end of the TFS within the Bozghush Range (see Figure 3 for location). Here, the strike-slip component of the NTF is accommodated along several oblique reverse faults and extrado extension located at the top of the Bozghush Range anti-form. NF; normal faults.

The seismic event of 1593 AD occurred in the Sarab region and could be related to the faults that bordered the northern flank of the Bozghush Range. More recently, in 1879 AD, a destructive earthquake also occurred in the eastern part of the Range.

Pattern of active deformation along the Tabriz Fault System

Our observations indicate that the amount of maximum cumulated horizontal displacement is different along the four mentioned parts of the fault system. It is of >500 and 300 meters for the two west and east central portions respectively, however it is close to zero in the western and eastern east-west trending portions. We interpret that horizontal component of displacements along the west and east central parts of the fault system are being absorbed within the Mishu and Bozghush Ranges as two fault terminations.
Moreover, the time window that corresponds to the maximum cumulated dextral offsets along both west and east central portions of the fault system is not inevitably the same. This alone

assertion doesn't allow us to interpret the different cumulative displacements as different slip rates. To answer the question of slip rate variation along these portions of the fault system the paleoseismological approach can be considered as a good solution.
In the first paleoseismological study along the NTF (Hessami et al., 2003), the seismic characteristics of the NW segment of the fault have been investigated. Based on this study, the NW segment of the North Tabriz fault since 3600 B.P. has been ruptured at least during four large earthquakes with mean recurrence interval of 820-/+170 years, including the last one, which occurred in 1780AD.
The study of the other segment of the fault (SE segment) is then of major interest for seismic hazard assessment in the Tabriz region where total population exceed more than two millions but also to better understand present day geodynamic of NW Iran.
In the present study, to complete and to better assess the seismic hazard, we focused our paleoseismological analysis along the SE segment of the fault.

III) Paleoseismological study of the SE segment of the North Tabriz Fault

To identify the paleoearthquakes that occurred on the SE segment of the NTF, we focused our studies along this portion of the fault that is supposed to have ruptured during the 1721 AD (M=7.3) SE Tabriz earthquake (e.g. Ambraseys and Malville, 1982; Berberian, 1997; Berberian and Yeats, 1999). This earthquake was the last macroseismic event along this fault segment and severely damaged the Tabriz city and especially other urbanizations such as Shebli and Bostanabad (see Figures 1, 3 and 5 for situation). As shown before, the region surrounding the Ghurugol Lake is one of the best places where the fault zone shows clear geomorphic evidences of repeated co-seismic surface ruptures that include most probably the last seismic event of 1721 AD (see Figures 3 and 8). In this area, the fault cut Late Quaternary deposits and several drainages trending normal to the fault direction. All of these features make this zone very suitable to perform a paleoseismologic study and detailed quantitative geomorphic observations. Streambeds and gullies are, indeed, systematically offset along the fault trace. The most spectacular feature among them is a recent channel located between the Ghurugol lake and Bostanabad, which has been displaced right-laterally (Figure 11). At this location, the stream channel was offset by about 9.0 -/+ 0.5 m, which is the smallest amount of displacement that we have observed along the SE segment of the NTF. This displacement may correspond to one or several large seismic events. If we assume this offset corresponds to two events then the slip amount per event is about 4.5 m, which is similar to the one, proposed by Hessami et al. (2003) for the NW segment of the NTF. However, we will discus later, others possibilities.

Figure 11: Clear right-lateral offset drainage bed (9 -/+ 0.5m) observed along the SE segment of the NTF west of Bostanabad (looking north east).

Offsets of several drainages elsewhere (more to northwest) along this section of the fault contain evidence for cumulative displacements by several individual offset events. In some cases, these offsets are difficult to interpret. The amount of measured cumulated dextral offset features along this segment of the NTF varies from 9, 45, 105, 150 and 250 to about 300 m. The maximum 300 m dextral offsets can be measured using aerial photos and by matching drainage systems and ridges (see Figures 8 and 12).
Along this portion of the fault segment, the vertical component of displacement varies from place to place between 5 and 10 m, but in any case, the dip-slip component is subsidiary to the main right-lateral strike-slip movement, or it may represent slip distribution on secondary dip slip fault branches close to the main strike-slip fault. In fact, although the southern block seems systematically downthrown relative to the north side, the strike-slip movement along the fault has created scarps facing both north and south by shifting the topography laterally in this relatively high-relief terrain.

As we mentioned before, we observed west of Bostanabad that the fault deformations are morphologically distributed at least along three N135°E parallel fault branches. However, the evidences of nearly pure right-lateral strike-slip deformation are concentrated along the main (see section 3) fault trace of the NTF (see also Figures 2 and 11). Here, along the main fault branch we focused our studies on two sites (Figures 12 and 13). Within the sites one and two, we opened three trenches across the main dextral fault branch and one trench across the southern thrust fault branch.

Site 1:

1.2 km east of the Ghurugol Lake, the NTF zone crosscuts well developed Quaternary alluvial fans that drape the southern flank of a fault parallel range where Eocene volcanics outcrop (see Figures 8, 12 and 13). The southern part of these alluvial fans is dammed by several hills associated to large shutter ridges. These hills correspond to displaced topographies, which formed successively during the past surface faulting events along the fault zone.

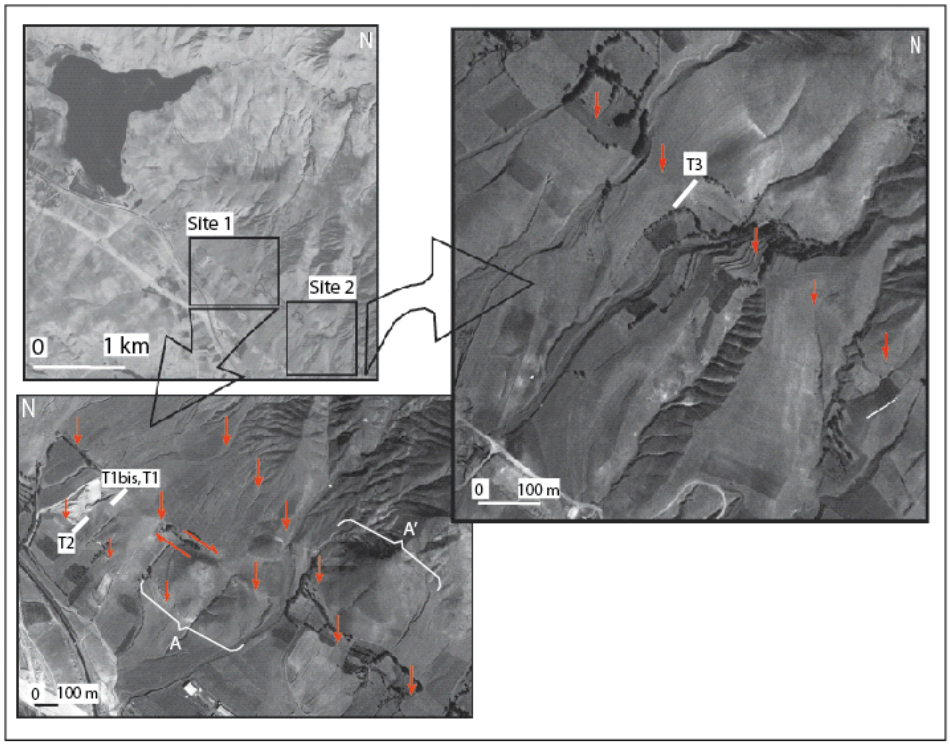

Figure 12: As shown on these aerial photos, the trench sites are located east of the Ghurugol Lake. A total of four trenches (perpendicular to the trend of the fault zone) were dug. The horizontal displacement between A and A' piercing points is 310 m.

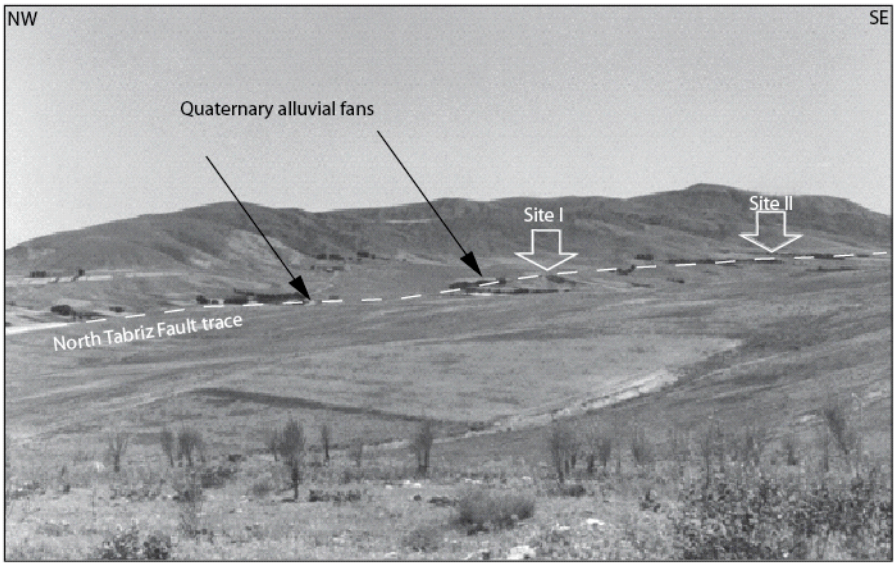

Figure 13: Perspective view (looking northeast) of the trench sites east of Ghurugol Lake. Here, the NTF zone crosscuts several Quaternary alluvial fans issued from the erosion of the topographic ridge made of Eocene volcanics trending parallel to the fault trace.

Based on field observations, some of them especially to the east are constituted by Eocene igneous rocks, while other ones toward the west are formed by younger (plio-quaternary) sedimentary formations. Quarry activity allowed us to study a large outcrop within the western hill. Here, uplifted and deformed alluvial fans deposited unconformably over Mio-Pliocene volcano-detritic formations of the Sahand volcano. These formations are folded and thrusted between the main-dextral and the secondary-reverse fault branches (Figure 14).

This cross section contains a synclinal, whose fold axis trends at N115°E (Figures 14, 15 and 16). Within this site, we excavated three trenches, two of them across the northern and the other one across the southern fault branch.

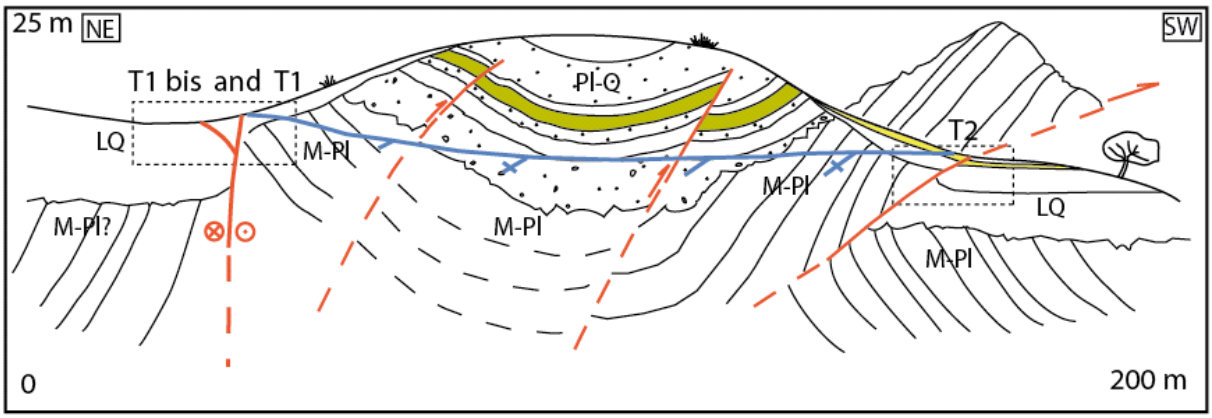

Figure 14: Schematic cross section at site 1 showing the geological situation of the folded Mio-Pliocene bed rock (M-Pl) and Plio-Quaternary fan deposits (Pl-Q). The Late Quaternary deposits (LQ) are affected by faults. The blue solid line shows the ground surface level. See text for more information.

To open the paleoseismological trenches, we first used large scale Digital Elevation Models (DEM) calculated from D-GPS (Differential Global Positioning System) surveying (Figure 16). The detailed DEM, allowed us to better determine the surface geometry of the fault branches and the uplifted fold.
All along the main fault trace, we found several evidences of recent horizontal displacement with typical offsets about 7 m -/+ 1m that correspond to the last seismic events (Figure 17).

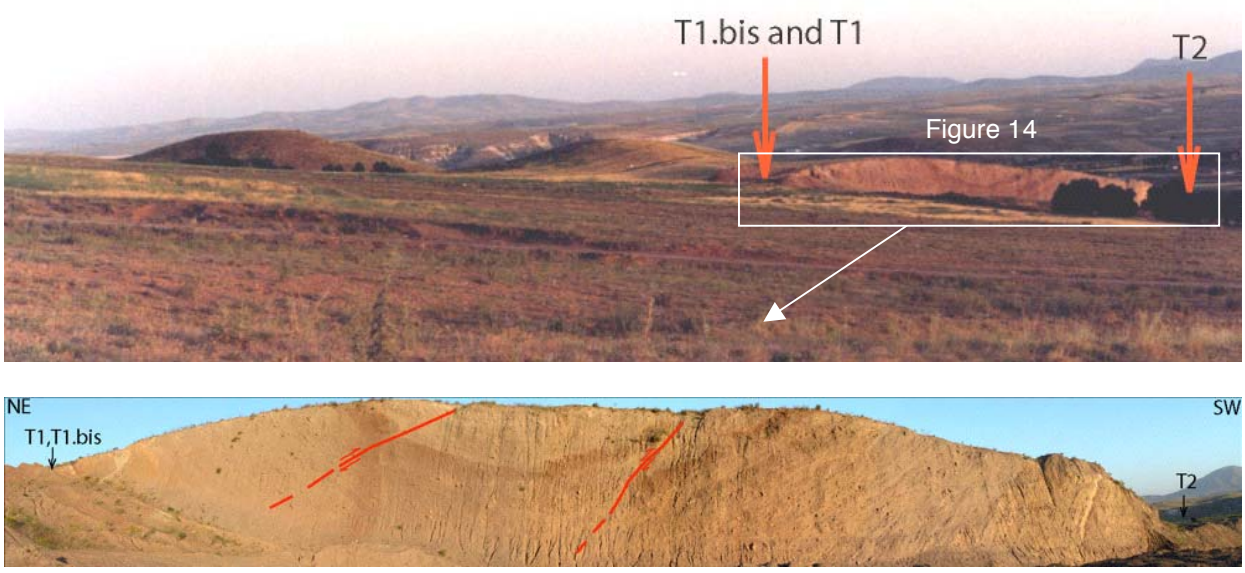

Figure 15: Paleoseismological trench site located on the SE segment of the NTF. Here, uplifted and dragged synclinal made of deformed Plio-Quaternary fan deposits can be observed within the fault zone. Fold axis strikes N115°E and several reverse faults affect the structure. Here, we opened three trenches along this section; trenches T1 bis and T1 were excavated on the NE flank to study the main strike-slip fault plane and T2 on the SW flank to study a reverse fault surface rupture.

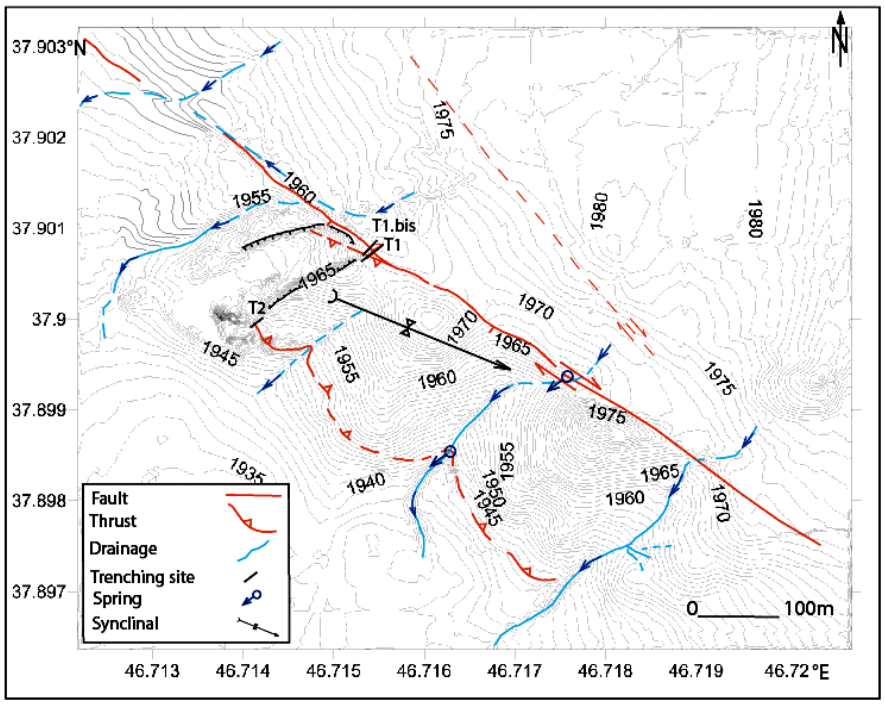

Figure 16: Detailed topographic map based on digital Elevation Model (DEM) of trench site number 1 and structural interpretation based on our field observations (see Figure 12 for situation). Within this site we dug three trenches for paleoseismological investigations.

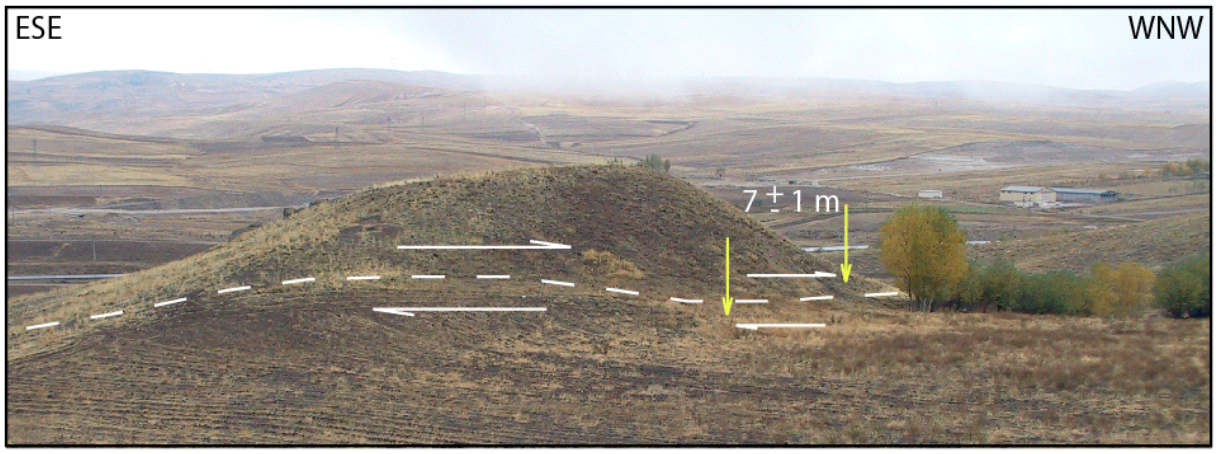

Figure 17: Example of recent right-lateral offset. This small hill, located at 200 m SE of trench site T1, is dextrally sheared by about 7 m -/+ 1 m.

Trenches T1 bis and T1:

At site 1, we opened the first and second trenches (T1bis and T1) on the main dextral fault branch of the NTF zone (Figures 18A, 18B, 19A and 19B). T1 bis and T1 trenches measure 14 and 15 meters long, respectively and were excavated very close each other at a distance about 4 m. However, we observed some essential differences in some seismite features within the trench walls. Within T1 bis and T1 trenches, during the past large seismic events, the bedrock to the south is sheared and thrusted over younger deposits to the north over a fault zone of 7-8 m width.

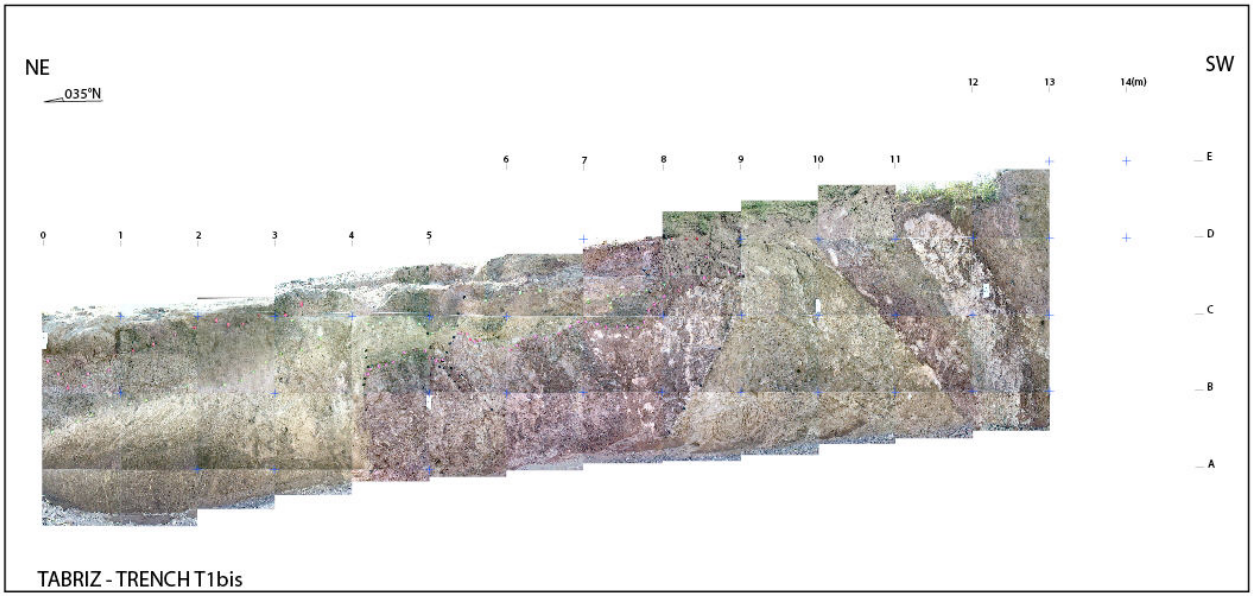

Figure 18A: Rectified photo mosaic of the first trench (T1bis) within the site 1 (see Figures 12, 14, 15 and 16 for situation). During the past large seismic events, the bedrock (to the south) is sheared and thrusted over younger soil and colluvium units (to the north). This situation is consistent with the fault scarp topography.

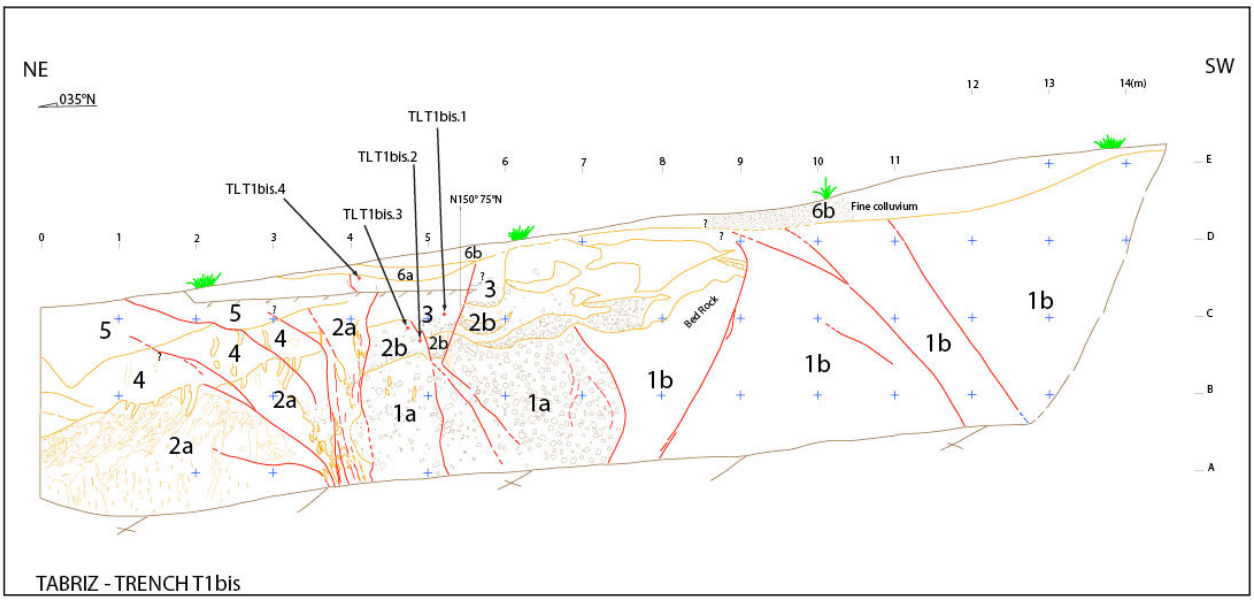

Figure 18B: T1bis trench log (site 1). The width of the fault zone is about 8 meters. However, the most recent faulting features are concentrated within a narrow fault zone (between benchmark 2 and 6). Here, a few faults reach the ground surface and can therefore be associated to the last macro-seismic events.

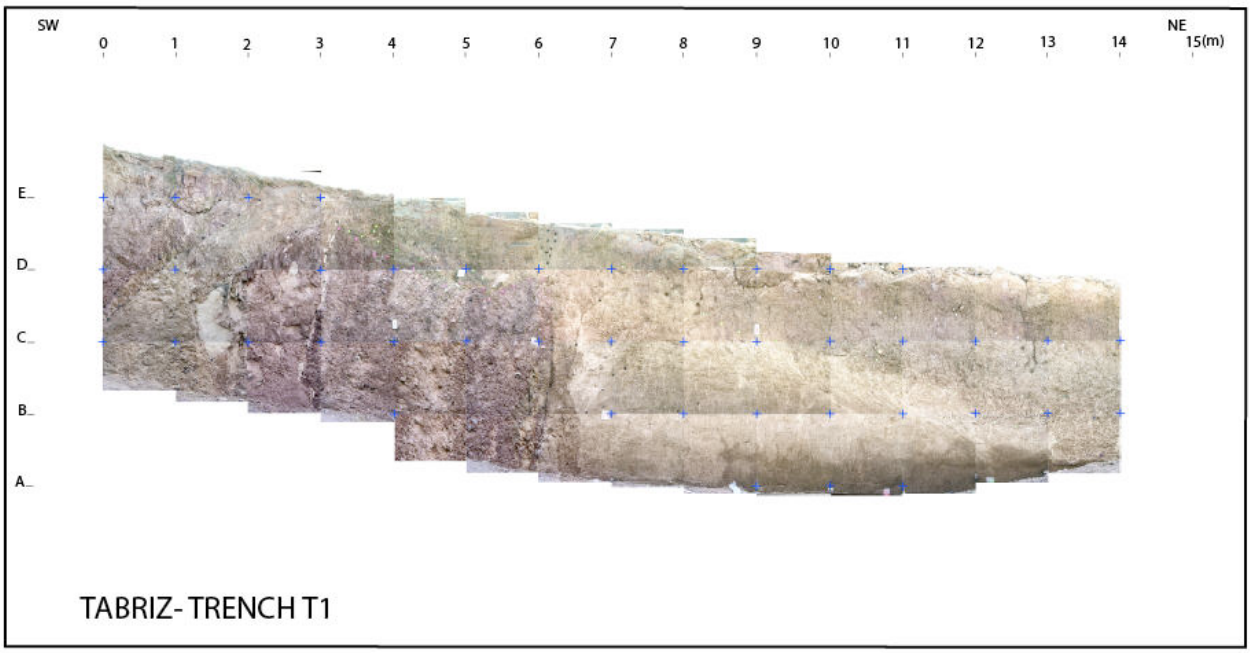

Figure 19A: Photo mosaic of T1 trench (site 1) (see Figures 12, 14, 15 and 16 for situation). To avoid geometric distortions and perform accurate measurements, we have ortho-rectified each picture individually by using the Envi 4.0 Software. This new technique allowed us a very good comparison between the mosaics and the trench logs. The bedrock (red formation) is also clearly sheared and thrusted toward north over younger deposits along several fault planes.

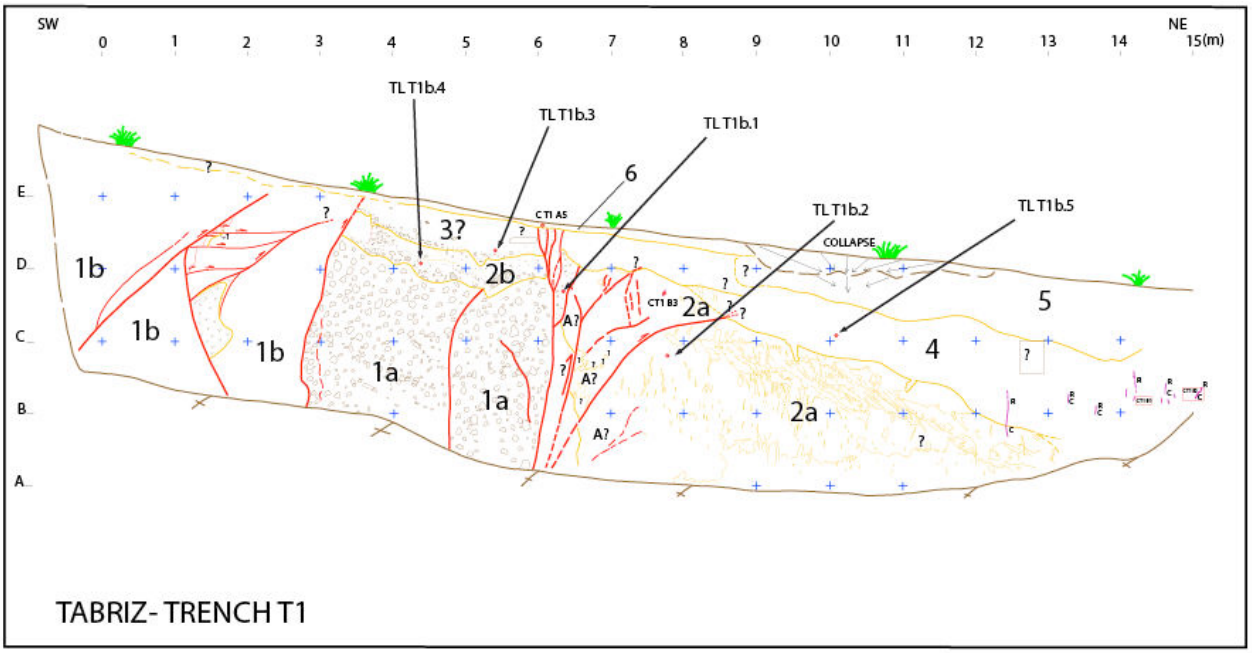

Figure 19B: T1 trench log (site 1). The width of the fault zone is about 7 meters. The evidences of the most recent faulting are concentrated within a narrow zone (between benchmark 6 and 9) that cut the ground surface during the last macro-seismic events.

Descriptions of the sedimentary units observable on the T1bis and T1 trench walls:

Unit 1: This unit corresponds to Mio-Pliocene formations (1b) and constitutes the basement of the southern compartment of the main fault zone. This unit includes a 3-5 meters wide fault brechia (1a) situated closed to the main fault.

Unit 2: This unit is located on the northern compartment of the fault zone. It is composed mainly by unstratified light ochre silty-clay and carbonate lake sediments (2a). No organic material has been found in this unit, which can be interpreted as deposits under cold climate conditions. This formation contains very well preserved seismites generated by paleo-earthquakes. These structures correspond to liquefaction features made of sandy-silty materials coming from the lower part of the formation, which is located now at a depth of 1-2.5 m (see Figures 18A, 19A and 20).
Based on these observations, we interpret the unit 2 as a sag pond deposit (lake sediments) because liquefaction phenomenon required generally water saturated unconsolidated sandy-silty materials located at a depth lower than 10 meters. Because sag pond deposits are covered by soils that are not affected by these seismites, it appears that the liquefaction features cannot be associated to the 1721 AD earthquake.

Figure 20: The flame form liquefaction feature in sandy-silty materials of unit 1 within trench T1bis (looking to east) (see Figure 18 for situation; between benchmarks 0 and 4).

Unit 2b: This unit is composed of colluvial deposits. The clasts of this formation are originated from the southern compartment while the matrix comprised mainly sag pound fine deposits from the northern compartment. Because elements of unit 2a appear inter-fingered in unit 2b, we interpret unit 2b as a lateral sedimentary variation of the sag pond formation (Figure 21). It must be note that the age of the base of this colluvial sub-unit (2b) varies, then,

laterally from north to south. Within main unit 2, isochrones are probably sub-horizontals. This observation is very important for seismic events interpretation in trenches T1bis and T1.

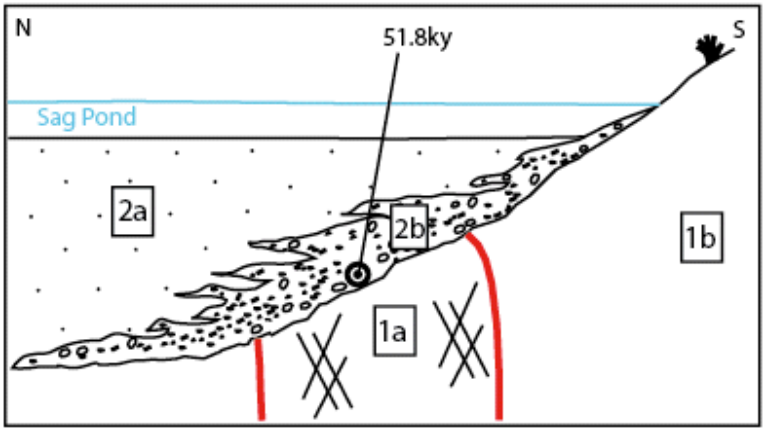

Figure 21: Schematic sketch of the sedimentary situation after the oldest observed paleo-event found in trenches T1bis and T1. Fault ruptures were sealed by the deposition of unit 2a and 2b.

Unit 3: Unit 3 corresponds to an unconsolidated, well washed grayish graded-bedding deposit associated to the infilling of a fossil gully. The gully is localized within the main fault zone in a graben bounded by two fault planes. Surface ruptures of the last seismic events affected this unit.

Unit 4: This unit consists of a dark developed paleosoil covering unit 2 conformably. This paleosoil contains mainly fine organic materials, fossil roots and carbonate reworked from unit 2 and rare clastic elements. This paleosoil indicates that sag pound conditions ends since that time.

Unit 5: This unit corresponds to a brown superficial soil that contains organic material, sand and numerous clasts of centimetric size. The base of this unit gullied the unit 2 (i.e. benchmark 0.5 in trench T1bis) indicating that an erosional surface has developed.

Unit 6: This unit, which is the most superficial one, is composed by a fine-grained modern soil to the north (6a) and by a colluvium to the south (6b) that contains an important fraction of organic material. The upper part of the unit 6 is reworked by agricultural activities.

Descriptions of the fault planes within T1bis and T1 trench walls:

On the trench walls, several fault planes are clearly visible. Generally, the fault planes consist of south dipping thrusts that become rapidly vertical at depth. Among them, some can be considered as the most recent ones because they crosscut the youngest formations (i.e. units 5, 6). However, the other ones seem to be older because they are covered by the same young formations (benchmark 7, trench T1bis).
The main fault (between benchmarks 3 and 4 in trench T1 bis) consists of a 50 cm wide sub vertical shear zone. This zone is limited on both sides by slip planes that cut young formations. The southern one clearly reaches the surface (benchmark 4 in T1bis and benchmark 8 in T1) (see Figures 18A, 18B, 19A and 19B).

Trench T2:

140 m south of the first (T1 bis) and second (T1) trenches at site 1, we dug another trench (T2) across the thrust fault scarp (Figures 22A and 22B). This trench measures 8 m long and 2.5 m deep.

Figure 22A: Picture looking south of the third trench T2 (within the site 1). This trench was excavated across a NE dipping thrust fault located just SW of T1 and T1bis trenches. The surface rupture associated to this fault is clearly visible in the morphology or in the aerial photos and can be followed for several hundred meters toward the SE (see Figures 12, 14 and 15 for situation).

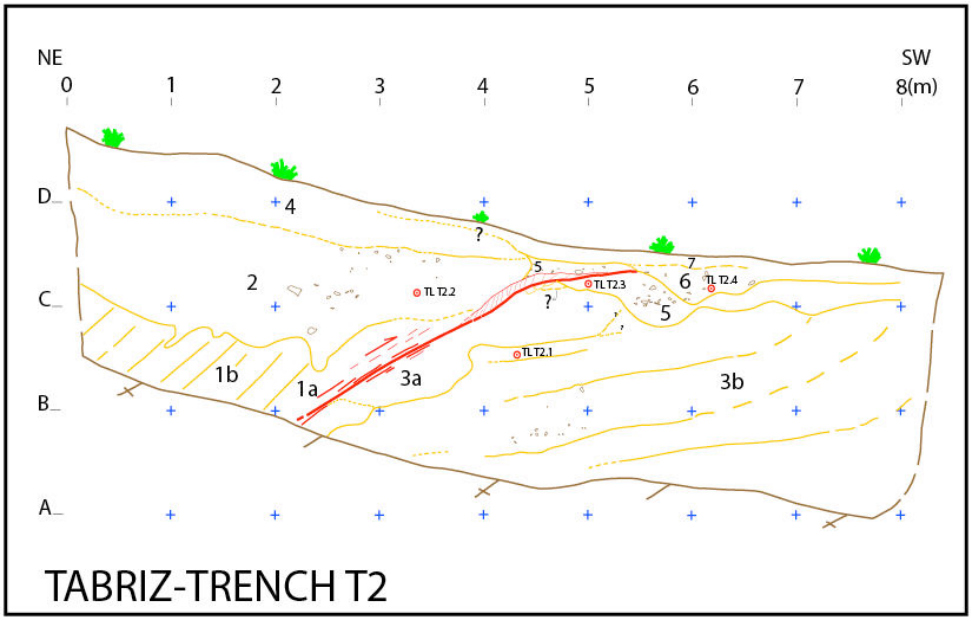

Figure 22B: Paleoseismological Log of the third trench (T2) that crosscut the thrust fault scarp of the NTF zone within site 1.

Descriptions of the sedimentary units within T2 trench wall:

Unit 1: This unit is composed by Mio-Pliocene sediments and constitutes the northern compartment (1b) of the fault zone. This unit includes a 20-30 centimeters wide shear zone (1a).

Unit 2: This unit consists of a grey consolidated colluvial deposit, which contains fine elements as a matrix with carbonate impregnations. Some fossil root traces associated to the paleosoil of the unit 4 are visible at the top of this unit. Some centimetric clasts are also present. This unit was deposited unconformably on the Mio-Pliocene bedrock (unit 1) as demonstrated by a very well developed erosional surface. Because unit 2 is at the same stratigraphical position than unit 5 in the trenches T1bis and T1, we assume that these two units have a same age. This unit exists only on the hanging wall of the fault.

Unit 3: This unit corresponds to a well-stratified alluvial fan deposit, hardened by carbonated impregnations. The unit contains coarse elements of decimetric size inter-bedded with fine sandy levels. Bedding dips gently (about ten degrees) toward the north.

Unit 4: Unit 4 is a reddish-Brown paleosoil partially hardened. It contains organic material and fine vertical lode of carbonate, which correspond probably to fossil root traces. This unit as for unit 2 exists only on the hanging wall of the fault.

Unit 5: It is a colluvial wedge formed at the immediate vicinity of the superficial trace of the fault. It contains clasts of centimetric size with some pebbles and a sparse matrix. This colluvial wedge has been clearly cut by the fault.

Unit 6: It corresponds to another colluvial wedge, which overlaps the unit 5. This unit contains material reworked from the unit 4.

Unit 7: This unit corresponds to the modern soil riches of organic material. It is partially reworked by recent agricultural activity.

Description of the fault planes within T2 trench wall:

As we mentioned before the fault scarp shows clear evidences of vertical component that could be corresponds to a low angle thrust fault (see section 3 above).
After digging the trench, we found a thrust fault plane dipping (33°) to the NE. Here, the deformation is concentrated along a narrow shear zone (20-30 cm). This fault plane cut the superficial units (such as unit5) showing its recent activity.

Site 2:

1.4 km east of the site 1, we found a nice outcrop of the NTF on an east-facing artificial riser made for agricultural purpose, which we dug and cleaned it again to study.

Here, the main dextral deformation zone of the NTF contains a narrow zone that cut a Quaternary fan deposits to the south and displaced against Neogene bedrock covered by a very young soil unit to the north (Figure 23, 24A and 24B). The outcrop is located just west of an offset riverbed.

Within the trench wall, sedimentary units geometry appear almost horizontal (on both side of the narrow fault zone), which indicate that the main fault slip component is strike-slip rather than dip-slip. However, there are some evidences of secondary order normal-vertical component of deformation distributed within a zone of about 4 meters along ruptures dipping SW (Figures 27 and 28).

The main difference between sites 1 and 2 is the situation of the bedrock. Within T1 bis and the T1 trenches, the Mio-Pliocene bedrock is located south of the main fault zone, however at site 2 the bedrock is situated north compare to the fault trace. This observation is characteristic of displaced topographies along strike slip faults.

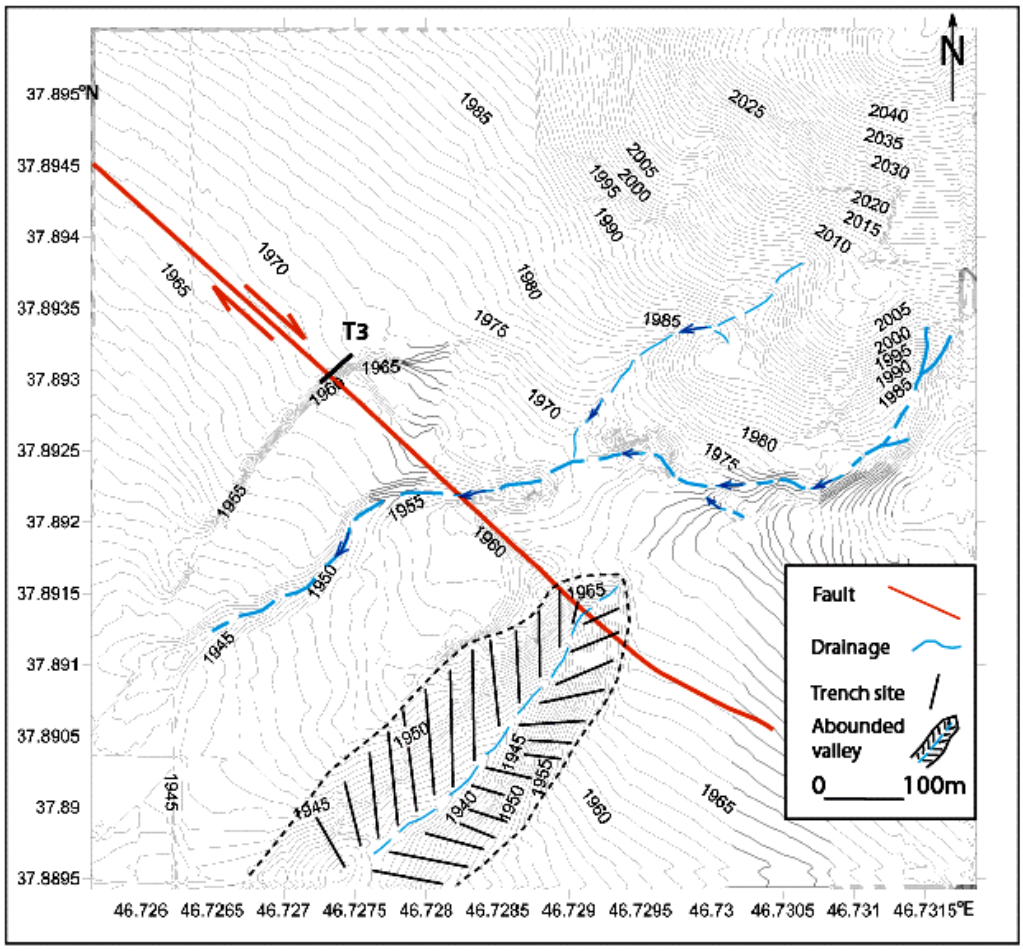

Figure 23: Detailed topographic map based on DEM of the site 2 calculated from GPS kinematics surveying (see Figure 12 for situation). Here, the fault cut and shifted 300 meters right laterally the riverbed. The abounded valley (situated on the southern side of the fault trace) is another morphological feature of the strike-slip faulting formed along the SE segment of the NTF.

Figure 24A: View of the trench T3 opened across the NTF at site 2. Here, the narrow steep shear zone of the main right-lateral strike-slip deformation separates the alluvial fan deposits (to the south) and Mio-Pliocene bedrock and its Late Quaternary cap (to the north).

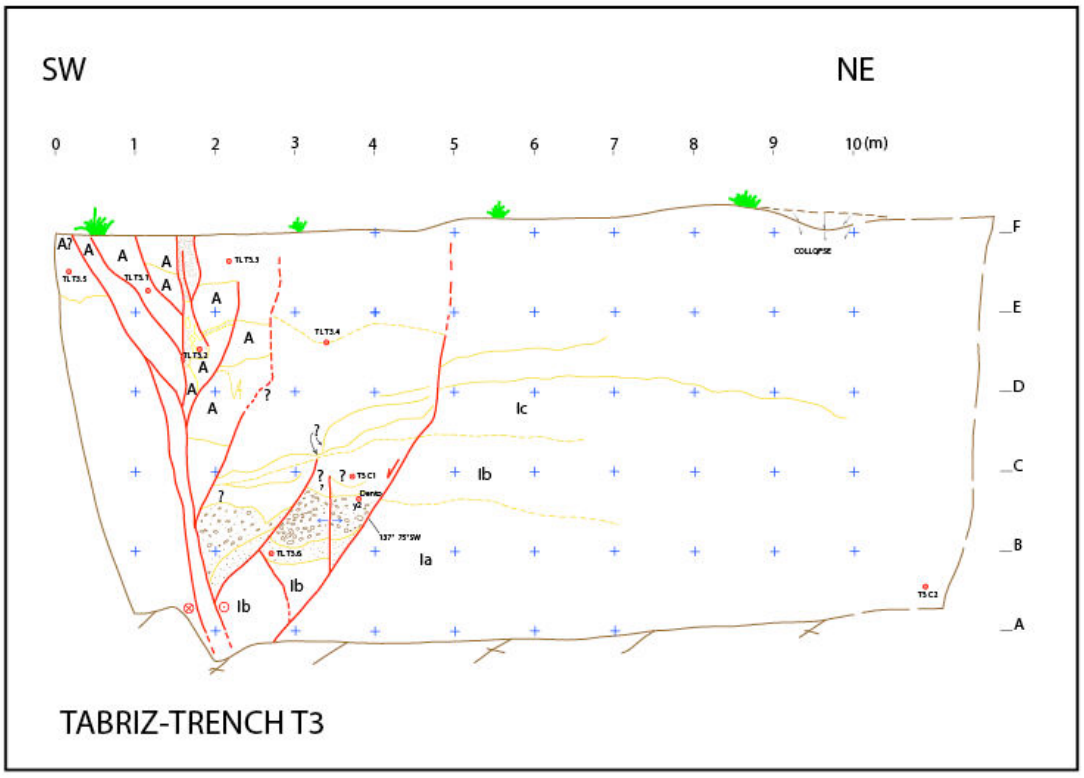

Figure 24B: Trench log T3 (site 2). The width of the fault zone is about 5 meters close to the surface and less than 2 m at a depth of about 5 meters. We observed that right-lateral strike-slip faulting is concentrated at depth in a narrow zone (between benchmark 1.8 A and 2.1 A). To the surface, the fault zone becomes wider (between benchmarks 1.0 F and 5.0 F). Some evidences of a normal component are observed on a few fault planes located at an intermediate depth (between benchmarks 2B and 4B).

Dating Analysis:

To determine the age of paleoearthquake evidences found in trench walls within site 1, we have chosen eight OSL (Optical Stimulated Luminescence) samples. In the following, we present the results:

Trench T1.bis

Samples	Age
……..	..……
TL-T1bis 1 (base U3)	33.5 ka (-/+ 10%)
TL-T1bis 3 (top U2b)	51.8 ka (-/+ 10%)
TL-T1bis 4 (top U3)	14.8 ka (-/+ 10%)

Trench T1 (west wall)

Samples	Age	
……..	..……	
TL-T1.b 2 (U2a)	24.5 ka (-/+ 10%)	
TL-T1 b 4 (U2b)	44.1 ka (-/+ 10%)	Prob. Error
TL-T1 b 5 (U4)	12.4 ka (-/+ 10%)	

Trench T2 (east wall)

Samples	Age	
……..	..……	
TL-T2-3 (U5)	18.5 ka (-/+ 10%)	
TL-T2-4 (U6)	24.4 ka (-/+ 10%)	Prob. Error

Based on these results, the age of analyzed units varies from -51.8 ka to -12.4 ka. This time window is relatively wide, however there is a normal chronological order. On the other hand, the most recent units (U5, U6a and U6b) are not yet dated.

Interpretation of paleo-seismic events within trenches:

In order to interpret the paleoearthquakes that occurred along this section of the SE segment of the NTF, we decided to focus our analysis on site 1 and especially within trenches T1bis and T1. Our decision is based on the difficulty to interpret unit geometries in trench T3 within the site 2 and available datations.

To reconstruct paleoearthquake chronology, which has been documented using the young units as seismits of trenches T1bis and T1, we model the events and their recurrence period's situations in following illustrations (see Figures 21 and 25 A to F). In these figures, each event horizon (i.e. the ground surface at the time of the faulting) for these paleoearthquakes is located in the following stratigraphic positions:

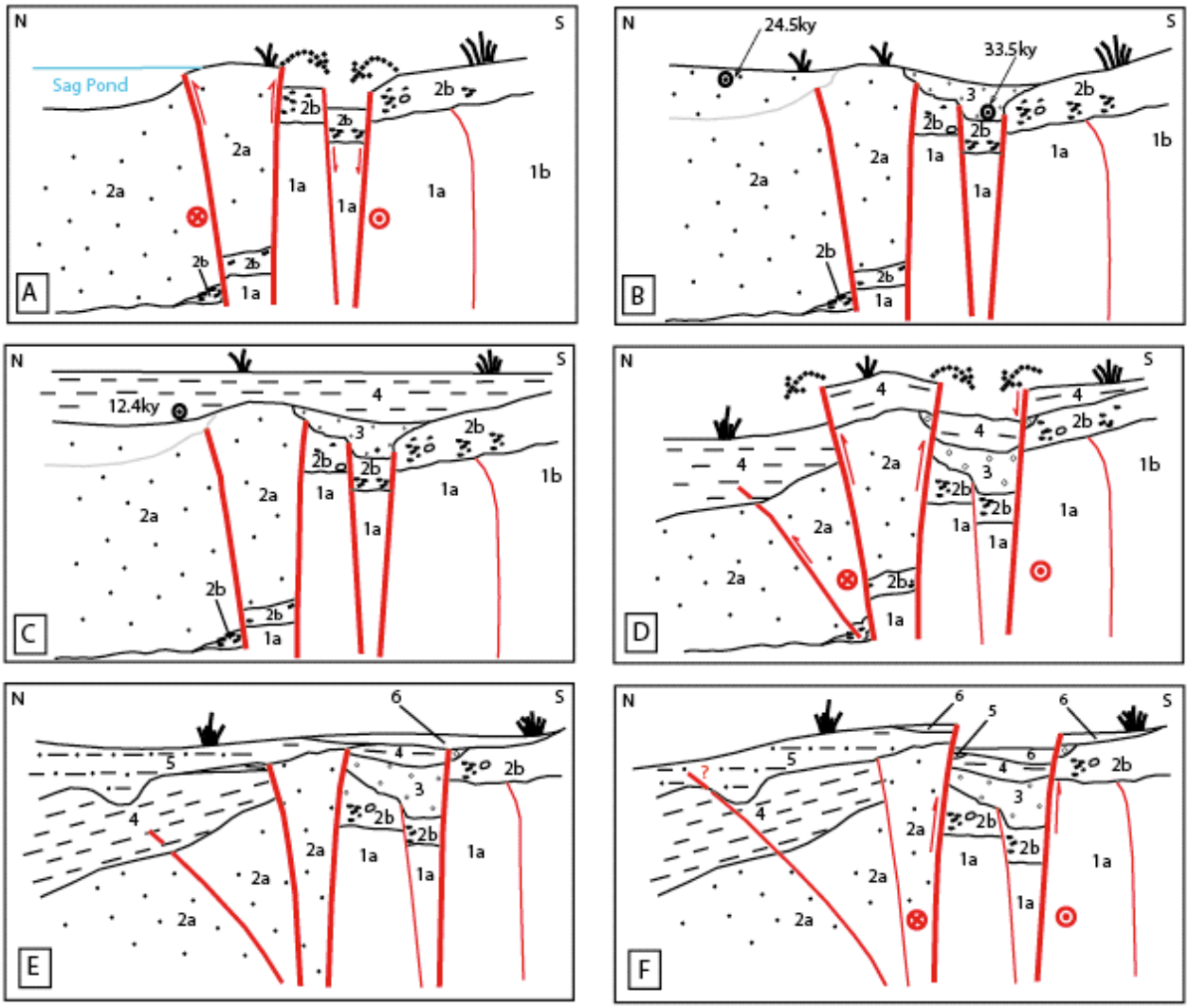

Figure 25: The chronological stages of co-seismic surface faultings and their recurrence period's situations after the first recorded paleo-event (see Figure 23) occurred within trenches T1bis and T1.

Figure 21 shows the situation after the first documented old strong earthquake observable within trench T1bis and T1. The erosion surface between the units 1 and 2 is the event horizon of the paleoearthquake. The unit 2b is a colluvial wedge as the equivalent of the unit 2a and can be interpreted as the post-event horizon for one or several seismic events. The observed liquefaction features within unit 2a (see Figure 20) allow us to conclude that one or probably more seismic events took placed during sedimentary process of the sag pond (51.8-24.5 kyr at minimum). In trenches T1bis and T1, the age of this oldest paleo-event is at minimum 51.8 +/- 5 Kyr.

Figure 25:

Figure A, shows the situation at the time of the surface faulting associate to the second strong earthquake. The unit 2b and its equivalent (unit 2a) are the event horizon of this paleo-event.
Figure B, shows an erosional stage that occurred after the second paleoearthquake. The basal portion of unit 3 (-33.5. +/- 3 Kyr), that covers the erosion surface, is interpreted as the post-event horizon of the second earthquake.

Figure C, shows the sedimentation of unit 4 before the third paleoearthquake. The base of this unit was dated to 12.4 +/- 1 Kyr.

Figure D, shows the situation at the time of a new surface faulting associated to the third strong earthquake. The top of unit 4 (ground surface) is the event horizon of this third paleo-event.

Figure E, shows an erosion surface that affected the top of units 2a and 4 and the deposition of units 5 and 6 that formed after the third paleoearthquake.

Figure F, shows the situation during the last surface faulting, which can be associated to the last strong seismic event of 1721 AD because it affects the uppermost soils situated close to the surface, except a discontinuous thin recent soil layer constituting the present day ground surface that developed during the last 300 yr (see paleoseismological logs in Figures 18A and 19A).

We also found the age of a seismic event within trench T2, which is older than 18.5 +/- 2 Kyr (unit 5 is the post event horizon) and that could be associated to one of the oldest seismic event documented within trench T1bis and T1. Within trench T2 a younger event (less than 18.5 +/- 2 Kyr) cut unit 5 and is covered by unit 6 corresponding to the last post event horizon). This last earthquake could be associated to the penultimate or the last (1721 earthquake) seismic event observable in trench T1bis and T1.

Discussion and Conclusions

1- The NTF is a portion of a regional fault system (Tabriz Fault System). The TFS with about 300 km long is the southeastern part of a large fault network (GSKT) that extends to the NW over more than 600 kilometers. Large right-lateral branches associated with E-W thrust and N-S normal fault segments mainly constitute this fault network (see Figure 1).

2- The northern termination of the GSKT fault network shows horsetail pattern of N-S normal faults associated with numerous active volcanoes whereas the southeastern termination within NW Iran (in Bozghush Range) is mainly characterized by active compression (see Figure 1). In fact, Bozghush Range not only is the eastern termination of the TFS but also it’s the eastern end of the GSKT fault network. This means that the fault network can be interpreted as a transform fault system between extensional and compressive deformations. This kinematics model is coherent with the N-S direction of convergence between Arabian-Eurasian plates. This interpretation doesn’t require that the NTF is the southeastern continuation of the North Anatolian fault as proposed by some authors (e.g. Westaway, 1990 and Jackson et al., 1992).

3- Our morphotectonics analysis of the TFS shows that the fault system contains four main portions. The two west and east central portions of it correspond to right-lateral strike-slip fault segments of the NTF. The western and eastern ends of the TFS contain oblique-slip (thrust and right-lateral) and dip-slip (thrust) faults. Our interpretations reveal that, these fault terminations correspond to compressional relays that accommodated most

of the horizontal displacement of the North Tabriz strike-slip fault. On both fault ends, strike-slip faulting is associated to pure to oblique thrusting. This deformation pattern reveals a transpressive tectonic regime. Normal faulting appears to be limited only to local extrado deformation associated to large scale folding within the Bozghush range.

4- The maximum cumulated right-lateral strike-slip offset observable in the morphology of the fault system is nearly twice along the west central section (more than 500 m) compare to the east central section (about 300 m) of the fault system. To verify if this significant difference of displacements is related to a variation of the slip rate along the fault segments, we used a paleosismological approach.

5- Our paleoseismological trenching along east central section of the fault system as the SE segment of the NTF revealed that the occurrence of at least three strong seismic events since the last 33.5 ky. Hessami et al (2003) show that the west central section of the fault system experienced a much higher rate with four large seismic events since 3600 years.

6- This can be interpreted in two ways:

1-The first possibility is a longer return period of seismic events along the east central section rather than the west central section of the fault system. We interpret this significant difference as evidence of decreasing co-seismic slip rate from NW towards SE along the fault. Indeed, the narrow fault zone of the NW segment of the NTF suggests a more concentrated active strike-slip faulting zone rather than the SE segment of the fault where the fault zone is wider and the deformation is more distributed.

Moreover, if we consider for the SE segment the longer time intervals of the earthquakes, the longer length of the segment (more than 60 km versus 50 km for the NW segment) and the larger mean value of about seven meters for the smallest observed dextral displacements (as slip per-event), the SE segment of the NTF could produce stronger seismic events than the NW segment of the fault.

The longer recurrence time intervals concern only strong earthquakes along the SE segment of the NTF but not moderate seismic events, which have logically shorter recurrence time intervals.

2-The second possibility is to interpret this difference by earthquake clustering as proposed by some authors (e.g. Berberian, 1997; Karakhanian et al., 2004). In this case, because of shorter recurrence time intervals there is not enough time to deposit any differentiated post-event horizons, so we lose consequently some internal seismic events.

-Acknowledgements
This research is based on collaboration between International Institute of Earthquake Engineering and Seismology (IIEES) and University of Montpellier 2. Founding for this joint project was provided by INSU Relief program, IIEES and French embassy. We wish to acknowledge the kind supports of the Mr. Rezai and his colleagues in prefecture of Bostanabad and also to Mr. Sadeghzadeh and his colleagues in Farazab Consulting Engineeres.

-References:

Ambraseys, N.N. &Melville, C.P., 1982. *A History of Persian Earthquakes, Cambridge Earth Science Series*, Cambridge University Press, London.

Barka, A. A., 1992, The North Anatolian Fault, Annales Tectonicae., VI, 164-195.

BERBERIAN,M. and S. ARSHADI, 1976. On the evidence of the youngest activity of the North Tabriz Fault and the seismicity of Tabriz city, *Geol. Surv. Iran Rep.*, **39**, 397-418.

Berberian, M., 1994. Natural hazards and the first earthquake catalog of Iran, Vol. 1: historical hazards in Iran prior 1900, I.I.E.E.S. report.

Berberian, M., 1997. Seismic sources of the Transcaucasian historical earthquakes. In: Giardini, D.,Balassanian, S. (Eds.), Historical and Prehistorical Earthquakes in the Caucasus. Kluwer Academic Publishing, Dordrecht, Netherlands, pp. 233–311.

BERBERIAN, M. and R.S. YEATS, 1999. Patterns of historical earthquake rupture in the Iranian plateau, *Bull. Seismol. Soc. Am.*, **89**, 120-139.

DEMETS, C., R.G. GORDON, D.F. ARGUS and S. STEIN, 1990, Current plate motions, *Geophys. J. Int.*, **101**, 425-478.

Eftekharnezhad, J., 1975. Brief history and structural development of Azarbaijan. Geological Survey of Iran, Internal Report, 8P.

Hessami, K., D. Pantosi, H. Tabassi, E. Shabanian, M. Abbassi, K. Feghhi, S. Sholaymani, 2003. Paleoearthquakes and slip rates of the North Tabriz Fault,NWIran : preliminary results, Ann. Geophys. 46 903–915.

JACKSON, J., 1992. Partitioning of strike-slip and convergent motion between Eurasia and Arabia in Eastern Turkey and the Caucasus, *J. Geophys. Res.*, **97**, 12471-12479.

Jackson, J., Priestley, K., Allen, M., Berberian, M., 2002. Active ectonics of the South Caspian Basin. Geophysical Journal International 148, 214– 245.

Kagan, Y.Y. and Jackson, D.D., 1991. Long-term earthquake clustering, Geophys. J. Int., 104, 117-133.

Karakhanian, A., Djrbashian, R., Trifonov, V., Philip, H., Arakelian, S., Avagian, A., 2002. Holocene-historical volcanism and active faults as natural risk factor for Armenia and adjacent countries. J. Volcanol. Geotherm. Res. 113 (1– 2), 319–344.

Karakhanian, A., R. Jrbashyan, V. Trifonov, H. Philip, A. Avagyan, K. Hessami, F. Jamali, M. Bayraktutan, H. Bagdassarian, S. Arakelian, V. Davtyan, A. Adilkhanyan, 2004. Active faulting and natural hazards in Armenia, eastern Turkey and Northern Iran, Tectonophysics, 380 189–219.

Masson, F., Djamour, Y., van Gorp, S., Ch´ery, J., Tatar, M., Tavakoli, F., Nankali, H. & Vernant, P., 2006. Extension in NW Iran driven by motion of the South Caspian Bosin, *Earth Planet. Sc. Lett.*, **252,** 180–188.

McQuarrie, N., J. M. Stock, C. Verdel, and B. P. Wernicke, 2003. Cenozoic evolution of Neotethys and implications for the causes of plate motions, Geophys. Res. Lett., 30(20), 2036, doi:10.1029/2003GL017992.

Nabavi, M. H., 1976. Preface to geology of Iran, Geological survey of Iran, 109 p. (in Persian)

F. Nilforoushan, F. Masson, P. Vernant, C. Vigny, J. Martinod, M. Abbassi, H. Nankali, D. Hatzfeld, R. Bayer, F. Tavakoli, A. Ashtiani, E. Doerflinger, M. Daignières, P. Collard, J. Chéry, 2003. GPS network monitors the Arabia–Eurasia collision deformation in Iran, J. Geody., 77, 411–422.

Sella, G. F., T. H. Dixon, and A. Mao , 2002. REVEL: A model for Recent plate velocities from space geodesy, J. Geophys. Res., 107(B4), 2081, doi:10.1029/2000JB000033.

Siahkali Moradi, A., 2008. Seismicity-Seismotectonic and velocity structure of the earth crust within the Bam and Tabriz strike-slip fault zones, Phd. Thesies, International Institute of Earthquake Engineering and Seismology (IIEES).

Solaymani Azad S., Dominguez, S., Philip, H., Hessami, K., Forutan M-R, Shahpasand Zadeh , M., Ritz, J-F, In preparation, The Zandjan Fault System; Morphological and tectonic evidences of a new active fault network in the NW of Iran, In preparation.

Stöcklin, J., 1968. Structural history and tectonics of Iran: a review. American Association of Petroleum Geologists Bulletin 52, 1229–1258.

Stöcklin, J., 1974. Mesozoic-Cenozoic Orogenic Belts: Data for Orogenic Studies. In: Spencer, A. (Ed.), Northern Iran: Alborz Mountains, 4. Geological Society Special Publication, London, pp. 213–234.

Vernant, P., F. Nilforoushan, D. Hatzfeld, M. Abbassi, C. Vigny, F. Masson, H. Nankali, J. Martinod, A. Ashtiani, R. Bayer, F. Tavakoli, J. Chery, 2004. Contemporary crustal deformation and plate kinematics in middle east constrained by GPS measurement in Iran and northern Oman, Geophys. J. Int., 157, 381–398.

Vernant, P., and J. Chery, 2006. Low fault friction in Iran implies localized deformation for the Arabia-Eurasia collision zone, Earth Planet. Sci. Lett., 246, 197-206.

WESTAWAY, R., 1990. Seismicity and tectonic deformation rate in Soviet Armenia: implications for local earthquake hazard and evolution of adjacent regions, *Tectonics*, **9**, 477-503.

CHAPITRE 4

LE SYSTEME DE FAILLES DE ZANDJAN

Dans les deux chapitres précédents, nous nous sommes intéressés au domaine oriental et occidental du Nord-ouest de l'Iran où sont localisées deux villes importantes. Dans le présent chapitre, nous nous focaliserons sur la région de Zandjan qui est située à la jonction entre trois domaines structuraux : celui de l'Alborz (à l'est), de Tabriz-Azerbaïdjan iranien (à l'ouest) et de l'Iran Central (au sud). Pourtant, sur la base des catalogues de la sismicité (historique et instrumentale) du Nord-ouest de l'Iran et des cartes sismotectoniques, cette région n'est pas considérée comme très active. Cependant, d'un point de vue tectonique, cette région appartient à un secteur-clé pour comprendre la géodynamique de la région car elle appartient à la zone de transition entre l'Alborz occidental, caractérisée entre autre par des failles décrochantes sénestres et le secteur Tabriz-Azerbaîdjan où les failles actives décrochantes sont dextres alors qu'elles ont la même direction NW-SE que celles de l'Alborz occidental.

The Zandjan Fault System: Morphological and tectonic evidences of a new active fault network in the NW of Iran

SOLAYMANI AZAD S. (1,2), DOMINGUEZ S. (1), PHILIP H. (1), HESSAMI K. (2), FORUTAN M-R (3), SHAHPASAND ZADEH M. (2), RITZ J.-F. (1)

1: Université Montpellier 2, Laboratoire Géosciences Montpellier, UMR 5243, Montpellier, France.
2: International Institute of Earthquake Engineering and Seismology (IIEES), Dibaji, 19531, Teheran-Iran.
3: Geological Survey of Iran, P.O.Box: 13185 1494, Teheran-Iran.

Abstract: In NW Iran, the Zandjan province is situated at the junction between the southern termination of the Tabriz right-lateral strike-slip fault and the western end of the Alborz active mountain range. Despite this strategic location in terms of active tectonics, there is no destructive earthquake reported in available historical seismicity catalogues. Even if a few low magnitude earthquakes have been recorded in the last century indicating that this area is actively deforming, the Zandjan region can be considered as a seismic gap. In the present study, based on Digital Elevation Models (DEM), satellite image and aerial photo interpretations together with detailed field investigations, we have identified a new major active fault network. It is mainly constituted by several west and north verging thrust faults, trending NW-SE to N-S, that clearly cut Late Quaternary and recent deposits. Evidences in the morphology indicate also that they accommodate a significant right-lateral slip component. This fault network can be divided into four major fault zones affecting Zandjan city (present day population over 510000) and part of the Zandjan-Mianeh basin more to the west. Based on fault geometrical characteristics (fault length, segmentation...) and kinematics, the Zandjan fault system is capable to produce moderate to large earthquakes and serious damages in surrounding areas. The study of these faults is, then, of major interest for seismic hazard assessment in Zandjan province where total population exceed 1.5 million but also to better understand present day geodynamics of NW Iran.

Key words: Iran, NW of Iran, Zandjan, seismic gap, morphotectonics, active faulting

I) Introduction:

Iran is part of the Alp-Himalayan orogenic belt that extends over more than 10000 km from west Europe to Southeast Asia (Figure 1). It is actively deforming in response to the northward motion of Arabia plate that collides with Eurasia (Figure 1). As indicated by the most recent published GPS measurements (e.g. Vernant et al. 2006; Relinger et al., 2006) convergence occurs at a present day shortening rate of about 23 to 25 mm/yr. In response, strong to moderate earthquakes strike regularly this region (Figure 1). Indeed, according to historical seismicity catalogues, at least 450 destructive earthquakes were reported in Iran since 600 BC (e.g. Ambraseys and Melville 1982; Berberian, 1994; Berberian and Yeats 1999 and 2001). In the last century, strong earthquakes (M>6.5) occurred at a similar rate, each five to six years in average (Silakhor (Ms=7.4, 1909), Salmas (Ms=7.4, 1930), Torud Ms=6.5, 1953), Lar (Ms=6.7, 1960), Buin Zahra (Ms=7.2, 1962), Dasht-e-Bayaz (Ms=7.4, 1968), Qir (Ms=6.9, 1972), Khorgu (Ms=7.0, 1977), Tabas (Ms=7.7, 1978), Qayen (Ms=7.1, 1979), Rudbar-Manjil (Ms=7.3, 1990), Sefidabeh (Ms=6.1,1994), Ardebil (Ms=6.1, 1997), Birjand (Ms=7.3, 1997) and Fandog (Mw=6.6, 1998)). The sources of all of these seismic events are well identified now and correspond to active reverse or strike-slip faults mainly concentrated in the south of Iran (Zagros fold-and-thrust belt), eastern Iran and north-west of Iran (Alborz ranges and Talesh-Azerbaijan region). However, it is important to point out that for some of these events, the seismic source was unknown before the occurrence of the earthquake because active fault mapping of Iran is still under progress.

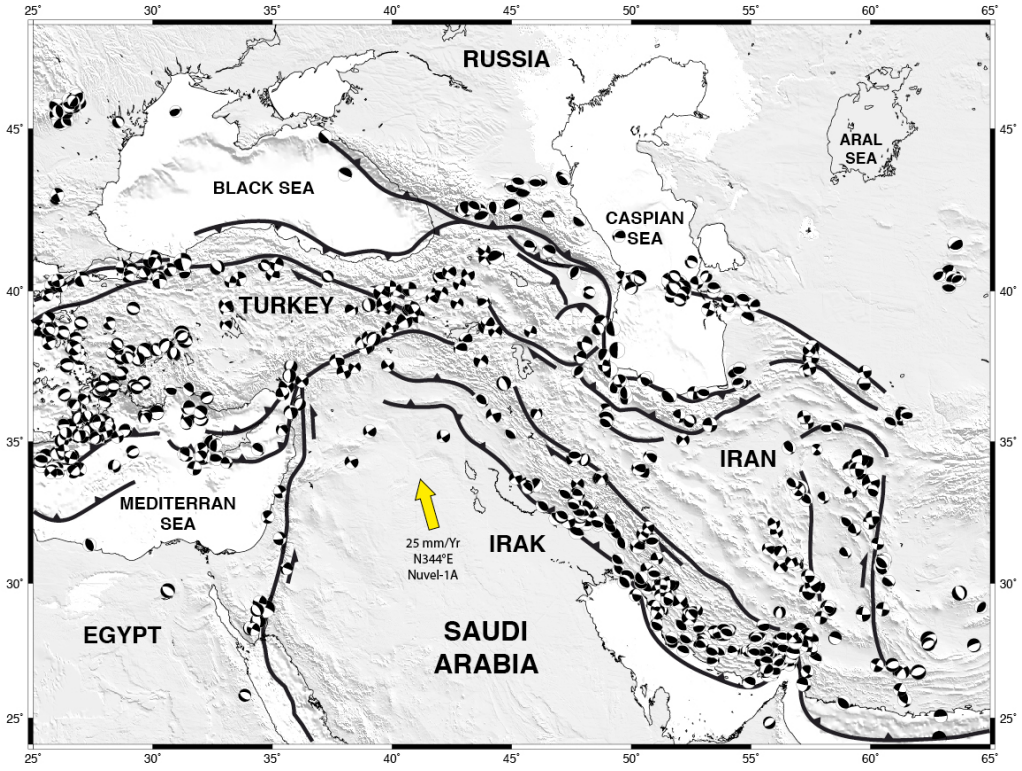

Figure 1: Geodynamic context of the Arabia-Eurasia collision. Focal mechanisms are from CMT Harvard (1976-2008).

Because climatic conditions are more favorable in the northern part of Iran and especially in north central (Teheran) and northwest of Iran (Tabriz), the population density is significantly

higher in these regions. Furthermore, as water resources are not very abundant, most of Iranian villages and main cities have developed in the vicinity of mountain range fronts and consequently often very close to active fault zones. Seismic hazard is, then, very high in the N and NW of Iran. Numerous works dedicated to the study of active faults and earthquakes were conducted in the past decades, especially in the NW Iran (e.g. Berberian 1983 and 1997; Cisternas and Philip 1997; Karakhanian et al. 1994, 2002 and 2004; Jackson et al. 1992 and 2002; Westawey 1990; Hessami et al. 2003; Coplay and Jackson 2006). In these works the NW of Iran is considered as a part of the Transcaucasian structural domain within the Turkish-Iranian Plateau (average elevation about 2 km) (e.g. Van Couvering and Miller 1971; Berberian 1997; Cisternas and Philip 1997; Copley and Jackson 2006). Based on Cisternas and Philip (1997), the recent geodynamics of the NW of Iran is controlled by its eastward motion since upper Miocene (Tortonian) which occurred synchronously with the opening of the Red Sea and northward motion of the Arabia Plate. Other works such as Jackson and McKenzie (1984), Priestly et al. (1994) and Westawey (1990), showed that the most important effect of this eastward motion is thrusting of NW Iran over the oceanic crust (Berberian 1983) of the South Caspian Basin.

At a general scale, the northern and southern borders of the Alborz Ranges are actively thrusting over the southern margin of the Caspian Sea and on the northern part of the Central Iranian block, respectively (e.g. Berberian 1983). Moreover, Jackson et al. (2002) based on seismic stress drop of earthquakes showed that nearly whole of tectonic deformation in NW Iran and E-Turkey is co-seismic. Berberian (1997) pointed out that the main seismotectonical characteristic of the NW Iran and Transcaucasia is the occurrence of very strong earthquakes, which historically occurred often in a cluster form. Berberian (1997) insisted on the possibility of contemporaneous surface rupturing of whole of the segments during a single strong earthquake along some fault systems in this region. Karakhanian et al. (1994 and 2004) also tried to complete the active fault mapping in the region of south Armenia and northwest of Iran. They studied also fault segmentation along some faults such as the North Tabriz Fault. These investigations, that significantly improved the evaluation of the seismic hazard assessments in these regions, were completed by some paleoseismological analysis. Trenching across the NW segment of the North Tabriz Fault, which is one of the main seismic sources of NW Iran showed that since 1600 B.C. four strong earthquakes occurred along this segment of the fault (Hessami et al., 2003). As a result, the slip rate along the portion of the North Tabriz Fault was estimated to be about 3.1-6.4 mm/yr. Moreover, morphotectonics and paleoseismological analyzes on the SE segment of the NTF (Solaymani et al., in preparation) reveals some evidences for slip rate variation along the fault.

In this paper, we investigate the seismic hazard situation of the Zandjan city, a populated city located between Teheran and Tabriz that could be considered up to now as a seismic gap, based on instrumental and historical seismicity data. Our work is based on seismotectonics and especially morphotectonics observations acquired during three field trips conducted in 2005, 2006 and 2007 that allowed us to discover and document a new fault network.

II) Geodynamic context and active tectonics of NW Iran

NW of Iran is situated nearby the most central part of the Arabia-Eurasia collision zone. This region is characterized by intense N-S finite shortening distributed over 500 km and experienced destructive historical earthquakes (e.g. Berberian, 1997; Allen et al., 2004). The geology of Iran (Figure 2) results from a long geodynamic evolution starting at the beginning of the Triassic with the closing of the Paleothetys and the opening of the Neothetys (e.g.

Sengör 1979; Stampfli 1991 and 2001). The subduction of Neothetys beneath the southern margin of Eurasia (south of the Central Iranian Plateau) during Jurassic and Cretaceous generated the formation of a calco-alkaline volcanic arc (Urumieh-Dokhtar Magmatic Arc, UDMA) (e.g. Förster et al., 1972) and associated HP-LT metamorphic belt (Sanandaj-Sirjan, Central Iran) (e.g. Berberian 1983; Ghassemi and Talbot 2006; Agar et al.; 2005). During the Eocene, back arc extension produced extensive volcanic and magmatic activity in Central Iran and Alborz ranges (Figure 2). The collision between Arabia and Eurasia occurs diachronously after closing the Neothetys, during the Oligocene in the northwest of Iran and during the Miocene in the southeast (Stoneley 1981; Yilmaz 1993). Consequently, the deformation of the Arabia passive margin resulted into the construction of the Zagros fold-and-thrust belt and the propagation of the deformation toward the north up to the Alborz and Caucasus (e.g. Berberian, 1983; Blanc, 2003; Ghasemi and Talbot, 2006). The present day topography of Iran is directly inherited from this last Alp-Himalayan phase of deformation but it is noticeable that some of the main active faults reactivate Paleozoic and Mesozoic inherited structures (Figure 2).

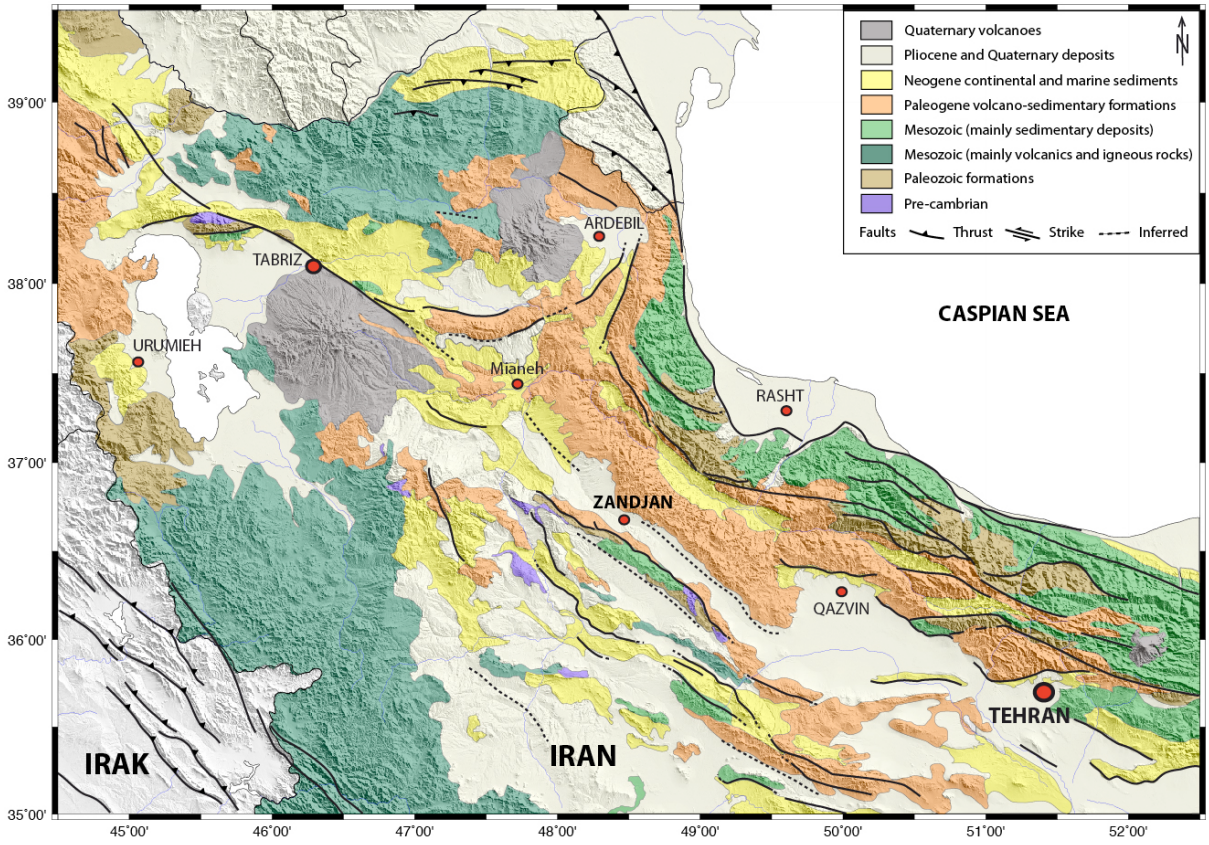

Figure 2: Simplified geological map of NW Iran merged with shaded topography.

Assessing current deformation of Iran with GPS monitoring reveals that the general direction of crustal motion in NW of Iran is toward the north at 22-23 mm/yr. (Nilforushan et al. 2003; Vernant et al. 2004 and 2006; Masson et al. 2006; Reilinger et al., 2006). When looking into more details, the GPS strain field can be divided into several areas (Figure 3). The central Iranian plateau appears to move N355° at 14 mm/yr. while north of Tabriz, the Talesh and Armenia move N10° at about 13 mm/yr. A significant part of the deformation (3 to 5 mm/yr.) seems also to be accommodated across the Alborz Range (Vernant et al., 2004). These kinematics differences are related to the activity of the N135° trending right-lateral strike-slip North Tabriz fault and the N175° trending right-lateral Talesh fault.

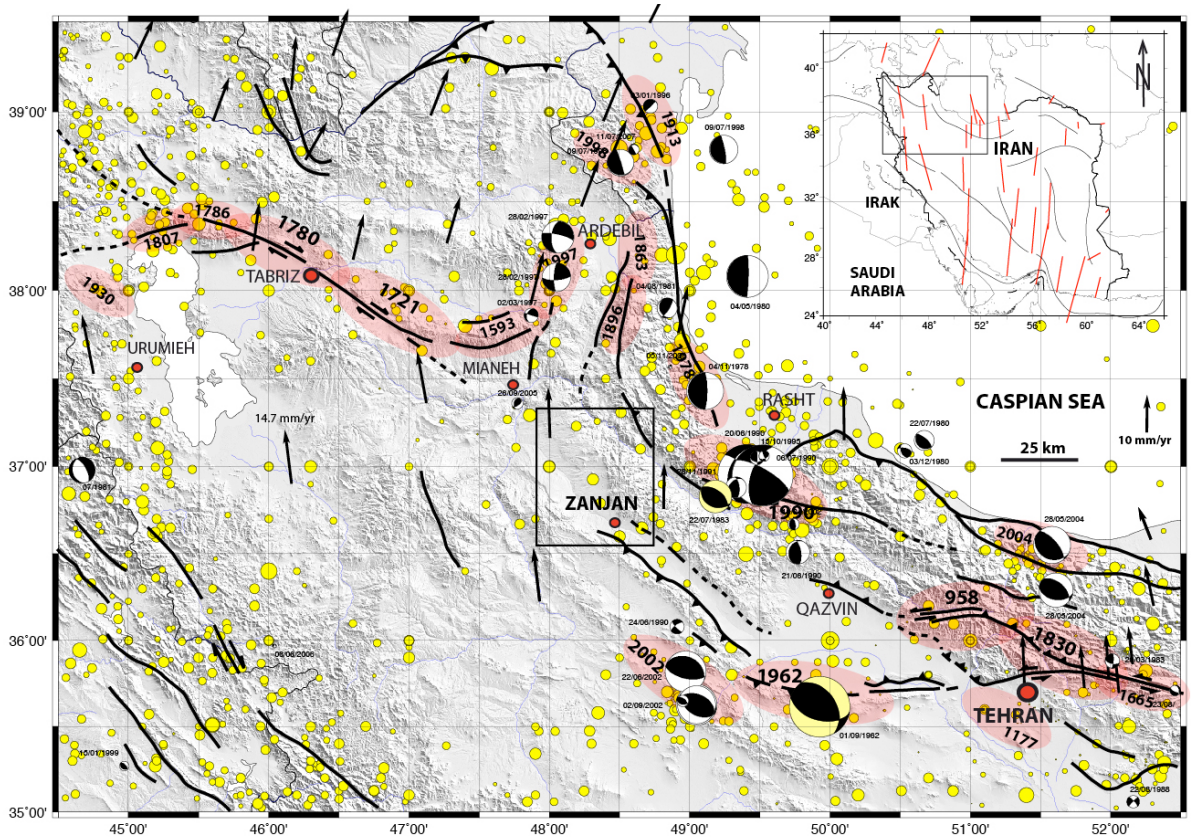

Figure 3: General seismotectonic map of NW Iran showing the main active faults, historical (Ambraseys and Melville, 1982; Berberian, 1997; Berberian and Yeats, 1999) and instrumental seismicity (IRIS), focal mechanism (Harvard CMT and Jackson et al, 2002). GPS vectors are from Reilinger et al., 2006.

Historical and instrumental seismicity records in NW of Iran show that the most active region corresponds to the Tabriz area, which experienced at least 12 destructive historical earthquakes since 858 AD (Figure 3). During the two last decades however, this part of NW Iran did not experienced any destructive seismic event. Two other strong seismic events in NW of Iran can be also mentioned, the Salmas earthquake (M>7, 1930) and the Chalderan earthquake (M>7, 1976) situated near the frontier between Iran and Turkey. In the north, a few historical and instrumental earthquakes were reported in the Talesh (1567(?), 1861, 1862) and near Ardebil (1997). In the north-central part of NW Iran, large earthquakes (M>6) have been also recorded north of Miyaneh (near Bozghush in 1593, 1679, 1844, 1879) and in the northeast (southeast of Ardebil in 1863 and in 1896 and north of Astara in 1913). To the east, several major earthquakes have been also recorded in the western termination and the central part of Alborz (near Teheran; 958, 1177, 1665 and 1830, Buinzahra; 1962, Qazvin, Avaj; 2002, Manjil-Rudbar; 1990).When considering the historical seismicity catalogues, it appears that the southwestern and south-central parts of NW Iran are characterized by a relative low level of seismic activity (e.g. Ambraseys and Melville 1982, Berberian 1994). The Zandjan region, in particular, seems to correspond to a seismic gap because no historical earthquake had affected this region. Up to now only a few low (M<5.5) magnitude earthquakes have been recorded in the last century indicating that this region is actively deforming. One possible explanation for such an anomaly is to consider that the recurrence time interval for large seismic events could reach several thousand years (e.g. 4000 years for the Manjil earthquake; Mw=7.3, 1990, Berberian and Yeats 2001). This remark is very important for assessing seismic hazard in the NW of Iran.

The distribution of mapped active faults in the NW of Iran shows noteworthy variations in trend and mechanism of faulting. In the northwestern part of the region, the North Tabriz Fault has been identified as the seismic source of the strong event of 1780 (Mw=7.4, Io=IX) (Berberian, 1997). It is a nearly pure right-lateral strike-slip fault, trending N135°E, with a slight reverse component as demonstrated by compressive deformations observable all along the fault trace (Nabavi 1976; Eftekharnezhad 1976; Berberian and Arshadi 1976; Karakhanian et al. 2004) and in trenches (Hessami et al. 2003; Solaymani et al., in prep.).
In the Talesh, active faults mainly correspond to south and north dipping thrust faults trending E-W in Central Talesh and nearly NW-SE in the east (near Lankaran) (e.g. Berberian 1997). In the southeast, these faults connect with the western termination of the Alborz ranges along a major right-lateral transfer reverse fault zone constituted by the north and south Talesh Faults (Figure 3). In the same region, the N20°E trending Sangavar Fault marks the transition between the eastern border of the Bozghush mountain range and the northwestern end of the Alborz ranges (e.g. Berberian 1997; Hessami et al., 2003). This fault is probably reverse with a right lateral strike-slip component (Berberian and Yeats 1999; Allen et al., 2003).
In the Alborz domain, the seismicity and active shortening is partitioned mainly along north and south dipping thrust faults, trending range parallel, but also on left-lateral strike-slip faults that accommodated the oblique component of the local plate convergence (e.g. Allen, 2003; Jackson et al., 2002). The thrust faults are often located at the base of mountain fronts (e.g. Khazar fault and western part of North Teheran faults) and the main strike-slip faults are situated generally in the region of high topography (e.g. Rudbar-Manjil, Taleghan and Mosha faults). As mentioned before, despite a lot of efforts (e.g. Berberian 1997, Hessami et al. 2003, Karakhanian 2004), active fault mapping of NW Iran is still under construction. For example, the seismic source of some events such as Avaj (Mw=6.5, 2002) was not identified before the earthquake (Solaymani and Feghhi 2003, Walker et al. 2005). Moreover, the relation between geometry and kinematics of active faults in northwest of Iran is not easy to interpret. Both left and right-lateral strike-slip components are observed along active faults shearing the same (WNW-ESE) direction (e.g. Salmas and North Tabriz faults to the west and Rudbar-Manjil, Taleghan, Ipak and Mosha faults to the east).
Finally, it is noticeable that no major seismic source is identified in the geological and active fault maps in the south central part of NW Iran and especially around the Zandjan city (see Figure 2). Indeed, even if a few faults are mapped east and south of Zandjan, no strong earthquake is reported in historical records (e.g. Ambraseys and Melville, 1982; Berberian, 1994). At the scale of NW Iran, it can be then considered as a seismic gap.

III) Morphotectonics analysis of the Zandjan Region

The Zandjan-Mianeh region is a key area because it constitutes the structural junction between the tectonic provinces of West Alborz in the east, Iranian Azerbaijan to the west and Central Iran in the south. Consequently, the morphology and tectonics of this region is controlled by interactions between NW-SE, N-S and E-W structural trends that characterize, respectively, these three geological domains (see Figures 2 and 3).
Using SRTM DEM analysis and geological maps of the Zandjan area, we discovered several topographic lineaments as escarpments affecting Plio-Quaternary deposits and morphologic anomalies disturbing the drainage network geometry (Figure 4).
North of Zandjan, we found a sharp NNW-SSE topographic lineament located at the boundary between the Eocene magmatic formations of West Alborz in the east and Quaternary alluvial deposits to the west (Figures 4). Its morphology is constituted by a topographic step of several meters, trending N 10° W parallel to the Gharadash mountain

front, that extends over more than seventy kilometers from north to south through the Zandjan city.
Based on additional works on DEM, satellite images and field investigations, we identified two other topographic anomalies associated to specific geomorphic surfaces north of the Zandjan River (Zandjan rud) (Figure 4). The orientation of these topographic lineaments evolve from east to west; the first one trends N 30° W and lies at the tow limits of a large Plio-Quaternary alluvial surface, the second N 45° W follows the general trend of the Zandjan river and affects Quaternary fluvial terrasses.
South of the Zanjan river, the alluvial surfaces of the Jahand Daghi range are disrupted by a sinuous topographic step trending roughly N45°W, parallel to the river. This topographic anomaly extends over more than 60 km (Figure 4).
All of these topographic lineaments converge and join progressively together toward the southeast, in the vicinity of Zandjan city.

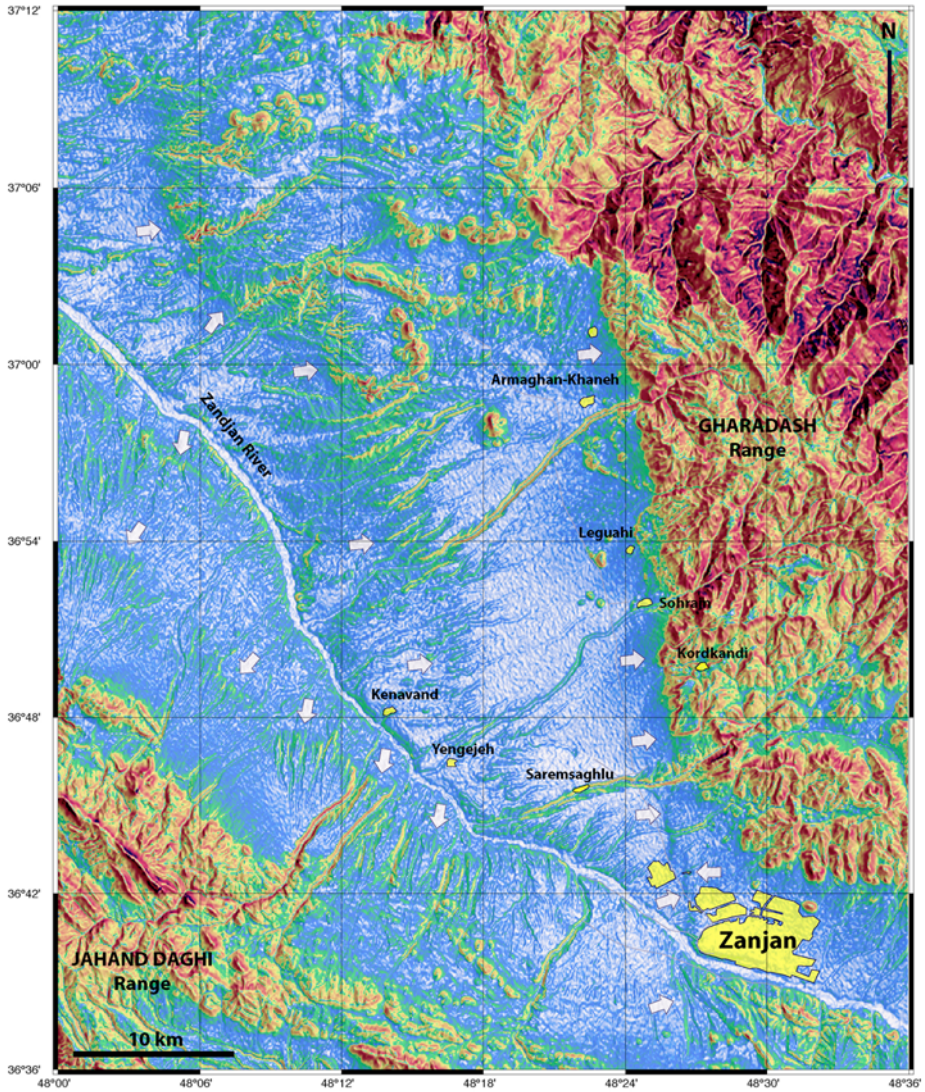

Figure 4: Slope map derived from SRTM DEM (NASA) showing the main morphological characteristics of the Zandjan region. Flat surfaces appear in white to blue colors and steep topographies appear in yellow and red. Several geomorphic surfaces, separated by escarpments can be evidenced, as well as incision anomalies in the drainage network. Just North of Zandjan city, we first found a main linear NNW-SSE escarpment located at the boundary between Eocene magmatic formations of West Alborz in the east (Yellowish part in this map) and Quaternary alluvial planes to the west (blue part in this map).

All of these observations are summarized in the geomorphological map presented in Figure 5. The studied region can be divided geomorphologically into 6 domains, separated by four topographic lineaments.

Because, each of these domains shows differential uplifts and are bounded by drainage anomalies (regressive incision, offset drainages…), we interpret these features as active fault zones. According to this interpretation, the geometry of the Zandjan Rud riverbed is probably largely controlled by the activity of these fault zones.

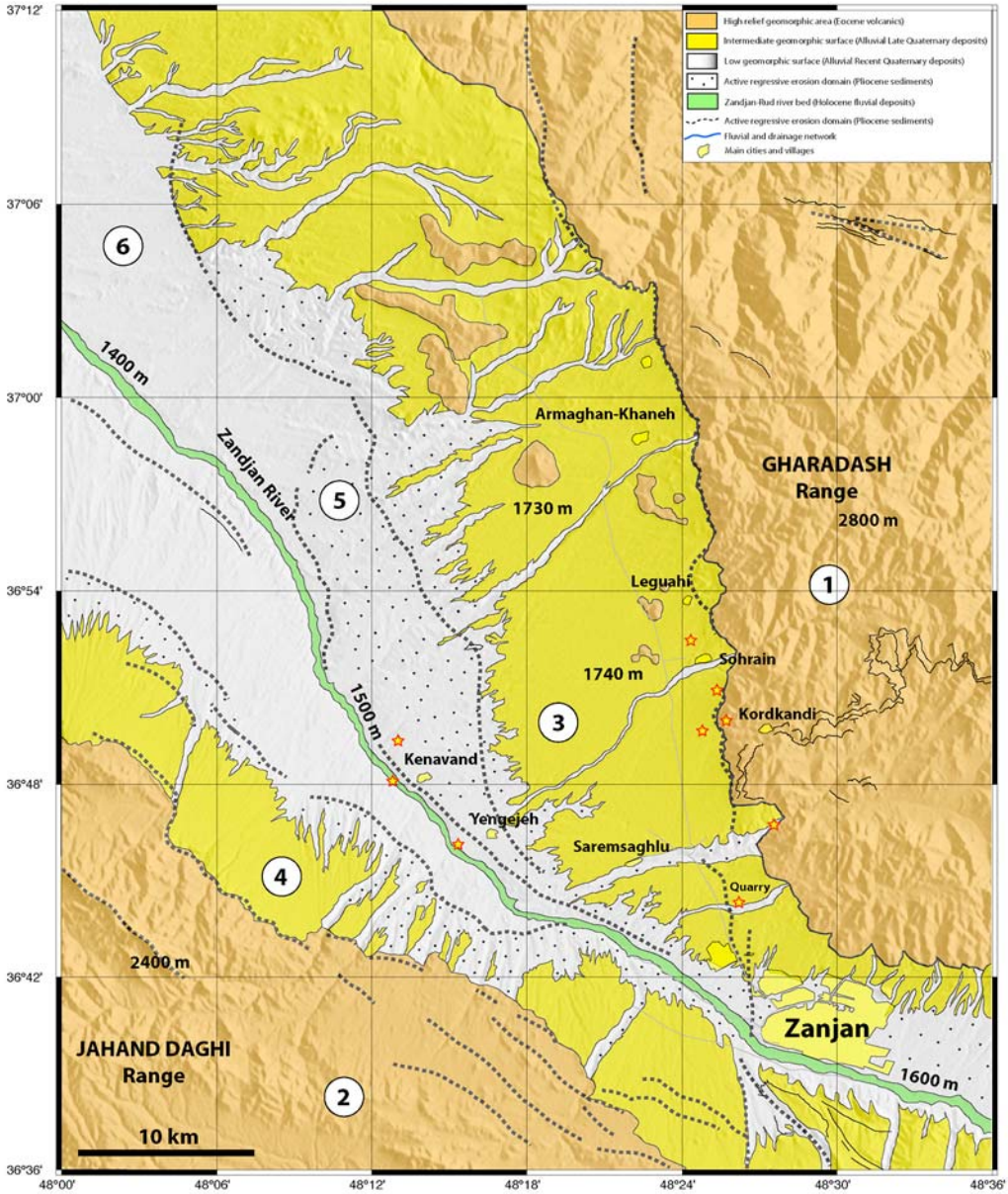

Figure 5: Synthetic geomorphological map showing first order geomorphic surfaces and topographic domains (1-6). Six distinct zones with differential uplifts have been identified. These geomorphic surfaces are separated by topographic steps that correspond to surface fault traces as demonstrated by local field observations realized in the framework of our study.

Based on these characteristics and fault kinematics considerations, these fault zones define a large fault network affecting most of the Zandjan-Mianeh basin over a large area (70 km x 40 km). To detail the characteristics (morphology, geometry and fault kinematics) of each of the four identified fault zones, we present hereafter a selection of the most interesting sites that were studied in the field (see Figure 5 for location).

III-1) The first fault zone (N10°W) of the Zandjan Fault Network (ZFN):

The sharp topographic contrast, observable between the Eocene Andesitic formations of the Gharadash ranges (to the east with 2800 meters high) and its western adjacent Quaternary plain (with 1800 meters high) north of Zandjan city, corresponds morphologically to an active mountain front (Figure 5 and 6). Its geomorphology shows evidences of oblique compressional features (such as dextral offset drainages, uplifted alluvial fans) indicating that it is actively deforming. The topography of the Gharadash Ranges is characterized by accordant summit feature, which is morphologically a good marker for relatively similar uplift rate (e.g. Martin-Kaye, 1963) occurring along the mountain range. Along this portion of the Gharadash ranges, the amount of Smf morphometric indices (mountain front sinuosity) is 1.15, suggesting that the mountain front contains potentially an active fault (Bull and McFadden 1989).

Moreover, the regular amount of about 140 m right-laterally offset streambeds observed along this mountain front shows some evidences of active strike-slip deformation (see Figure 6B). To determine fault characteristics in terms of fault plane geometry, slip kinematics and surface rupture morphology, we made detailed field investigations.

The selected site presented hereafter is situated near Kordkandi village (at about 17 kilometers north of Zandjan city). At this site, the fault zone contains morphologically two portions. The first one is situated in the mountain front domain and it is characterized by evidences of oblique deformation (thrust and right-lateral faulting) concentrated at the boundary between Eocene andesitic formations and Quaternary alluvial deposits within a narrow zone (40 m in width) (see Figure 6A and 6B). The fault zone contains several steep fault planes with a dip>70°, trending toward the east-northeast. The second portion, that lies parallel to the first one, is situated at a distance of about 400 to 700 m to the first one and contains one thrust fault scarp affecting Late Quaternary fan deposits (Figures 6C and D). The prolongation of this fault zone to the south, which can be traced along a NNW-SSE linear escarpment, moved progressively away from the mountain front. Near Zandjan, the fault zone is situated at a distance of about three km west of the mountain front domain (Figure 5 and 6).

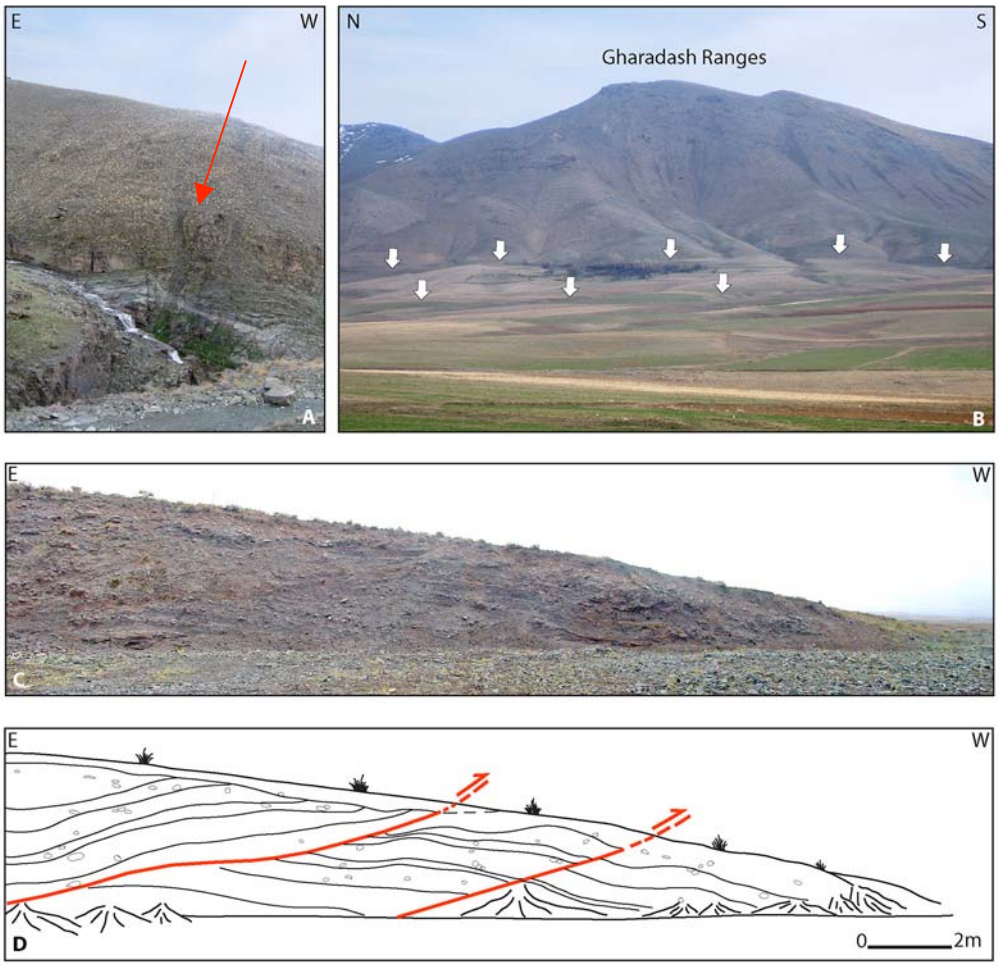

Figure 6: The first fault zone of the Zandjan fault network in Kordkandi area (see Figure 4 for situation). Within this area, the fault zone contains morphologically two portions. The first one is situated at the western mountain front of the Gharadash Range (A and B) and it is characterized by evidences of oblique deformation (thrust and right-lateral faulting) concentrated between Eocene andesitic and Quaternary alluvial formations (white arrows show the two fault traces). This feature indicates that it is actively deforming. The second portion contains a thrust fault scarp located in Late Quaternary fan deposits (C and D).

More to the south (5 km north of Zandjan city), we studied another site where fault deformation concentrated along a well-developed fault scarp, about 15-20 m high, which uplift Quaternary alluvial fans surfaces (Figure 7B). Here, quarry activity allowed us to study a large outcrop within the fault scarp. Our studies revealed that this NNW-SSE escarpment is controlled by a thrust fault zone dipping 20° toward the northeast (Figures 7C and 7D).

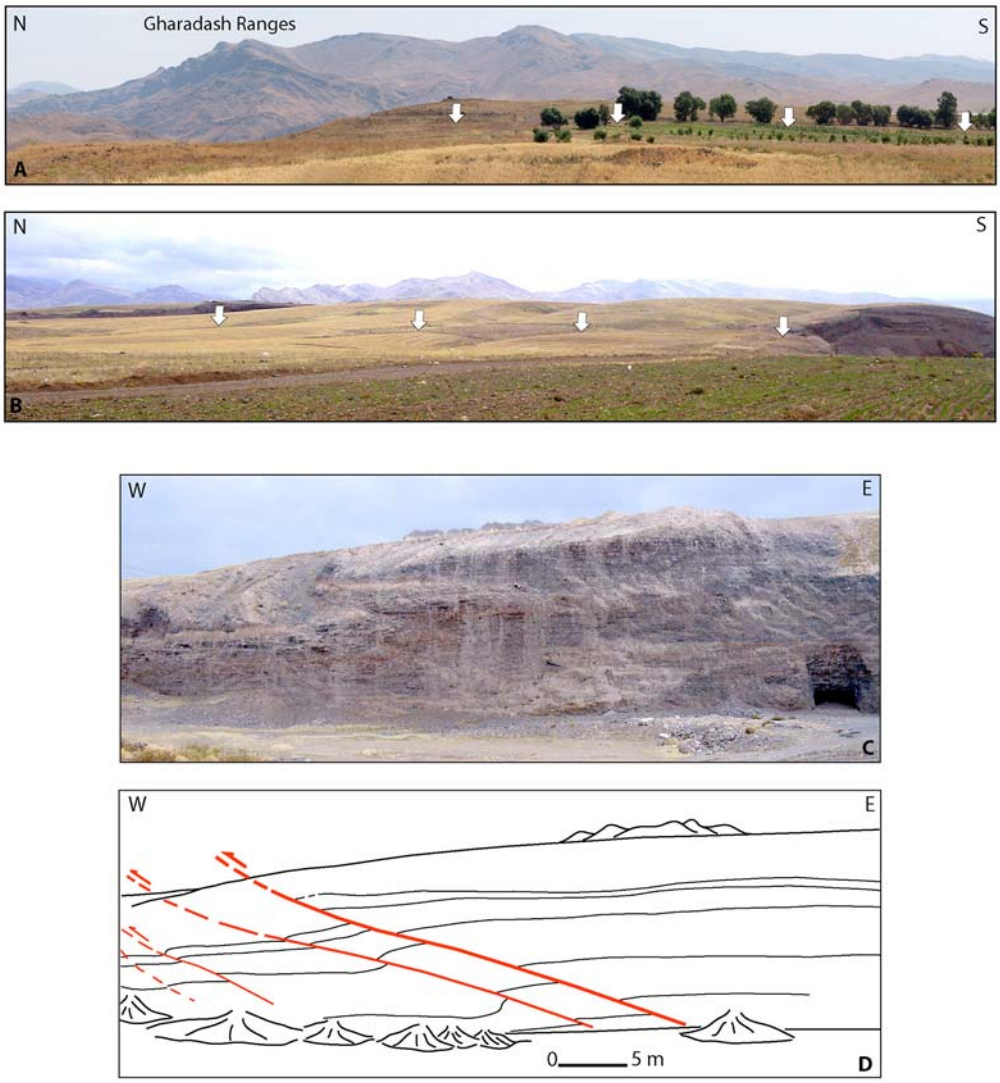

Figure 7: A; The Quaternary fault scarp along south prolongation of the first fault zone of the ZFN (8 km north side of Zandjan). The trace of the fault passes close to the trees. B; this picture shows the southern prolongation of the first fault zone of the ZFN (in 5 km north side of Zandjan city). Here, fault deformation is concentrated along a NNW-SSE fault scarp (with a height of about 15-20 m), which is located in Quaternary alluvial fans (white arrows show the trace of the fault at the tow of fault scarp). C and D; our studies within the fault scarp revealed that a thrust fault zone that formed the escarpment.

North of Zandjan city, the fault scarp offsets right-laterally (about 750 meters) three E-W trending riverbeds (Dareh Dash, Saremsaghlu and Sohrain rivers, see Figures 4 and 5 for situation). In the southern part, the trend of the fault zone changes slighltly toward the Soltanieh fault located in the southeast of the Zandjan-Teheran highway (Figure 5).

III-2) The second fault zone (N30°W) of the Zandjan Fault Network

DEM, satellite images and aerial photos allowed us to map another fault zone trending N 30° W. This fault zone lies at the tow limits of a large alluvial surface extending west of the first fault zone of the ZFN (see Figure 5). The broken sinuous-form of the fault trace can be interpreted as a thrust fault zone dipping toward the NE, which cuts Quaternary alluvial fan deposits (Figure 8). Several drainages, trending normal to the fault trace, are offset laterally suggesting this fault zone accommodate a dextral strike-slip component.

Intensive human activities, which developed on this alluvial surface, have modified and erased most of the recent morphological features concerning the surface faulting, precluding an easy observation of kinematics markers at field scale. The rheology of the surficial materials (almost gravels and soils) is the other important parameter in this relation. Moreover, the other possibility to explain the situation is that the activity of the fault zone is not as recent as the other fault zones found in this study.

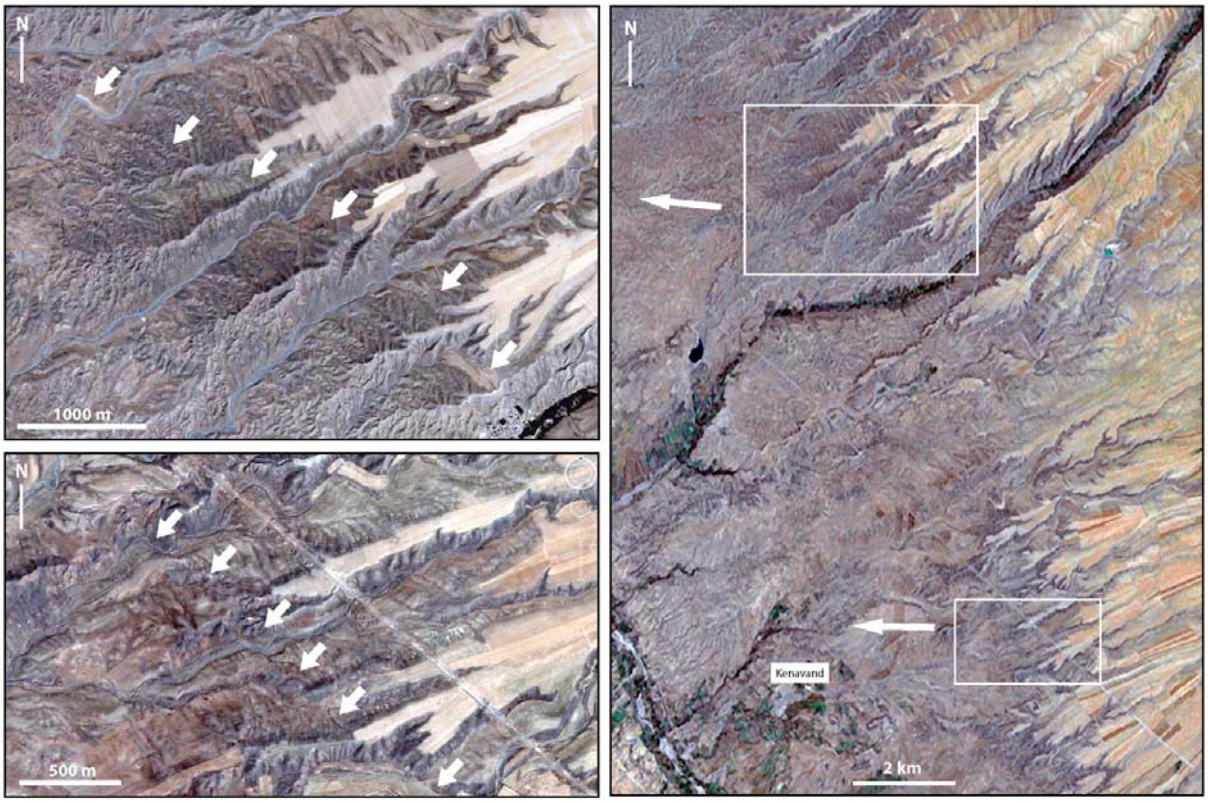

Figure 8: Google earth satellite image of two portions of the second fault zone of the ZFN, east of Kenavand region. Here, several offset drainage beds show evidences of dextral faulting associated to thrust fault deformation. The strike-slip evidences of faulting can be interpreted as an apparent component.

III-3) The Third fault zone (N50°W) of the Zandjan Fault Network

Six kilometers west of the second fault zone of the ZFN (at the right bank of the Zandjan River), we found another linear WNW-ESE topographic lineament (see Figure 4 and 5). It is a fault scarp that affects recent (Holocene to Upper Pleistocene) down-stream deposits of the alluvial fans (see Figures 5 and 9D and 9E). Generally, this fault zone extends over more than 30 km and it is constituted by two parallel faults. The first one is an active thrust fault, situated at the tow of the main fault scarp (to the south), which cut recent soil units containing ceramic particles. The second one, situated in the northeast side of the mentioned thrust fault (to the north), is mainly a strike-slip fault that displace right-laterally several drainages (Figures 9D and 9E).

These observations show that within this third fault zone, close to the surface, local shortening is partitioned along nearly pure dextral slips and thrusting. In terms of seismic hazard, this active fault zone is located at the west vicinity of the Zandjan city and then shows a high level of seismic risk for Zandjan city.

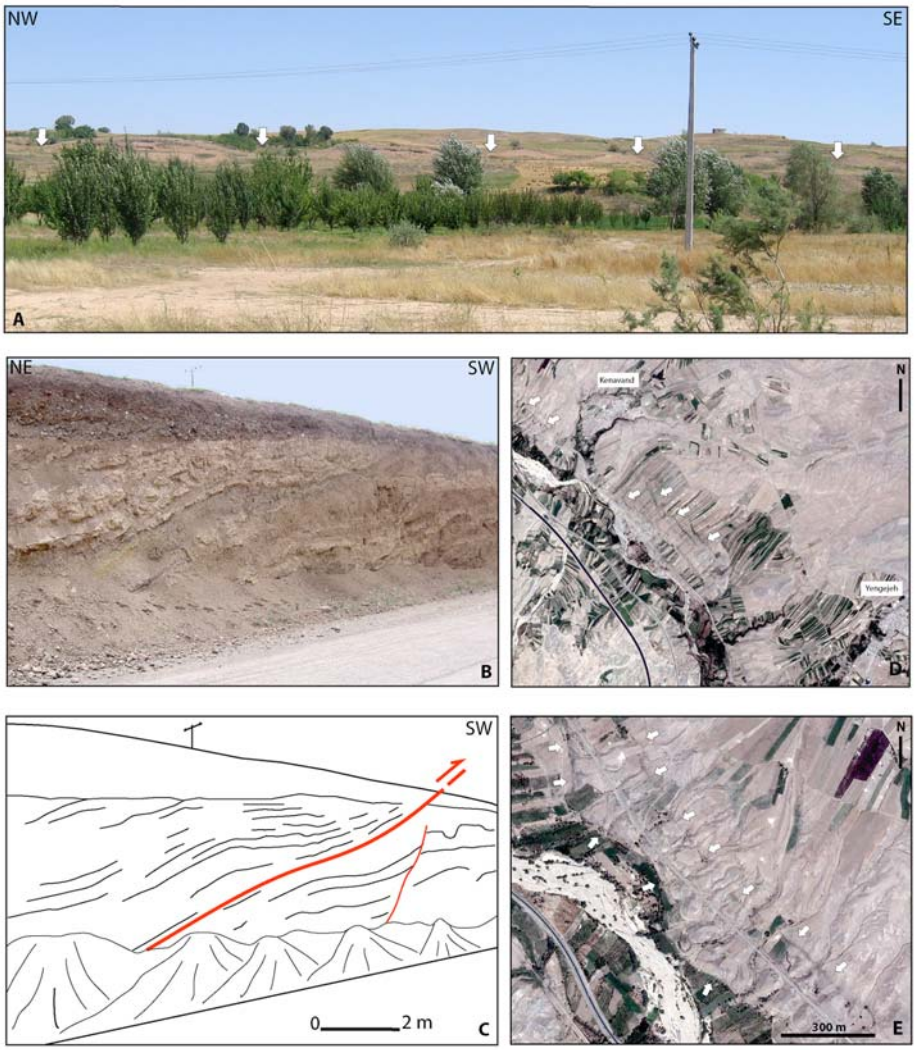

Figure 9:A; Cumulated fault scarp located north of the Kenavand village (see Figure 4 for situation). B and C; active thrust fault concern to the first part of the third fault zone of the ZFN west side of the Yengejeh village (see Figure 4 for situation). This fault cuts Holocene soil units containing ceramic particles. D and E show Google earth satellite image of the fault zone in the northwest vicinity of Kenavand village (see Figure 4 for situation). The fault scarp contains two right-lateral strike-slip and thrust faults (see text for details).

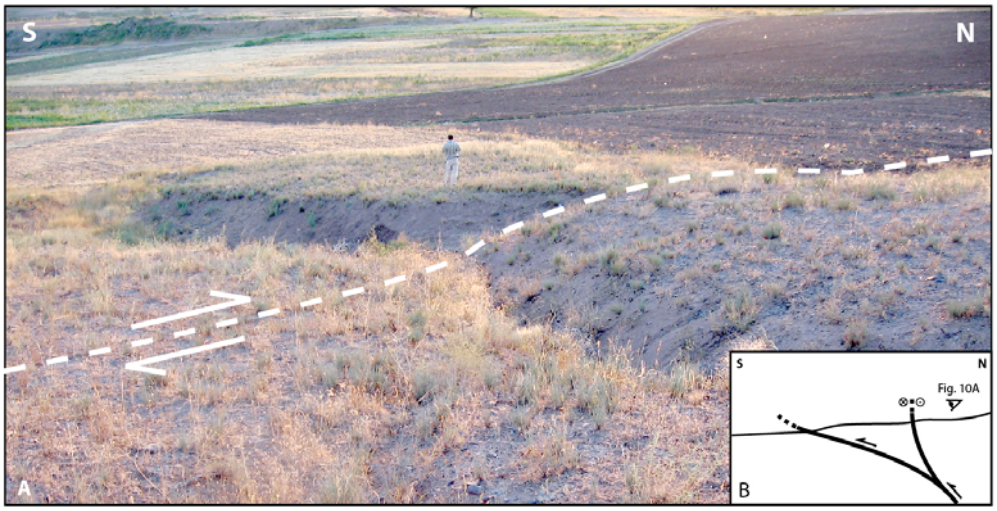

Figure 10: Cumulated fault scarp located north of the Kenavand village (see Figure 4 for situation).

III-4) The Fourth fault zone (N50°W) of the Zandjan Fault Network

Based on aerial photo interpretations, several uplifted alluvial surfaces can be observed on the left bank of the Zandjan River (south of the third fault zone of the ZFN). These surfaces are incised and are limited on their northern sides by a topographic scarp, trending N50°W, that extends over more than 50 km. This scarp corresponds to an active fault that affects Quaternary to Holocene fan deposits. Its surface geometry corresponds to a thrust fault dipping to the southwest (Figure 9). More to the south, at the base of Jahan-Daghi mountain front (with 2400 meters high), the uplifted alluvial surfaces are also cut by another fault that bounds the northern limb of N50-60°W trending folds. Based on its surface geometry, it corresponds to a thrust fault with a little dextral component (Figure 4 and 9). This fault zone can be interpreted as the NW prolongation of the Soltanieh fault.

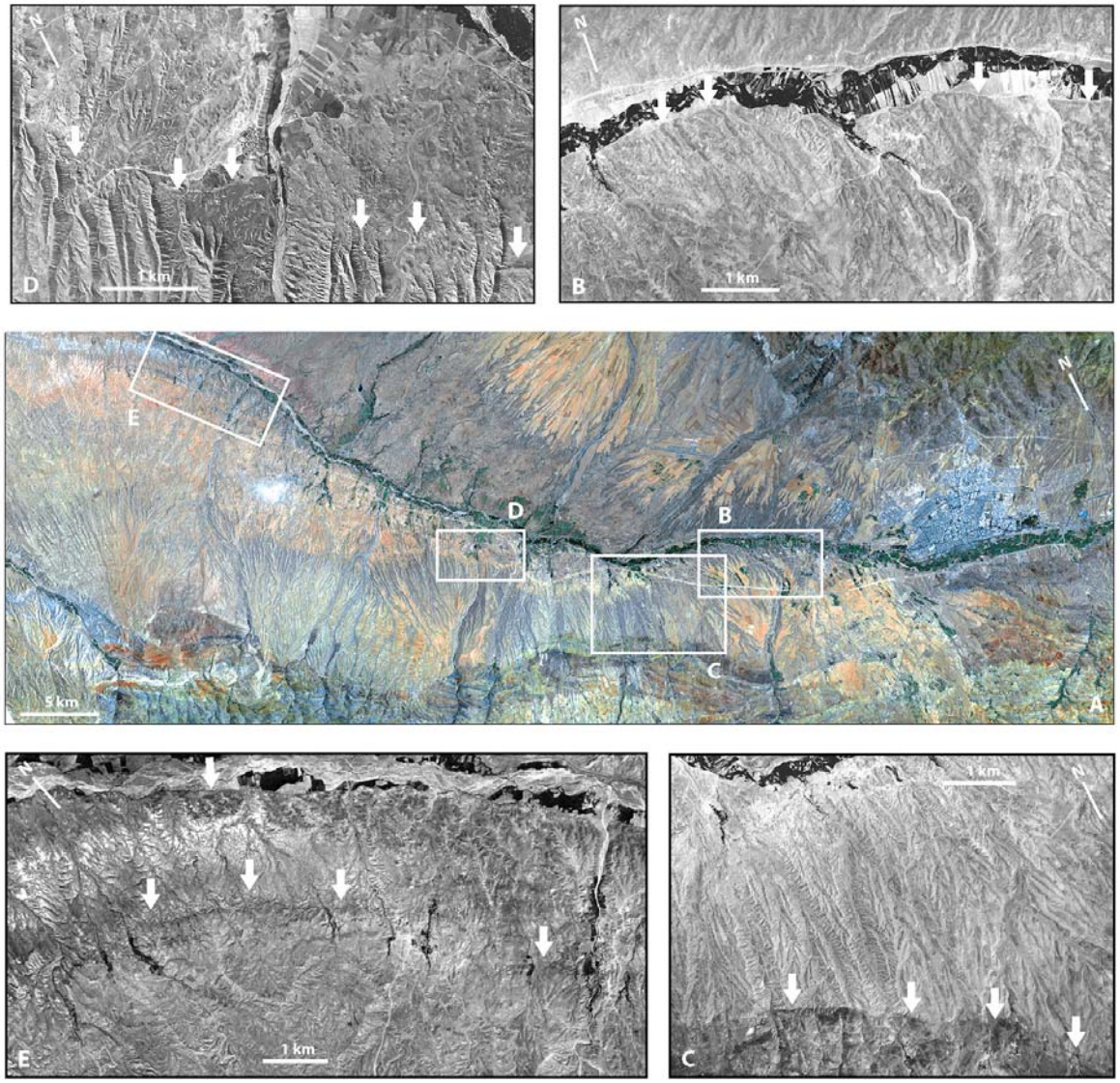

Figure 11: Landsat 7 satellite image (A) and aerial photos (B, C, D, E) showing clear morphological evidences of surface ruptures and deformations affecting alluvial fan deposits of the northen piedmont of the Jahan Daghi Range (white arrows show the fault traces).

IV) Discussion

Figure 12 presents the synthesis of our morphostructural investigations of the Zandjan fault network (Figure 12). According to this map, the Zandjan city (with more than 510,000 peoples) appears to be located at the junction of four major fault zones. These fault zones define a large fault network (Zandjan Fault Network: ZFN), which affects the SE termination of the Zandjan-Mianeh Basin and covers an area of 2800 km^2 .

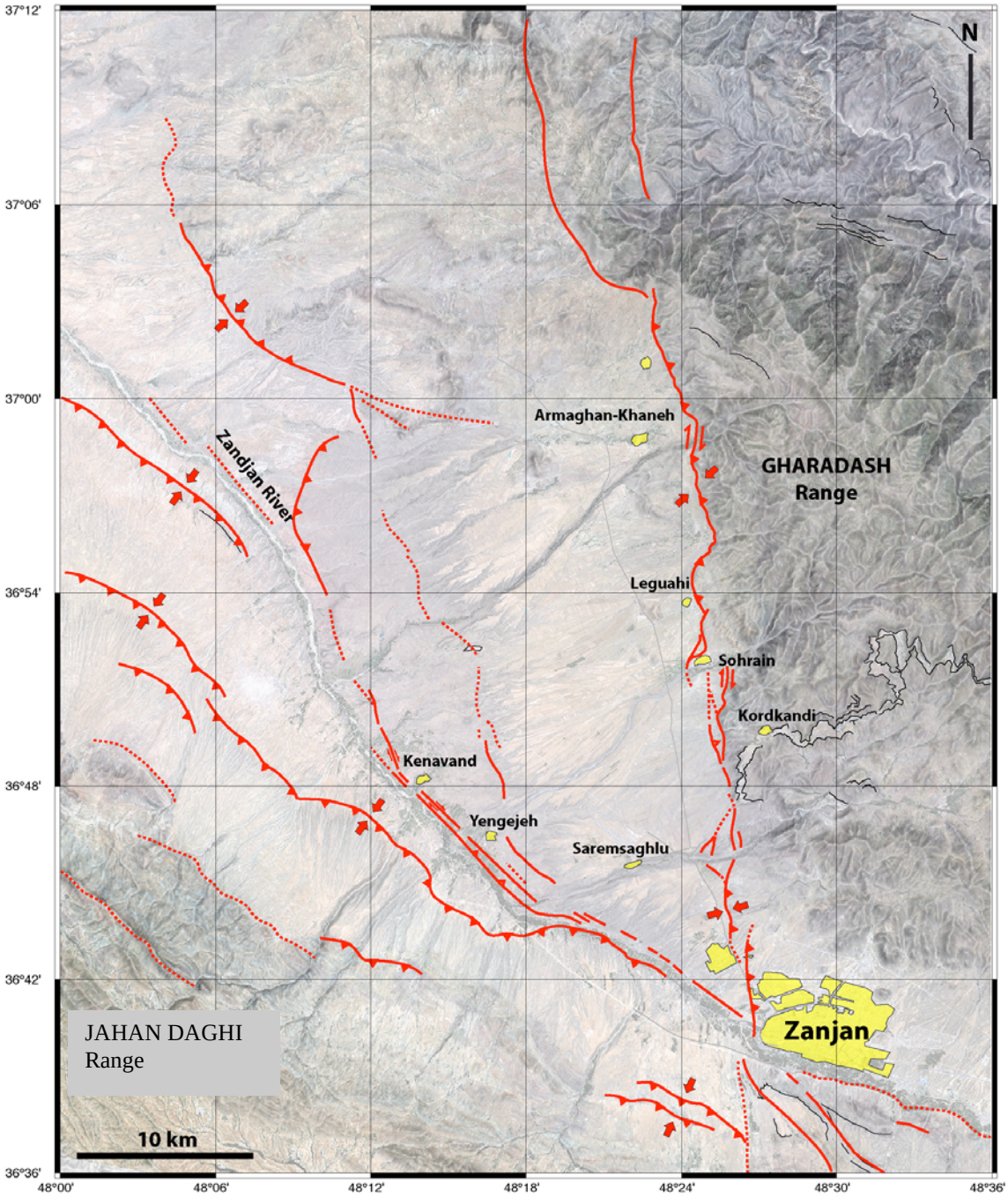

Figure 12: Tectonic map of the Zandjan fault network showing several fault zones converging towards the Zandjan City. These faults are mainly pure thrusts associated sometime to right-lateral strike-slip faults. The pointed lines show the active folds axis.

The ZFN contains at least four major fault zones striking N-S to NW-SE. The orientation of these fault zones evolves from east to west from N-S to NW-SE, respectively (Figure 12). The first fault zone trending N 10° W, is parallel to the Gharadash mountain front. The second one trending N 30° W, lies at the tow limits of a large Plio-Quaternary alluvial surface which cover the Gharadash's piedmont. The third one, N 45° W, follows the general trend of the right bank of the Zanjan Rud river and affects Late Quaternary fluvial materials. The last one, within the left bank of the Zanjan Rud river, follows also the general trend of the river and affects Late Quaternary alluvial fan deposits. These fault zones are mainly constituted by active thrusts and dextral faults. They converge toward the southeast, in the vicinity of Zandjan city (Figure 12, 13).
No strong earthquake has been reported in this region (Ambraseys and Melville, 1982; Berberian, 1994). As shown by historical and pre-historical earthquake records (e.g. Manjil area or Sagzabad-Qazvin area), the occurrence of strong earthquakes in NW of Iran is often characterized by long-term recurrence intervals (e.g.Berberian and Yeats, 2001). Therefore, the Zandjan region corresponds to a seismic gap (Figure 3).
In terms of seismic hazard, the first and third fault zones of the ZFN should be taken into much consideration because they cross the Zandjan city and cut the most recent soil units. There seismic potential is high because they extend over more then 50 km and could produce M=7 magnitude earthquakes (Figure 13). A strong earthquake occurring along one of these fault could produce very strong damages to the Zanjan city and significant loses of population. To better constrain the kinematics and fault geometry of the ZFN, more field investigations are still required, especially for the fault zone bounding the northern piedmont of the Jahand Daghi range which could represent the NW prolongation of the Soltanieh Fault. The seismic hazard associated to this fault zone increases dramatically the potential of damages for the Zandjan city.

Our study brings also new data to better understand the complex present day geodynamics setting of NW Iran.

The geometry and kinematics of the Zandjan Fault Network (NW-SE pure thrusts, oblique NNW-SSE reverse faults and N-S dextral strike slip faults) are compatible with a regional NE-SW direction of compression (Figure 14). This direction of crustal shortening is consistent with Plio-Quaternary deformations observable in the Zandjan region (e.g. folds and faults of the Jahan Daghi Range, antiform structure of the Gharadash Range). It is also compatible with the available focal mechanisms situated in the western termination of Alborz (earthquakes of rezvanshahr, (M=6, 1978), Shaft (M=5.6, 1983), Rudbar (M= 7.4, 1990), see Figure 3).
This observation strongly suggest that since Pliocene, at least, the azimuth of horizontal shortening in this part of NW of Iran did not changed so much. In response to the Arabia-Eurasia collision, the Central Iranian Plateau started colliding with the Caspian Sea Block resulting into the formation of Alborz. The deformation propagated towards the SW, closing progressively the intramontaneous basin trapped between two consecutive compressive crustal structures. Presently, the Zandjan-Mihaneh basin experiences the same evolution and will close probably in the next millions years.

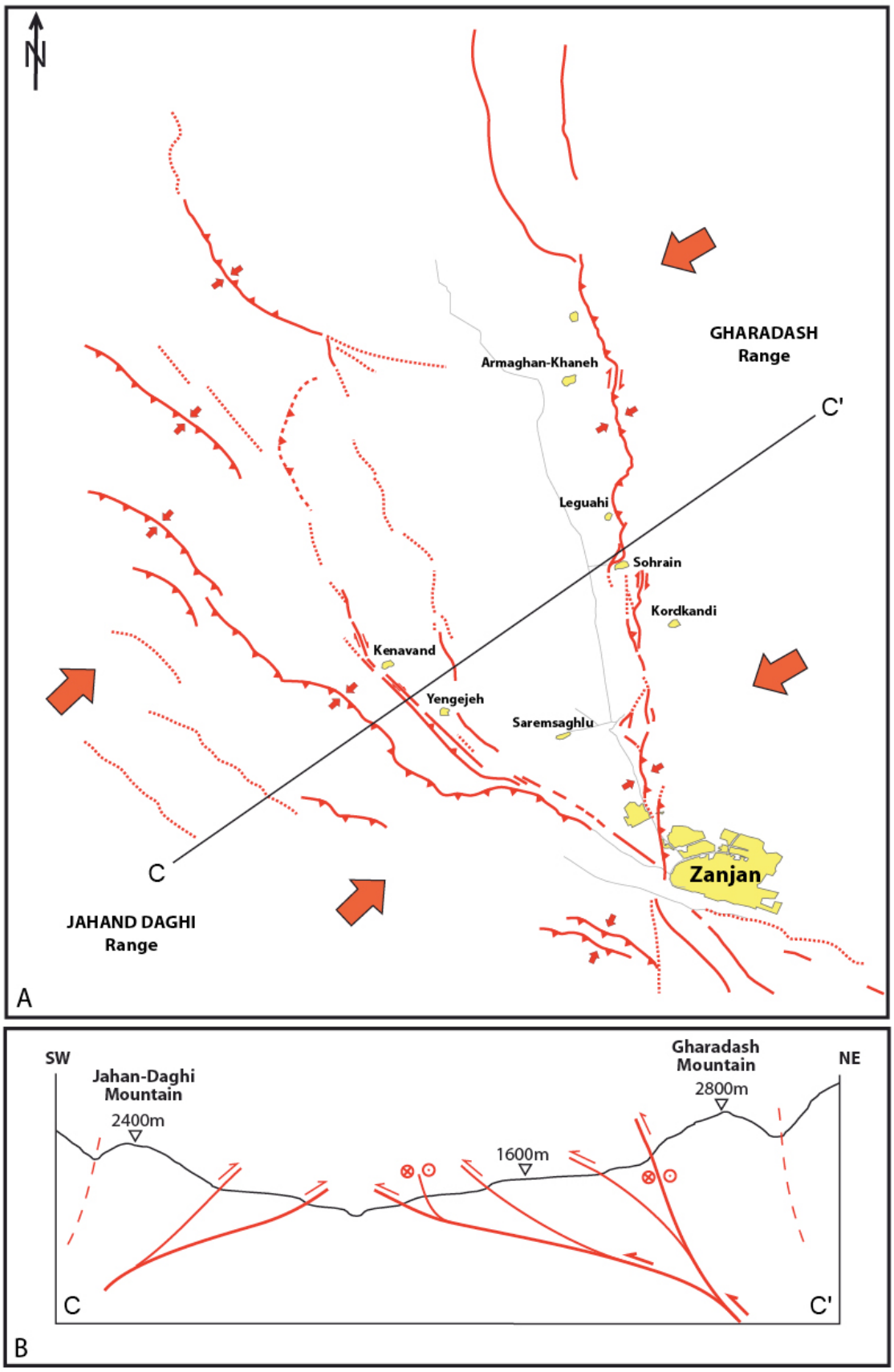

Figure 13: A: Synthetic structural maps at the scale of the studied area and NW of Iran and (B) simplified cross-section trending SW-NE

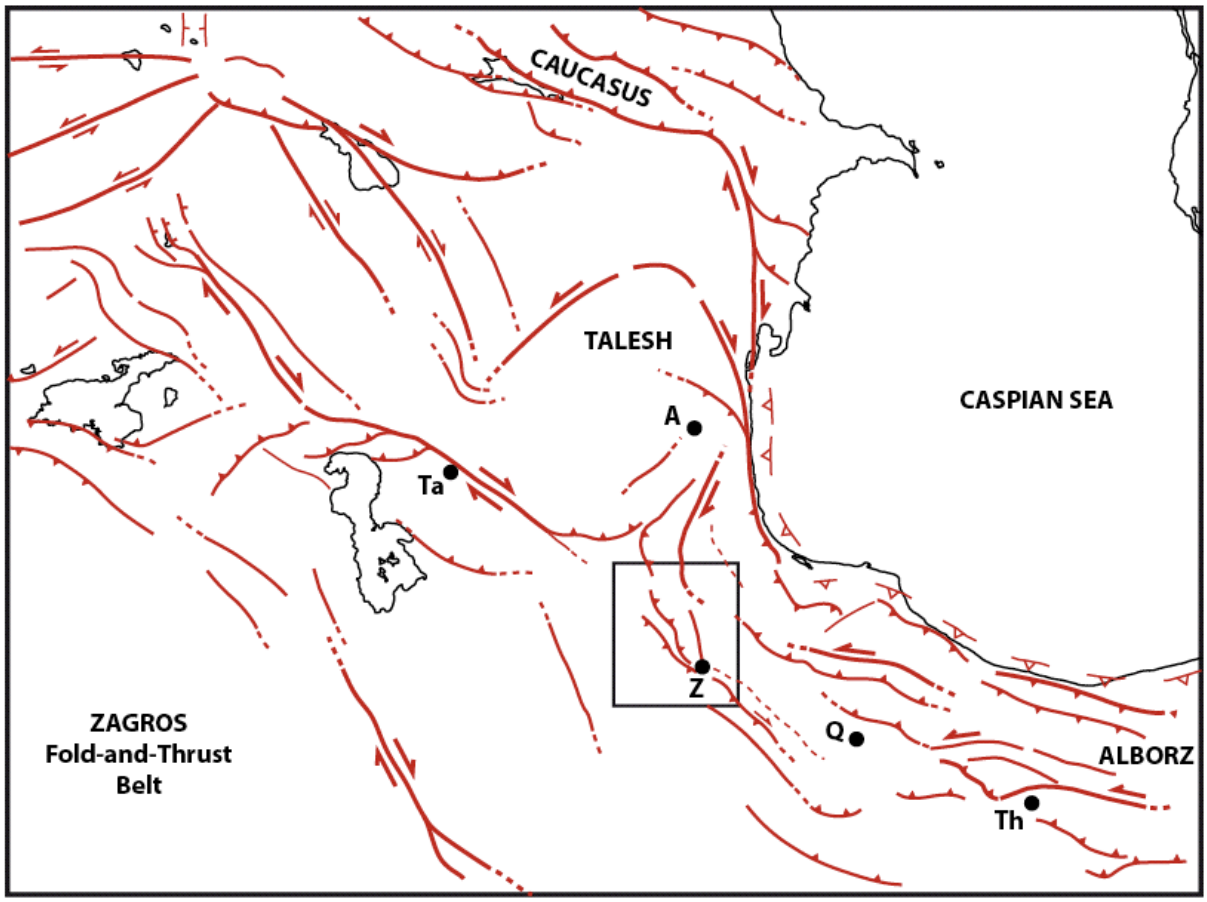

Figure 14: Simplified geodynamic map of the NW of Iran and Transcaucasian region. Th; Tehran, Q; Qazvin, Z; Zandjan, Ta; Tabriz, A; Ardebil.

The ZFN constitutes also a part of the southern prolongation of the Alborz virgation toward the north, which connect the Alborz termination to the Talesh Arc through the Nur and Astara faults. This observation could explain why the azimuths of the Zandjan fault zones evolve from NW-SE, south of Zandjan to N-S, north of Zandjan.

References:

Agard, P., J. Omrani, L. Jolivet, and F. Mouthereau (2005), Convergence history across Zagros Iran):Constraints from collisional and earlier deformation, I n t . J . Earth Sc i ., 94, 401 – 419, doi:10.1007/s00531-005-0481-4.

Allen, M.B., S.J. Vincent, I. Alsop, A. Ismail-zadeh, R Flecker, 2003a. Late Cenozoic deformation in the South Caspian region: effects of a rigid basement block within a collision zone, Tectonophysics 366, 223– 239.

Allen, M.B., Ghassemi, M.R., Shahrabi, M., and Qorashi, M., 2003b, Accommodation of late Cenozoic oblique shortening in the Alborz range, northern Iran: Journal of Structural Geology, v. 25, p. 659–672.

Allen, M., J. Jackson, and R. Walker ,2004, Late Cenozoic reorganization of the Arabia-Eurasia collision and the comparison of short-term and long term deformation rates, Tectonics, 23, TC2008, doi:10.1029/2003 TC 001530.

Ambraseys, N.N. &Melville, C.P., 1982. *A History of Persian Earthquakes, Cambridge Earth Science Series*, Cambridge University Press, London.

Blanc, E.J.-P., Allen, M.B., Inger, S.and Hassani, H., 2003. Structural styles in the Zagros simple Folded zone, Iran. *J. Geol. Soc. London*, **160,** 401–412.

Berberian, M. and S. Aarshadi, 1976 : On the evidence of the youngest activity of the North Tabriz Fault and the seismicity of Tabriz city, *Geol. Surv. Iran Rep.*, **39**, 397-418.

Berberian, M., 1983. The southern Caspian: a compressional depression floored by a trapped, modified oceanic crust. Canadian Journal of Earth Sciences 20, 163–183.

Berberian, M., 1994. Natural hazards and the first earthquake catalog of Iran, Vol. 1: historical hazards in Iran prior 1900, I.I.E.E.S. report.

Berberian, M. and R.S. Yeats, 1999 : Patterns of historical earthquake rupture in the Iranian plateau, *Bull. Seismol. Soc. Am.*, **89**, 120-139.

Berberian, M., 1997. Seismic sources of the Transcaucasian historical earthquakes. In: Giardini, D., Balassanian, S. (Eds.), Historical and Prehistorical Earthquakes in the Caucasus. Kluwer Academic Publishing, Dordrecht, Netherlands, pp. 233–311.

Berberian, M., Yeats, R.S., 2001. Contribution of archaeological data to studies of earthquake history in the Iranian plateau. J. Struct. Geol. 23, 563– 584.

Cisternas, A. and Philip, H., 1997, Seismotectonics of the Mediterranean Region and the Caucasus, In: Giardini, D., Balassanian, S. (Eds.), Historical and Prehistorical Earthquakes in the Caucasus. Kluwer Academic Publishing, Dordrecht, Netherlands, pp. 39-77.

Copley, A. and Jackson, J., 2006, Active tectonics of the Turkish-Iranian Plateau, Tectonics, Vol. 25, TC6006, doi : 10.1029/2005TC001906.

Eftekharnezhad, J. (1975): Brief history and structural development of Azarbaijan. Geological Survey of Iran, Internal Report, 8P

Förster et al., 1972

Ghassemi, A. and Talbot, C. J., 2006, A new Tectonic scenario for the Sanandaj-Sirjan Zone (Iran), Journal of Asian Earth sciences, XX, 1-11.

Hessami, K., D. Pantosi, H. Tabassi, E. Shabanian, M. Abbassi, K. Feghhi, S. Sholaymani, 2003. Paleoearthquakes and slip rates of the North Tabriz Fault, NWIran : preliminary results, Ann. Geophys.,46, 903–915.

Hessami, K., Jamali, F., Tabassi, H., 2003, the map of major active faults of Iran, International Institute of Earthquake Engineering and Seismology

Jackson, J. & McKenzie, D. 1984, "Active tectonics of the Alpine- Himalayan Belt between western Turkey and Pakistan.", Geophysical Journal - Royal Astronomical Society, vol. 77, no. 1, pp. 185-264.

Jackson, J., 1992 : Partitioning of strike-slip and convergent motion between Eurasia and Arabia in Eastern Turkey and the Caucasus, *J. Geophys. Res.*, **97**, 12471-12479.

Jackson, J., Priestley, K., Allen, M., Berberian, M., 2002. Active tectonics of the South Caspian Basin. Geophysical Journal International, 148, 214– 245.

Karakhanian, A., 1993. The active faults of the Armenian Upland. In: *Proc. of the Scientific Meeting on Seismic Protection*, Dipartamento per la Geologia e le Attivita estrattive, Regione del Veneto, Venice, Italy, pp. 88–94.

Karakhanian, A.S., 1992. Some features of active tectonics in the 1988 Spitak earthquake zone. *Izvestia AN Armenii, Nauki o zemlie* **1**, pp. 3–11 (in Russian) .

Karakhanian, A.S. and Balassanian, V.S., 1992. Active dynamics of the 1988 Spitak earthquake zone. *Izvestia AN Armenii, Nauki o Zemlie* **2**, pp. 12–21 (in Russian) .

Karakhanian, A., Jamali, F.H., Hessami, K.T., 1996. An investigation of some active faults in the Azarbaidjan region (NW Iran). Report IIEES. Tehran, 7.

Karakhanian, A.S., Trifonov, V.G., Azizbekian, O.G. and Hondkarian, D.G., 1997. Relationship of the late Quaternary tectonics and volcanism in the Khonarassar active fault zone, the Armenian Upland. *Terra Nova* **9**, pp. 131–134. View Record in Scopus | Cited By in Scopus (8)

Karakhanian, A.S., Djrbashyan, R.T., Trifonov, V.G., Philip, H. and Ritz, J.-F., 1997. Active faults and strong earthquakes of the Armenian Upland. In: Giardini, D. and Balassanian, S., Editors, 1997. *Historical and Prehistorical Earthquakes in the Caucasus*, Kluwer Academic Publishing, Dordrecht, Netherlands, pp. 181–187.

Karakhanian, A., Bagdassarian, H., Arakelian, S., Avagyan, A., Davtian, V., Adilkhanian, A., Balassanian, V. and Abgaryan, Y., 2000. In: *Landslide Hazard and Risk: Geographic Information System on Landslide Hazard and Risk Assessment in the Republic of Armenia*, UNDP, Yerevan, p. 274.

Karakhanian, A., Djrbashian, R., Trifonov, V., Philip, H., Arakelian, S. and Avagian, A., 2002. Holocene-historical volcanism and active faults as natural risk factor for Armenia and adjacent countries. *J. Volcanol. Geotherm. Res.* **113** 1–2, pp. 319–344. **Article** | PDF (2463 K) | View Record in Scopus |

Martin-Kaye, P. H. A. "Accordant Summit Levels in the Lesser Antilles." *Carib. J. Sci.* Vol. 3 (1963), pp. 181-184.

Masson, F., Djamour, Y., van Gorp, S., Ch´ery, J., Tatar, M., Tavakoli, F., Nankali, H. & Vernant, P., 2006. Extension in NW Iran driven by motion of the South Caspian Bosin, *Earth Planet. Sc. Lett.*, **252,** 180–188.

Mirzaei, 2003. Basic Parameters of Earthquakes in Iran, Daneshnegar, 183p. (in Persian).

Nabavi, M. H., 1976. Preface to geology of Iran, Geological survey of Iran, 109 p. (in Persian).

Nilforoushan, F., F. Masson, P. Vernant, C. Vigny, J. Martinod, M. Abbassi, H. Nankali, D. Hatzfeld, R. Bayer, F. Tavakoli, A., Ashtiani, E. Doerflinger, M. Daignières, P. Collard, J. Chéry, 2003. GPS network monitors the Arabia–Eurasia collision deformation in Iran, J. Geody., 77, 411–422.

Priestley, K., Baker, C., and Jackson, J., 1994, Implications of earthquake focal mechanism data for the active tectonics of the south Caspian basin and surrounding regions: Geophysical Journal International, v. 118, p. 111–141.

Reilinger, R., et al. (2006), GPS constraints on continental deformation in the Africa-Arabia-Eurasia continental collision zone and implications for the dynamics of plate interactions, J. Geophys. Res., 111, B05411

Stampfli, G.M., Marcoux, J., and Baud, A., 1991, Tethyan margins in space and time, *in* Channell, J.E.T., Winterer, E.L., and Jansa, L.F., eds., Paleogeography and paleoceanography of Tethys: Palaeogeography, Palaeoclimatology, Palaeoecology, p. 373–410.

Stampfli, G.M., Borel, G., Cavazza, W., Mosar, J. and Ziegler, P.A. 2001. The paleotectonic atlas of the Peritethyan domain on CD ROM , A presentation, EGS 26th General assembly. Geophysical research abstracts, Nice, GRA3, 878.

Sengör, A. M. C., 1979, Mid-Mezozoic closure of Permo-Triassic Tethys and its implications, Nature, 279, p. 590-593.

Solaymani, S., Feghhi, K., 2003. Report of surface faulting and Morphotectonics of Avaj Region Earthquake on June 22, 2002.Website: http://www.iiees.ac.ir/English/bank/Avaj/avaj_report.html.

Solaymani Azad, S., Philip, H., Dominguez, S., Hessami, K., Shahpasand Zadeh, M., Forutan, M-R, Tabassi, H., Lamothe, M., Paleoseismological and morphological evidences of slip variations along the North Tabriz Fault (NW Iran), in preparation.

Stoneley, R. 1981. The geology of the Kuh-e Dalneshin area of southern Iran, and its bearing on the evolution of southern Tethys. Journal of the Geological Society, London, 138, 509-526.

Van Couvering, J. A., and J. A. Miller. 1971. Late Miocene marine and non-marine time scale in Europe. Nature, 230: 559-563.

Vernant, P., F. Nilforoushan, D. Hatzfeld, M. Abbassi, C. Vigny, F. Masson, H. Nankali, J. Martinod, A. Ashtiani, R. Bayer, F. Tavakoli, J. Chery, Contemporary crustal deformation and plate kinematics in middle east constrained by GPS measurement in Iran and northern Oman, 2004, Geophys. J. Int., 157, 381–398.

Vernant, P., and J. Chery, 2006, Low fault friction in Iran implies localized deformation for the Arabia-Eurasia collision zone, Earth Planet. Sci. Lett., in press.

Walker, R. T., Bergman, E., Jackson, J., Ghorashi, M., Talebian, M., 2005, The 2002 June 22 Changureh (Avaj) earthquake in Qazvin province, northwest Iran : epicentral relocation, source parameters, surface deformation and geomorphology, Geophys. J. Int., 160, 707-720.

Westaway, R., 1990 : Seismicity and tectonic deformation rate in Soviet Armenia: implications for local earthquake hazard and evolution of adjacent regions, *Tectonics*, **9**, 477-503.

Yilmaz, Y., 1993, New evidence and model on the evolution of the southeast Anatolian orogen: Geological Society of America Bulletin, v. 105, p. 251–271, doi: 10.1130/0016- 7606(1993) 105<0251:NEAMOT> 2.3. CO;2.

CHAPITRE 5

SYNTHESE DES RESULTATS ET CONCLUSIONS

SYNTHESE ET CONCLUSIONS

Les études que nous avons menées dans trois secteurs-clé du NW de l'Iran nous ont permis d'améliorer l'évaluation de l'aléa sismique associé aux failles actives majeures, en précisant leurs cinématiques actuelles et le potentiel sismogénique des différents segments constituant ces failles et de contribuer à l'élaboration d'un modèle géodynamique à l'échelle régionale.
Notre travail contribue à préciser le risque sismique pour trois grandes villes d'Iran (Téhéran, Tabriz, Zandjan) qui présentent par ailleurs une vulnérabilité importante liée en partie à un accroissement démographique rapide dû à un exode rural important. Dans les trois secteurs, le risque sismique est accentué par le fait que les failles, capables de produire des séismes de magnitudes supérieures à 7, ont un tracé qui traverse les zones urbanisées de la périphérie de ces villes.

Dans la région de Téhéran (les failles de Mosha et de Nord Téhéran) :

Dans la capitale de l'Iran, Téhéran, nous nous sommes concentrés sur le système de faille active de Mosha-Nord Téhéran. Nos travaux démontrent que ce système est essentiellement décrochant sénestre. Nos analyses morphotectoniques et paléosismologiques nous ont permis de montrer que :

1- Les failles de Mosha et de Nord Téhéran (situées dans le sud de l'Alborz Central) sont les sources sismiques les plus proches au nord de la capitale Téhéran (15 millions des habitants).

2- Basés sur nos études morphotectoniques, les tracés récents et actifs de ces deux failles, principalement décrochantes, ne suivent pas toujours les tracés des failles-anciennes qui correspondent à des mouvements chevauchants plus anciens (mio-Pliocène).

3- Les mouvements les plus récents sur ces failles majeures sont principalement des mouvements décrochants sénestres. Ils sont concentrés sur des plans de failles orientés E-W avec des pendages très forts vers le nord ou vers le sud et une géométrie segmentée en échelon left-stepping à l'est et right-stepping à l'ouest.

4- La transmission de ce mouvement sénestre au nord de la ville de Téhéran se fait par la faille de Niavaran et vers la ville de Karadj par trois branches en échelon right-stepped dans la partie occidentale de la faille de Nord Téhéran.

5- Au niveau de la cinématique récente, les parties NW-SE de ces failles sont principalement inverses ou sénestres inverses.

6- D'un point de vue général, nous interprétons la partie décrochante-sénestre-active (mentionnée en 3 et 4) comme un même système de faille : le système de faille Mosha-Nord Téhéran.

7- L'analyse paléosismologique de la partie orientale de ce système dans la vallée de Tar (sur le segment oriental de la faille de Mosha) montre que depuis 10000 BP elle a été la source de sept grands séismes (M>7). Ces mêmes études ont permis de calculer à partir des vitesses de glissement (horizontal: 2,2 +/- 0,5 mm/an et vertical : 0.45 mm/an), l'intervalle de récurrence des grands séismes sur cette partie de la faille de Mosha qui se situe entre 1100-1400 ans.

8- La même analyse dans la partie centrale du système Mosha-Nord Téhéran suggère que le dernier grand événement sismique (M>7) a eu lieu pendant les derniers 1120 ans.
D'un autre côté, d'après Berberian et Yeats (1999), la localisation de ce grand (M>7.1) événement sismique est cohérant avec la localisation de l'aire pléistoséiste (Io) du séisme historique qui a eu lieu en 1830 AD.

Dans la région de Tabriz (la faille de Nord Tabriz) :

Dans la région de Tabriz, nos études montrent que la faille Nord Tabriz, qui correspond à la portion centrale d'un système de faille plus important (TFS), est constituée par deux segments NW et SE décrochants dextres. Nous nous sommes intéressés plus particulièrement au segment SE de cette faille où nous avons réalisés plusieurs études paléosismologiques et morphostructurales. Nos résultats montrent que :

1- La faille de Tabriz est une structure majeure du NW de l'Iran de 300 km de long qui appartient à un système de faille (GSKT) plus vaste, qui s'étend vers le NW sur plus de 600 km de long, et qui relie une zone d'extension active dans la partie centrale de la collision Arabie-Eurasie (en Turquie orientale et Sud de l'Arménie) et une zone de compression active à l'Est (en Iran).
La faille de Tabriz comporte plusieurs branches : une partie centrale, elle-même segmentée, qui correspond à une cinématique décrochante dextre et deux branches E-W caractérisées par de la compression le long des massifs de Mishu et de Bozghush où une grande partie du déplacement horizontal dextre de la partie centrale est accommodée par des plis et des chevauchements.
Le système de faille GSKT comporte, à son extrémité NW, un ensemble de failles normales N-S en « queue-de-cheval » associées à du volcanisme récent alors que sa terminaison SE au niveau du massif de Bozghush) est caractérisée par de la compression active. Cette disposition permet d'interpréter ce système comme transformant et cohérent avec la direction de convergence N-S Eurasie-Arabie.

2- L'ensemble des déformations observées au NW de l'Iran et en particulier dans le secteur de la faille de Nord Tabriz correspond à un régime tectonique transpressif. Les failles normales sont limitées aux déformations à l'extrados des grands plis (Bozghush). Les extrémités ouest (Mishu) et est (Bozghush) de ce système correspondent à des zones compressives qui absorbent les déplacements horizontaux sur les segments NW et SE.

3- Nos études paleosismologiques sur le segment SE de la partie centrale de la faille ont permis de mettre en évidence trois événements majeurs depuis 33500 ans alors que les études de Hessami et al. (2003) sur le segment NW ont montré que quatre séismes de forte magnitude (M>7) se sont produits depuis 3600 ans. De plus, en comparant nos résultats sur le segment SE avec ceux obtenus sur le segment NW on observe des déplacements cumulés plus important sur

le segment NW (500 à 800 m) que sur le segment SE (300 m). On peut proposer trois hypothèses pour expliquer cette situation :

A- Une période de retour plus longue pour les séismes de fortes magnitudes sur le segment SE que sur le segment NW avec une décroissance d'ouest en est de la vitesse de glissement et des séismes plus importants sur le segment SE, ce qui serait cohérent avec des déplacements élémentaires observés : de 7 +/- 1 m le long du segment SE.
B- L'effet d'une interaction entre séismes (earthquake clustering) sur le segment SE. Des séismes trop rapprochés dans le temps ne permettent pas de les différencier à partir des seules données paléosismologiques car la vitesse de sédimentation n'est pas assez rapide dans la zone étudiée pour enregistrer tous les évènements sismiques.
C- La déformation est distribuée sur plusieurs branches dans la partie SE, dont toutes n'ont pas encore été étudiées.

Dans la région de Zandjan (la faille de Zandjan) :

Enfin, à Zandjan qui est une ville située dans une région de lacune sismique, nous avons découvert un important réseau de failles actives. La cinématique des différentes failles qui composent ce réseau indique que cette région est soumise à un régime tectonique général transpressif. Notre étude basée sur une approche morphotectonique montre que :

1- La ville de Zandjan est située à la convergence d'un réseau de failles actives qui comporte quatre zones de failles principales, dont certaines traversent la ville. On peut donc considérer au niveau de l'aléa sismique que Zandjan et sa région présentent une probabilité d'occurrence de séisme de forte magnitude très élevée.

2- Ce réseau est constitué majoritairement de failles inverses, d'orientations NW-SE à N-S, associées à des décrochements dextres. Parmi les zones de faille identifiées, la zone de failles située le plus à l'est correspond au front montagneux, entre le massif de Ghara Dash et le bassin pliocène à quaternaire de Zandjan-Mianeh. Cette zone de failles présente deux failles parallèles : la plus à l'est, située entre les séries volcaniques de l'Eocène et du Quaternaire a un pendage fort (>70°) vers l'est et correspond à une cinématique décrochante dextre. La deuxième, faiblement inclinée vers l'est et située dans les cônes d'alluvion, correspond à une cinématique en faille inverse.
La deuxième zone de faille qui correspond à des failles inverses à pendage (<35°) vers l'est, affecte les surfaces des grands cônes plio-quaternaires qui forment le piedmont du massif de Ghara Dash.
La troisième zone de faille située à l'est de la rivière Zandjan-Rud comporte deux segments parallèles, l'un est décrochant dextre et l'autre inverse. Les failles affectent des formations d'âge Holocène contenant des céramiques.
La quatrième zone de faille est située sur la rive gauche de la rivière Zandjan Rud. Elle présente un pendage vers le SW et correspond à un chevauchement.

3- Les déplacements correspondant au dernier séisme (2-3 mètres), observés sur la troisième zone de faille, montrent que des séismes de magnitudes supérieures à 7 peuvent affecter cette région.

En conclusion, les localisations et les cinématiques des systèmes de faille étudiés sont discutées dans le cadre géodynamique général de la collision Arabie-Eurasie. Le NW de l'Iran se trouve dans une région particulièrement intéressante du point de vue géodynamique, à cheval sur le secteur central de la collision Arabie-Eurasie et sa bordure Est, là où les structures tectoniques de l'Alborz se terminent pour se connecter à celles du Grand Caucase par un système de failles décrochantes (faille Ouest Caspienne) à valeur de faille transformante.

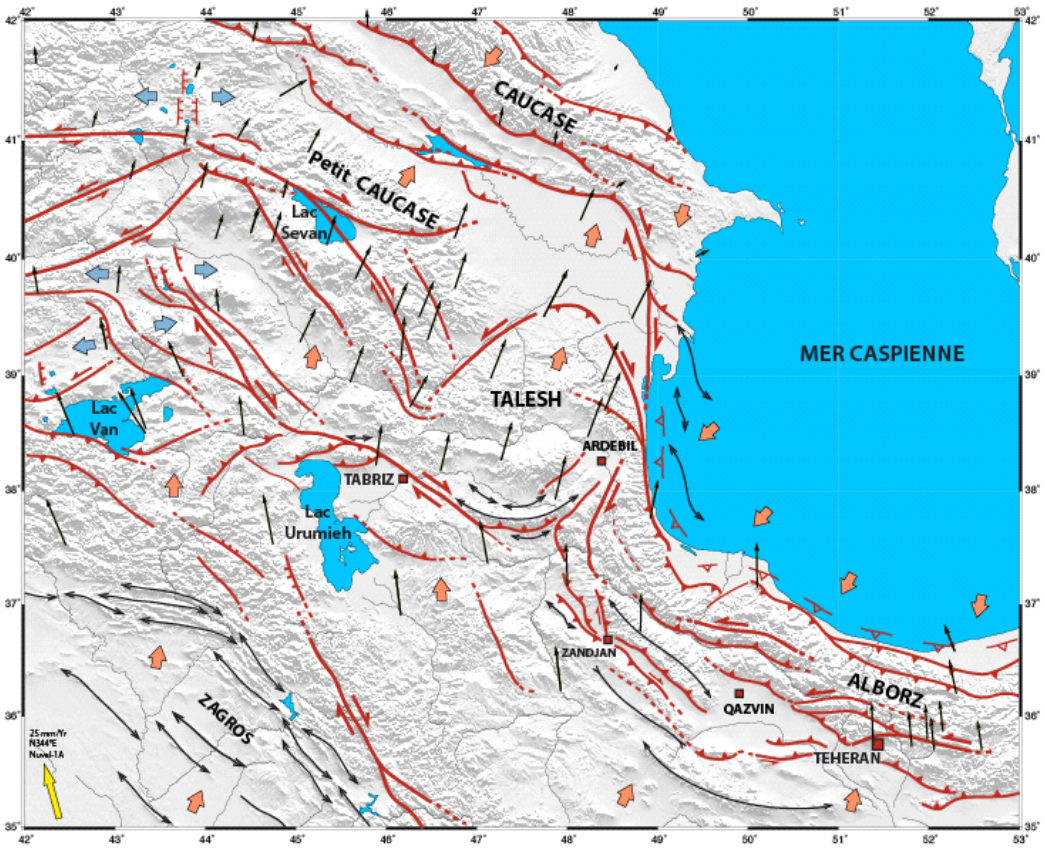

Carte interprétative géodynamique du Nord-ouest de l'Iran. Les failles avec les triangles représentent les chevauchements ; celles avec les barbules les failles normales. Les flèches orange indiquent les directions de compression actives et les flèches bleues, les direction d'extension actives. Les axes de plis sont indiqués par des doubles flèches et les vecteurs GPS par des flèches noires (Reilinger et al., 2006).

On remarquera que la faille majeure de Nord Tabriz qui correspond essentiellement à un décrochement dextre à la même direction NW-SE que les décrochements sénestres présents dans la chaîne de l'Alborz (les failles de : Mosha, Talaghan et Manjil). Cette observation implique une variation de la direction de compression entre ces deux régions. Dans la région de Tabriz (située à l'ouest de notre zone d'étude), basé sur les cinématiques des failles principales et les directions

d'axes des plis Plio-Quaternaires, la direction de la compression active est globalement N-S, tandis que dans le domaine de l'Alborz (située à l'est de notre zone d'étude) la direction de la compression active est orientée NE-SW.

Dans ce schéma général, le Bassin Sud Caspien jouerait un rôle passif de môle résistant solidaire de l'Eurasie dont il représenterait un diverticule autour duquel viendrait se mouler les chaînes péri caspiennes. Les résultats des mesures de positionnement GPS semblent soutenir ce modèle. En effet, les vecteurs vitesse calculés avec l'Eurasie fixe montrent :

- que l'essentiel de la convergence Arabie Eurasie est absorbée au niveau du Grand Caucase avec une forte diminution au franchissement du chevauchement majeur qui borde la chaîne au Sud.
- Cette diminution des vecteurs vitesse est très nette de part et d'autre de l'accident transformant Ouest Caspien, ce qui confirme : 1- le jeu décrochant dextre de cet accident d'importance lithosphérique. 2- que le bloc Sud Caspien est solidaire (cinématiquement) de l'Eurasie.

Dans la partie ouest, essentiellement en Turquie et en Arménie, les déformations actuelles et récentes sont caractérisées par la présence de failles normales NS associées à du volcanisme actif et à de grands décrochements dextres NW-SE et sénestres NE-SW. Ces derniers dessinent des arcs ouverts vers le Sud et dont les sommets sont occupés par des failles inverses actives (faille du séisme de Spitak de 1988 en Arménie). Les déformations récentes et actuelles correspondent donc cette région à de l'extension EW et par un raccourcissement NS sub-parallèle à la convergence Arabie Eurasie. Par contre, dans la partie Est où le volcanisme est moins présent et ne présente pas un caractère actif, la compression est dominante. Le système de faille GSKT auquel appartient la faille de Tabriz relie la partie ouest en extension à la partie est en compression. Cette faille joue donc un rôle important transformant entre extension et compression et se marque à son passage par une rotation dextre des vecteurs vitesse (GPS) ce qui lui confère un rôle actif prédominant par comparaison avec d'autres accidents décrochant qui lui sont parallèles plus au Nord (en Arménie). L'hypothèse d'une connexion plus ou moins directe avec la faille Nord Anatolienne est à écarter.

La terminaison Est de la faille de Nord Tabriz correspond à un vaste anticlinal actif (Bozghush) de forme arqué qui absorbe les déplacements horizontaux de la partie centrale de la faille de Tabriz, mais aussi partiellement ceux du système de faille GSKF. La structure arquée de l'anticlinal vient tangenter les accidents décrochants dextres chevauchants qui correspondent à la terminaison ouest de l'Alborz et auquel participe la faille de Zandjan. Basé sur nos études dans la région de Zandjan (située au centre de notre zone d'étude) la direction de la compression active est NE-SW, ce qui est cohérent avec nos interprétations au niveau de Tabriz et de l'Alborz.

Les perspectives

Pour améliorer l'évaluation de l'aléa sismique associé aux failles actives majeures autour des villes importantes de Téhéran, Tabriz et Zandjan, nos priorités sont ;

- Compléter les études paléosismologiques sur le secteur occidental du système de faille active de Mosha-Nord Téhéran où la faille de Niavaran transfère les mouvements essentiellement décrochantes sénestre (avec une composante verticale inverse) vers l'ouest. Malgré le fait que ce secteur est presque entièrement anthropisé (à cause de l'urbanisation), il existe encore quelques sites favorables pour faire des tranchées. Ensuite, il faut étudier les sources sismiques potentielles, situées à l'est de la capitale Téhéran, comme la faille de Arreh-Kuh ou les failles situées au sud et l'ouest de Guilavand.

- Densifier les études paléosismologiques sur le segment SE de la faille de Nord Tabriz pour déterminer si l'intervalle de récurrence des grands séismes sur ce segment est réellement plus long que celui du segment NW ou bien si cela est dû à du clustering?

- Dans la région de Zandjan, il faut commencer les études paléosismologiques. La priorité dans ce secteur est de faire des tranchées paléosismologiques sur le tracé de la faille décrochante dextre située à l'ouest de Kenavand. Ensuite, il faut compléter les études morphotectoniques sur la quatrième zone de faille que nous avons identifiée au sud de la rivière Zandjan-Rud (le secteur Jahan Daghi).

- Pour améliorer l'évaluation de l'aléa sismique associé aux failles actives majeures de la région peuplée de nord-ouest de l'Iran, nous proposons d'étendre les études paléosismologiques aux villes importantes comme Qazvin et Mianeh.

Annexe

* Article en préparation**:**

Ritz J-F., Solaymani S., Balescu S., Nazari H., Vernant P., Abbassi M. R., Chery J., Farbod Y., Feghhi K., Lamothe M., Massault M., Michelot J-L., Shabanian E. and Tabassi H., Geometry, kinematics, slip Rate and recurrence intervals of earthquakes along the eastern Mosha fault (Central Alborz, Iran), in prep for the Journal of Geophysical Research.

NB : Article en préparation synthétisant sous forme de figures l'ensemble des résultats concernant l'étude paléosismologique du segment oriental de la faille de Mosha.

* Article publié à Geology en 2006 :

Ritz J-F., Nazari H., Ghassemi A., Salamati R., Shafei A., Solaymani S. and Vernant P., 2006, Active transtension inside Central Alborz: A new insight of the Northern Iran-Southen Caspian Geodynamics, Geology, 34, 477-480, doi : 10.1130/G22319.1.

Geometry, Kinematics, Slip Rate and Recurrence of Earthquakes Along the Eastern Mosha Fault (Central Alborz, Iran)

Ritz J-F.[1], Solaymani S. [1,2], Balescu S. [3], Nazari H. [4], Vernant P. [1], Abbassi M. R. [2], Chery J. [1], Farbod Y. [2], Feghhi K. [2], Lamothe M. [5], Massault M.[6], Michelot J-L.[6], Shabanian E. [2] and Tabassi H. [2].

1: Laboratoire Géosciences Montpellier - UMR 5243, Université Montpellier 2, France
2: International Institute of Earthquake Engineering and Seismology (IIEES), Dibaji, 19531, Tehran-Iran.
3: Laboratoire de Préhistoire et Quaternaire – UMR 8018, Université des Sciences et Technologies de Lille, 59655 Villeneuve d'Ascq Cedex, France.
4: Institute for Earthsciences, Geological Survey of Iran, PO Box: 13185 1494, Tehran-Iran.
6: UMR CNRS-UPS "IDES" Université Paris-Sud, Bat. 504, 91405, Orsay, France.
5: US Geological Survey, Box 25046, M.S. 974, Denver CO 80225, USA

Abstract

The Eastern Mosha fault is one of the major active faults menacing the 15 millions peoples leaving in Tehran metropolis and its suburbs areas. Located at the southern piedmont of Central Alborz, it has been described as the source of several large historical earthquakes in in 1665 AD and 1830 AD. To assess the seismic hazard associated with this fault, we carried paleoseismological studies. We found many evidences at different scales, of left-lateral strike slip movements associated with a small normal component showing that the Mosha active fault is mainly a left-lateral strike-slip fault, and not a revere fault as previously described. Our paleoseismological investigations allowed us to determine a minimum slip rate of 2.2 ± 0.5 mm/yr along the eastern part of the Mosha fault. Along this segment, trenches analyses brr evidences for several seismic ground ruptures having occurred during the past ~10000 years - including the 1665 AD or the 1830 AD historical earthquakes. Combining stratigraphical and kinematics evidences allowed us to conclude that these ruptures were caused by seismic events with Magnitude Mw >7. Using radiocarbon and optically stimulated luminescence dates, we estimated the return periods for these large events to be comprised between 1100 and 1400 years.

Key words: Iran, Alborz, Mosha fault, paleoseismology, slip rate, recurrence intervals

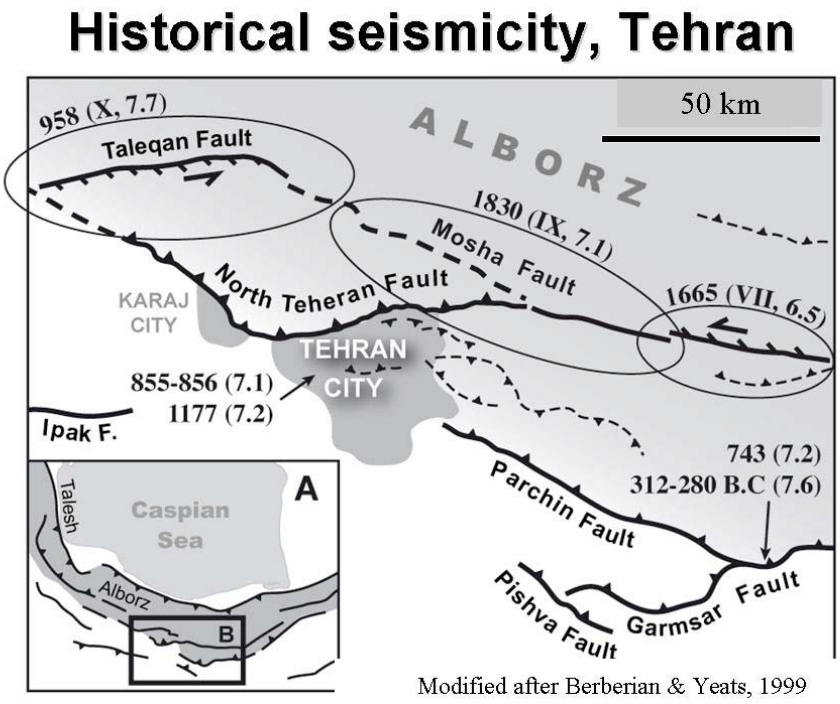

Figure 1: Sketch map of the active faults and associated damaging historical earthquakes within the Tehran region at the southern border of the Central Alborz mountain range (in grey). The macroseismal areas are from Berberian and Yeats (1999) and their evaluated intensities and magnitudes are from Ambraseys and Melville (1982).

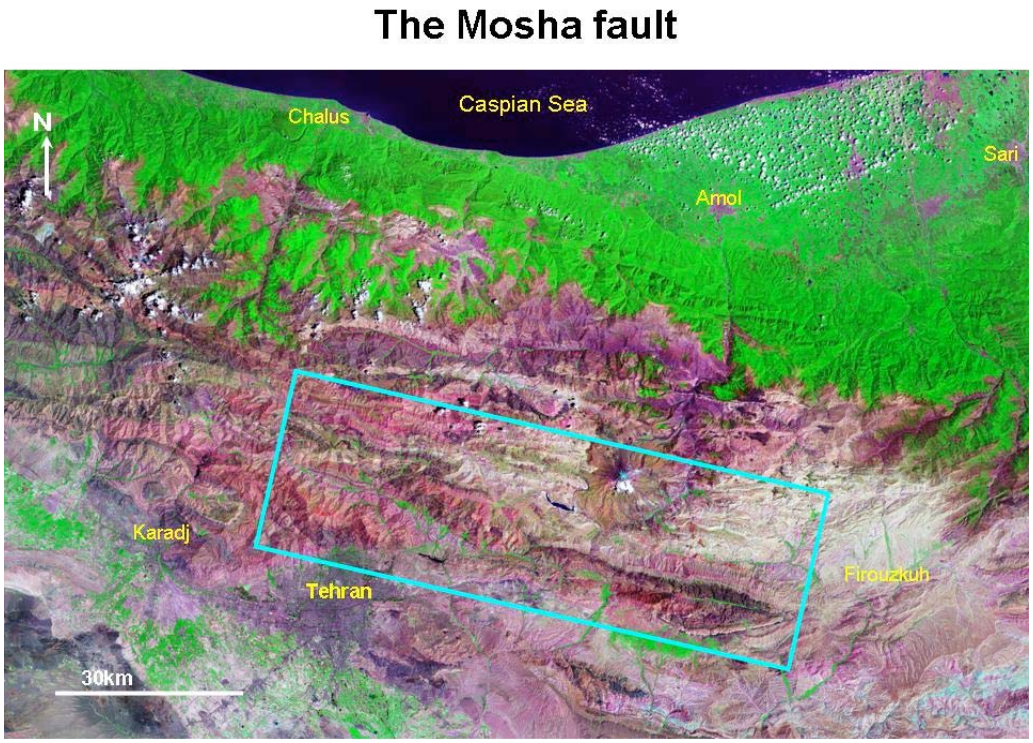

Figure 2: Landsat Satellite image of the Central Alborz mountain range showing range-parallel faults and folds. The green area corresponds to the wetter northern flak of the range undergoing the moisture of the South Caspian sea. The Mosha fault is located in the blue frame.

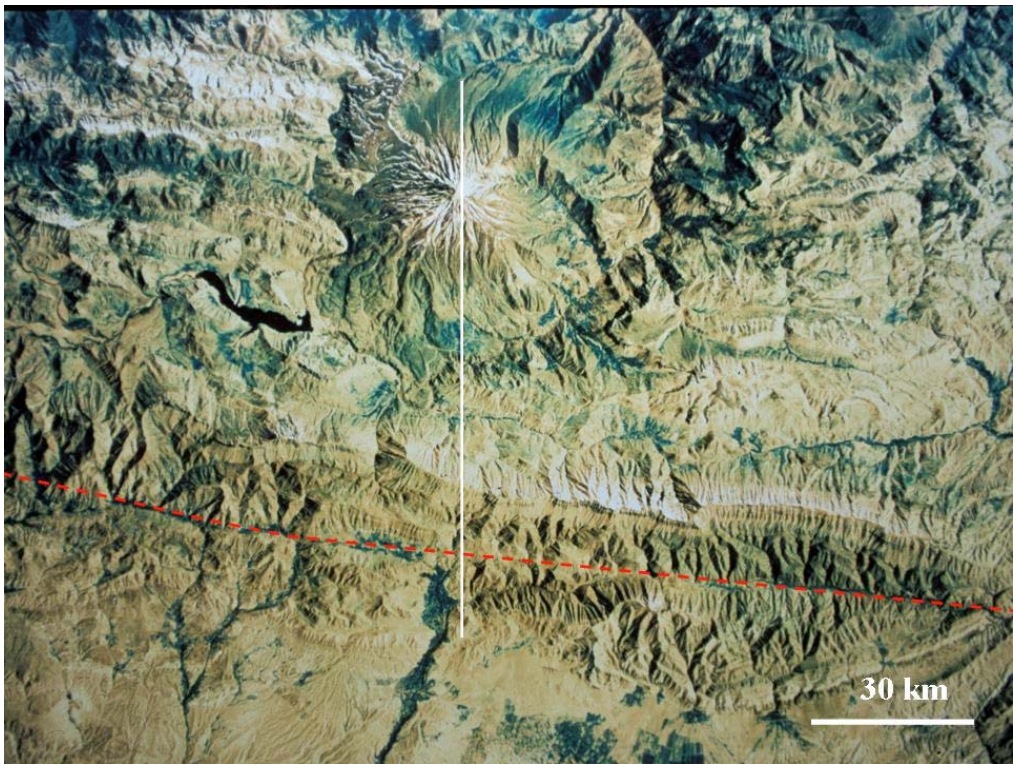

Figure 3: Cosmos satellite image of the eastern part of the Mosha fault (red dashed line). Due to repeating earthquake surface ruptures the Mosha fault has a clear surface expression along most of its trace and exhibits clear features of recent activity. The straight trace of the fault shows that the fault plane has a steep dip. The white line shows the situation of the cross section presented in Figure 4. Note the Damavand volcano 50 km northwards the fault.

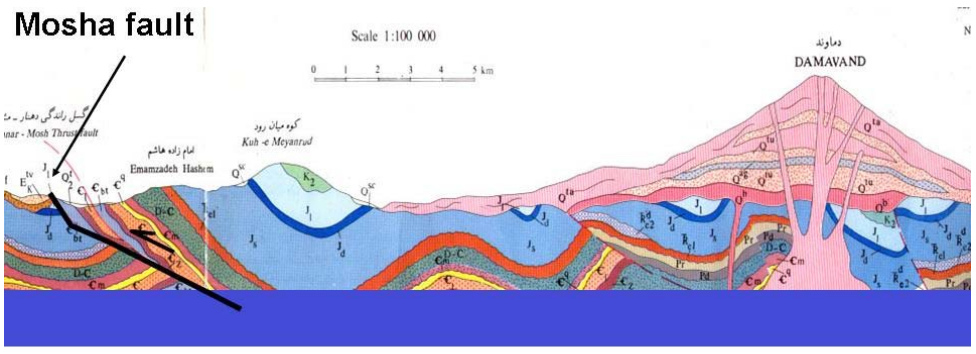

Figure 4: Geological cross section of the southern part of the Central Alborz Range showing the thrusting towards the South of the Mesozoic and older formations over the Cenozoic and younger formations along the Mosha fault (e.g. Berberian, 1983). As noted below the cross section, few neotectonics studies showed evidences for active oblique-slip (thrust and left-lateral) deformation along the fault (See the Figure 3 for situation).

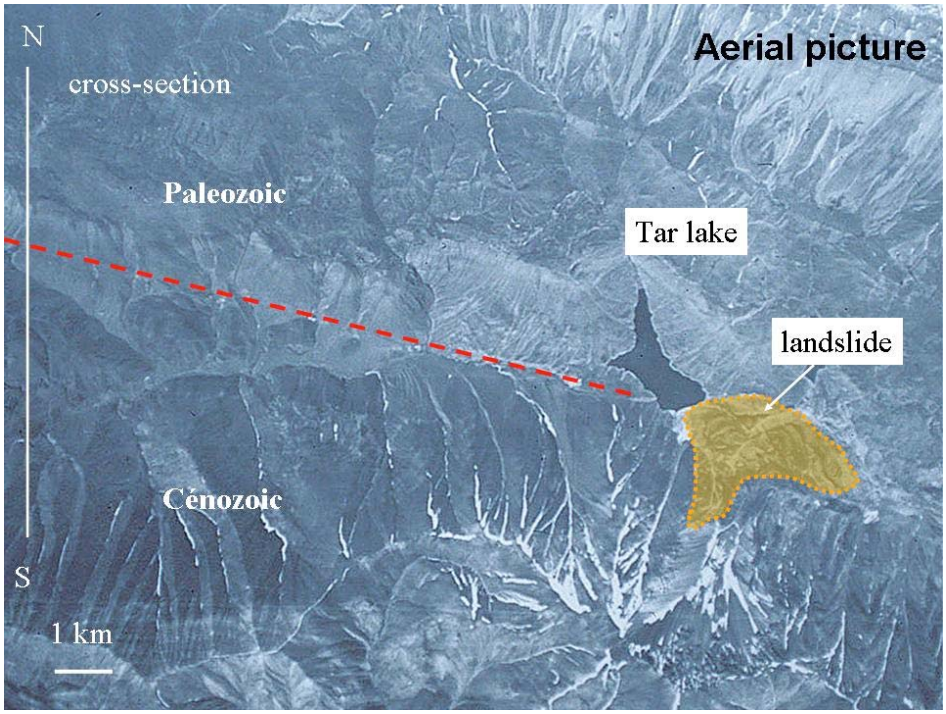

Figure 5: Aerial photograph of the eastern the Mosha fault within the Tar Valley. The straight trace of the fault (red dashed line) shows a steep narrow fault zone. Note that the Tar Lake sets within a pass and was formed by a landslide that dammed the drainage coming from the North. The white line corresponds to the natural cross section shown in Figure 7.

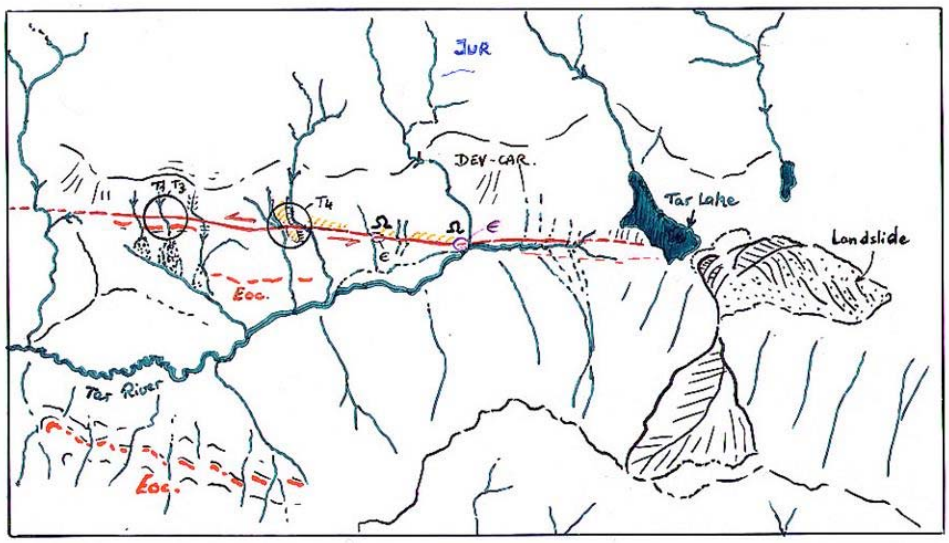

Figure 6: Interpretation of the aerial photo shown in Figure 5. The Mosha active fault reactivates an old thrusting contact between the Cambrian-Devonian-Carboniferous formations and the Cenozoic formations (Karaj). Quarries in Cambrian quartzites are dug all along the fault line. Circles point out evidences for of active left-lateral deformation along the fault, where we focused our trench study (T1, T3, T4 indicates labels of trenches).

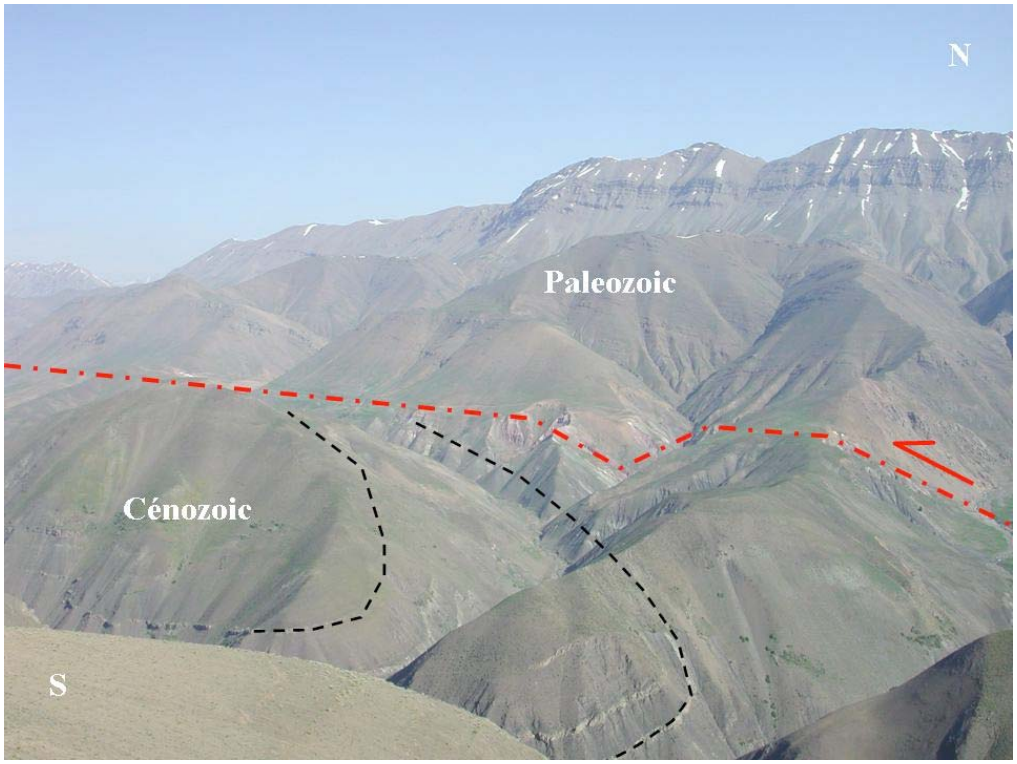

Figure 7: Northwest view showing a cross section of the Mosha fault zone between the Mosha and Tar valleys (see white line in Figure 5). The Paleozoic formations thrusted over the cenozoic Karadj formation forming an overturned syncline. This long-term thrusting deformation is not anymore active, as shown by the Upper-Pleistocene and Holocene features (shown in Figure 6 and followings) characterizing a left-lateral strike-slip normal deformation.

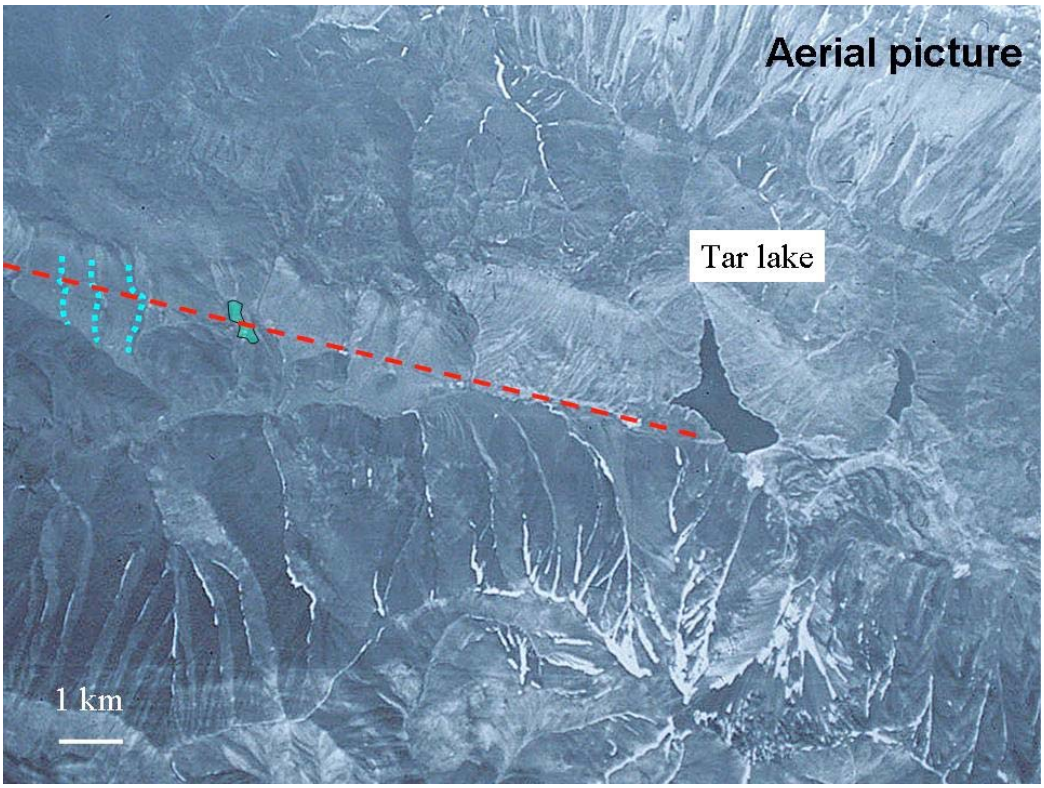

Figure 8: Aerial picture showing the two sites where we studied left-lateral offset features. The offset drainages corresponds to site 1 and the offset surface corresponds to the site 2.

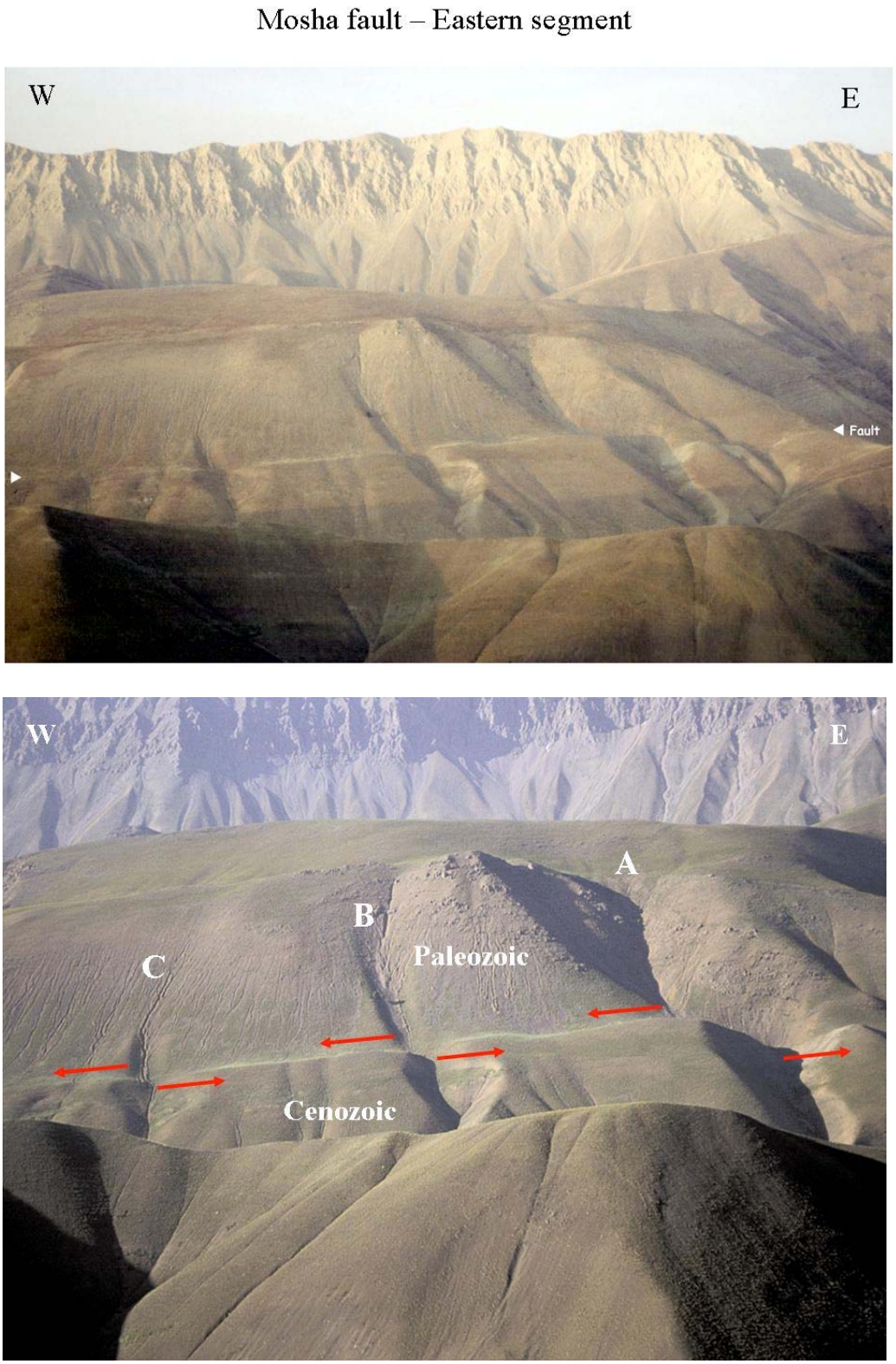

Figure 9: Two panoramic views showing the three left-laterally offset drainages within site 1 (note that offsets are not the same showing that the drainages have different ages (C is the the youngest drainage, A the oldest).

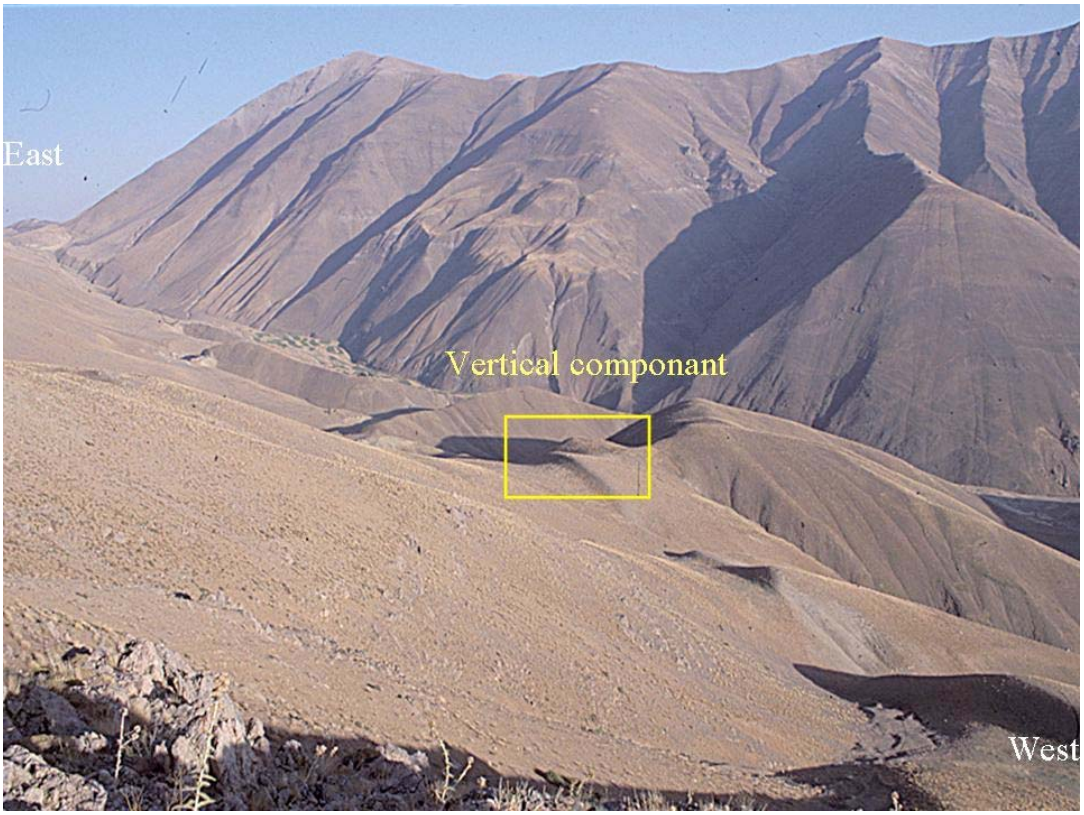

Figure 10: View towards the SE, showing the Mosha fault scarp from the upstream drainage A in the site 1. Note the shutter ridges characterizing the left-lateral strike-slip deformation. The yellow frame, within a crest line, points out the small vertical deformation associated with the horizontal deformation.

Figure 11: Westwards view of drainage B, where were dug 3 trenches. Note also the slight vertical deformation associated with the horizontal deformation.

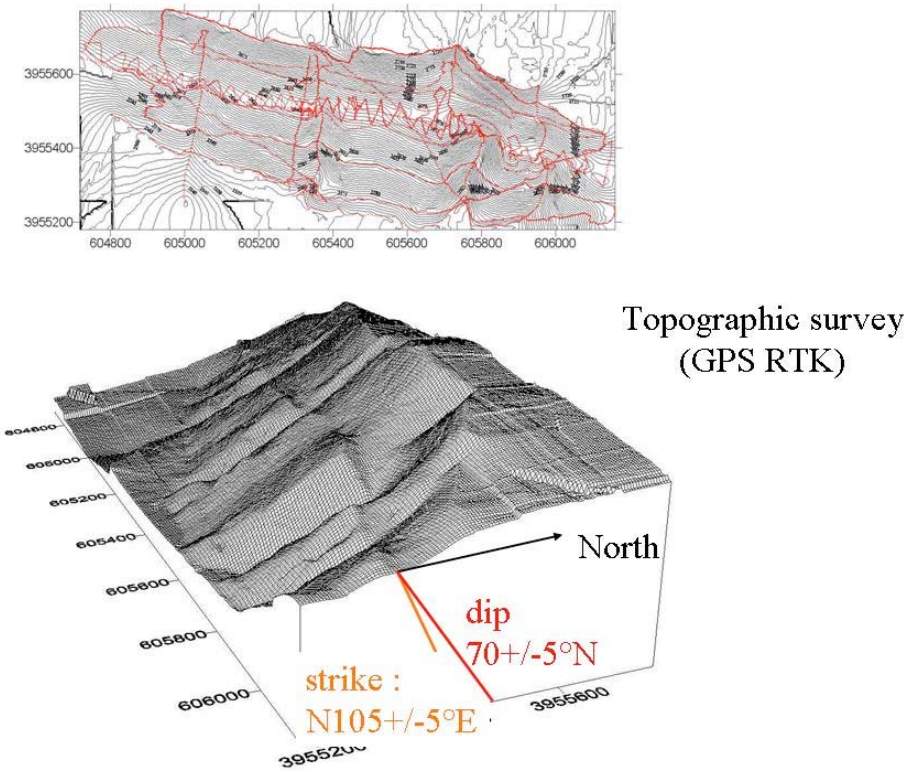

Figure 12: Digital Elevation Model (DEM) of site 1 obtained from GPS RTK survey, from which were calculated the strike, dip and rake of the eastern Mosha fault.

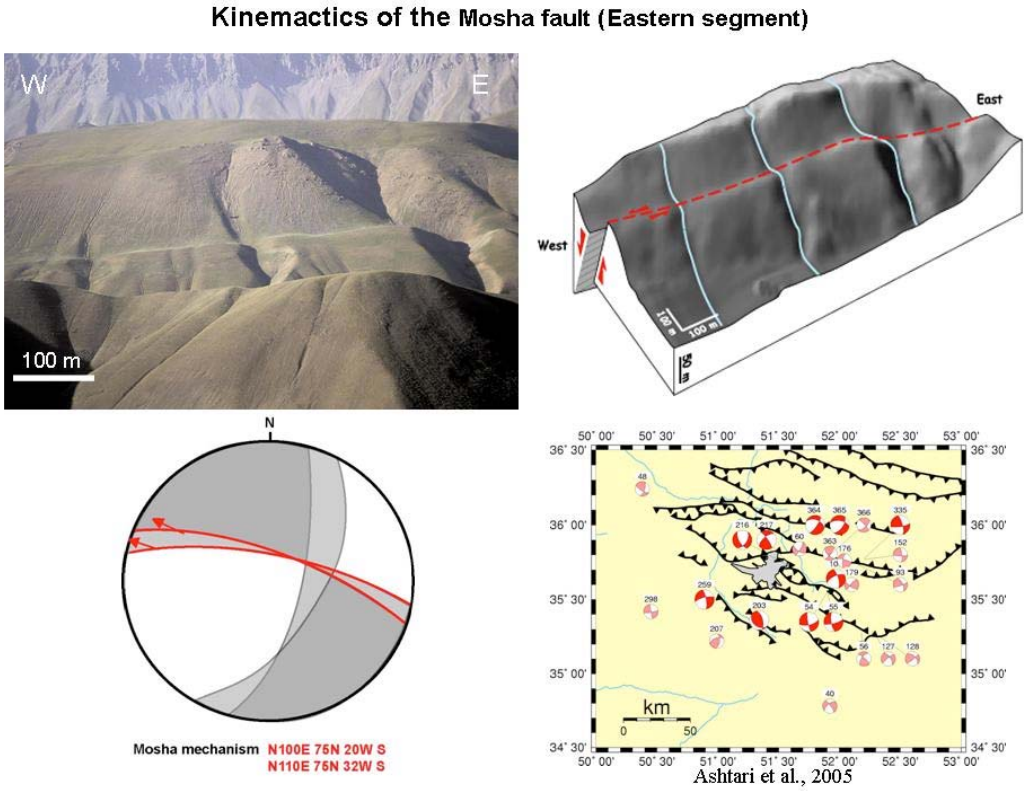

Figure 13: Summary of the kinematics study within site 1 along the eastern Mosha fault showing a panoramic view of the site from distance, a 3D representation of the DEM, the focal mechanism calculated from the DEM (280 75 – 20/-32), and focal mechanisms from microseismicity data (Ashtary et al., 2005) for comparison.

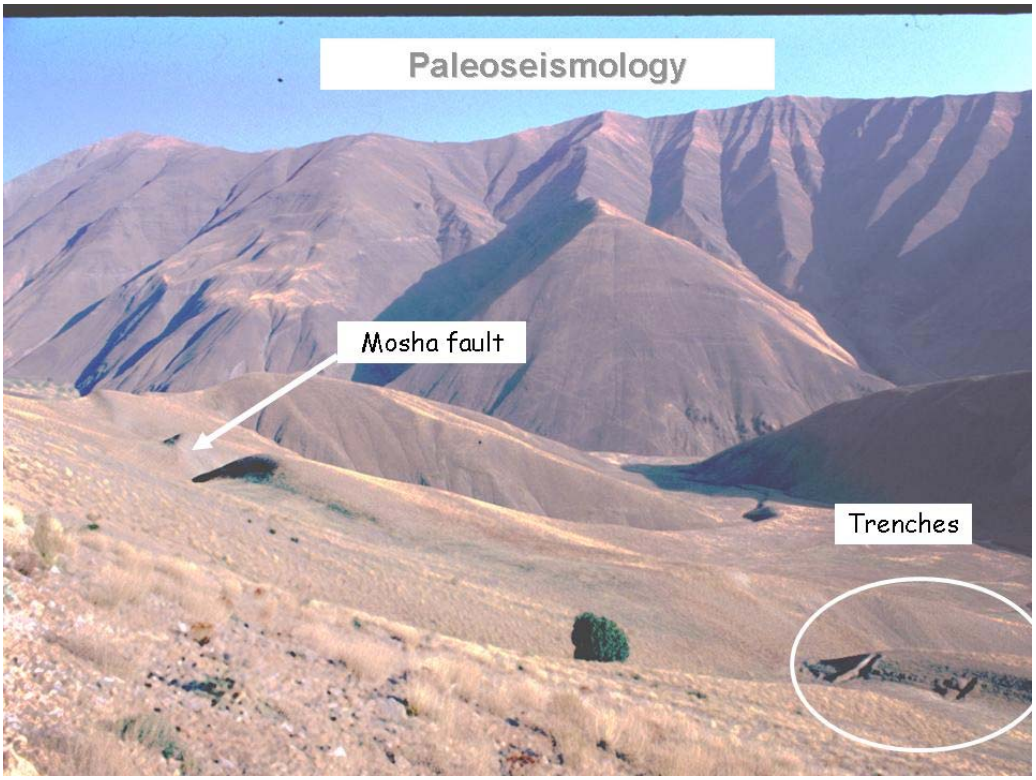

Figure 14: Picture looking southeast, taken upstream drainage B, showing three of trenches that were dug across the fault scarp.

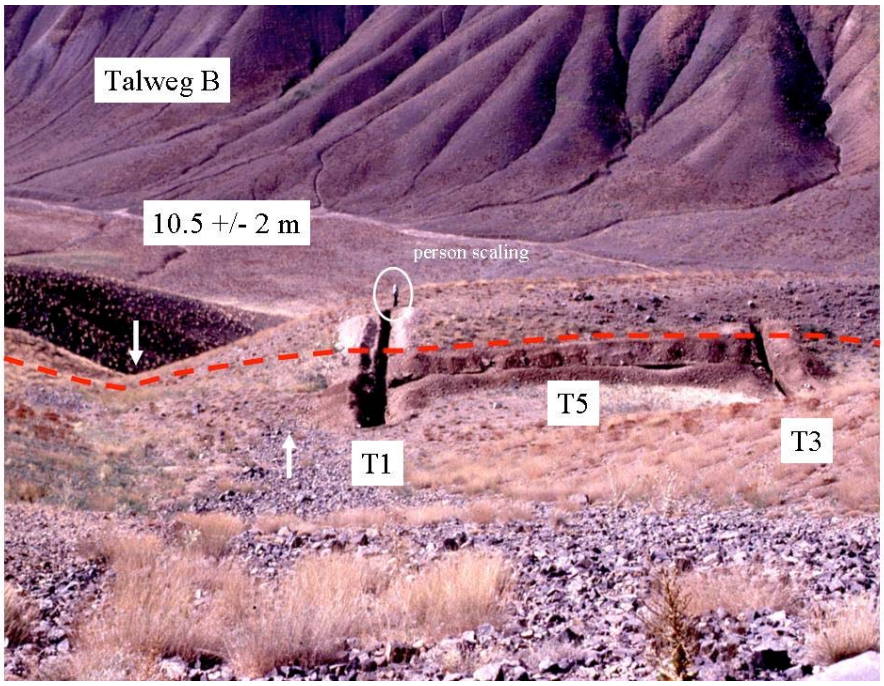

Figure 15: Southwards view of trenches T1, T3 and T5, dug at the right bank of the offset talweg B (see figure 9 for situation). The trench T5 was dug to analyse the correlation between units observed in T1 and T3.

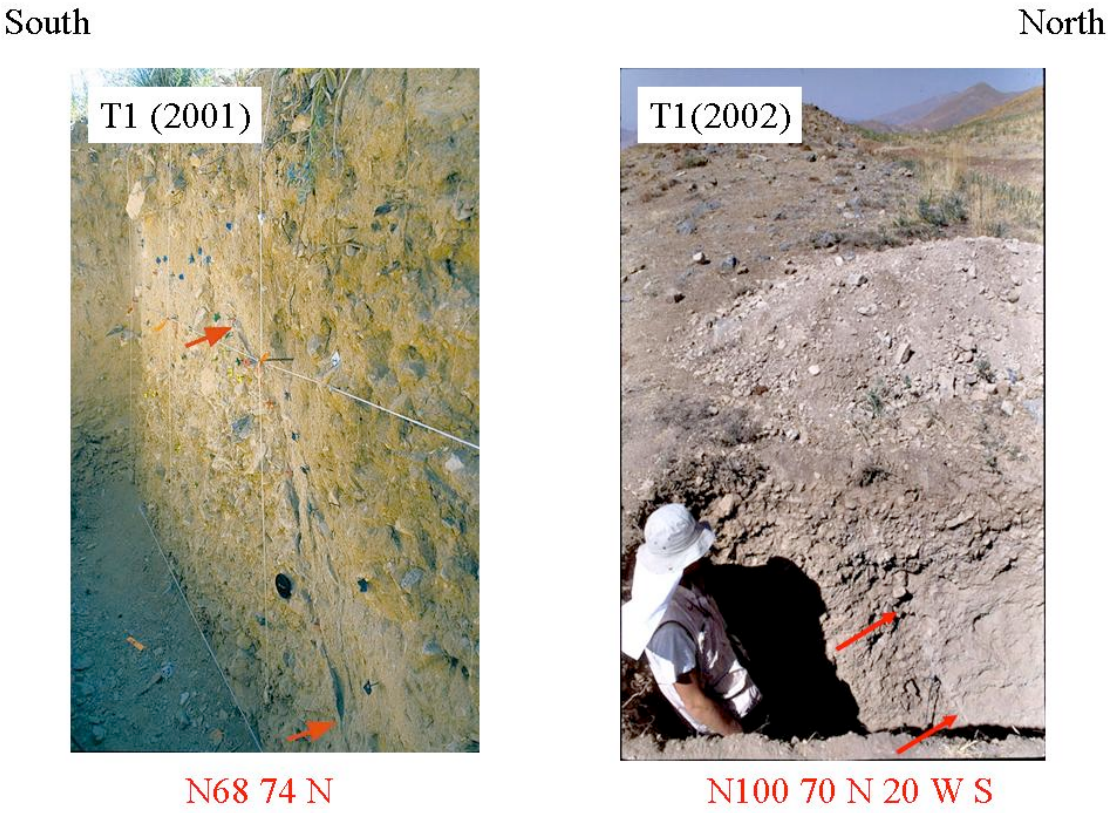

Figure 16: Westwards view of the steep north-dipping fault zone within the western wall of trench T1. Fault measurements within the fault zone attest of a main left-lateral motion with a small normal component.

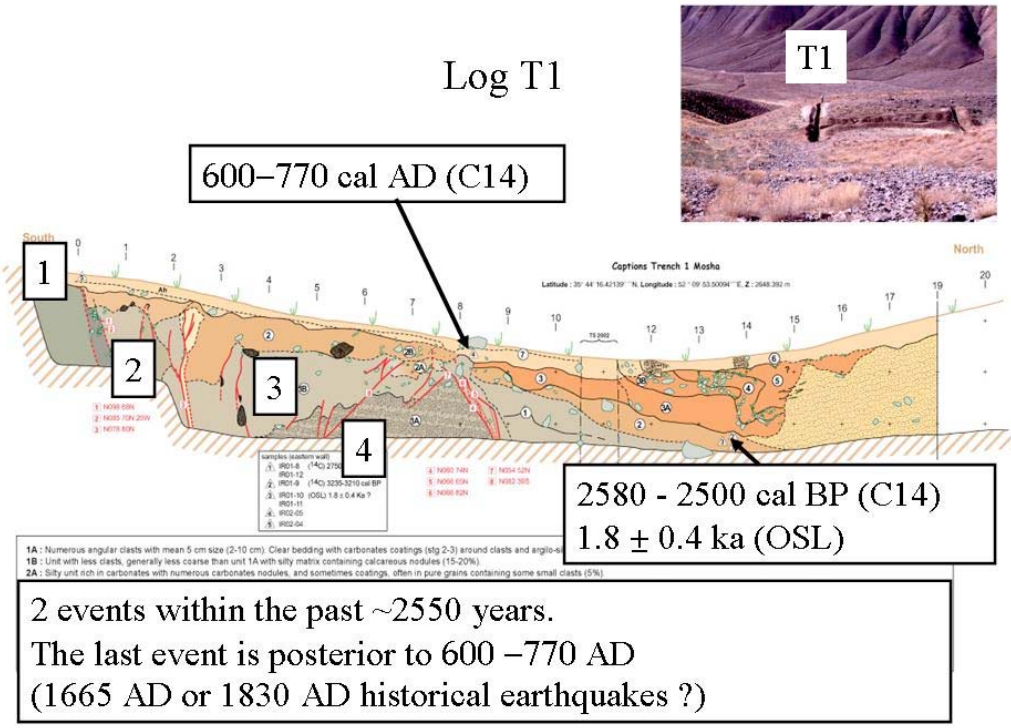

Figure 17: Log of the western wall of the trench T1. Based on fault terminations, we found evidences for at least four co-seismic surface-ruptures within the trench wall. From dating analysis (OSL and C14), we interpret that two events occurred since ~2,550 years. The most recent event is posterior to 600-770 AD, and could corresponds to the 1665 AD and 1830 AD historical earthquakes.

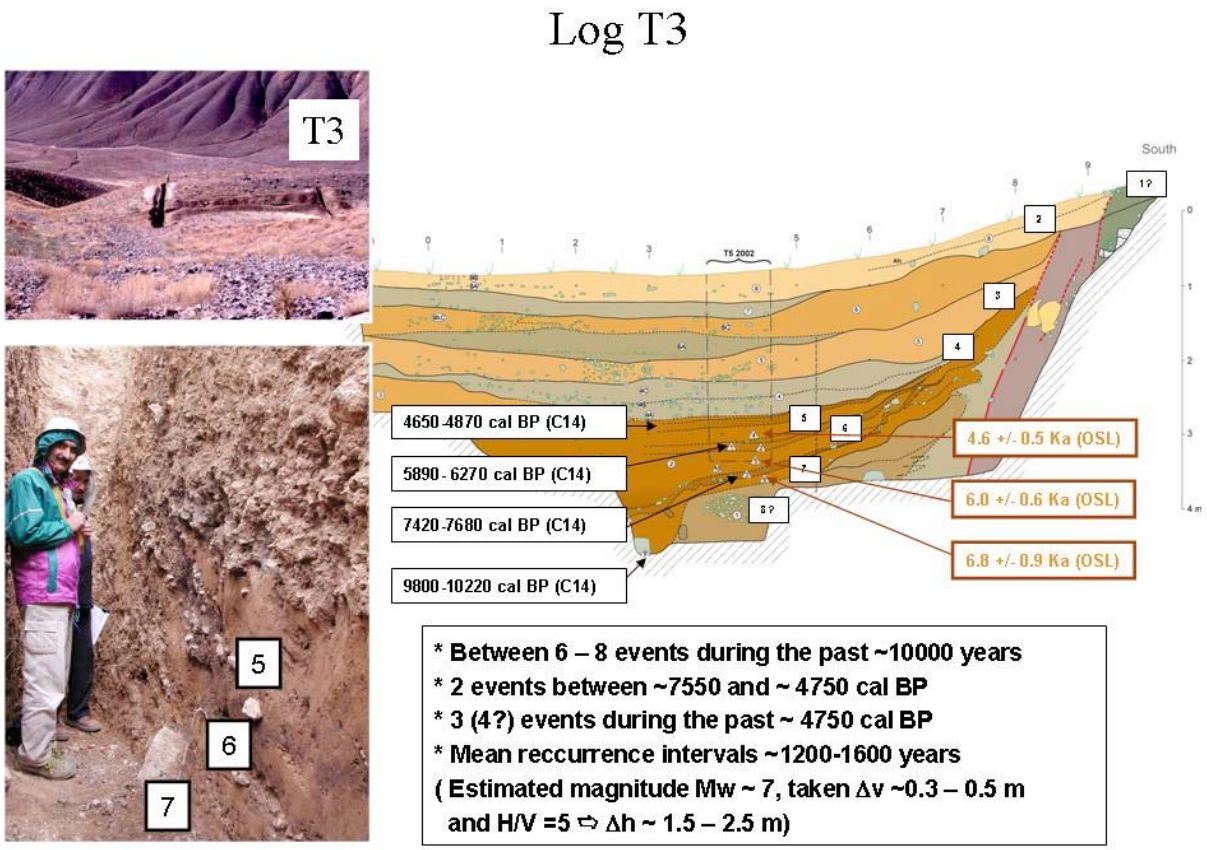

Figure 18: Summarised interpretation of the log of the trench T3. Here, we interpreted the colluvium units dipping north from the fault as scarp-derived colluviums. In the lower part of the trench, these colluviums units postdate thin paleosoil units (event horizons) that cap ponded silt units. We interpreted between 6 and 8 events. After the radiocarbon dating of paleosoils and the OSL dating of ponded silt, these 6 or 8 events occurred during the past 10,000 years. 2 events occurred between ~7,550 years and ~4,750 years cal BP, and between 3 and 4 events occurred during the past ~4,750 years. This yields a mean recurrence intervals of 1400 ± 200 years. Assuming that the north-dipping colluvium units results mainly from the destruction of a fault scarp, which height was roughly equal to or larger than the thickness of the deposits (e.g. McCalpin, 1996; Philip et al., 2001), we estimated a mean vertical component per event comprised between 30 and 50 cm. Combining these estimates with the fault rake allows us to estimate that the mean horizontal slip per events was comprised between 1.5 m and 2.5 m. Therefore, combining stratigraphical and kinematics evidences allowed us to conclude that these event ruptures were caused by seismic events with Magnitude Mw >7.

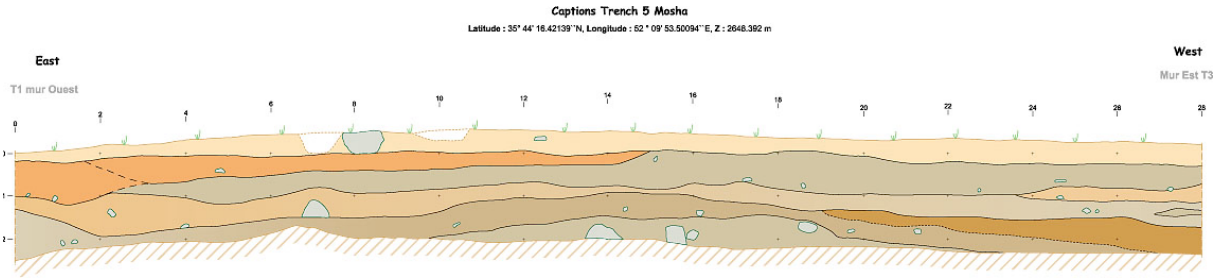

Figure19: Log of the southern wall of trench T5 correlating the units observed in trenches T1 and T3.

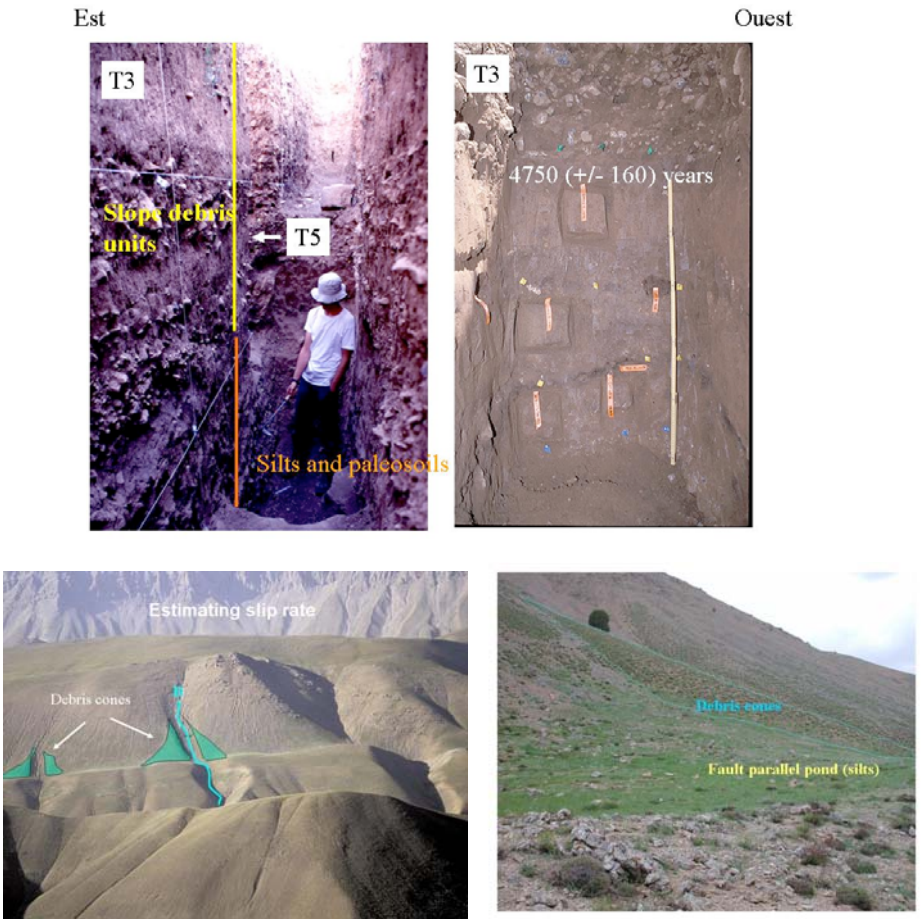

Figure 20: Pictures showing the abrupt change in the stratigraphy observed in trench 3, and its correlation with the morphology: the coarse debris units observed on the upper part of trench 3 corresponds to debris cones covering the fine silty and organic-rich units that accumulated along the scarp within an elongated depression. Note that this abrupt change which occurs soon after ~4,750 years cal BP is certainly due to a drastic change in the regional climate.

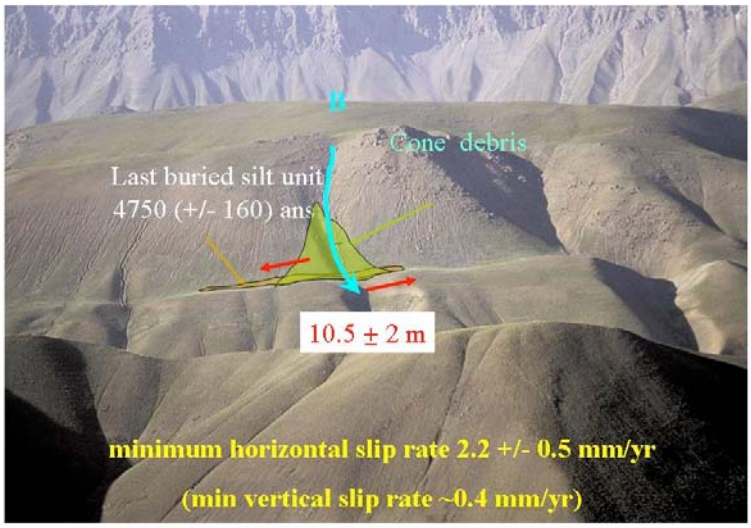

Figure 21: We used features described in Figure 20 to estimate the horizontal slip rate along the eastern Mosha fault. We considered that the onset of the stream incisions started when the debris cone, filling up the depression, allowed the stream to overbank the scarp. Therefore the 10.5 ± 2 m offset occurred after ~4,750 ± 160 years, the age of the top silt units. This yields a minimum horizontal slip rate of 2.2 ± 0.5 mm/yr.

Figure 22: Southwards view of site 2 (see figure 8 for situation). Here, the main and secondary branches of the Eastern Mosha fault offset left-laterally a young glacial surface. The vertical components observed on both faults give a graben-like style to this morphotectonics feature. Note the large shutter ridge along the Southern rupture. T4 and T6 show the locations of our paleoseismological trenches within the site.

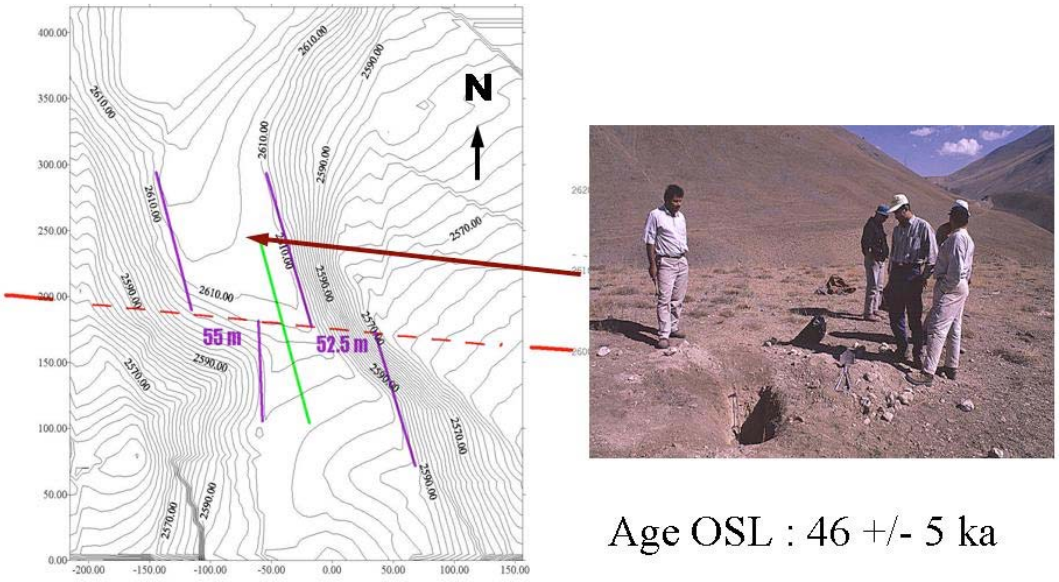

Minimum Upper Pleistocene horizontal slip rate
1.2 +/- 0.1mm/yr

Figure 23: (Left) Detailed DEM of the deformed glacial surface showing a ~53 m left-lateral offset along the main fault branch. (Right) Picture showing the soil pit dug on the surface (see figure 21 for situation) to collect OSL sample. Taken the ~53 m offset as a minimum offset, the OSL age (46 +/- 5 ky) yields a minimum horizontal slip rate of 1.2 ± 0.1 mm/yr.

Figure 24: Northwards view of the site 2 showing the locations of trenches T4 and T6 (see figure 21 for situation).

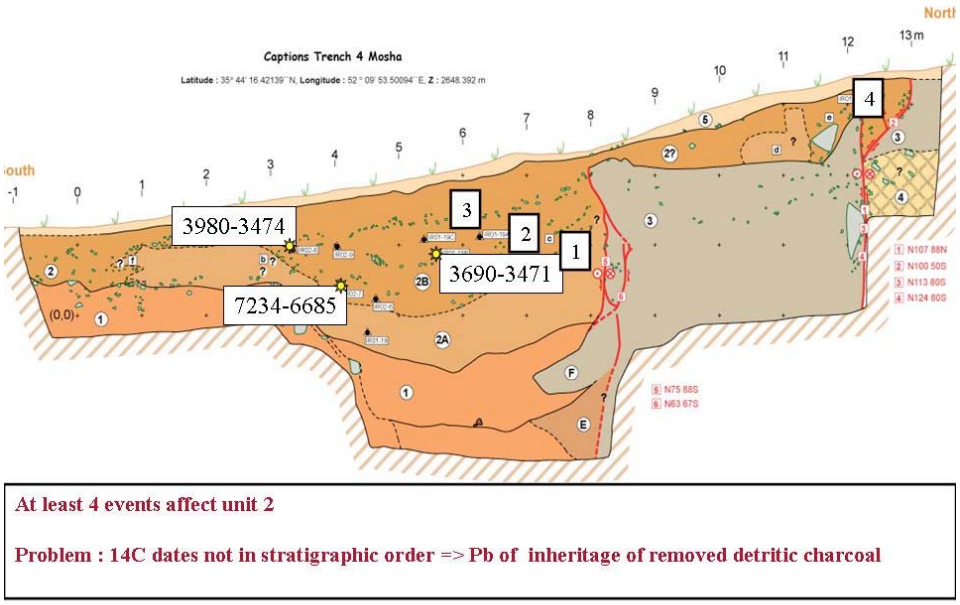

Figure 25: Log of trench T4 dug across the main fault branch (see Figure 21 for situation). Several events can be interpreted from the log. We found some charcoal in unit 2 that postdating till units. Considering the gradual bend of layers in unit 2 as tectonics features, we tentatively interpreted 3 events along a first plane, plus a fourth one along another one in the northern part of the trench. Therefore, four events would have occurred since the past ~6.9ky. This interpretation has to be considered with caution taken the fact that all radiocarbon ages are not in good stratigraphical order..

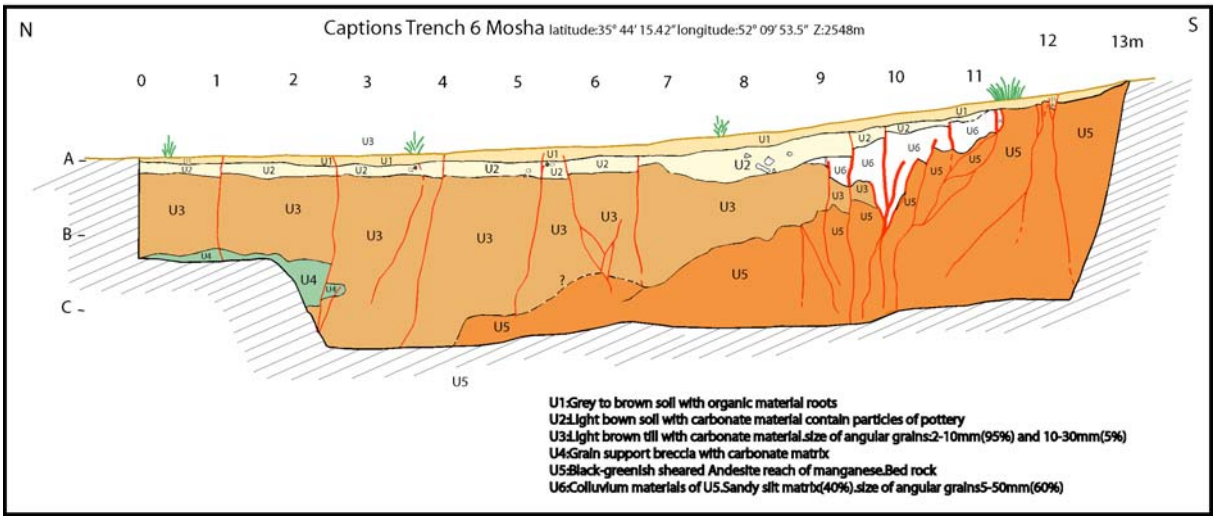

Figure 26: Log of trench T6 within the site 2. We dug this trench across the secondary fault branch (see Figure 21 for situation). Here, the southern fault branch cut clearly the ground surface during the most recent event. After radiocarbon dating, the age of this event is older than 7000 years, suggesting that the seismic activity along this fault branch is older and secondary compared to the northern branch.

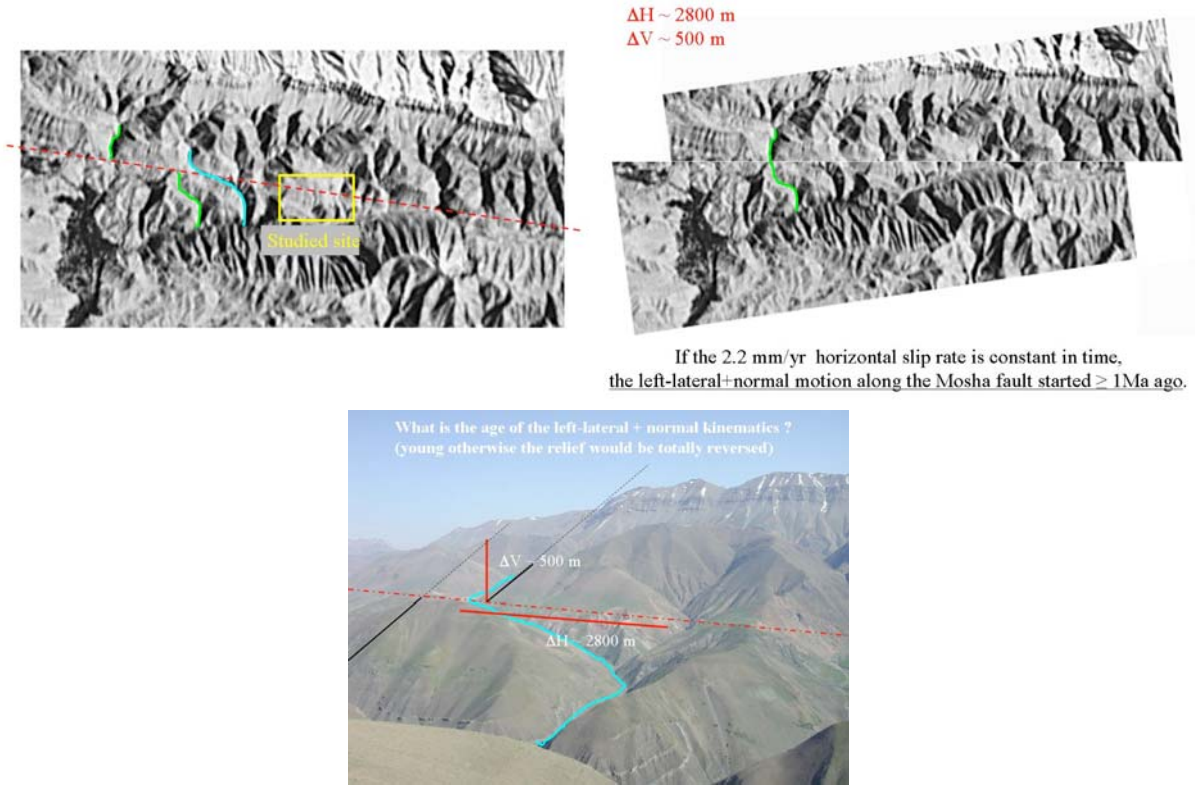

Figure 27: The large offset river bed and related topography found at the western side of the Tar valley, shows a maximum cumulative horizontal offset of 2800 m. The cumulative vertical offset is 500 m which yields a ratio H/V of ~5 similar to the ration H/V calculated from the DEM in site 1. Dividing the cumulative horizontal offset by the 2.2 ± 0.5 mm/yr slip-rate (assuming it was constant through time) places the onset of the left-lateral strike-slip faulting along the eastern Mosha fault between 1 and 1.5 Ma.

* Article publié à Geology en 2006 :

Ritz J-F., Nazari H., Ghassemi A., Salamati R., Shafei A., Solaymani S. and Vernant P., 2006, Active transtension inside Central Alborz: A new insight of the Northern Iran-Southen Caspian Geodynamics, Geology, 34, 477-480, doi : 10.1130/G22319.1.

Active transtension inside central Alborz: A new insight into northern Iran–southern Caspian geodynamics

J.-F. Ritz Laboratoire Dynamique de la Lithosphère, UMR 5573, Université Montpellier 2, 34095 Montpellier Cedex 05, France
H. Nazari Laboratoire Dynamique de la Lithosphère, UMR 5573, Université Montpellier 2, 34095 Montpellier Cedex 05, France, and Geological Survey of Iran, P.O. Box 13185 1494, Tehran, Iran
A. Ghassemi, R. Salamati, A. Shafei Geological Survey of Iran (GSI), P.O. Box 13185 1494, Tehran, Iran
S. Solaymani International Institut of Earthquake Engineering and Seismology (IIEES), Dibaji, 19531, Tehran, Iran
P. Vernant Laboratoire Dynamique de la Lithosphère, UMR 5573, Université Montpellier 2, 34095 Montpellier Cedex 05, France

ABSTRACT

The tectonic activity in the Alborz mountain range, northern Iran, is due both to the northward convergence of central Iran toward Eurasia, and to the northwestward motion of the South Caspian Basin with respect to Eurasia inducing a left-lateral wrenching along this range. These two mechanisms give rise to a NNE-SSW transpressional regime, which is believed to have affected the entire range for the last 5 ± 2 m.y. In this paper, we show that the internal domain of central Alborz is not affected by a transpressional regime but by an active transtension with a WNW-ESE extensional axis. We show that this transtension is young (middle Pleistocene). It postdates an earlier N-S compression and may have been initiated when the South Caspian Basin started moving. Consequently, our results suggest that the South Caspian Basin motion may have taken place more recently than previously proposed.

Keywords: Iran, central Alborz, South Caspian Basin, active tectonics, transtension.

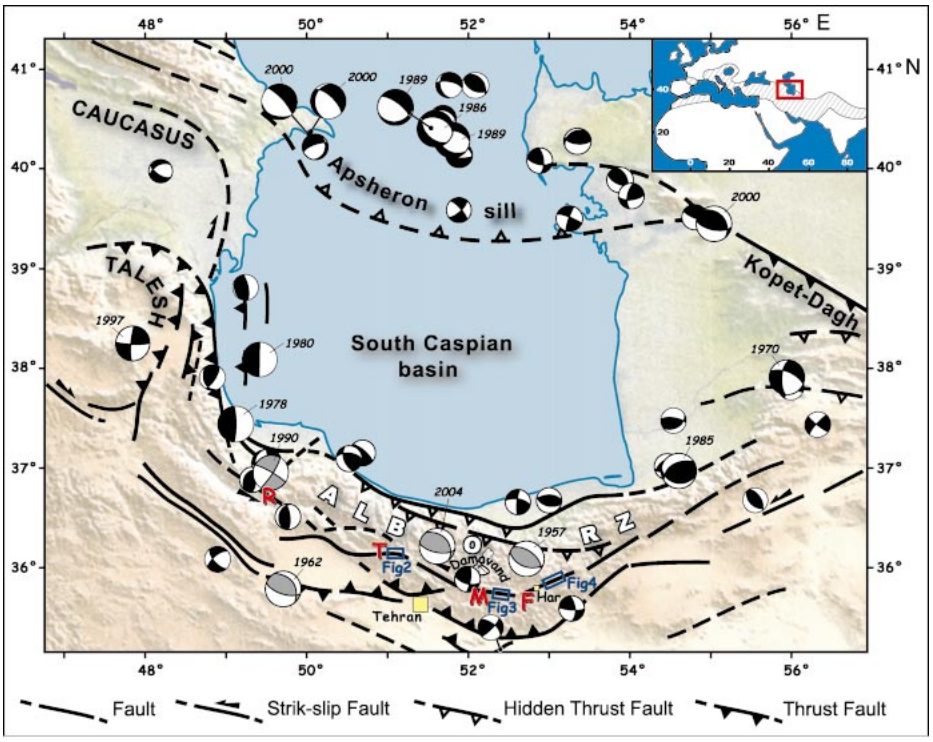

Figure 1. Map of the South Caspian region with active faults and focal mechanisms (larger spheres with dates correspond to earthquakes having magnitude ≥6). Focal mechanisms are from Jackson et al. (2002) for Apsheron sill and Kopet Dagh area, and from Ashtari et al. (2005) for Alborz. Gray spheres are from McKenzie (1972) for 1957 earthquake, from Jackson et al. (2002) for 1962 and 1990 earthquakes, and from U.S. Geological Survey for 2004 earthquake. Abbreviations: T—Taleghan fault, M—Mosha fault, F—Firuzkuh fault, R—Rudbar fault, Har—Harandeh village.

INTRODUCTION

Surrounding the South Caspian Basin, the Alborz mountain range shows strong tectonic activity with several destructive earthquakes in the past (Berberian and Yeats, 2001). A V-shaped structure characterizes its central part (longitudes 50°E to 54°E) with folds and faults trending NW-SE in the western Alborz and trending NE-SW in the eastern Alborz (Fig. 1). Structural and seismological data for the Alborz show that the deformation is partitioned along range-parallel thrusts and left-lateral strike-slip faults (Jackson et al., 2002; Allen et al., 2003). A recent global positioning system (GPS) study showed that N-S shortening across the Alborz occurs at 5 ± 2 mm/yr and that the left-lateral shear across the overall belt has a rate of 4 ± 2 mm/yr (Vernant et al., 2004). Seismological data recorded in Alborz and other areas surrounding the South Caspian Basin allowed Jackson et al. (2002) to conclude that the South Caspian Basin is moving NW with respect to Eurasia; using the global GPS data set, the maximum northern component of the South Caspian plate movement is 5–6 mm/yr. This model accounts for the seismic activity along the Apsheron ridge, the eastward overthrusting of the Talesh, and the left-lateral movement along the WNW-ESE Rudbar fault, to the north, west, and southwest of the South Caspian Basin, respectively (Fig. 1). Coupled with the N-S convergence of central Iran, the southwestward motion of the South Caspian Basin with respect to central Iran leads to a NNE-SSW transpressional regime in Alborz. This transpression would have started between 3 and 7 m.y. ago. Before this date, right-lateral movements observed along range-parallel strike-slip faults in western Alborz suggest that the range was deforming against the rigid and stable South Caspian domain under a N-S compressional regime (Axen et al., 2001; Jackson et al., 2002; Allen et al., 2003).

However, in the internal domain of central Alborz, morphotectonic features do not fit with the above kinematical and chronological model. These features concern the Taleghan, the eastern Mosha, and the Firuzkuh faults, which are three main active faults, each

around 70–80 km long that trend E-W, WNW-ESE, and NE-SW, respectively (Fig. 1). These three faults are more or less connected and belong to a range-parallel shear zone inside the central Alborz. The area covered by these faults is 250 × 50 km^2, between 50°30′ and 53°00′E longitude, and includes the Damavand, a dormant volcano corresponding to the highest peak in the Middle East (5670 m).

During historical seismicity, these three faults have been the sites of large earthquakes (Berberian and Yeats, 2001), but so far, the absence of strong instrumental events along them has not allowed us to determine their focal mechanisms. On the geological maps, these faults are indicated as thrust faults along which Mesozoic, Paleozoic, or Proterozoic deposits overthrust Cenozoic deposits. These thrusting movements are considered still active (e.g., Berberian et al., 1996) and associated with left-lateral strike-slip faulting along the eastern Mosha fault (e.g., Allen et al., 2003) and the Firuzkuh fault (e.g., Berberian et al., 1996; Jackson et al., 2002). Study of recent morphological features and associated structures affecting the Quaternary deposits along these faults allows us to propose a different interpretation of their present kinematics. This has implications in terms of understanding the recent geodynamical evolution of the central Alborz–South Caspian region.

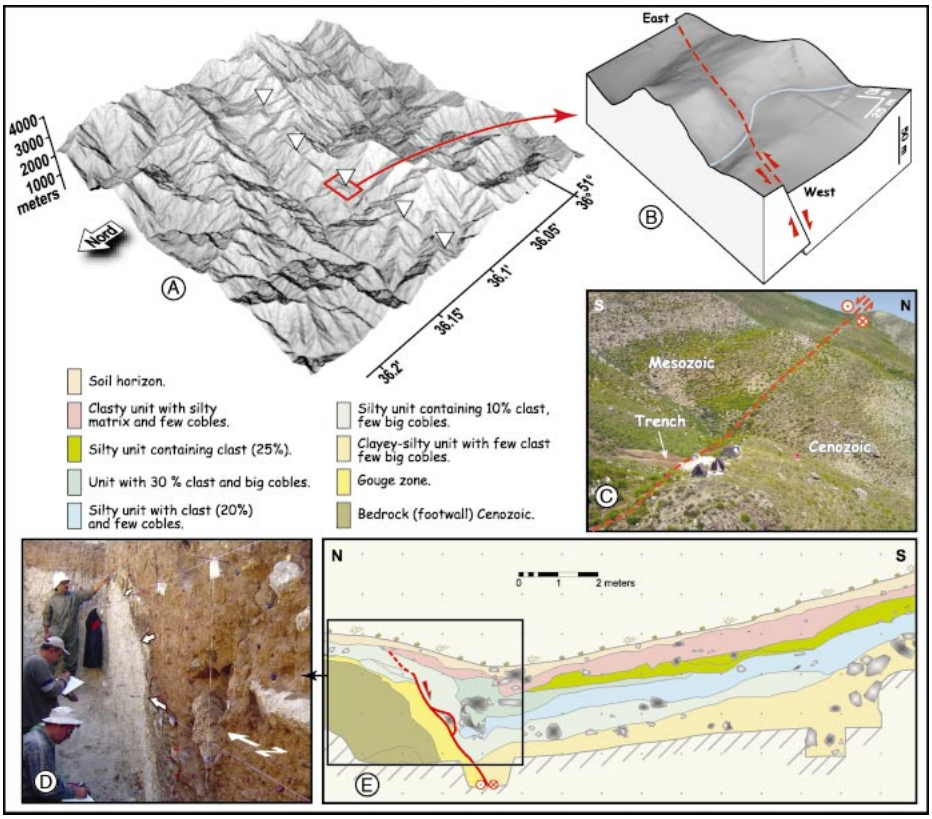

Figure 2. A: Digital elevation model (DEM) obtained from "Asara" 1:50,000 topographical map showing Taleghan fault scarp. B: DEM obtained from global positioning system (GPS) kinematics survey. C: Picture of the fault scarp. D: View of the Taleghan fault in trench and (E) corresponding log.

MORPHOTECTONICS AND STRUCTURAL ANALYSES

Along the three mentioned faults, we analyzed satellite pictures, air photographs, and the large-scale digital elevation models (DEM; generated from digitizing 1:50,000 scale topographic maps). Then we did extensive field work within selected sites, analyzing the morphology, using small-scale DEMs generated from GPS kinematics surveys, and the structures affecting the recent deposits within paleoseismological trenches dug across fault scarps.

Figure 2 shows a synthesis of our observations along the Taleghan fault. At all scales, we observe a clear fault scarp attesting to the recent (Pleistocene-Holocene) surface rupture along the fault. The morphology of the scarp indicates that the dip of the Taleghan fault is toward the south. Therefore, the counterslope observed all along the scarp clearly indicates that the recent movements have a normal component (Figs. 2A and 2B) associated with left-lateral displacement as shown by the shifting of the talwegs and the ridges. According to the DEM in Figure 2B, the ratio *H*/*V* between the horizontal (H = 13 m) and the vertical (V = 17 m) components is 0.76. In trenches, the geometry and kinematics of the fault affecting the recent deposits are consistent with what is observed at a larger scale in the morphology (Figs. 2D and 2E). From the compilation of our observations, the mean strike, dip, and pitch for the Taleghan fault in its eastern part are N105°E, 60°S, and 50°E, respectively. This makes it a normal left-lateral strike-slip fault.

Along the eastern Mosha fault, the shifting of the talwegs and ridges (Figs. 3A and 3B) attests to the predominant left-lateral wrenching, as mentioned by Allen et al. (2003) and Bachmanov et al. (2004), along a north-dipping fault plane. However, the shutter ridges cannot explain the counterslope morphology of the scarp observed all along the fault (Figs. 3B and 3C). There is a clear slight normal component associated with the left-lateral horizontal movement. The ratio *H*/*V* between horizontal (H = 100 m) and vertical (V = 20 m) components is 5, according to the digital elevation model (Fig. 3B). The mean strike, dip, and pitch of the fault are N100°E, 70°S, and 20°W, respectively. This makes it a left-lateral normal fault. These geometry and kinematics are also observed in trenches at smaller scale, where a main north-dipping surface rupture associated with conjugated horst and graben structures is affecting Holocene deposits (Fig. 3D). Along the main fault plane (Fig. 3E), we measured fault-slip data of N098°E, 70°N, and 20°W, indicating a left-lateral normal movement. More to the west, at the junction between eastern and central parts of the Mosha fault, where the fault bends to the NW (see Fig. 1), our preliminary observations suggest that the fault has a pure left-lateral movement.

The morphology along the Firuzkuh fault clearly shows a counterslope scarp as observed along the Taleghan and the eastern Mosha faults. Between Firuzkuh city and Harandeh village, along the southern part of the Firuzkuh fault, the geometry of the fault scarp indicates that the dip of the fault is toward the SE (Figs. 4A and 4B), which is consistent with the observation in Harandeh village of a main (pluri-decametric) fault plane affecting the Mesozoic deposits trending N060°E and dipping 55°SE. Figure 4A shows that the talwegs have shifted with apparent and opposed strike-slip movements along a counterslope scarp, suggesting that the fault has a normal movement associated with a slight left-lateral component. North of Firuzkuh city, we surveyed a site showing a dried valley perched on the northern side of the fault, whereas on the southern side, the corresponding present stream appears downthrown and shifted left-laterally (Figs. 4C and 4D). Against the scarp, we found lacustrine deposits that have been incised by regressive erosion. These features are consistent with those observed to the south of Firuzkuh and suggest that the fault is dipping south and has a main normal component associated with a slight left-lateral movement. From the digital elevation model (Fig. 4D),

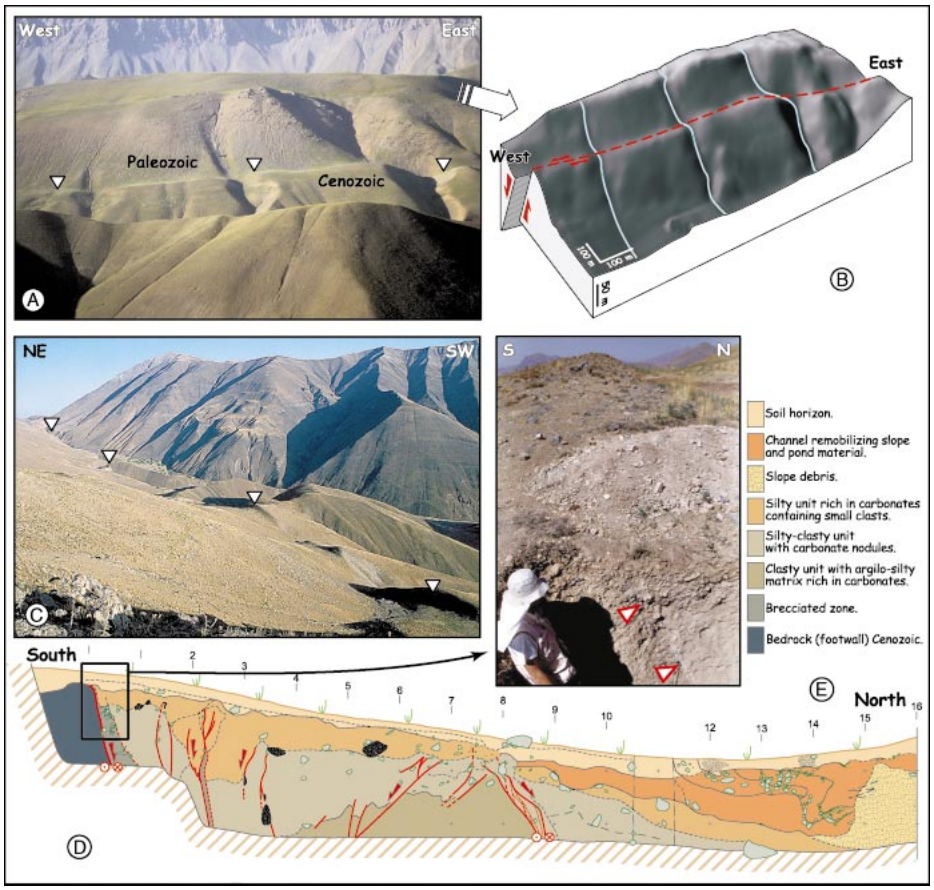

Figure 3. A: Eastern Mosha fault scarp in landscape. B: Corresponding digital elevation model (DEM) obtained by global positioning system (GPS) kinematics survey. C: Picture of fault scarp. D: Log of one of trenches dug across fault scarp (modified after Ritz et al., 2003). E: Picture of main rupture.

we estimated a ratio of $H/V = 0.6$ between the horizontal ($H = 15$ m) and the vertical ($V = 25$ m) components for the main stream displacement. This is consistent with the geometrical and kinematical parameters measured along the Taleghan and eastern Mosha faults, also taking into account the NE-SW trend of the Firuzkuh fault.

Put together, the recent morphological and structural features observed along the Taleghan, eastern Mosha, and the Firuzkuh faults characterize an active transtensional deformation occurring in the internal domain of central Alborz. The constant WNW-ESE direction of slip vectors throughout the studied area shows that this transtension is not related to the apex of the curved Alborz Mountains. Moreover, this transtension regime does not accumulate enough deformation to reverse the large-scale topography associated with previous thrusting movements. This suggests that the transtensional tectonic events along these faults are recent.

How recent? From paleoseismology, Ritz et al. (2003) estimated an ~2 mm/yr horizontal slip rate along the eastern Mosha fault over the Holocene and a ratio $H/V = 5$ between horizontal and vertical components. This ratio is also obtained if we use larger-scale morphological features, such as left-lateral shifted streams and the corresponding accumulated vertical offset of the mountain slopes (Fig. 5): From the satellite image (Fig. 5A), we measured an ~2 km accumulated horizontal displacement for the stream shown in Figure 5B, corresponding to accumulated vertical offset of ~350 m (the accumulated vertical displacement along the Taleghan fault is also ~350 m). This yields a ratio $H/V = 5.7$, suggesting that the kinematics of the fault have remained stable through the time.

On the satellite picture (Fig. 5A), the largest shifted drainage that we can observe is displaced a maximum of 3 km. Consequently, assuming a 2 mm/yr horizontal slip rate stable through the time, this yields an age of 1–1.5 Ma for the beginning of the transtensional regime along the Mosha fault.

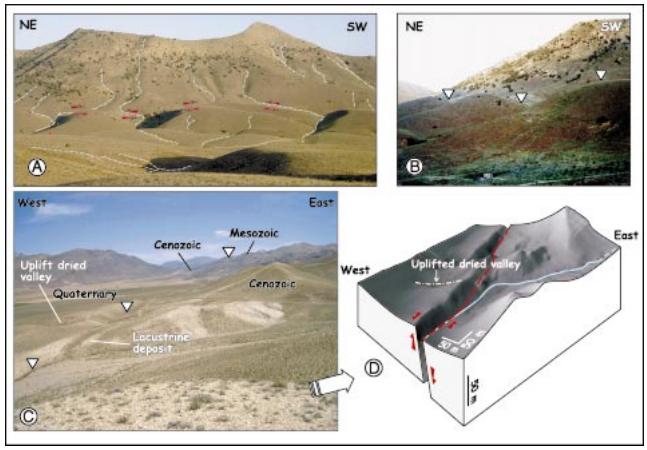

Figure 4. A–B: Firuzkuh fault scarp in landscape. C: Picture of fault scarp studied north of Firuzkuh. D: Corresponding digital elevation model (DEM) obtained from global positioning system (GPS) kinematics survey.

DISCUSSION

Our observations show that the present general left-lateral shear observed inside the central Alborz mountain range is associated with transtensional deformation. These observations are supported by microseismic data recorded along the eastern Mosha fault showing steep north-dipping, N100°E-trending left-lateral strike-slip focal mechanisms associated with normal components (Ashtari et al., 2005). Moreover, the analysis of Shuttle Radar Topography Mission (SRTM) images in western Alborz suggests that the same kind of features (normal movements associated with left-lateral wrenching) are occurring along the Rudbar fault. Compared to the cumulative transpressive deformation and the large-scale topography associated with the Neogene structures (e.g., geological maps; Allen et al., 2003), our observations show that there has been a transition of the internal domain of the central Alborz from transpression to active transtension in very recent time.

This transtension is tightly associated with the geometry of pre-existing faults that are involved in the general left-lateral shear inside the range. Meanwhile, the borders are still affected by a transpressive regime. The whole kinematic picture is compatible with a general strike-slip regime (with $\sigma 1$ and $\sigma 3$ trending horizontally NNE-SSW and WNW-ESE, respectively) and the permutation of $\sigma 1$ with the vertical stress axis between the borders and the internal domain (Fig. 6).

Our results show that the highest reliefs in the internal part of the range are decreasing. This appears to be consistent with the reconstruction of sedimentation history in the South Caspian Basin (Brunet et al., 2003), which suggests a recent diminishing of the sedimen-

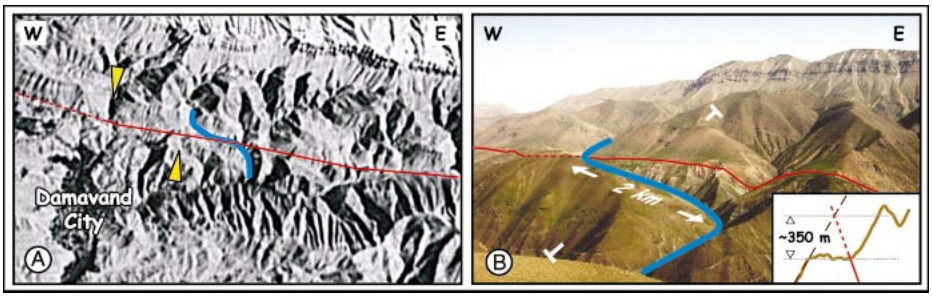

Figure 5. A: Iconos satellite image showing eastern Mosha fault and offset streams (stream underlined in blue is the one shown in B); yellow arrows show largest shifted stream (3 km). B: Picture showing cumulative horizontal and vertical displacements within an offset stream.

tation rate between the Pliocene (when the Alborz was higher and under compression) and the Pleistocene.

This recent kinematical change in the Alborz has to be considered also with the present deformation in the Talesh at the southwestern border of the Caspian Basin, where GPS measurements show the occurrence of a NNE-SSW extension (Masson et al., 2005). All these new observations tend to show that a recent regional kinematic reorganization has occurred at the scale of the South Caspian Basin and its surrounding mountain ranges.

According to our estimates, the transtension started between 1 and 1.5 Ma and appears to be contemporaneous with the Damavand volcanic activity, dated between 1.8 Ma and 7 ka (Davidson et al., 2004). The transtension is clearly linked to the partitioning of deformation in the central Alborz, which is itself associated with the westward component of the South Caspian Basin motion with respect to Eurasia (Jackson et al., 2002). It could also be proposed that the general left-lateral shearing in Alborz is related to the clockwise rotation of the South Caspian Basin (Fig. 6B). Therefore, our results suggest that the latter events could be at least three times younger (middle Pleistocene) than has been previously proposed (middle Pliocene), which used interpretations of industry-image subsurface growth structures in the northwestern South Caspian sedimentary stack (Devlin et al., 1999).

CONCLUSIONS

Our results suggest that the beginning of the South Caspian Basin northwestward motion to Eurasia and/or its clockwise rotation is Pleistocene in age. This motion provoked not only the change from a general N-S compression to a general NNE-SSW transpression in Alborz but also the expression of transtension in the internal domain of the range. Not only have the horizontal movements along the strike-slip faults in the western Alborz been reversed but also the vertical component of the thrusting faults in the internal part of the range; this is an outstanding example of extensional phenomena occurring within a compression-dominated region.

ACKNOWLEDGMENTS

This work was supported by a French-Iranian research program on the study of the recent and active tectonics in Iran (coordination D. Hatzfeld). We are grateful to the Centre National de la Recherche Scientifique (CNRS), the French Embassy in Iran, and the Geological Survey of Iran (GSI) and the International Institut of Earthquake Engineering and Seismology (IIEES) for their support. We thank M. Abbassi, R. Bayer, J. Chéry, S. Dominguez, K. Hessami, D. Hatzfeld, J. Lavé, M. Ghassemi, F. Masson, M. Ghorashi, H. Philip, A. Saidi, and R. Walker for fruitful discussions. We also thank G. Ganem, R. Tailleux, B. Anderson, and J. Jackson for their comments on the text, and A. Delplanque for drawings. This manuscript benefited from the comments of G. Axen, B. Guest, and T. Niemi during a first review, and D. Stockli and an anonymous referee during a second review.

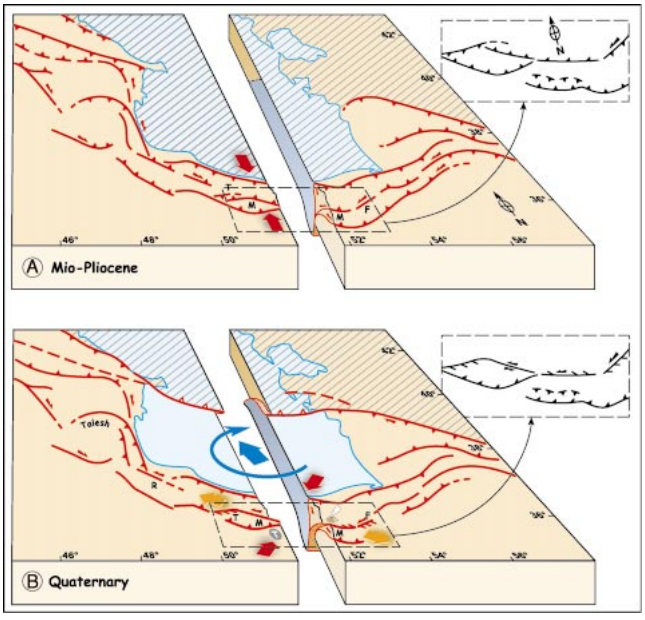

Figure 6. Three-dimensional sketches illustrating recent change of kinematics in central Alborz associated with northwestward motion of South Caspian Basin (blue arrow) and/or its clockwise rotation. Red arrows indicate general compressive axis across central Alborz; orange arrows indicate extensional axis in internal domain of range along range-parallel left-lateral shear zone. Symbols are same as Figure 1. Faults with small dashes indicate predominant normal faulting along Taleghan and Firuzkuh faults. T—Tehran city.

REFERENCES CITED

Allen, M.B., Ghassemi, M.R., Shahrabi, M., and Qorashi, M., 2003, Accommodation of late Cenozoic oblique shortening in the Alborz range, northern Iran: Journal of Structural Geology, v. 25, p. 659–672.

Ashtari, M., Hatzfeld, D., and Kamalian, M., 2005, Microseismicity in the region of Tehran: Tectonophysics, v. 395, p. 193–208.

Axen, G.J., Lam, P.S., Grove, M., Stokli, D.F., and Hassanzadeh, J., 2001, Exhumation of the west-central Alborz mountain, Iran, Caspian subsidence, and collision-related tectonics: Geology, v. 29, p. 559–562.

Bachmanov, D.M., Trifonov, V.G., Hessami, Kh.T., Kozhurin, A.I., Ivanova, T.P., Rogozhi, E.A., Hademi, M.C., and Jamali, F.H., 2004, Active faults in the Zagros and central Iran: Tectonophysics, v. 380, p. 221–241.

Berberian, M., and Yeats, R.S., 2001, Contribution of archeological data to studies of earthquake history in the Iranian Plateau: Journal of Structural Geology, v. 23, p. 563–584.

Berberian, M., Ghorashi, M., Shoja Taheri, J., and Talebian, M., 1996, Seismotectonic and earthquake-fault hazard investigations in the Semnan region, Volume VII: Tehran, Geological Survey of Iran (GSI), p. 268 (in Persian).

Brunet, M.F., Korotaev, M.V., Ershov, A.V., and Nikishin, A.M., 2003, The South Caspian Basin: A review of its evolution from subsidence modelling: Sedimentary Geology, v. 156, p. 119–148.

Davidson, J., Hassanzadeh, J., Berzins, R., Stockli, D.F., Bashukooh, B., Turrin, B., and Pandamouz, A., 2004, The geology of Damavand volcano, Alborz Mountains, northern Iran: Geological Society of America Bulletin, v. 116, p. 16–29.

Devlin, W.J., Cogswell, J.M., Gaskins, G.M., Isaksen, G.H., Pitcher, D.M., Puls, D.P., Stanley, K.O., and Wall, G.R.T., 1999, South Caspian Basin: Young, cool and full of promise: GSA Today, v. 9, no. 7, p. 1–9.

Jackson, J., Priestley, K., Allen, M., and Berberian, M., 2002, Active tectonics of the South Caspian Basin: Geophysical Journal International, v. 148, p. 214–245.

Masson, F., Vangorp, S., Chéry, J., Tavakoli, F., Tatar, M., and Nankali, H., 2005, Extension in NW Iran inferred from GPS enlightens the behavior of the south Caspian basin [abs.]: Eos (Transactions, American Geophysical Union), v. 86, no. 52, Fall Meeting Supplement.

McKenzie, D.P., 1972, Active tectonics of the Mediterranean region: Geophysical Journal of the Royal Astronomical Society, v. 30, p. 109–185.

Ritz, J.F., Balescu, S., Sleymani, S., Abbassi, M., Nazari, H., Feghhi, K., Shabanian, E., Tabassi, H., Farbod, Y., Lamothe, M., Michelot, J.L., Massault, M., Chéry, J., and Vernant, P., 2003, Geometry, kinematics and slip rate along the Mosha active fault, central Alborz: Nice, France, EGU-AGU-EUG Joint Assembly, Abstract EAE03-A-06057.

Vernant, P., Nilforoushan, F., Chéry, J., Bayer, R., Djamour, Y., Masson, F., Nankali, H., Ritz, J.F., Sedighi, M., and Tavakoli, F., 2004, Deciphering oblique shortening of central Alborz in Iran using geodetic data: Earth and Planetary Science Letters, v. 223, p. 177–185.

Manuscript received 19 October 2005
Revised manuscript received 19 January 2006
Manuscript accepted 20 January 2006

Printed in USA

REFERENCES BIBLIOGRAPHIQUES

REFERENCES

Abbassi, M. R., Farbod, Y., 2009. Faulting and folding in quaternary deposits of Tehran's piedmont (Iran). Journal of Asian Earth Science 34, 522–531.

Alavi, M., 1996. Tectonostratigraphic synthesis and structural style of the Alborz mountain system in northern Iran. J. Geodyn. 21, 1 – 33.

Allen, M.B., S.J. Vincent, I. Alsop, A. Ismail-zadeh, R Flecker, 2003a, Late Cenozoic deformation in the South Caspian region: effects of a rigid basement block within a collision zone, Tectonophysics 366, 223– 239.

Allen, M.B., Ghassemi, M.R., Shahrabi, M., and Qorashi, M., 2003b, Accommodation of late Cenozoic oblique shortening in the Alborz range, northern Iran: Journal of Structural Geology, 25, p. 659–672.

Allenbach, P., 1966, Geologie und petrographie des Damavand und seiner Umgebung (Zentral Elburz), Iran., Geol. Mitt. Geol. Inst. ETH Univ. Zurich, n. s., 63, 144p.

Ambraseys, N.N. & Melville, C.P., 1982. *A History of Persian Earthquakes*. Cambridge University Press, New York.

Ashtari, M., Hatzfeld, D., and Kamalian, M., 2005, Microseismicity in the region of Tehran: Tectonophysics, 395, p. 193–208.

Axen, G. J., P. J. Lam, M. Grove, D. F. Stockli, andJ. Hassanzadeh (2001), Exhumation of the westcentral Alborz mountains, Iran, Caspian subsidence,and collision-related tectonics, Geology, 29, 559 – 562, doi:10.1130/0091-7613(2001)029<0559:EOTWCA>2.0.CO;2.

Bachmanov, D.M., Trifonov, V.G., Hessami, Kh.T., Kozhurin, A.I., Ivanova, T.P., Rogozhi, E.A., Hademi, M.C., and Jamali, F.H., 2004, Active faults in the Zagros and central Iran: Tectonophysics, v. 380, p. 221–241.

Ballato, P., N. R. Nowaczyk, A. Landgraf, M R. Strecker, A. Friedrich, and S. H. Tabatabaei (2008), Tectonic control on sedimentary facies pattern and sediment accumulation rates in the Miocene foreland basin of the southern Alborz mountains, northern Iran. Tectonics, 27, TC6001, doi:10.1029/2008TC002278. (3.413).

Berberian, M., 1976. Contribution on the Seismotectonics of Iran: Part I. Geological Survey of Iran, Tehran. 517 pp.

Berberian, M., 1983. The southern Caspian: a compressional depression floored by a trapped, modified oceanic crust. Canadian Journal of Earth Sciences 20, 163–183.

Berberian, M., Qorashi, B., Arzhang-ravesh, A., Mohajer-Ashjai, 1985. Recent tectonics, seismotectonics and earthquake fault hazard investigations in the greater Tehran region: contribution to the seismotectonics of Iran: Part V, Geological Survey of Iran, report 56, 316 pp, 1985.

Berberian, M., Yeats, R.S., 1999. Patterns of historical earthquake rupture in the Iranian plateau. Bulletin of the Seismological Society of America 89, 120–139.

Berberian, M., Yeats, R.S., 2001. Contribution of archaeological data to studies of earthquake history in the Iranian plateau. J. Struct. Geol. 23, 563– 584.

Berberian,M .(1994).Natural Hazards and the First Earthquake catalogue of Iran, vol. 1, Historical Hazards in Iran Prior to 1900,A U NESCO/IIEES Publication during UN/IDND International Institute of Earthquake Engineering and Seismology Tehran, 603 + 66 pp.

Dellenbach, J., 1964. Contribution a l'etude geologique de la region situee a l'est de Teheran (Iran). Faculte de Science de l'Universite Strassbourg (France), 117pp.

Djamour, Y., Bayer, R., Vernant, P., Hatam, Y., Ritz, J. F., Hinderer, J., Luck, B., Nankali, H., Le Moigne, N., Sedighi, M., Boy, J. P., 2008, The present-day deformation in Alborz (Iran) depicted by GPS and absolute gravity observations: Paris, France, SGF

Djamour, Y., 2004, Contribution de la Géodésie (GPS et nivellement) à l'étude de la déformation tectonique et de l'aléa seismique sur la région de Téhéran (montagne de l'Alborz, Iran), Faculte de Sciences et de techniques du Languedoc l'Université Montpellier II (France), 180pp.

Dresch, J., 1961, Le piedmont de Téhéran, Les observations de géographie physique en Iran septentrional : Centre Docum. Cart. Geogr., Mem. et Docum., 8, 85-101.

Geological Survey of Iran, 1993. 1:100,000 Geology map of Tehran. Geological Survey of Iran, Tehran.

Guest, B., D. F. Stockli, M. Grove, G. J. Axen, P. S. Lam, and J. Hassanzadeh ,2006b, Thermal histories from the central Alborz mountains, northern Iran: Implications for the spatial and temporal distribution of deformation in northern Iran, Geol. Soc. Am. Bull., 118, 1507 – 1521, doi:10.1130/B25819.1.

Guest, B., G. J. Axen, P. S. Lam, and J. Hassanzadeh , 2006a, Late Cenozoic shortening in the west central Alborz mountains, northern Iran, by combined conjugate strike-slip and thin-skinned deformation, Geosphere, 2, 35 – 52, doi:10.1130/GES00019.1.

Hedayati, A., Brander, J.L., Berberian, M., 1976. Microearthquake survey of Tehran region, Iran. Bull. Seismol. Soc. Am. 66, 1713–1725.

Hessami, K., Jamali, F., Tabassi, H., 2003, the map of major active faults of Iran., International Institute of Earthquake Engineering and Seismology.

Holingsworth, J., Jackson, J., Walker, R., Nazari, H., 2008, Extrusion tectonics and subduction in the eastern South Caspian, J. Geology, V. 36, N. 10, 763-766.

Hollingsworth, J., 2007, Active Tectonics of NE Iran , PhD thesis University of Cambridge, 220 pp.

Ritz J-F, H. Nazari, H.A., R. Salamati, A. Shafeii, S. Solaymani, 2006, Active transtension inside Central Alborz: a new insight into the Northern Iran–Southern Caspian geodynamics, Geology 34, 477–480.

Jackson, J., Priestley, K., Allen, M., Berberian, M., 2002. Activetectonics of the South Caspian Basin. Geophysical Journal Internationa 148, 214– 245.

Knill and Jones , K.S., 1968, Ground water conditions in Greater Tehran. Quart. J. Eng. Geol., 1, 181-194.

Nabavi, M. H., 1976, Preface to geology of Iran, Geological survey of Iran, 109 p.

Nazari H., Ritz J-F., A. Shafei, A. Ghassemi, R. Salamati, J-L. Michelot and M. Massault, Morphological and paleoseismological analyses of the Taleghan fault, Alborz, Iran, GJI, accepted

Nazari H., Ritz J-F., BALESCU S., LAMOTHE M., R. Salamati, A. Ghassemi, A. Shafei, M. GHORAISHI, A. SAIDI, J-L. Michelot and M. Massaut. Paleoseismological analysis of the North Tehran Fault, Iran: Analysing Prehistoric ruprures for the past 30.000 years, JGR, in revision

Nazari, H., 2006, Analyse de la tectonique récente et active dans l'Alborz Central et la région de Téhéran : Approche morphotectonique et paléoseismologique, Faculte de Sciences et de techniques du Languedoc l' Université Montpellier II (France), 246pp.

Negahban, E.O., 1977. Report of Preliminary excavations at Tapeh Sagzabadin the Qazvin plain. Marlik, Journal of the Institute and Department of Archaeology, 2, Faculty of Letters and Humanities, Tehran University, pp. 26 and 45 (in Persian and English).

Pedrami, M., 1983, Plio-Pleis resch, J., 1961, Le piedmont de Téhéran, In observations de géographie physique en Iran septentrional : Centre Docum.Cart. Geogr.,Mem. et Docum., 8, 85-101.

Rieben, E.H., 1955. The geology of Tehran plain. American Journal of Science 253, 617–639.

Ritz J.-F., Extrusion tectonics and subduction in the eastern South Caspian region since 10 Ma: Comment, Geology, in press.

Ritz, J.-F., Balescu, S., Soleymani, S., Abbassi, M., Nazari, H., Feghhi, K., Shabanian, E., Tabassi, H., Farbod, Y., Lamothe, M., Michelot, J.-L., Massault, M., Che´ry, J., Vernant, P., 2003. Determining the long-term slip rate along the Mosha fault, Central Alborz, Iran. Implications in Terms of Seismic Activity, S.E.E. 4 Meeting, Tehran, 12–14 May.

Sieber, N., 1970, Zur geologie des gebietes sudlich des Taleghan-tales, Zentral Elburz (Iran), Europaische Hochsch, Schrschriften, 19(2), 126p.

Solaymani, Sh., Feghhi, Kh., Shabanian, E., Abbassi, M.R., Ritz, J.F., 2003. Preliminary paleoseismological studies on the Mosha Fault at Mosha Valley. International Institute of Earthquake Engineering and Seismology, 89 p. (in Persian).

Steiger, R., 1966, Die geologie der west-Firuzkuh area (Zentral Elburz/Iran), Mitteilung Geologisches Institut, ETH-Zurich, 145p.

Stöcklin, J. 1974. Northern Iran: Alborz Mountains. *In* Mesozoic-Cenozoic belts. *Edited by* A. M. Spencer. Geological Society of London, Special Publications, 4, pp. 213-234.

Stöcklin, J., 1968. Structural history and tectonics of Iran. A review: Bull. Amer. Assoc. Petrol.Geol. 52 (7), pp. 1229-1258.

Tala'i, H., 1998. Preliminary report of the 10th excavation season (1998) at Tappeh Sagzabad, Qazvin Plain. Archaeological Institute, Tehran University, unpublished internal report, 31 p.

Tatar, M., Hatzfeld, D., 2009, Microseismic evidence of slip partitioning for the Rudbar-Tarom earthquake (*M*s 7.7) of 1990 June 20 in NW Iran, Geophisical Journal International, **176,** 529–541

Tchalenko, J.S., 1975. Seismotectonics framework of the North Tehran fault. Tectonophysics 29, 411– 420.

Tchalenko, J.S., Berberian, M., Iranmanesh, H., Bailly, M., Arsovsky, M., 1974. Tectonic framework of the Tehran region, Geological Survey of Iran, Report n0 29.

Trifonov, V.G., Hessami, K.T., Jamali, F., 1996. West-Trending Oblique Sinitral–Reverse Fault system in Northern Iran. IIEES Special Pub., vol. 75. Tehran, Iran.

Vernant, P., Nilforoushan, F., Che´ry, J., Bayer, R., Djamour, Y., Masson, F., Nankali, H., Ritz, J.F., Sedighi, M., and Tavakoli, F., 2004, Deciphering oblique shortening of central Alborz in Iran using geodetic data: Earth and Planetary Science Letters, v. 223, p. 177–185.

Zanchi , A., F. Berra, M. Mattei, M.R. Ghassemi and J. Sabouri, 2006. Inversion tectonics in central Alborz, Iran, J. Struct. Geol., 20, 1-15.

Ambraseys, N.N. &Melville, C.P., 1982. *A History of Persian Earthquakes, Cambridge Earth Science Series*, Cambridge University Press, London.

Barka, A. A., (1992): The North Anatolian Fault, Annales Tectonicae., VI, 164-195.

BERBERIAN,M. and S. ARSHADI (1976): On the evidence of the youngest activity of the North Tabriz Fault and the seismicity of Tabriz city, *Geol. Surv. Iran Rep.*, **39**, 397-418.

Berberian, M., 1994. Natural hazards and the first earthquake catalog of Iran, Vol. 1: historical hazards in Iran prior 1900, I.I.E.E.S. report.

Berberian, M., 1997. Seismic sources of the Transcaucasian historical earthquakes. In: Giardini, D.,Balassanian, S. (Eds.), Historical and Prehistorical Earthquakes in the Caucasus. Kluwer Academic Publishing, Dordrecht, Netherlands, pp. 233–311.

BERBERIAN, M. and R.S. YEATS (1999): Patterns of historical earthquake rupture in the Iranian plateau, *Bull. Seismol. Soc. Am.*, **89**, 120-139.

DEMETS, C., R.G. GORDON, D.F. ARGUS and S. STEIN, 1990, Current plate motions, *Geophys. J. Int.*, **101**, 425-478.

Eftekharnezhad, J. (1975): Brief history and structural development of Azarbaijan. Geological Survey of Iran, Internal Report, 8P.

Hessami, K., D. Pantosi, H. Tabassi, E. Shabanian, M. Abbassi, K. Feghhi, S. Sholaymani, Paleoearthquakes and slip rates of the North Tabriz Fault,NWIran : preliminary results, Ann. Geophys. 46 (2003) 903–915.

JACKSON, J. (1992): Partitioning of strike-slip and convergent motion between Eurasia and Arabia in Eastern Turkey and the Caucasus, *J. Geophys. Res.*, **97**, 12471-12479.

Jackson, J., Priestley, K., Allen, M., Berberian, M., 2002. Active ectonics of the South Caspian Basin. Geophysical Journal International 148, 214– 245.

Kagan, Y.Y. and Jackson, D.D., 1991, Long-term earthquake clustering, Geophys. J. Int., 104, 117-133.

Karakhanian, A., Djrbashian, R., Trifonov, V., Philip, H., Arakelian, S., Avagian, A., 2002. Holocene-historical volcanism and active faults as natural risk factor for Armenia and adjacent countries. J. Volcanol. Geotherm. Res. 113 (1– 2), 319–344.

A. Karakhanian, R. Jrbashyan, V. Trifonov, H. Philip, A. Avagyan, K. Hessami, F. Jamali, M. Bayraktutan, H. Bagdassarian, S. Arakelian, V. Davtyan, A. Adilkhanyan, Active faulting and natural hazards in Armenia, eastern Turkey and Northern Iran, Tectonophysics 380 (2004) 189–219.

Masson, F., Djamour, Y., van Gorp, S., Ch´ery, J., Tatar, M., Tavakoli, F., Nankali, H. & Vernant, P., 2006. Extension in NW Iran driven by motion of the South Caspian Bosin, *Earth Planet. Sc. Lett.*, **252,** 180–188.

McQuarrie, N., J. M. Stock, C. Verdel, and B. P. Wernicke, 2003, Cenozoic evolution of Neotethys and implications for the causes of plate motions, Geophys. Res. Lett., 30(20), 2036, doi:10.1029/2003GL017992.

Moinvaziri, H. and Aminsobhani, A., 1986, volcanology and volcanosedimentology of the Sahand volcano, Tarbiat Moallem Press.

Nabavi, M. H., 1976, Preface to geology of Iran, Geological survey of Iran, 109 p. (in Persian)

F. Nilforoushan, F. Masson, P. Vernant, C. Vigny, J. Martinod, M. Abbassi, H. Nankali, D. Hatzfeld, R. Bayer, F. Tavakoli, A. Ashtiani, E. Doerflinger, M. Daignières, P. Collard, J. Chéry, 2003, GPS network monitors the Arabia–Eurasia collision deformation in Iran, J. Geody., 77, 411–422.

Sella, G. F., T. H. Dixon, and A. Mao , 2002, REVEL: A model for Recent plate velocities from space geodesy, J. Geophys. Res., 107(B4), 2081, doi:10.1029/2000JB000033.

Siahkali Moradi, A., 2008, Seismicity-Seismotectonic and velocity structure of the earth crust within the Bam and Tabriz strike-slip fault zones, Phd. Thesies, International Institute of Earthquake Engineering and Seismology (IIEES).

Solaymani Azad S., Dominguez, S., Philip, H., Hessami, K., Forutan M-R, Shahpasand Zadeh , M., Ritz, J-F, In preparation, The Zandjan Fault System; Morphological and tectonic evidences of a new active fault network in the NW of Iran, In preparation.

Stöcklin, J., 1968. Structural history and tectonics of Iran: a review. American Association of Petroleum Geologists Bulletin 52, 1229–1258.

Stöcklin, J., 1974. Mesozoic-Cenozoic Orogenic Belts: Data for Orogenic Studies. In: Spencer, A. (Ed.), Northern Iran: Alborz Mountains, 4. Geological Society Special Publication, London, pp. 213–234.

Vernant, P., F. Nilforoushan, D. Hatzfeld, M. Abbassi, C. Vigny, F. Masson, H. Nankali, J. Martinod, A. Ashtiani, R. Bayer, F. Tavakoli, J. Chery, Contemporary crustal deformation and plate kinematics in middle east constrained by GPS measurement in Iran and northern Oman, 2004, Geophys. J. Int., 157, 381–398.

Vernant, P., and J. Chery, 2006, Low fault friction in Iran implies localized deformation for the Arabia-Eurasia collision zone, Earth Planet. Sci. Lett., in press.

WESTAWAY, R. (1990): Seismicity and tectonic deformation rate in Soviet Armenia: implications for local earthquake hazard and evolution of adjacent regions, *Tectonics*, **9**, 477-503.

……..

Agard, P., J. Omrani, L. Jolivet, and F. Mouthereau (2005), Convergence history across Zagros Iran):Constraints from collisional and earlier deformation, I n t . J . Earth Sc i ., 94, 401 – 419, doi:10.1007/s00531-005-0481-4.

Allen, M.B., S.J. Vincent, I. Alsop, A. Ismail-zadeh, R Flecker, 2003a. Late Cenozoic deformation in the South Caspian region: effects of a rigid basement block within a collision zone, Tectonophysics 366, 223– 239.

Allen, M.B., Ghassemi, M.R., Shahrabi, M., and Qorashi, M., 2003b, Accommodation of late Cenozoic oblique shortening in the Alborz range, northern Iran: Journal of Structural Geology, v. 25, p. 659–672.

Allen, M., J. Jackson, and R. Walker, 2004, Late Cenozoic reorganization of the Arabia-Eurasia collision and the comparison of short-term and long term deformation rates, Tectonics, 23, TC2008, doi:10.1029/2003 TC 001530.

Ambraseys, N.N. &Melville, C.P., 1982. *A History of Persian Earthquakes, Cambridge Earth Science Series,* Cambridge University Press, London.

Blanc, E.J.-P., Allen, M.B., Inger, S.and Hassani, H., 2003. Structural styles in the Zagros simple Folded zone, Iran. *J. Geol. Soc. London,* **160,** 401–412.

Berberian, M. and S. Aarshadi, 1976 : On the evidence of the youngest activity of the North Tabriz Fault and the seismicity of Tabriz city, *Geol. Surv. Iran Rep.*, **39**, 397-418.

Berberian, M.,1983. The southern Caspian: a compressional depression floored by a trapped, modified oceanic crust. Canadian Journal of Earth Sciences 20, 163–183.

Berberian, M., 1994. Natural hazards and the first earthquake catalog of Iran, Vol. 1: historical hazards in Iran prior 1900, I.I.E.E.S. report.

Berberian, M. and R.S. Yeats, 1999 : Patterns of historical earthquake rupture in the Iranian plateau, *Bull. Seismol. Soc. Am.*, **89**, 120-139.

Berberian, M., 1997. Seismic sources of the Transcaucasian historical earthquakes. In: Giardini, D., Balassanian, S. (Eds.), Historical and Prehistorical Earthquakes in the Caucasus. Kluwer Academic Publishing, Dordrecht, Netherlands, pp. 233–311.

Berberian, M., Yeats, R.S., 2001. Contribution of archaeological data to studies of earthquake history in the Iranian plateau. J. Struct. Geol. 23, 563– 584.

Cisternas, A. and Philip, H., 1997, Seismotectonics of the Mediterranean Region and the Caucasus, In: Giardini, D., Balassanian, S. (Eds.), Historical and Prehistorical Earthquakes in the Caucasus. Kluwer Academic Publishing, Dordrecht, Netherlands, pp. 39-77.

Copley, A. and Jackson, J., 2006, Active tectonics of the Turkish-Iranian Plateau, Tectonics, Vol. 25, TC6006, doi : 10.1029/2005TC001906.

Eftekharnezhad, J. (1975): Brief history and structural development of Azarbaijan. Geological Survey of Iran, Internal Report, 8P

Förster et al., 1972

Ghassemi, A. and Talbot, C. J., 2006, A new Tectonic scenario for the Sanandaj-Sirjan Zone (Iran),Journal of Asian Earth sciences, XX, 1-11.

Hessami, K., D. Pantosi, H. Tabassi, E. Shabanian, M. Abbassi, K. Feghhi, S. Sholaymani, 2003. Paleoearthquakes and slip rates of the North Tabriz Fault, NWIran : preliminary results, Ann. Geophys.,46, 903–915.

Hessami, K., Jamali, F., Tabassi, H., 2003, the map of major active faults of Iran, International Institute of Earthquake Engineering and Seismology

Jackson, J. & McKenzie, D. 1984, "Active tectonics of the Alpine- Himalayan Belt between western Turkey and Pakistan.", Geophysical Journal - Royal Astronomical Society, vol. 77, no. 1, pp. 185-264.

Jackson, J., 1992 : Partitioning of strike-slip and convergent motion between Eurasia and Arabia in Eastern Turkey and the Caucasus, *J. Geophys. Res.*, **97**, 12471-12479.

Jackson, J., Priestley, K., Allen, M., Berberian, M., 2002. Active tectonics of the South Caspian Basin. Geophysical Journal International, 148, 214– 245.

Karakhanian, A., 1993. The active faults of the Armenian Upland. In: *Proc. of the Scientific Meeting on Seismic Protection*, Dipartamento per la Geologia e le Attivita estrattive, Regione del Veneto, Venice, Italy, pp. 88–94.

Karakhanian, A.S., 1992. Some features of active tectonics in the 1988 Spitak earthquake zone. *Izvestia AN Armenii, Nauki o zemlie* **1**, pp. 3–11 (in Russian) .

Karakhanian, A.S. and Balassanian, V.S., 1992. Active dynamics of the 1988 Spitak earthquake zone. *Izvestia AN Armenii, Nauki o Zemlie* **2**, pp. 12–21 (in Russian) .

Karakhanian, A., Jamali, F.H., Hessami, K.T., 1996. An investigation of some active faults in the Azarbaidjan region (NW Iran). Report IIEES. Tehran, 7.

Karakhanian, A.S., Trifonov, V.G., Azizbekian, O.G. and Hondkarian, D.G., 1997. Relationship of the late Quaternary tectonics and volcanism in the Khonarassar active fault zone, the Armenian Upland. *Terra Nova* **9**, pp. 131–134. View Record in Scopus | Cited By in Scopus (8)

Karakhanian, A.S., Djrbashyan, R.T., Trifonov, V.G., Philip, H. and Ritz, J.-F., 1997. Active faults and strong earthquakes of the Armenian Upland. In: Giardini, D. and Balassanian, S., Editors, 1997. *Historical and Prehistorical Earthquakes in the Caucasus*, Kluwer Academic Publishing, Dordrecht, Netherlands, pp. 181–187.

Karakhanian, A., Bagdassarian, H., Arakelian, S., Avagyan, A., Davtian, V., Adilkhanian, A., Balassanian, V. and Abgaryan, Y., 2000. In: *Landslide Hazard and Risk: Geographic Information System on Landslide Hazard and Risk Assessment in the Republic of Armenia*, UNDP, Yerevan, p. 274.

Karakhanian, A., Djrbashian, R., Trifonov, V., Philip, H., Arakelian, S. and Avagian, A., 2002. Holocene-historical volcanism and active faults as natural risk factor for Armenia and adjacent countries. *J. Volcanol. Geotherm. Res.* **113** 1–2, pp. 319–344. **Article** | PDF (2463 K) | View Record in Scopus |
Martin-Kaye, P. H. A. "Accordant Summit Levels in the Lesser Antilles." *Carib. J. Sci*. Vol. 3 (1963), pp. 181-184.

Masson, F., Djamour, Y., van Gorp, S., Ch´ery, J., Tatar, M., Tavakoli, F., Nankali, H. & Vernant, P., 2006. Extension in NW Iran driven by motion of the South Caspian Bosin, *Earth Planet. Sc. Lett.*, **252,** 180–188.

Mirzaei, 2003. Basic Parameters of Earthquakes in Iran, Daneshnegar, 183p. (in Persian).

Nabavi, M. H., 1976. Preface to geology of Iran, Geological survey of Iran, 109 p. (in Persian).

Nilforoushan, F., F. Masson, P. Vernant, C. Vigny, J. Martinod, M. Abbassi, H. Nankali, D. Hatzfeld, R. Bayer, F. Tavakoli, A., Ashtiani, E. Doerflinger, M. Daignières, P. Collard, J. Chéry, 2003. GPS network monitors the Arabia–Eurasia collision deformation in Iran, J. Geody., 77, 411–422.

Priestley, K., Baker, C., and Jackson, J., 1994, Implications of earthquake focal mechanism data for the active tectonics of the south Caspian basin and surrounding regions: Geophysical Journal International, v. 118, p. 111–141.

Reilinger, R., et al. (2006), GPS constraints on continental deformation in the Africa-Arabia-Eurasia continental collision zone and implications for the dynamics of plate interactions, J. Geophys. Res., 111, B05411

Stampfli, G.M., Marcoux, J., and Baud, A., 1991, Tethyan margins in space and time, *in* Channell, J.E.T., Winterer, E.L., and Jansa, L.F., eds., Paleogeography and paleoceanography of Tethys: Palaeogeography, Palaeoclimatology, Palaeoecology, p. 373–410.

Stampfli, G.M., Borel, G., Cavazza, W., Mosar, J. and Ziegler, P.A. 2001. The paleotectonic atlas of the Peritethyan domain on CD ROM , A presentation, EGS 26th General assembly. Geophysical research abstracts, Nice, GRA3, 878.

Sengör, A. M. C., 1979, Mid-Mezozoic closure of Permo-Triassic Tethys and its implications, Nature, 279, p. 590-593.

Solaymani, S., Feghhi, K., 2003. Report of surface faulting and Morphotectonics of Avaj Region Earthquake on June 22, 2002.Website: http://www.iiees.ac.ir/English/bank/Avaj/avaj_report.html.

Solaymani Azad, S., Philip, H., Dominguez, S., Hessami, K., Shahpasand Zadeh, M., Forutan, M-R, Tabassi, H., Lamothe, M., Paleoseismological and morphological evidences of slip variations along the North Tabriz Fault (NW Iran), in preparation.

Stoneley, R. 1981. The geology of the Kuh-e Dalneshin area of southern Iran, and its bearing on the evolution of southern Tethys. Journal of the Geological Society, London, 138, 509-526.

Van Couvering, J. A., and J. A. Miller. 1971. Late Miocene marine and non-marine time scale in Europe. Nature, 230: 559-563.

Vernant, P., F. Nilforoushan, D. Hatzfeld, M. Abbassi, C. Vigny, F. Masson, H. Nankali, J. Martinod, A. Ashtiani, R. Bayer, F. Tavakoli, J. Chery, Contemporary crustal deformation and plate kinematics in middle east constrained by GPS measurement in Iran and northern Oman, 2004, Geophys. J. Int., 157, 381–398.

Vernant, P., and J. Chery, 2006, Low fault friction in Iran implies localized deformation for the Arabia-Eurasia collision zone, Earth Planet. Sci. Lett., in press.

Walker, R. T., Bergman, E., Jackson, J., Ghorashi, M., Talebian, M., 2005, The 2002 June 22 Changureh (Avaj) earthquake in Qazvin province, northwest Iran : epicentral relocation, source parameters, surface deformation and geomorphology, Geophys. J. Int., 160, 707-720.

Westaway, R., 1990 : Seismicity and tectonic deformation rate in Soviet Armenia: implications for local earthquake hazard and evolution of adjacent regions, *Tectonics*, **9**, 477-503.

Yilmaz, Y., 1993, New evidence and model on the evolution of the southeast Anatolian orogen: Geological Society of America Bulletin, v. 105, p. 251–271, doi: 10.1130/0016- 7606(1993) 105<0251:NEAMOT> 2.3. CO;2.

Evaluation de l'aléa sismique pour les villes de Téhéran, Tabriz et Zandjan dans le NW de l'Iran, Approche; morphotectonique et paléosismologique.

……

RESUME L'objectif de ce mémoire de thèse est l'étude de la tectonique récente et l'évaluation de l'aléa sismique pour trois villes importante, Téhéran, Tabriz et Zandjan, situées dans le nord-ouest de l'Iran. Dans la capitale de l'Iran, Téhéran, nous nous sommes concentrés sur le système de faille active de Mosha-Nord Téhéran. Nos travaux démontrent que ce système est essentiellement décrochant sénestre. Nos analyses paléosismologiques sur la portion est de ce système (dans la vallée de Tar) montrent au minimum les évidences de sept grands événements sismiques (M>7) pendant les derniers 10000 ans (l'intervalle de récurrence est de 1100 à 1400 ans). Les études que nous avons mené dans la partie centrale de ce système (région d'Abali) révèlent qu'il pourrait être la source du dernier événement sismique ayant affecté la ville de Téhéran en 1830 AD. Dans la région de Tabriz, nous nous sommes intéressés au segment SE de la faille décrochante dextre de Nord Tabriz où nous avons trouvé les évidences de trois grands séismes pendant les derniers 33500 ans. Nos études montrent que la faille Nord Tabriz qui est la portion centrale d'un système de faille (TFS) est constituée par deux segments NW et SE dextres. Notre étude paléosismologique suggère une variation de la vitesse qui diminue du NW vers SE le long de ces segments. Les extrémités ouest (Mishu) et est (Bozghush) de ce système correspondent à des zones compressives qui absorbent les déplacements horizontaux sur les segments NW et SE. D'un point de vue général la TFS est une partie d'un système de failles régionales (GSKT) qui relie une zone d'extension active dans la partie centrale de la collision Arabie-Eurasie et une zone de compression active à l'Est. Enfin, à Zandjan qui est une ville située dans une région de lacune sismique, nous avons découvert un important réseau de failles actives. Le tracé sud-est de ce réseau de failles passe par la ville de Zandjan. En conclusion, les localisations et les cinématiques des systèmes de faille étudiés sont discutées dans le cadre géodynamique général de la collision Arabie-Eurasie. On remarquera que la faille majeure de Nord Tabriz qui correspond essentiellement à un décrochement dextre a la même direction NW-SE que les décrochements sénestres présents dans la chaîne de l'Alborz (les failles de : Mosha, Talaghan et Manjil). Cette observation nécessite une variation de la direction de compression entre ces deux régions.

Mots clés : Aléa sismique, Iran, NW Iran, Paléosismologie, Morphotectonique, Téhéran, Tabriz, Zandjan

……

Seismic hazard assessment for Tehran, Tabriz and Zandjan cities (NW Iran) based on morphotectonical and paleoseismological approaches.

……

SUMMARY This thesis aims to analyze the active tectonics and the seismic hazard for three main cities of NW Iran (Tehran, Tabriz and Zandjan) using morphotectonics and paleoseismology. Within the Tehran capital, we focused our analysis on the Mosha-North Tehran (M-NT) active fault system. Our investigations show that this fault system is mainly dominated by left-lateral faulting. Along the eastern part of the M-NT fault system, we found evidences of at least seven strong (M>7) paleoearthquakes during the past 10 ka (recurrence interval: 1100-1400 yrs). Our study along the central portion of the fault system (in Abali region) suggests that it corresponds probably to the source of the 1830 AD historical earthquake (M=7.1, Io= IX). Within Tabriz region, we studied the SE segment of the North Tabriz fault. We found evidences of at least three strong events, which occurred during the past 33.5 ka. The North Tabriz dextral fault corresponds to the central portion of a fault system (TFS), and contains two fault segments (NW and SE). Our paleoseismological analysis shows a variation of the slip rate, which decreases from NW to SE along the strike-slip fault. The western (Mishu) and eastern (Bozghush) terminations of the fault system correspond to oblique-compression zones. TFS belongs to the eastern portion of a regional fault system (GSKT), linking the active extension within the central part of the collision and the active compression to the East. Finally, we focus on the Zandjan area, where no important historical seismicitiy is recorded. There, based on morphotectonics analysis we discovered a large active fault network, whose southeastern part affects the Zandjan city.

To conclude this work, we replace our observations within the general geodynamic framework of the Arabia-Eurasia collision. One of the striking pictures is the occurrence of opposite kinematics along the M-NT (and other range parallel faults within the south Central Alborz) and the North Tabriz fault systems that have the same trend. This shows the rapid variation of the regional stress field in the Northern Iran.

Key words: Seismic hazard assessment, Iran, NW Iran, Paleoseismology, Morphotectonics, Tehran, Tabriz, Zandjan

……..

Discipline : Structure et Evaluation de la Terre et des Planètes

……

Laboratoire Géosciences Montpellier – UMR 5243 – Université Montpellier II, Cc060, Place E. Bataillon, 34095 Montpellier Cedex 5, France.